Dissertation zur Erlangung des Doktorgrades
der Fakultät für Chemie und Pharmazie
der Ludwig-Maximilians-Universität München

Internal Plasticized Glycidyl Azide Copolymers For Energetic Solid Propellant Binders

Sven Tobias Hafner
aus
Stuttgart, Deutschland
2019

Erklärung

Diese Dissertation wurde im Sinne von §7 der Promotionsordnung vom 28. November 2011 von Herrn Prof. Dr. Thomas M. Klapötke betreut.

Eidesstattliche Versicherung

Diese Dissertation wurde eigenständig und ohne unerlaubte Hilfe erarbeitet.

Karlsruhe, 12.11.2019

.....

(Sven Tobias Hafner)

Dissertation eingereicht am: 26.07.2019
1. Gutachter: Prof. Dr. Thomas M. Klapötke
2. Gutachter: Prof. Dr. Konstantin Karaghiosoff
Mündliche Prüfung am: 09.10.2019

Meiner Familie in tiefer Dankbarkeit gewidmet.

Danksagung

Mein besonderer Dank gilt Prof. Dr. Thomas M. Klapötke für die Betreuung dieser Arbeit. Seine Hilfsbereitschaft und Offenheit ermöglichten mir das Thema der Dissertation frei zu gestalten und zu bearbeiten. Prof. Dr. Konstantin Karaghiosoff danke ich für die Übernahme des Zweitgutachtens und die fachliche Unterstützung in Fragen zur NMR-Spektroskopie an Polymeren.

Insbesondere möchte ich mich bei Dr. Thomas Keicher bedanken, dessen kontinuierliche Unterstützung in hohem Umfang zum Gelingen dieser Arbeit beigetragen hat. Ferner danke ich ihm für die Weitergabe seiner Expertise in der Synthese und Handhabung energetischer Materialien im Allgemeinen, sowie den unzähligen fachlichen und privaten Diskussionen.

Mein Dank gilt ebenfalls Dr. Jürgen Hürttlen, Dr. Volker Gettwert, Dr. Stefan Löbbecke und Carolyn Fisher für das Korrekturlesen der vorliegenden Arbeit. Für zahlreiche Diskussionen und die Unterstützung in wissenschaftlichen Fragestellungen danke ich Jürgen Antes, Dr. Uwe Schaller, Hartmut Kröber, Marcel Holler, Ligia Radulescu, Michael Wittek, Sebastian Fischer und Claudio Tagliabue.

Bei Dr. Gregor Fröhlich, Dr. Daniel Borowski, Dr. Daniel Schmollinger und Dr. Max Rieger möchte ich mich für die moralische Unterstützung auf den akademischen Wegen und Irrwegen bedanken.

Für die Hilfe am Fraunhofer ICT und im Labor bedanke ich mich bei Gudrun Dornick, Isabel Wilhelm, Maurice Kleine-Beek, Jan-Benedict Müller, Marko Maier und Sarah Steinert. Weiterer Dank gilt der ganzen EM Analytik-Mannschaft, insbesondere Heike Schuppler, Jasmin Aniol, Wenka Schweikert, Stefan Müller, Manuela Dörich, Christian Müller, Gunnar Kronis, Hermann Popp, Werner Reinhard, Dr. Ulrich Förter-Barth sowie Tanja Jahnke und Alexander Baier.

Besonderer Dank gilt vor allem auch meiner Familie und allen Freunden, die mich über die Jahre hinweg begleitet und stets verlässlich unterstützt haben.

Contents

Abstract

Energetic polymers are crucial components of next-generation composite propellants with enhanced performance. A solid rocket motor requires propellants that retain their mechanical properties over a wide range of temperatures. Compared to the state-of-the-art binder systems based on HTPB, the literature shows that energetic polymers, including the well-known glycidyl azide polymer (GAP), often exhibit bad low-temperature properties. The aim of this thesis is the synthesis of novel energetic glycidyl azide copolymers with improved low-temperature properties, and their characterization with special emphasis on their use as prepolymeric binders for cast-cured composite propellants. Comonomers with nonpolar *n*-alkyl side chains were incorporated in the molecular structure of GAP. They act as internal plasticizers that are not able to migrate in the cured propellant formulation, providing improved low-temperature properties and better processability of the copolymer. The first part of the thesis describes the small-scale synthesis of various glycidyl azide copolymers with a systematic variation of the *n*-alkyl side chain lengths and molecular compositions via cationic ring-opening polymerization. The molecular structure of the copolymers was characterized with spectroscopic and chromatographic techniques (IR, NMR, GPC). Their energetic and thermal properties were investigated using thermal analysis methods (DSC, TGA, bomb calorimetry). Further properties that are essential for binder development such as density, viscosity and equivalent weight were also determined. The results of the experiments were discussed and compared to the commercially available GAP homopolymer, which was selected as a reference compound. The second part of the thesis covers the scale-up of one selected copolymer with the most interesting properties in order to obtain enough material for further evaluation concerning its use as a suitable binder system for composite propellants. The third part of the thesis presents formulation studies of the copolymer, starting with a theoretical evaluation using the ICT thermodynamic code, followed by the investigation of binary polymer-plasticizer mixtures. Finally, model propellants with ammonium dinitramide (ADN) as an oxidizer were prepared in a cast-cure process in order to study the influence of the novel copolymer on the processability and mechanical properties of cured composite propellant specimen.

Acronyms

Abbreviations

ACPA 4,4'-Azobis(4-cyanopentanoic acid)

ACPC 4,4'-Azobis(4-cyanopentanoyl chloride)

AD Anno Domini

ADN Ammonium dinitramide

Al Aluminum

AMMO 3-Azidomethyl-3-methyl oxetane

AP Ammonium perchlorate

ATR Attenuated total reflection

ATRP Atom transfer radical polymerization

BAM Bundesanstalt für Materialforschung und -prüfung (DEU)

BAMO 3,3-Bis(azidomethyl) oxetane

BCMO 3,3-Bis(chloromethyl) oxetane

BDNPA Bis(2,2-dinitropropyl) acetal

BDNPA/F 50:50 (w/w) mixture of BDNPA and BDNPF

BDNPF Bis(2,2-dinitropropyl) formal

BDO 1,4-Butanediol

BTTN Butanetriol trinitrate

BuNENA *N*-Butylnitratoethyl nitramine

CEMA Chloromethyl methacrylate

CL-20 Hexanitrohexaazaisowurtzitane, also referred to as HNIW

CMDB Composite-modified double-base propellant

CTPB Carboxyl-terminated polybutadiene

DBTDL Dibutyltin dilaurate, also referred to as D22

DCM Dichloromethane

DDC *N,N*-Diethyl dithiocarbamate

DEGBAA Diethylene glycol bis(azidoacetate)

DEHA Di-(2-ethylhexyl) adipate

DIN Deutsches Institut für Normung (DEU)

DINCH 1,2-Cyclohexane dicarboxylic acid diisononyl ester

DINP Diisononyl phthalate

DMAP 4-Dimethylaminopyridine

DMF *N,N*-Dimethylformamide

DMSO Dimethylsulfoxide

DNDA-5 2,4-Dinitro-2,4-diazapentane

DNDA-6 2,4-Dinitro-2,4-diazahexane

DNDA-7 3,5-Dinitro-3,5-diazaheptane

DNDA-57 Mixture of DNDA-5, DNDA-6, DNDA-7 approx. 43:45:12 (w/w/w)

DOA Dioctyl adipate

DOS Dioctyl sebacate

DRA Defence Research Agency (GBR)

DSC Differential scanning calorimetry

ECH Epichlorohydrin

EG Ethylene glycol

EGBAA Ethylene glycol bis(azidoacetate)

EGDN Ethylene glycol dinitrate

ETPE Energetic thermoplastic elastomer

EUR Europe

EW Equivalent weight

FOI Totalförsvarets forskningsinstitut (SWE)

FRP Freezing point

FW Formula weight

GA Glycidyl azide

GALCIT Guggenheim Aeronautical Laboratory of the California Inst. of Technology

GAP Glycidyl azide polymer

GAP-A Azido-terminated glycidyl azide polymer ($M_n < 1000\,\mathrm{g/mol}$)

GN Glycidyl nitrate

GPC Gel permeation chromatography

GPO Dioctyl terephthalat

HMMO 3-Hydroxymethyl-3-methyl oxetane

HMX Cyclotetramethylene tetranitramine, also referred to as octogen

HNVP 3-Hexyl-1-vinyl-2-pyrrolidone

HR Heating rate

HTPB Hydroxyl-terminated polybutadiene

ICT Fraunhofer Institute for Chemical Technology (DEU)

IM Insensitive munitions

IR Infrared radiation

JATO Jet-assisted take-off

KPG Kerngezogenes Präzisionsglasgerät (special type of glass stirrer)

LOVA Low-vulnerability ammunition

MCPI *N*-Methyl-2-chloropyridinium iodide

MMA Methyl methacrylate

MWD Molecular weight distribution

NATO North Atlantic Treaty Organization

NENA Nitrato ethyl nitramine

NC Nitrocellulose

NG Nitroglycerin

NHTB Nitrated hydroxyl-terminated polybutadiene

NMP *N*-Methyl-2-pyrrolidone

NMR Nuclear magnetic resonance

NVP 1-Vinyl-2-pyrrolidone

OHV Hydroxyl value

PAEMA Poly(azidoethyl methacrylate)

P(AMMO) Poly(3-azidomethyl-3-methyl oxetane)

PBAA Polybutadiene-acrylic acid

P(BAMO) Poly(3,3-bis(azidomethyl) oxetane)

PBAN Polybutadiene acrylonitrile

P(BCMO) Poly(3,3-bis(chloromethyl) oxetane)

PBX Polymer-bonded explosive

PDI Polydispersity index

PECH Polyepichlorohydrin

PEG Polyethylene glycol

PETKAA Pentaerythritol tetrakis(azidoacetate)

PGAAT Poly(glycidyl azide-*r*-3-azido tetrahydrofuran)

PGN Poly(glycidyl nitrate)

PMMA Poly(methyl methacrylate)

P(NIMMO) Poly(3-3-nitratomethyl-3-methyl oxetane)

Py Pyridine

ppm Parts per million

PS Polystyrene

PVAc Poly(vinyl acetate)

PVN Poly(vinyl nitrate)

RDX 1,3,5-Trinitro-1,3,5-triazacyclohexane, also referred to as hexogen

RID Refractive index detector

RT Room temperature

RU Repeating unit

SRM Solid rocket motor

STS Space transportation system

STANAG Standardization agreement

TA Triacetin

TEA Triethyl amine

TEGDN Triethylene glycol dinitrate

TGA Thermogravimetric analysis

THF Tetrahydrofuran

TMETN Trimethylolethane trinitrate

TMP Trimethylolpropane

TMS Tetramethylsilane

TOTM Trioctyl trimellitate

TsCl *p*-Toluenesulfonyl chloride

USA United States of America

UN United Nations

UV Ultraviolet

WWI World War One

WWII World War Two

Symbols

Å Ångström

T_B Boiling point

T_b Brittle point

δ Chemical shift

T_c Combustion chamber temperature

T_d Decomposition temperature

ρ Density

$\Delta_c U$ Energy of combustion

$\Delta_c H$ Enthalpy of combustion

ΔH_{Dec} Enthalpy of decomposition

T_g Glass transition temperature

T_m Melting temperature

M_n Number average molecular weight

Ω Oxygen balance

$\Delta_c H_m^0$ Molar standard enthalpy of combustion

$\Delta_f H_m^0$ Molar standard enthalpy of formation

M_p Peak molecular weight

D Polydispersity index

I_{sp} Specific impulse by weight

I_{spv} Volumetric specific impulse

$\Delta_f H^0$ Standard enthalpy of formation

η Viscosity

$\tilde{\nu}$ Wave number

M_w Weight average molecular weight

List of Figures

List of Tables

1 Introduction

The earliest rockets in the Western world were described as 'flying fires' in around 1300 AD. They emerged from fireworks, which had been invented by the Chinese more than 700 years earlier [1, 2]. Pyrotechnic compositions of potassium nitrate, charcoal and sulfur, which are known as black powder, were the propellants of these forerunners of modern rockets [2]. Major advances in the evolution of solid propellants were achieved in the 19th and 20th century. After the invention of nitrocellulose by Schönbein and Böttger in 1846 [3], black powder was replaced by more effective and reliable double base propellants at the end of the 19th century, which are still applied in some missiles today [4, 5]. The development of more powerful composite rocket propellants was strongly driven by incidents during the Cold War that required reliable missile systems providing a high performance. Composites are still the state-of-the-art solid propellant systems used in military and space applications nowadays [6]. Beside the classification of propellants according to their applications, a convenient approach starts with the energy source (nuclear, solar, chemical). Contemporary space propulsion systems are based on chemical propellants, but they may be replaced in the future by other energy sources [8]. During the high-pressure combustion process of the reaction partners of a chemical propellant, high-temperature gaseous products are formed (2500 °C to 4100 °C). They are expanded in a nozzle and accelerated to high velocities (1800 m/s to 4300 m/s), generating thrust for the rocket propulsion [8]. Depending on the physical state of the reaction partners, chemical propellants can be classified into several groups which is presented according to the literature in Figure 1.1 [7]. Today's high-performance solid propellants are usually heterogeneous composites that consist of three main components

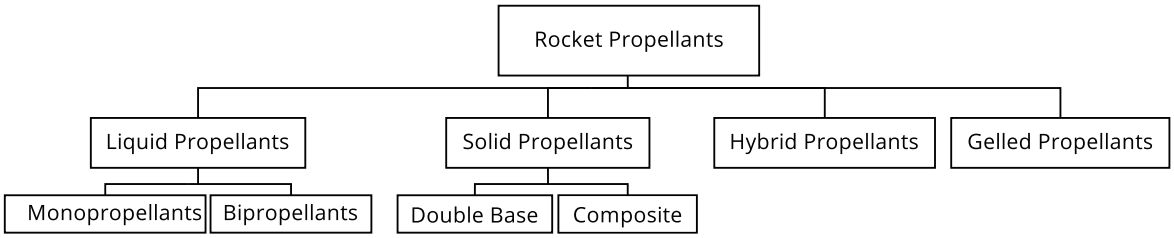

Figure 1.1 Simplified classification of rocket propellants in terms of their physical state [7].

beside other additives: An oxygen-rich solid oxidizer, which delivers oxygen for the combustion process, a combustible metal fuel for improved performance and an organic polymer that is used as a binder acting as an elastic matrix for the solid filler particles [9]. Composite propellants are manufactured in a cast-cure process. The fillers are mixed in kneaders with liquid prepolymers and additives before the obtained propellant slurry is cast into the rocket motor mold. Depending on curing agents, catalysts and curing temperature, the mixture is cured within a few hours to several days to deliver the final propellant grain [5]. Though its percentage in propellant formulations is rather low, the binder fulfills several fundamental functions. First of all, it retains the shape and the structural integrity of the propellant grain. Furthermore, it absorbs the thermal and mechanical stress that occurs during storage and combustion while the rocket is launched. The sensitivity of the propellant towards impact and friction is reduced by the binder, because it separates the oxidizer and metal particles from each other and is therefore essential to ensure the insensitivity of the propellant grain. Last but not least, the binder serves as a fuel for the combustion process. Modern solid propellant binders are predominantly based on hydroxyl-terminated polybutadiene (HTPB), which is crosslinked by curing reactions with isocyanates, forming urethane linkages to build a rubber-like elastomer. This binder system provides superior mechanical properties in the widely used formulations containing ammonium perchlorate (AP) as an oxidizer and aluminum (Al) as a metal fuel [10, 11].

By replacing the inert binder with an alternative that contains energetic functional groups (e.g. nitramine-, nitro-, azido-groups or nitrate esters), additional energy can be provided to the combustion process. Such energetic binder systems can be applied for rocket propellants with enhanced performance. Though a lot of research in the field of energetic binders has been carried out during the past decades, the literature reports almost no application of energetic polymers in composite propellants, because they suffer from various drawbacks like bad processability, insufficient mechanical properties, low stability or high costs due to complicated synthesis and expensive raw materials. This thesis is directed towards the development of novel energetic propellant binder systems that are appropriate for next generation composite propellants for both military and space applications. The present work reports on glycidyl azide copolymers with improved low-temperature properties, which is a major topic of energetic binder research. Starting from the copolymer synthesis via cationic ring-opening polymerization, a systematic variation of the molecular compositions is followed by experimental investigations on binary polymer-plasticizer mixtures and cast-cured model composite propellants.

2 Concepts

2.1 Motivation and Objectives

The performance enhancement of modern composite propellants demands suitable energetic binders that are able to increase the overall energy released during the combustion process. Research and investigation concerning energetic binder materials started in the early 1950s [12] and is still ongoing. Though many different energetic polymers have been reported in the scientific literature, they still barely find technical applications in space flight or missile systems, except nitrocellulose (NC). The reason for this are the various requirements for propellant binders that are difficult to meet with energetic polymers, already reported in the literature. These polymers generally suffer from drawbacks in terms of:

- Processability: Low viscosities are needed to achieve high filler loadings, which is crucial for the performance of the propellant.
- Stability: Some molecular structures and energetic functional groups have a negative impact on the stability.
- Sensitivity: Low sensitivity towards mechanical stimuli and electric discharge are important for the manufacturing of insensitive munition (IM).
- Mechanical properties: Most published energetic polymers exhibit insufficient mechanical properties and do not meet the required standards in composite formulations.
- Costs: Complicated and expensive multiple-step synthesis procedures often prevent the large-scale production of interesting materials.

Taking these factors into account, the most promising energetic polymer today is glycidyl azide polymer (GAP) (Figure 2.1). GAP is currently the only commercially available energetic polymer and is sold by 3M (USA) under the trademark GAP-5527 Polyol [13] and by Eurenco Bofors (EUR) under the trademark GAP Diol [14]. Though

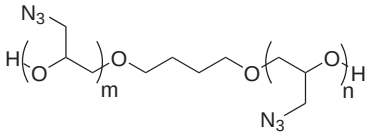

Figure 2.1 Molecular structure of glycidyl azide polymer (GAP).

GAP provides excellent properties like a high enthalpy of formation and good thermal stability, it still suffers from a high glass transition temperature (T_g) of approximately $-43\,°C$ [15] that further increases during the curing process [13]. Because the specified service temperatures of solid rocket propellants are usually in a range of $-54\,°C$ to $71\,°C$ [16, 17], depending on the operation purpose, a high content of plasticizers has to be used for GAP-based propellants to obtain the low-temperature properties that are required. When using high contents of plasticizers, the propellant grain often suffers from migration phenomena and also insufficient mechanical properties which can cause severe safety issues (Chapter 3.4).

The main objective of this thesis was the development of novel energetic polymers with improved low-temperature properties that are suitable for use in energetic binder systems for solid propellants. The following aspects had to be considered:

- Cheap and commercially available reactants
- Scalable synthesis procedure avoiding multiple synthesis steps
- Thermal stability comparable to GAP
- Good interaction with established plasticizers

The desired benefit of developing novel energetic polymers with better low-temperature properties is to avoid the need for plasticizers or at least to limit the necessary amount in order to reduce the associated problems with migration phenomena. This main objective was divided into three consecutive tasks (Figure 2.2). Firstly, synthesis

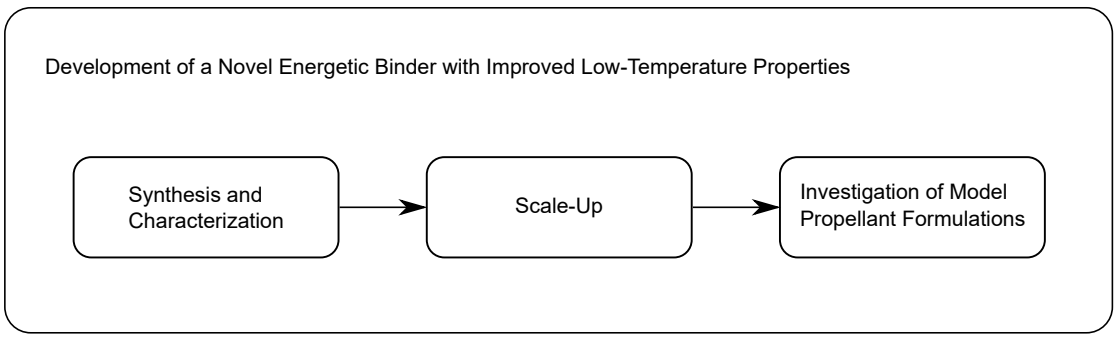

Figure 2.2 Consecutive tasks of energetic binder development.

in small-scale batches up to a few grams had to be performed as an efficient and economical approach to investigate many different materials in a manageable amount of time and without excessive use of resources. After selecting the most promising polymer, a scale-up procedure was elaborated in order to obtain enough material for further characterization and evaluation in propellant formulations. Finally, application studies in model propellant formulations were necessary to evaluate the influence of a novel energetic binder on the properties of cured propellant specimen.

Because of the promising properties of glycidyl azide units, in particular their high enthalpy of formation and good thermal stability [18], it was decided to adopt the polymer system of glycidyl azide polyethers and to apply the concept of internal plasticization that is known for other polymer systems like polymeric acrylates (Chapter 3.4). The incorporation of nonpolar side chains reduces the intra-/ and intermolecular forces between the backbone chains, thereby providing the desired plasticizing effect that is needed to improve the low-temperature properties and to avoid brittleness. As the internal plasticizer is bound to the molecular structure of the polyether, no migration phenomena can occur, in contrast to external plasticizers. The plasticizing effect of the side chains is expected to show several desirable influences on the copolymer properties:

- Decreased glass transition temperature (T_g)
- Lowered process viscosity during mixing in the propellant cast-cure process
- Decreased sensitivity towards mechanical stimuli compared to GAP because of a lower nitrogen content

The synthesis of such internal plasticized glycidyl azide copolymers starts from epichlorohydrin and commercially available comonomers (Figure 2.3). Substituted oxiranes were identified as suitable comonomers since they are known to undergo cationic ring-opening polymerization under comparable conditions to epichlorohydrin [19]. An evaluation

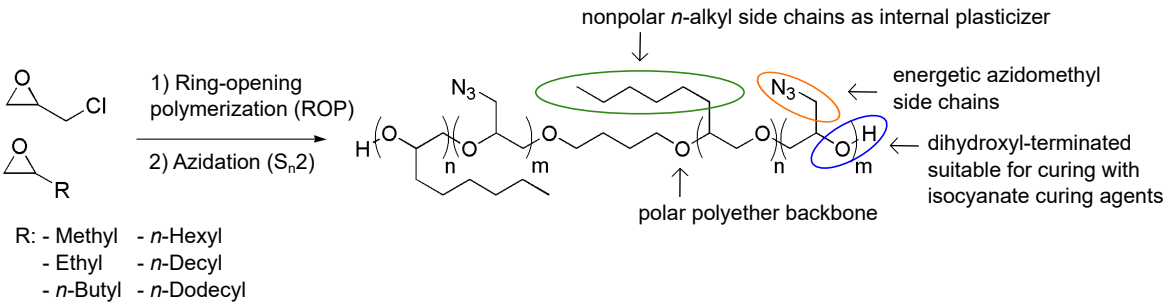

Figure 2.3 Concept of using nonpolar n-alkyl side chains as an internal plasticizer for glycidyl azide copolymers.

of commercially available oxiranes with nonpolar substituents led to the decision to focus the study on *n*-alkyl-substituted oxiranes because *n*-alkyl chains are known to have excellent plasticizing properties that are even better than branched chains [20]. Furthermore, *n*-alkyl-substituted oxiranes turned out to be cheap and readily available from different suppliers. They are offered over a wide range of side chain lengths from C1 (methyl moiety) to C12 (dodecyl moiety), therefore providing the possibility of a comprehensive evaluation of the side chain influence on the glycidyl azide copolymer properties. This evaluation of *n*-alkyl side chains as internal plasticizers for glycidyl azide copolymers finally determined the following subtasks that are addressed by the different parts of the thesis:

1. Synthesis and characterization:
    - Optimization of a synthesis procedure for the copolymerization of *n*-alkyl-substituted oxiranes and epichlorohydrin
    - Realization of a convenient azidation process of epichlorohydrin copolymers
    - Investigation of the influence of side chain length and molecular composition on the copolymer properties with special focus on their use as prepolymers for energetic binder systems
    - Selection of the copolymer with the most promising properties for further studies in propellant formulations
2. Scale-up:
    - Evaluation of the reproducibility of the copolymerization procedure
    - Scale-up of the established synthesis to deliver a sufficient amount of copolymer material for model propellant formulation studies
3. Formulation of model propellants:
    - An evaluation using the ICT thermodynamic code to calculate the expected performance of propellants based on the novel copolymer in comparison to GAP
    - Miscibility studies with commercial plasticizers in order to find a suitable plasticizer for further improvement of the mechanical properties
    - Formulation and characterization of first model propellants based on the oxidizer ammonium dinitramide (ADN) to study the influence of the novel copolymer on the properties of cured propellant specimen

2.2 Structure of the Thesis

Chapter 1 and 2: Introduction and Concepts A brief introduction to the topics and objectives of the thesis.

Chapter 3: Background Provides an overview of the current status quo in the literature concerning solid propellant binders, with a special focus on energetic polymers based on glycidyl azide units. Because of their high importance in modern binder materials, external plasticizers are also briefly discussed, including an introduction to migration phenomena and internal plasticization.

Chapter 4: Characterization Methods Describes all characterization methods that were used in the different parts of the thesis in a comprehensive chapter.

Chapter 5: Synthesis and Characterization of Glycidyl Azide Copolymers Reports on the synthesis of novel *n*-alkyl-substituted glycidyl azide copolymers and their characterization with respect to their use as prepolymers for energetic solid propellant binders. The first section covers the optimization of polymerization conditions concerning molecular weight, monomer/initiator ratio ([M]/[I]) and end groups using the example of 1,2-epoxyhexane as a comonomer with a moderate side chain length. By a variation of the comonomers, the influence of the side chain length on properties like glass transition temperature and processability was investigated in the second section. 1,2-Epoxyoctane turned out to be the most interesting comonomer for further investigation. The molecular composition between epoxyoctane (EpO) units and glycidyl azide (GA) units was therefore varied in the third section and P($GA_{0.75}$-*co*-$EpO_{0.25}$) was selected as the copolymer with the most promising properties for further studies in cast-cured model propellant formulations.

Chapter 6: Scale-Up Experiments Covers the scale-up experiments that were needed to provide enough material for formulation studies. The synthesis was scaled-up to a 100 g polymerization batch size, which was repeated several times. The batches were analyzed and compared regarding their properties in order to confirm the maintenance of the product quality in multiple synthesis procedures. Individual batches were combined to master batches and azidated in a subsequent synthesis step, providing sufficient amount of the selected azido-copolymer P($GA_{0.75}$-*co*-$EpO_{0.25}$) for the subsequent formulation studies.

Chapter 7: Formulation Studies This chapter is divided into three sections that report on the application of the novel synthesized copolymer in model propellant formulations. First of all, the selected copolymer P($GA_{0.75}$-*co*-$EpO_{0.25}$) is evaluated regarding its impact on the performance of solid propellants using the ICT thermodynamic code. This is followed by an experimental investigation of binary mixtures of the most important nonenergetic plasticizers and the copolymer. The aim was to find the most suitable plasticizer that can be added in small amounts to propellant formulations in order to obtain propellants with excellent low-temperature properties. The last section describes the formulation and characterization of propellants with the novel copolymer in comparison to similar formulations based on the commercially available GAP to investigate the performance and influences of the novel copolymer on cured composite propellant specimen.

3 Background

3.1 A brief History of Binders for Composite Rocket Propellants

After the development of nitrocellulose double base (DB) propellants, limits were reached when the demands on propellant grains became very complex concerning their size and geometry. The emerging composite propellants were soon able to outperform the performance of the established DB propellants. The evolution of modern composite propellants is closely related to the synthesis of new polymers and enhanced casting techniques after WWII. The goal was to utilize viscous prepolymers that can be mixed with solid oxidizers, metal fuels and additives to form a slurry that can be casted in suitable motor molds and cured subsequently after the casting step by using specific curing agents. A simple comparison of a first booster charge developed for JATO (jet assisted take-off) aircraft, which had a mass of approximately 28 kg, to a giant booster used for the Space Shuttle with a total mass of 504 t propellant illustrates how the requirements on the technology of solid propellants and also the binder materials themselves increased over time [21].

Different types of polymers have been developed for the application as binders in composite propellants. They can be roughly classified into three different categories [5]:

- Linear amorphous binders (asphalt, polyisobutylene)
- Linear crystalline binders (nitrocellulose, polyvinylchloride)
- Cross-linked binders (polysulfides, polybutadienes, polyurethanes)

The first specific binder for composite rocket propellants was invented by the Guggenheim Aeronautical Laboratory of the California Institute of Technology (GALCIT) during the development of solid propellants for JATO aircrafts. These type of propellants were based on a dispersion of potassium perchlorate in molten asphalt and reached specific impulses between $1750\,\mathrm{N\,s\,kg^{-1}}$ and $2150\,\mathrm{N\,s\,kg^{-1}}$ (GALCIT 53) but provided very poor elasticity and low achievable filler contents [5, 21]. The journey of modern

cross-linked binders started in 1946, when a new type of composite was formulated by mixing Thiokol LP-3 polysulfides with potassium perchlorate at the Jet Propulsion Laboratories. The polymer was cross-linked by oxidative coupling using curing agents like *p*-chinonedioxime or manganese dioxide to provide an elastic rubbery binder matrix with good elongation properties over a wide range of operation temperatures [22]. However, a major drawback of the polysulfide binders was the generation of sulfur dioxide during combustion, which causes the formation of combustion gases with a high average molar mass, thus decreasing the specific impulse (I_{sp}). Furthermore, the binder system was incompatible with metal fuels due to water formation during the cross-linking process, which limited the performance of such propellants significantly [5]. Other propellants developed during this period included formulations based on polyesters, polyurethanes, polyvinylchloride (plastisol propellants) or epoxy resins [23].

The need for binders that are suitable for high performance propellants ended up in the application of polyurethane systems based on butadienes in the 1950s (Figure 3.1). The first prepolymer of this category was PBAA, a liquid copolymer of butadiene and acrylic acid, which exhibited low viscosity and therefore high achievable solid loadings but suffered from poor mechanical properties and rapid aging [24]. These problems were overcome by PBAN, which is the terpolymer of butadiene, acrylonitrile and acrylic acid. Epoxides or aziridines were used as curing agents providing propellants with a high specific impulse and improved mechanical properties. Binders based on PBAN were

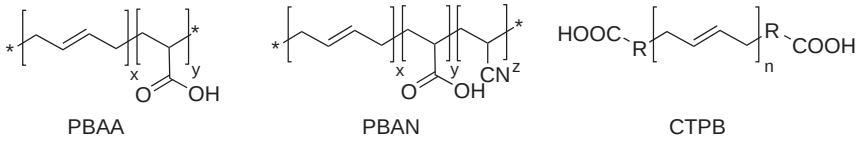

Figure 3.1 Molecular structures of different polybutadiene prepolymers containing carboxyl groups for curing.

therefore soon applied in many propellants, for example in the TP-H-1011 formulation for space transportation system solid rocket motors (STS SRMs) and the Space Shuttle booster [6, 23, 24]. Carboxyl terminated polybutadiene (CTPB) was developed by Thiokol in the late 1950s. While PBAA and PBAN have carboxylic functions that are statistically distributed, CTPB has the major advantage of a strictly telechelic structure, which increases the reproducibility of the propellant properties drastically. These binder systems are characterized by superior mechanical and ballistic properties compared to PBAA and PBAN. The tensile strength is almost two times higher compared to PBAA binders, which is beneficial especially for the manufacturing of complex grain geometries [5]. CTPB based propellants showed the highest performances at that time and replaced

many of the polyether-polyurethane systems that were developed simultaneously in the mid 1950s [6].

Todays almost exclusively utilized binder systems for composite propellants are based on hydroxyl-terminated polybutadiene (HTPB), which is commercialized under the trade mark R-45M by ARCO chemicals (Figure 3.2). HTPB is known to be the first prepolymer that was specifically designed for rocket propulsion systems [5, 6, 12]. It is synthesized by the free radical reaction of 1,3-butadiene using a peroxide initiator. Isocyanates are used as curing agents to form urethane linkages and HTPB can therefore

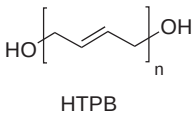

HTPB

Figure 3.2 Simplified molecular structure of hydroxyl-terminated polybutadiene (HTPB).

be considered as the link between the simultaneously developed polybutadiene and polyurethane families. The prepolymer showed advantages over CTPB considering performance (I_{sp}) and achievable filler content. Furthermore, it provides excellent strain performance at low temperatures and good aging properties. HTPB has therefore become the most widely used prepolymer in binders for composite propellants in military as well as in space applications, for example in the Ariane V booster rockets [25]. The later binder research focused on the development of energetic alternatives that are able to provide enhanced performance.

3.2 Energetic Polymers for Composite Propellant Binders

Concerning the improvement of modern propellant formulations, maximizing the specific impulse (I_{sp}) and optimization of the mechanical properties are key issues. The challenge to increase the energy of the binder material involves the replacement of the former discussed inert binders by energetic polymers. They contain explosophoric groups that are able to deliver additional energy to the combustion process. These functional groups involve amongst others:

- Nitro group: $-NO_2$
- Nitrate ester group: $-ONO_2$
- Azido group: $-N_3$

- Nitramine group: $-NNO_2$
- Tetrazoles

This overview is focusing on the most important developments in the field of energetic polymers, which are currently receiving the most attention. A full review on this topic would be far beyond the scope of this chapter. The section is divided according to the types of the energy delivering functional groups, which are covalently bond to the polymer backbone. Polymers based on nitrate esters and azido groups are still the most promising candidates for the application as prepolymers for energetic composite propellant binder systems and are therefore exclusively discussed.

3.2.1 Energetic Polymers Based on Nitrate Esters

Nitrato-polymers are a specific class of energetic polymers, characterized by nitrate ester groups ($-ONO_2$) that are attached to the polymer backbone. The most famous representative of this substance class is nitrocellulose (NC), also being one of the first known energetic materials and still widely applied in double base propellants as an energetic binder (Figure 3.3). NC was independently discovered by Schönbein and Böttger between 1845 and 1847 and improved by Sir Frederick Abel in his patent describing the preparation of nitrocellulose involving pulping steps, which increases the stability and provides suitable material for the manufacturing of propellants [3]. Nitrocellulose is synthesized by the nitration of cellulose, which is a linear polymer of β-1,4-linked D-glucopyranose units [26]. In general, NC is made from cotton, which is a natural product. Because of the unsteady characteristics of cotton depending on origin and seasonal variations, a constant quality of NC is hard to ensure and needs strict product quality control [12]. This is one major disadvantage of NC together with the autocatalytic decomposition of the nitrate ester groups which demands the use of external stabilizers.

In order to overcome the challenges of NC as a natural product, novel synthetic nitrato-spolymers were discovered over the years. Commonly known examples of this substance class are poly(vinyl nitrate) (PVN), poly(glycidyl nitrate) (PGN) and poly(3-nitratomethyl-3-methyloxetane), which is referred to as P(NIMMO) or poly(NIMMO)

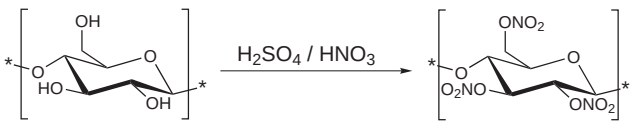

Figure 3.3 Synthesis of nitrocellulose (NC).

in the literature. One of the first hydroxyl-terminated energetic polymers used for composite propellant binders was poly(glycidyl nitrate) (PGN). It was published in 1950 by Thelan et al. from the Naval Warfare Center in the USA [12]. The monomer glycidyl nitrate (GN) was synthesized by a nitration of glycidol, using a nitration mixture consisting of acetic anhydride and nitric acid followed by a complicated purification process. This nitration process was later improved by the use of dinitrogen pentoxide N_2O_5 as nitration agent, facilitating a safer nitration process with high yields and high purity [27]. The polymerization of GN is performed via cationic ring-opening polymerization, using a lewis acid catalyst in the presence of a polyol initiator, usually ethylene glycol (EG) or 1,4-butanediol (BDO) (Figure 3.4). The PGN product can be isolated as a pale yellow viscous liquid with a T_g of −35 °C, which can be cured with isocyanate based curing agents [28, 29].

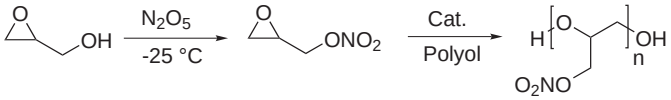

Figure 3.4 Synthesis of poly(glycidyl nitrate) (PGN). Nitration of glycidol with N_2O_5 is subsequently followed by cationic ring-opening polymerization [27].

A polymer-analogous modification providing nitrated HTPB (NHTPB) was achieved by a combination of epoxidation and nitration of HTPB (Figure 3.5). The properties of the resulting polymer are strongly depending on the ratio of remaining double bonds and the incorporated nitrate ester groups [30]. The viscosity and glass transition temperature are increasing with the content of nitrate ester groups. It turned out that a nitration level of approximately 10 % is most suitable for the manufacturing of propellants, because the viscosity is still low enough to be processed with a high content of solid fillers. The T_g of the 10 % nitrated product is higher compared to the pure HTPB polymer but it provides miscibility with common energetic plasticizers, which can be considered as a clear advantage over HTPB [31].

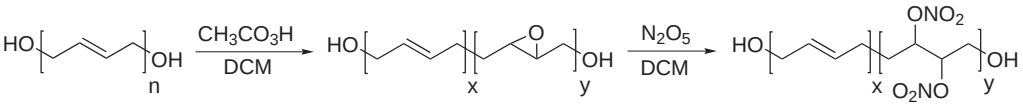

Figure 3.5 Synthesis of nitrated hydroxyl-terminated polybutadiene (NHTPB) [30].

Polyvinyl nitrate (PVN) is a solid, fibrous polymer that can be easily synthesized by the nitration of polyvinyl alcohol [32]. The properties of the material show a strong dependence on the nitration level. The major drawback of PVN as a replacement for nitrocellulose is the low softening temperature in the range of 40 °C to 65 °C [33] and a

poor long-term stability, which can be partially improved by adding suitable stabilizers to the formulation [32].

Manser et al. reported the synthesis of P(NIMMO) subsequently to the discovery of energetic polyoxetanes based on azides at Aerojet in 1984 [12]. The starting material, 3-nitratomethyl-3-methyl oxetane (NIMMO) can be synthesized following different routes. Like for the synthesis of PGN, the main challenge is a safe and economic procedure for the nitration reaction of the monomer synthesis. The starting material is synthesized by the cyclization of 2-methyl-2-hydroxymethyl propanediol using diethylcarbonate in the presence of KOH [34]. The following nitration of the cyclic ether can be performed via two different procedures. The proposed method of Manser using acetyl nitrate results in good yields and purity, but has the disadvantage of the hazardous nature of the nitration agent [34]. Golding et al. proposed a method using N_2O_5, which also provided high purity together with the improvement of a safer process. This variation was used for the commercial production of P(NIMMO) at DRA [35]. The NIMMO monomer can be polymerized via cationic ring-opening polymerization, using BF_3 and 1,4-butanediol to yield a pale yellow liquid polymer (Figure 3.6) [33, 36]. As for other cationic ring-opening polymerizations, the reaction should not be carried out in bulk to avoid the contamination with cyclic species that are caused by backbiting side reactions. By slow monomer feed over time, the content of low-molecular impurities can be significantly reduced [37].

The additional energy that is provided by the molecular structure of polymers based on nitrate esters is released due to the oxidation of the backbone chain, starting by the scission of $-O-NO_2$ bonds. This means that a nitrate ester based polymer contains both fuel and oxidizer in the same molecular structure [12]. In contrast to azido-polymers, nitrato-polymers offer the advantage of a better oxygen balance but usually suffer from

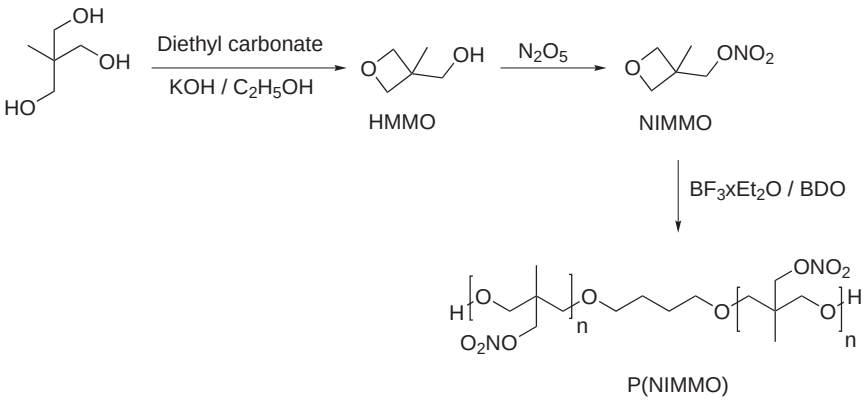

Figure 3.6 Synthesis of P(NIMMO) via a three-step process starting from 2-methyl-2-hydroxymethyl propanediol [35, 36].

low stability and very limited shelf-life due to autocatalytic decomposition processes of the nitrate ester groups over time.

3.2.2 Energetic Polymers Based on Azido Groups

Polymers with a high nitrogen content, typically exhibit a high positive enthalpy of formation. During the combustion process, additional energy is released due to the formation of molecular nitrogen [12]. Beside polymers based on triazoles and tetrazoles that are not covered by this review, the majority of this class consists of polymers based on azido-groups. The energetic potential of the azido group is attributed to the highly exothermic scission of the $-N_3$ bond (approximately 685 kJ/mol) [15]. The most prominent examples of azido-polymers are glycidyl azide polymer (GAP), poly(3-azidomethyl-3-methyl oxetane) (P(AMMO)) and poly(3,3-bis(azidomethyl) oxetane) (P(BAMO)) (Figure 3.7). GAP is currently the most readily available energetic polymer due to low production costs and superior binder properties compared to other literature reported polymers [38]. The compound is commercially available from 3M under the trademarks GAP-5527 Polyol and GAP-Diol from Eurenco Bofors.

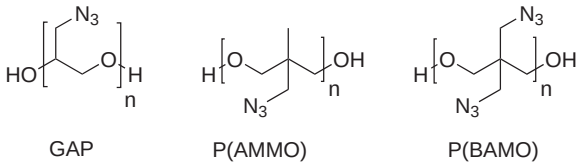

Figure 3.7 Common energetic polymers based on azido groups.

Energetic polyoxetanes were developed by the group of Manser in the early 1980s at Aerojet and represent one of the most interesting literature published energetic polymer classes [36, 39]. Such polymers are synthesized via cationic ring-opening polymerization of the respective oxetane monomer, using BF_3 as a catalyst. The most critical step of the production is typically the synthesis and purification of the monomer. P(BAMO) can be synthesized by using two different synthesis routes (Figure 3.8). Both routes start from the reactant 3,3-bis(chloromethyl) oxetane (BCMO) which can be prepared by ring-closure reaction of the trichloro derivative of pentaerythritol [40]. The first variation involves the azidation of BCMO by treatment with sodium azide in DMF, followed by the polymerization using BF_3-etherate in the presence of 1,4-butanediol as an initiator at $-5\,°C$. This procedure has a highly hazardous potential due to the sensitivity of the monomer 3,3-bis(azidomethyl) oxetane (BAMO), which has an impact sensitivity comparable to nitroglycerine. The alternative synthesis procedure involves a change in the sequence. To avoid the isolation of the sensitive BAMO monomer, the

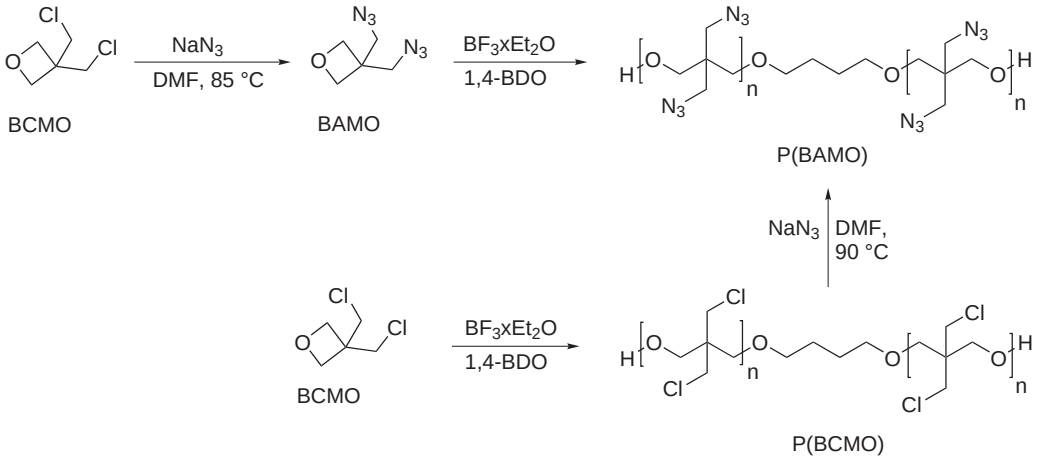

Figure 3.8 Synthesis of P(BAMO) by two different routes.

BCMO monomer is polymerized to yield P(BCMO) and azidated in a subsequent step using NaN_3 in DMSO at 115 °C [41]. The pure P(BAMO) homopolymer is solid at room temperature, which hampers the use as a binder for cast-cure processing. The melting point of the polymer is in a temperature range of 70 °C to 90 °C, depending on the crystallization conditions. The equilibrium melting temperature was found to be 129 °C [42]. In order to make this polymer suitable for cast-cure processing, copolymers with THF were synthesized to deliver a liquid energetic azido copolymer [42, 43].

The synthesis of P(AMMO) is very similar to the synthesis procedure of P(BAMO). It starts by the azidation of 3-hydroxymethyl-3-methyl oxetane (HMMO) forming the AMMO monomer, which is polymerized via cationic ring-opening polymerization using BF_3 and BDO (Figure 3.9). The published synthesis procedures differ in the azidation reactions of HMMO. The first variation involves the chlorination of HMMO by using a mixture consisting of triphenylphosphine and carbon tetrachloride, which acts as a solvent and the chlorine source. The product ClMMO is azidated in a subsequently following step, using sodium azide and DMF as the solvent [44]. Liu et al.

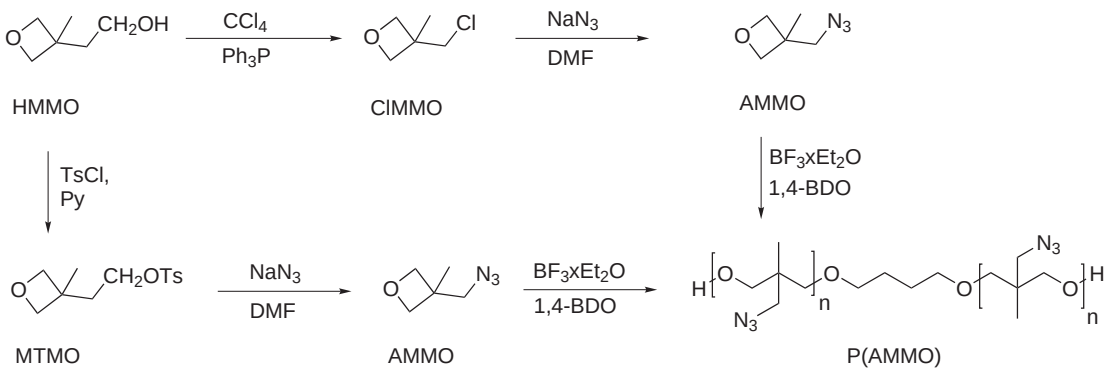

Figure 3.9 Synthesis of P(AMMO).

published a different synthesis route starting from HMMO, which is tosylated by using *p*-toluenesulfonyl chloride (TsCl) and pyridine (Py). A following nucleophilic substitution of the −OTS group using sodium azide delivers the AMMO monomer, which can be polymerized as described above [45]. A quasi-living cationic polymerization of AMMO was realized by using a bis(chlorodimethylsilyl)benzene / $AgSbF_6$ initiating system. The reaction was carried out in DCM at −78 °C. Because of the quasi-living conditions, it was possible to increase the number average molecular weight (M_n) linearly with increasing [M]/[I] ratio [46]. In contrast to P(BAMO), the P(AMMO) polymer is liquid at room temperature by exhibiting a glass transition temperature of approximately −41 °C.

3.3 GAP and Copolymers with Glycidyl Azide Units

3.3.1 Synthesis of GAP

The theoretical monomer of GAP is glycidyl azide (GA). It can be synthesized by a reaction of in-situ generated hydrazoic acid with epichlorohydrin (ECH) yielding 1-azido-3-chloro-2-propanol, which can be treated with a base forming the cylic product GA (Figure 3.10) [47]. Attempts to synthesize GAP from GA via cationic ring-opening polymerization failed. It turned out that the monomer GA suffers from a low reactivity and high sensitivity to mechanical stimuli. Therefore, another synthesis procedure starting from polyepichlorohydrin (PECH) was developed [18].

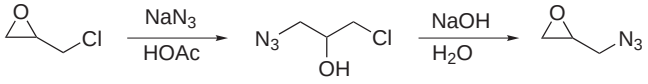

Figure 3.10 Synthesis of glycidyl azide (GA) [47].

The linear hydroxyl-terminated GAP prepolymers are usually synthesized in a simple procedure by two consecutive steps (Figure 3.11). The first one is the synthesis of polyepichlorohydrin (PECH) via cationic ring-opening polymerization of ECH in the presence of a diol (e.g. 1,4-butanediol or ethylene glycol) and a lewis acid (e.g. a BF_3-complex or $SnCl_4$). The second step, a nucleophilic substitution of the chlorine

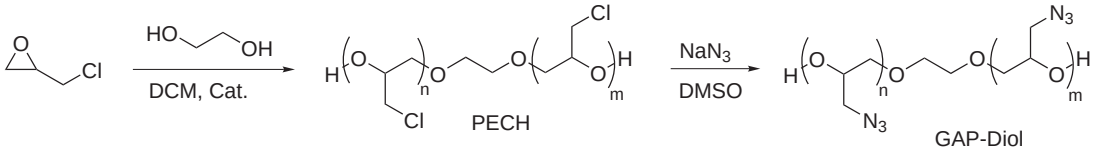

Figure 3.11 Synthesis of difunctional glycidyl azide polymer (GAP) [18].

groups, is carried out by using an excess of sodium azide (NaN_3) in a dipolar aprotic solvent (e.g. DMF or DMSO) [18, 48–52]. An aqueous procedure using a phase-transfer catalyst (methyl tricapryl ammonium chloride) has also been reported but multiple days were required for full conversion while the standard procedure using an aprotic solvent provided a much faster reaction time of approximately 12 h to 18 h [53, 54].

Trifunctional GAP can be synthesized by using glycerol instead of 1,4-butanediol as an initiator (Figure 3.12). Frankel et al. established the synthesis of GAP-triol at Rocketdyne in 1976 but it turned out that GAP with functionalities closer to two would enable improved mechanical properties of formulated propellants [18]. Therefore, research efforts shifted to the above discussed synthesis of strictly difunctional GAP-diol by using ethylene glycol or 1,4-butanediol. A major issue of the described azidation process is a significant deceleration of the reaction rate after 90 % conversion, which is supposed to be a consequence of the association of the metal cation (e.g. Na^+ or Li^+) of the azide salt with the solvent in which the salt has a limited solubility. To overcome this problem, Wagner developed a solvent-free molten salt method. By mixing PECH with low-melting quaternary ammonium azides like tetrabutylammonium azide instead of sodium azide and trace amounts of water, conversions over 90 % during three hours at approximately 100 °C could be achieved in small-scale experiments [55].

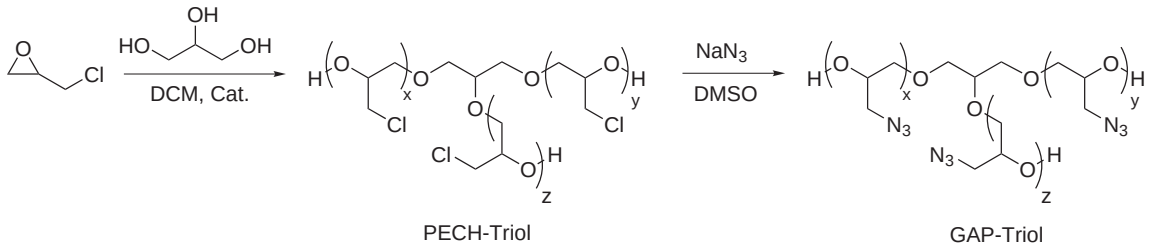

Figure 3.12 Synthesis of GAP-triol [18].

In order to avoid a time consuming and cost intensive multiple-step synthesis procedure, a one-pot process for the preparation of hydroxyl-terminated GAP has been described. In this process, a mixture of ethylene glycol, ECH and sodium azide in a dipolar aprotic solvent (e.g. DMF or DMSO) is heated up to an initial temperature of 70 °C where an exothermic reaction takes place by ring-opening of ECH. To complete the reaction, stirring is continued at 90 °C for approximately 30 min. This process delivers GAP with a low number average molecular weight (M_n) of around 500 g/mol [56]. Low molecular weight GAP ($M_n \approx 500$ g/mol) is not suitable as a prepolymer for binder networks but can be used instead as an azido-based plasticizer. However, the free hydroxyl end groups undergo an unwanted reaction with the isocyanates during the propellant curing process. This was improved by the synthesis of GAP-A [57].

Ampleman reported this azido-terminated version of GAP, which is synthesized by the tosylation of the hydroxyl end groups of GAP followed by a subsequent azidation (Figure 3.13). Another patent describes the synthesis of GAP-A by a nitration of the free hydroxyl groups of PECH followed by the azidation [58].

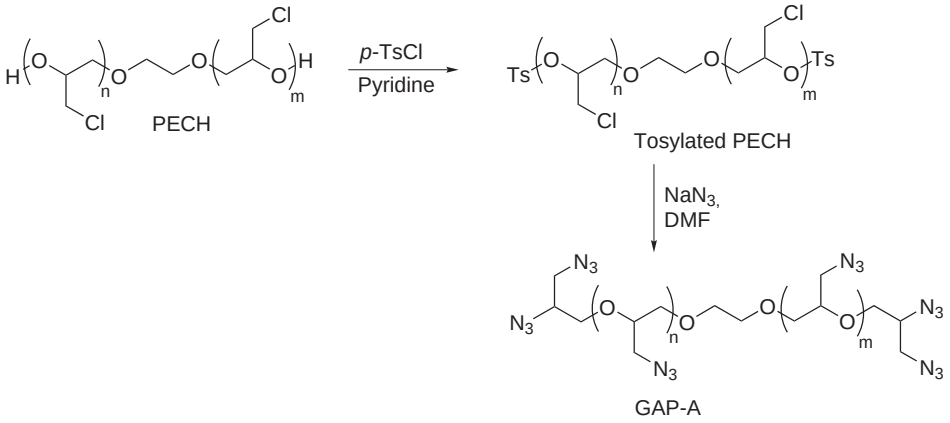

Figure 3.13 The synthesis of GAP-A. An azido-plasticizer based on low molecular weight GAP [57].

Ahad et al. reported the synthesis of a branched GAP by simultaneous degradation and azidation in a one-step process. The procedure involves high molecular weight PECH, which is treated with the epichlorohydrin monomer in the presence of alkali metal azides at higher temperatures (70 °C to 100 °C). By changing the ratio between PECH rubber and ECH monomer, the molecular weight of the resulting branched GAP can be adjusted [59]. The following patents report an improved synthesis making use of basic cleaving agents like sodium ethoxide or lithium methanolate avoiding the use of epoxide monomers. The molecular weight of the resulting material is controlled by the type and amount of the utilized cleaving agent [60–62].

A patent from Ampleman describes the synthesis of GAP with functionalities higher than two. Polyepichlorohydrin is regiospecific epoxidized at the hydroxyl end groups by using sodium hydride or potassium hydroxide. The epoxides can be readily opened by water (doubling the functionality), tris-1,1,1-hydroxymethyl ethane (tripling the functionality) or pentaerythritol (quadrupling the functionality). The following azidation is performed in the conventional manner by using sodium azide in DMF at 100 °C (Figure 3.14) [63].

Though GAP is already investigated for over 40 years, there are still publications in the recent literature discussing the optimization of the synthesis procedure and the characterization of the polymer. This indicates the continuing interest in the compound as an prepolymer for energetic binders, which can be applied in solid propellants and explosives [64–69].

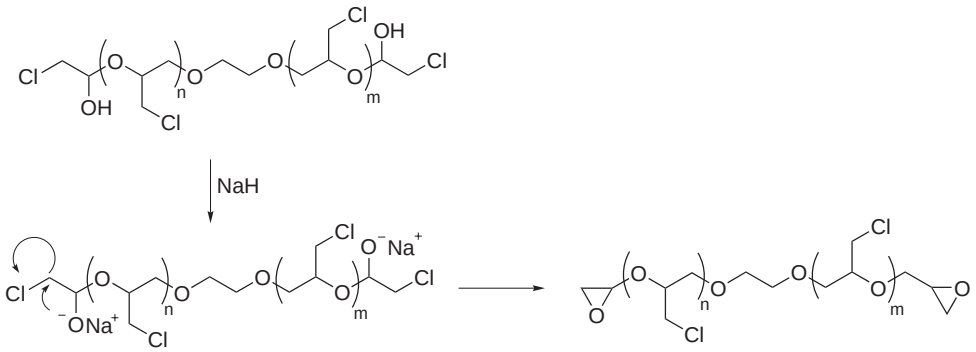

Figure 3.14 Preparation of PECH with various functionalities. The epoxides can be readily opened by different polyols [63].

3.3.2 Copolymers of GAP: Current Status

The literature related to copolymers of GAP is strongly driven by the intention to improve the mechanical properties of GAP and the respective binder materials that can be made based on these energetic prepolymers. Because of the commercial availability of GAP, block copolymers received more attention especially in the earlier literature while the synthesis of novel random copolymers is still limited to only a few published copolymer systems.

Block and Graft Copolymers of GAP

Triblock copolymers of PEG and PECH were synthesized by using PEGs with different molecular weights as diol compounds in the cationic ring-opening polymerization of epichlorohydrin, followed by azidation with sodium azide leading to GAP-*b*-PEG-*b*-GAP copolymers (Figure 3.15). These copolymers showed low glass transition temperatures down to −72 °C and decomposition properties similar to GAP [70].

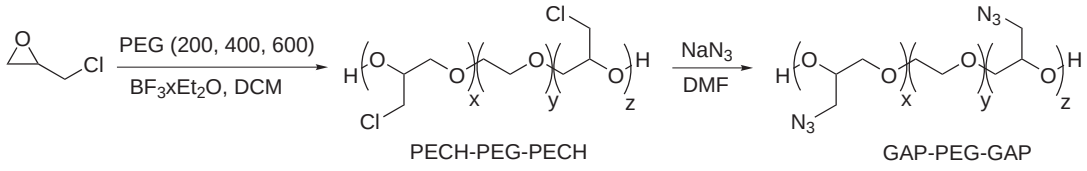

Figure 3.15 Synthesis of GAP-PEG-GAP block copolymers [70].

Subramanian et al. reported the synthesis of GAP-*b*-HTPB triblock copolymers by the azidation of PECH-*b*-HTPB using sodium azide in a dimethyl acetamide-toluene mixture at 95 °C. The halogenated precursor was synthesized by using HTPB as a macroinitiator for the cationic ring-opening polymerization of epichlorohydrin [71]. Another publication

reports the synthesis of GAP-HTPB blockcopolymer by a conventional procedure using a DMF/NaN_3 mixture [72].

GAP based block copolymers containing poly(styrene) (PS) or poly(vinyl acetate) (PVAc) segments were reported by Eroglu [73]. The published synthesis route involves the synthesis of macro-azo-inititiators by a reaction of 4,4'-azobis(4-cyanopentanoyl chloride) (ACPC) with GAP. A following block copolymerization with styrene and vinyl acetate monomers delivers PS-*b*-GAP and PVAc-*b*-GAP polymers, respectively (Figure 3.16).

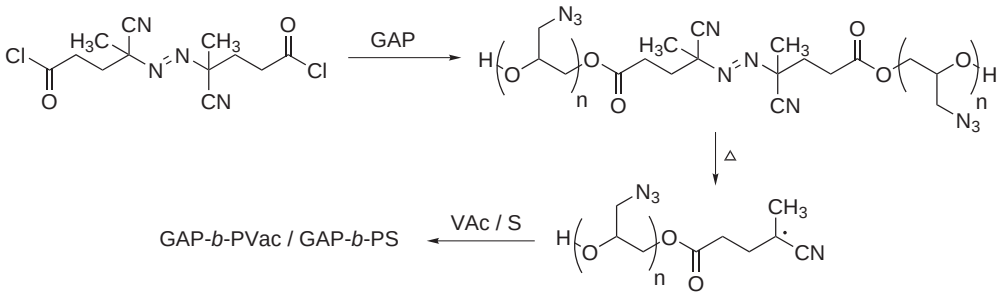

Figure 3.16 Synthesis of GAP-*b*-PVAc and GAP-*b*-PS block copolymers [73].

Eroglu et al. reported the graft copolymers HTPB-*g*-GAP [74]. A GAP macroinitiator was obtained by the reaction of GAP with ACPC in the presence of triethyl amine (TEA) as discussed for the PS/PVAc-GAP copolymers. GAP was grafted on HTPB by using a reaction of the former synthesized macro-azo-iniatiator with HTPB. The product was isolated by fractional precipitation. A DSC analysis revealed that the two segments are immiscible by showing two distinct glass transition temperatures. Murali et al. also reported the synthesis of graft copolymers of HTPB and GAP by applying a two-step procedure. In the first step, the macroinitiator was synthesized by a condensation of GAP-diol and 4,4'-azobis(4-cyanopentanoic acid) (ACPA) in the presence of *N*-methyl-2-chloropyridinium iodide (MCPI). This macroinitiator was used for the crosslinking or graft reaction with HTPB in the second step. Thermal analysis confirmed the results of Eroglu et al. by showing two distinct T_g at $-74.03\,°C$ and $-35.84\,°C$, indicating the incompatibility of the two chain segments [75].

Block copolymers of GAP and PMMA (PMMA-*b*-GAP) were synthesized by a redox polymerization utilizing a ceric ammonium nitrate/HNO_3 initiator system. It turned out that the method provided the possibility to incorporate GAP segments in amounts up to 45 mol % [76]. Another published procedure from Al-Kaabi reports the synthesis of

GAP with pendant *N*,*N*-diethyl dithiocarbamate groups (GAP-DDC) that was utilized as a macro-photoinitiator for the graft polymerization of methyl methacrylate (MMA). The reaction using UV radiation at 300 nm successfully yielded GAP-*g*-PMMA graft copolymers and showed a single glass transition temperature at approximately 75 °C, indicating the compatibility of the two different chain segments [77].

Zhang et al. recently reported a synthesis of GAP-*b*-PAEMA block copolymers. The reaction of PECH with 2-bromoisobutyryl bromide delivers a macroinitiator that was used to initiate the atom transfer radical polymerization (ATRP) of chloromethyl methacrylate (CEMA). After a subsequent azidation procedure of the PECH-*b*-CEMA precursor by using a DMF/NaN_3 mixture, the product GAP-*b*-PAEMA could be isolated with a yield of 92 %. Thermal analysis revealed two distinct glass transition temperatures at −18 °C and 36 °C [78].

A lot of research effort has been carried out, aiming at the block-copolymerization of energetic hard chain segments combined with energetic soft chain segments, to built energetic thermoplastic elastomers (ETPEs). This includes the combination of crystalline block segments of the former discussed P(BAMO) with soft chain segments consisting of GAP leading to GAP-BAMO copolymers [79]. In general, ETPEs are prepared either by linking the blocks of the different chain segments with isocyanates or sequential copolymerization [12]. They provide the remarkable property to be melt-castable, thus allowing extrusion processing techniques and environmental friendly recyclability of binders. Energetic thermoplastic elastomers are a seperate topic in the field of energetic binder research. For further information, there are excellent reviews on that topic available in the literature [12, 80].

Random Copolymers of GAP

Only few publications in the literature to-date report on random copolymers of GAP. They are basically focusing on GAP-THF and GAP-BAMO copolymer systems. In comparison to GAP, P(BAMO) has the major advantage of having a significantly higher nitrogen content as discussed in the general section about energetic polymers. Unfortunately, the crystalline nature of this polymer prevents the direct application as a binder prepolymer for composite propellants. Kawamoto et al. published the synthesis of a random copolymer consisting of BAMO and GAP segments to ensure an amorphous character of the polymer, while still providing a higher nitrogen content compared to the GAP homopolymer [81]. This offers the possibility to achieve higher performances of propellant formulations containing an energetic binder based on this particular copolymer [81–83]. The copolymer is synthesized via cationic ring-opening

copolymerization using 1,4-butanediol as an initiator and BF_3xEt_2O as a catalyst (Figure 3.17). A successful scale-up of the GAP-BAMO copolymer on kg scale was reported bei Keicher et al. providing a synthesis procedure to produce sufficient amount of material for first propellant evaluations [84, 85]. Curing studies with the material delivered very promising elastomeric rubbers with good mechanical properties. These results implicated that the material has a high potential to be used as a binder in future propellant formulations [83]. Pei et al. recently published DSC investigations about the compatibility of the GAP-BAMO copolymer with oxidizers (RDX, HMX and CL-20), energetic plasticizers (TMETN, BuNENA, NG) and metal fuels (Al, B). The measurements confirmed good compatibilities concerning these materials [86].

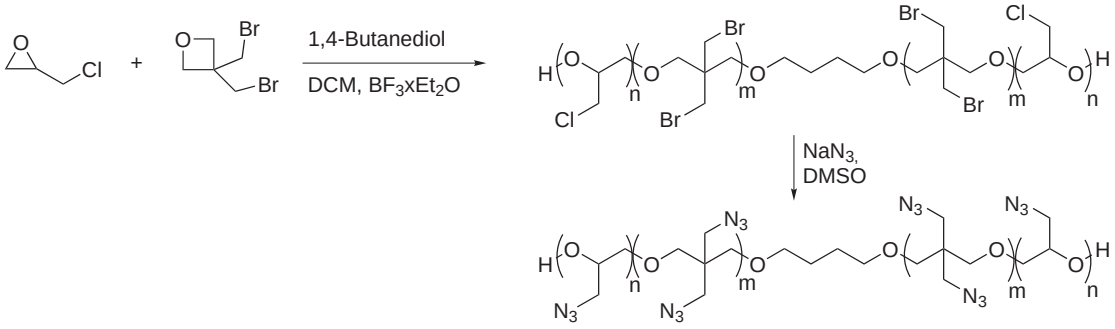

Figure 3.17 Synthesis of random copolymer GAP-BAMO [81].

A publication from Mohan et al. describes the synthesis of a random GAP-THF copolymer in order to improve the low-temperature properties of GAP [87]. The copolymer is synthesized via a two-step process, involving the cationic ring-opening polymerization of a ECH/THF monomer mixture using BF_3 as a catalyst, followed by a subsequent azidation using sodium azide in DMF or DMSO (Figure 3.18). The GAP-THF copolymers turned out to have interesting properties as precursors for energetic binder systems including a low glass transition temperature down to −64 °C [87]. Another slightly modified procedure by Lee et al. was recently patented, using a 1,4-butanediol/BF_3xTHF initiator system instead of EG/BF_3xEt_2O. The patent claims

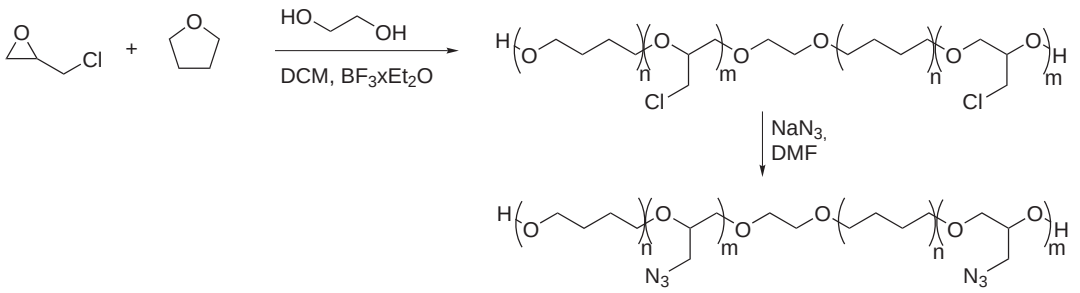

Figure 3.18 Two-step synthesis procedure of a random GAP-THF copolymer [87].

a synthesis providing high functionalities, a wide range of copolymer compositions and low fractions of cylic oligomers [88].

Dong et al. published a synthesis of poly(glycidyl azide-*r*-3-azidotetrahydrofuran) as a novel candidate for energetic binder systems (Figure 3.19) [89]. The material showed a promising glass transition temperature of −60 °C and high decomposition energy (1798 J/g measured by DSC) but demands a multiple-step synthesis procedure.

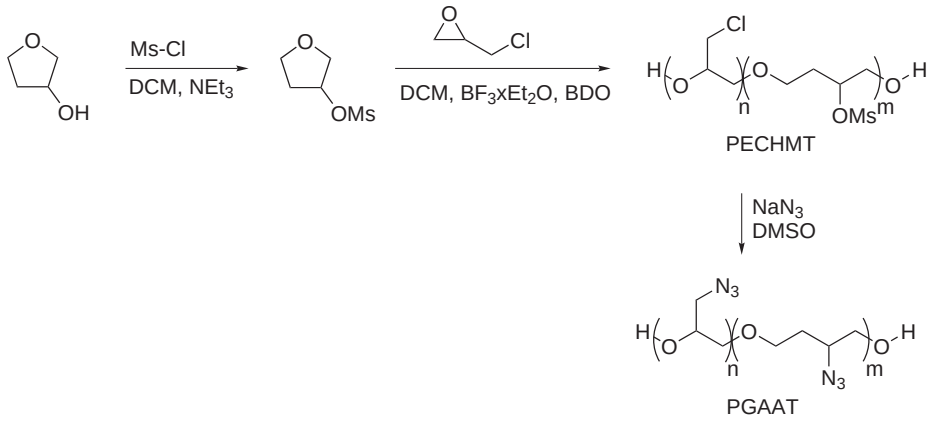

Figure 3.19 Synthesis of PGAAT as a novel azido-copolymer [89].

3.4 Plasticizers for Solid Propellants

In order to optimize the processability of a propellant mixture as well as the thermo-mechanical properties of the cured solid propellant, almost every formulation contains plasticizers [6]. According to Immergut, a plasticizer is usually defined in terms of the desired properties of a given polymer-plasticizer system [90]. In case of solid rocket propellants, this means an additive that is responsible for changing the properties of the material by reducing stiffness and providing better flexibility of the cured binder systems. Furthermore, a lower viscosity of the uncured propellant mixture allows a better mixing process before the formulation is casted into the motor mold. Due to the influence of plasticizer molecules, which reduce the intra- and intermolecular forces between the polymer backbone chains, E-modulus and tensile strength are decreased. A major purpose is always to improve the material properties in order to absorb the mechanical stress that occurs during launching or during storage and transport because of thermal strain.

Another important characteristic that is improved by adding plasticizers, is the low-temperature behavior of the binder matrix. When a solid propellant is cooled down below the specific glass transition temperature (T_g), the binder will lack of elasticity and

become brittle. This causes severe safety issues, because a brittle binder matrix looses its capability of absorbing mechanical stress. The formation of cracks in the propellant can be a consequence and therefore an uncontrolled accelerated combustion reaction after launching the missile, which may lead to an explosion of the rocket motor. Hence, the minimum requested service temperatures are very low. Usually a propellant T_g of at least $-54\,°C$ for military applications in tactical air-to-air missiles is specified in the literature [91–93]. Depending on the binder system, plasticizers are thus often needed in propellant formulations to lower the T_g in order to achieve the required low-temperature properties.

3.4.1 Common Energetic and Non-energetic Plasticizers

Similar to the polymeric binders, plasticizers can be distinguished between energetic and non-energetic. Typical non-energetic plasticizers that are used for the manufacturing of solid propellants are long-chain alkyl esters of mono-, di-, and tri-basic carboxylic acids. Common examples are di-(2-ethylhexyl) adipate (DEHA) often also referred to as dioctyl adipate (DOA), dioctyl sebacate (DOS) and triacetin (TA) amongst others (Figure 3.20) [6, 7, 94]. Because they do not deliver additional energy to the combustion process, their main functionality is to improve the mechanical properties at ambient and low temperatures together with the reduction of the viscosity of the formulation during the mixing process. The predominant disadvantage of non-energetic plasticizers is obviously the performance reduction of the propellant formulation, usually along with a negative influence on the oxygen balance.

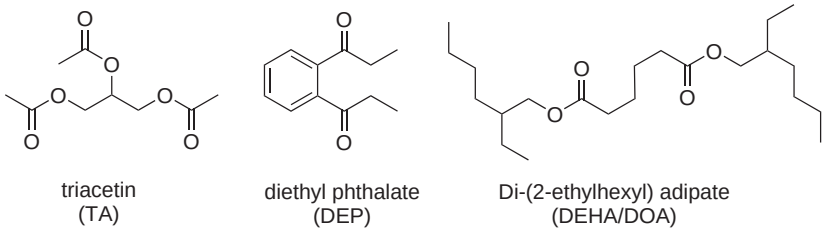

Figure 3.20 Examples of common non-energetic plasticizers.

To overcome these issues, energetic plasticizers were developed. Additionally to the discussed improvements, energetic plasticizers are supposed to give a contribution to the oxygen balance and to the overall energy of the formulation [38]. Since the development of the first known energetic plasticizer nitroglycerine (NG) in 1846 [3], several energetic plasticizers based on different explosophoric groups have been discovered. As nitroglycerine, some of the most widely used energetic plasticizers are based on nitrate esters for instance ethyleneglycol dinitrate (EGDN), butanetriol trinitrate (BTTN) or

trimethylolethane trinitrate (TMETN) (Figure 3.21). Most of the nitrate ester based plasticizers are explosives with high sensitivities to mechanical stimuli and exhibit low critical diameters along with a high volatility. They also show significant physiological effects, which make these substances difficult to handle. NG for example is known for causing dilation of arteries and severe headache [95]. Nevertheless, nitrate esters are still widely used energetic plasticizers in solid propellant formulations, especially in double and triple base propellants [7].

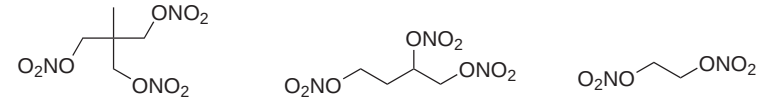

trimethylol ethane trinitrate (TMETN) | butanetriol trinitrate (BTTN) | ethylene glycol dinitrate (EGDN)

Figure 3.21 Examples of energetic plasticizers based on nitrate esters.

The most prominent example for nitro-based plasticizers is the BDNPA/F eutectic mixture (Figure 3.22). It usually consists of a 50:50 (w/w) ratio of bis(2,2-dinitropropyl) acetal and bis(2,2-dinitropropyl) formal and found applications in several LOVA gun propellants as well as in insensitive HMX-based explosives [38].

bis(2,2-dinitropropyl)acetal (BDNPA) | bis(2,2-dinitropropyl)formal (BDNPF)

Figure 3.22 BDNPA/F plasticizers, typically used as 50:50 (w/w) mixtures.

While GAP is mainly applied as a prepolymer for energetic binders, Ampleman developed a low-molecular GAP-A plasticizer with a number average molecular weight of 700 g/mol to 900 g/mol [57]. It provides a T_g of −56 °C together with a low volatility and good miscibility with azido-polyethers due to the structural similarity. A relatively new class of azido-plasticizers with very low glass transition temperatures ranging down to −71 °C and good thermal stabilities were synthesized by Drees et al. at Fraunhofer ICT namely ethylene glycol bis(azidoacetate) (EGBAA), diethyleneglycol bis(azidoacetate) (DEGBAA), trimethylol nitromethane tris(azidoacetate) (TMNTA) and pentaerythritol tetrakis(azidoacetate) (PETKAA) [96].

Nitramine plasticizers likewise found applications in modern solid propellants, for example the nitratoethyl nitramines (NENA derivatives). They are synthesized by a nitration of the respective commercially available alkyl ethanolamine (Figure 3.23) [38]. NENAs provide a high enthalpy of formation [12] but generally suffer from the problems

of autocatalytic decomposition and plasticizer migration causing poor long-term stability and reduced shelf-life [38].

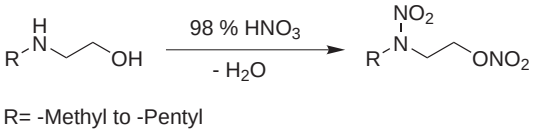

Figure 3.23 Synthesis of NENA derivatives by nitration of ethanolamines [38].

3.4.2 Migration Effects

In additive-polymer systems, migration is defined as the diffusion of an additive from the polymer matrix to another contacting material. This process involves several steps [97]:

- Diffusion of plasticizer from material bulk towards the surface
- Interface phenomena
- Sorption into the surrounding medium

The migration of plasticizers is a commonly observed problem for solid propellants (composites as well as double base) and has an important impact on aging mechanisms [98–104]. Migration processes can not only occur for plasticizers but also for other additives like burning rate catalysts [105], stabilizers or curing agents, before the propellant is fully cured [103].

The depletion of plasticizer due to diffusion phenomena of mobile species has serious influences on the rocket motor properties. It changes the chemical and thermo-mechanical properties of the propellant. Furthermore, the bonding between propellant and insulation is affected and combustion characteristics are strongly influenced which has severe impact on the rocket motor ballistics [100, 101, 103]. Several approaches are discussed in order to reduce plasticizer migration in solid propellants [38, 97, 103]:

- Insulation material equilibrated to the plasticizer concentration in the grain
- Barrier coatings
- Development of insulation materials resistant to migration
- Use of plasticizers with low migration tendency

The diffusion rate of plasticizers migrating into the insulation as well as the deposition and accumulation on the material surface depends on a number of parameters that are summarized in the literature [97, 103, 106, 107]. The molecular weight of the plasticizer molecule is known to have a huge influence [108]. Plasticizers with a number average molecular weight (M_n) within the range of 400 g/mol to 1000 g/mol are considered to provide optimum plasticizing effects. Plasticizers with a molecular weight below 200 g/mol may be more effective in reducing the glass transition temperature but are highly mobile and volatile species with a strong tendency to migrate out of the formulation [38]. Further crucial factors are:

- Concentrations in bulk, surface, insulation
- Temperature
- Solubility and compatibility of respective plasticizer and polymer matrix depending on the chemical structure of the plasticizer molecule
- Volatility of the plasticizer: Rate of migration can be controlled by the ease of loss from the surface (surface controlled) or by the rate of diffusion to the surface (diffusion control)

Plasticizer migration is not only a problem in case of solid propellants but also for many other important areas like medical applications or packaging of food [97].

3.4.3 Internal Plasticization

Beside the classification in energetic and non-energetic, plasticizers can also be divided in different terms into two main groups: internal and external plasticizers. In contrast to the already discussed external plasticizers, internal plasticizers are a part of the polymer itself by being incorporated comonomers that are directly bond to the polymer backbone structure. Suitable comonomers make the copolymer less ordered and therefore reduce the intermolecular forces between the polymer chains leading to the desired plasticizing effects. This principle is transferred for example to styrene-butadiene or butadiene-acrylonitrile copolymers. Usually the monomer whose polymer shows the better low-temperature properties is designated as internal plasticizer [90]. The same strategy is reported for energetic polymers like the former discussed GAP-*co*-BAMO and GAP-*co*-THF copolymers.

Another variation of internal plasticization that is described in the literature, is the introduction of *n*-alkyl side chains to polyacrylates [109]. Due to the influence of the unpolar substituents, intra- and intermolecular forces between the polymer backbone

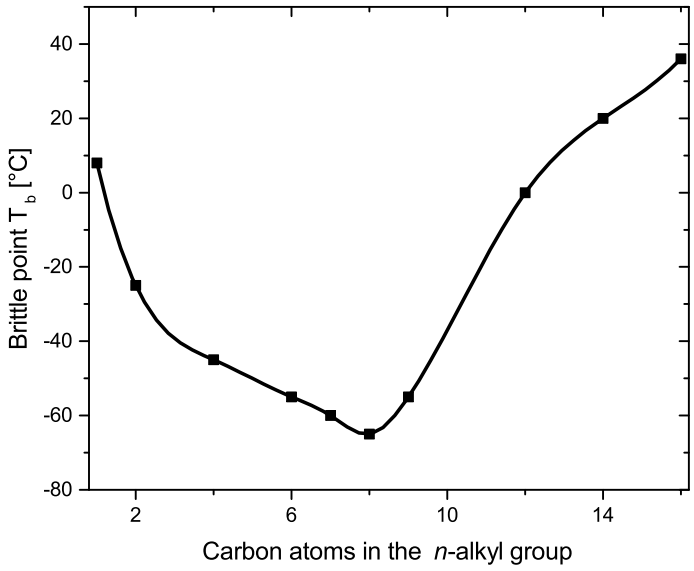

Figure 3.24 Brittle points (T_b) of selected polymeric n-alkyl acrylates [110].

chains are lowered. Figure 3.24 shows the brittle point temperatures T_b of polymeric n-alkyl acrylates. The curve exhibits a minimum at $-65\,°C$ for a C8 substituent, while T_b increases for longer chains because of side chain crystallinity, which occurs when the substituents become too long. Rehberg et al. also investigated brittle points of branched-chain alkyl acrylate ester polymers [20]. It turned out that the brittle points increased with the complexity of the branching. For example, while the polyacrylate with a n-butyl substituent showed a brittle point of $-45\,°C$, the polyacrylate with isobutyl substituent showed a 21 K higher T_b of $-24\,°C$. Therefore, for n-alkyl substituted polyacrylates it can be concluded that:

- n-Alkyl side chains provide a plasticizing effect to the polymer by decreasing the intra- and intermolecular forces between the polymer backbone chains.
- When the side chains become too long, phase separation and side-chain crystallinity can cause an antiplasticizing effect.
- Bulky side chains hinder the mobility and the free rotation of the C-C bonds in the backbone chain, leading to higher brittle points T_b compared to the corresponding n-alkyl chain substituents.

Introducing side chains as internal plasticizers was described in the literature also for other copolymer systems. For example, 3-hexyl-1-vinyl-2-pyrrolidone (HNVP) was used

as a n-hexyl substituted comonomer for the copolymerization with 1-vinyl-2-pyrrolidone (NVP). It turned out that the alkyl substitution in 3-position on the pyrrolidone ring does not affect the radical reactivity of the monomer but leads to a lower glass transition temperature [111]. Sasthav et al. reported the improvement of polyimide processability by internal plasticization [112]. The studies showed that n-alkyl side chains were very effective in lowering the T_g up to a chain length of eight carbon atoms. Any further increase of the alkyl chain length did not improve the T_g but caused semicrystalline polymers.

The use of energetic reactive plasticizers was recently reported for GAP, which is another possibility for the irreversible incorporation of plasticizer molecules into the polymer chains [113, 114]. Reactive plasticizers can be considered as a sub-category of internal plasticizers. A low-molecular weight compound is added to the prepolymer and reacts irreversible, getting covalently bond to the polymer chains. In the work reported by Ma et al., activated alkyne functionalised energetic plasticizers were added to the PU curing mixture (Figure 3.25). During pot-life, the alkyne groups reacted as expected with the azido moieties of GAP by Huisgen azide-alkyne 1,3-dipolar cycloaddition. The cured binder showed a higher tensile strength compared to the pure GAP binder.

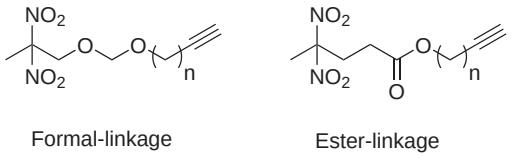

Figure 3.25 Energetic reactive plasticizers for GAP [113].

This was explained by the increased steric requirement of the formed triazole rings, preventing free torsion of the polymer backbone. The binary GAP/plasticizer mixtures showed reduced T_g but no glass transition temperatures of the final cured binder were presented. The use of reactive or internal plasticizers has the major advantage of avoiding problems with the above discussed plasticizer migration and is therefore an interesting approach for the development of future binders for composite propellants.

4 Characterization Methods

4.1 Instrumental Analysis

4.1.1 NMR Spectroscopy

The ^{1}H and ^{13}C NMR spectra were recorded using a Bruker Avance 400. All compounds were measured in $CDCl_3$ if not stated differently in the respective experimental section. All chemical shifts are stated in ppm relative to TMS as an external standard. The presented molecular compositions were calculated by comparing the integrals of the *n*-alkyl side chain protons with the integrals of the polymer backbones and chloromethyl units (azidomethyl units respectively).

4.1.2 Infrared Spectroscopy

Infrared (IR) spectra were recorded of the pure substance, using a Thermo Scientific Nicolet 6700 FT-IR-Spectrometer equipped with Durascope diamond ATR accessory in the range of 700 cm^{-1} to 4000 cm^{-1}. Signals are reported in wave numbers (cm^{-1}). The respective intensities are reported in parentheses, distinguishing between weak (w), medium (m) and strong (s).

4.1.3 Elemental Analysis

Elemental analyses were performed with a vario EL cube (Elementar Analysensysteme GmbH) using sample sizes between 1 mg and 2 mg. Each sample was measured three times and the arithmetic mean value for the carbon, hydrogen and nitrogen content is reported in wt. %.

4.1.4 Gel Permeation Chromatography (GPC)

Molecular weight distributions were measured by using a GPC Agilent Series 1100 system equipped with a RID detector and a set of four PSS SDV columns (50/100/1000/105 Å). THF was used as a solvent with a flow rate of 1.0 ml/min. Polystyrene standards with

molecular weights ranging from 162 g/mol to 246 000 g/mol were used for calibration. This setup showed good separation even at low molecular masses. The analysis was performed using the PSS WinGPCUniChrom software.

4.1.5 Density Measurements

Density measurements were performed by helium pycnometry using a Pycnomatic ATC (Porotec) following the procedure described in DIN 66137-2 [115] at 20 °C. Each sample was measured four times and the arithmetic mean value is reported.

4.2 Chemical Analysis

4.2.1 Determination of Hydroxyl Values and Equivalent Weight

Hydroxyl values were determined by titration following the routine described in DIN 53240-2 [116]. The hydroxyl value (OHV) is defined as the amount of potassium hydroxide (KOH) that is equivalent to the amount of acetic acid that is consumed during the acetylation of 1 g substance and is given in mg/g.

The weighed sample was acetylated using 30 ml of a catalyst solution consisting of 1 wt. % DMAP in NMP together with 10 ml of an acetylation solution consisting of 10 wt. % acetic anhydride in NMP. The reaction mixture was kept at RT for at least 15 minutes. Polyols containing secondary hydroxyl groups need a reaction time of at least 60 min according to DIN 53240-2 [116]. After quenching with 3 ml demineralised water and additional stirring for 12 min, the excess reagent was titrated with a potassium hydroxide solution. A blank value was always determined by the same procedure. The hydroxyl value (OHV) was calculated by the following equation:

$$\mathrm{OHV} = \frac{(b-a) * c * 56.1}{E} \tag{4.1}$$

Where a is the consumption of KOH solution (ml) during the titration of the sample, b is the consumption of KOH solution (ml) in the blank experiment, c is the concentration of the standardized KOH solution (mol/l) and E is the sample weight (g).

The equivalent weight indicates how many grams of substance contain 1 mole of hydroxyl groups. The hydroxyl value (OHV) kann be conveniently converted into the equivalent weight (EW, Eq. weight):

$$\mathrm{EW} = \frac{56\,100\,\mathrm{mg/mol}}{\mathrm{OHV}} \tag{4.2}$$

4.2.2 Karl Fischer Titration

Water contents of the chemicals and reagents were determined prior to the polymerization experiments by Karl Fischer (KF) titration using a KF-Titrino 795 from Metrohm with Vesuv software. Extra dry methanol from Roth Chemicals (specific grade for KF titration) was used as a suspension medium and Hydranal Composite 2 from Fluka was used as titration medium. The measurements were performed with a burette volume of 5 ml. All analysis results are stated in ppm.

4.3 Thermal Analysis

4.3.1 Differential Scanning Calorimetry (DSC)

All DSC measurements were performed using a TA Instruments Q 2000 calorimeter. The device was calibrated by indium, tin, zinc and lead standards with a heating rate of 5 K/min. Samples were weighed in aluminum pans with pierced lids (sample mass: max. 1 mg) and measured in the temperature range between −90 °C and 350 °C under a nitrogen flow of 50 ml/min with a heating rate of 5 K/min. The DSC decomposition temperatures (T_{Dec}) are reported as onset values, melting points (T_m) as peak values of the respective DSC curves. The glass transition temperatures (T_g) were determined by cooling down the sample to −90 °C followed by a heating curve with 10 K/min up to room temperature, results were taken at the second cycle. The T_g values were determined according to STANAG 4515 [117].

4.3.2 Thermogravimetric Analysis (TGA)

TGA measurements were performed using a TA Instruments Q 5000 analyzer. Samples were measured in platinum pans (sample mass: 1 mg to 2 mg) at a heat rate of 5 K/min. The applied temperature range was between 20 °C and 700 °C, which was sufficient for total decomposition of the investigated samples. To eliminate the influence of residual moisture, the samples were dried *in vacuo* under elevated temperatures prior to the experiments. The reported TGA decomposition points are determined by the inflection points (I) of the mass loss curve.

4.3.3 Bomb Calorimetry

Heats of combustion were measured with an IKA C 2000 bomb calorimeter following the procedure described in DIN 51900-2 [118]. Benzoic acid IKA C 723 was used as a

calibration standard, providing a certified heat of combustion of 26 461 J/g RSD 0.03 %. The calibration was performed in oxygen atmosphere at a pressure of 30 bar (3 MPa). All measurements of the liquid polymers were performed in glass crucibles. The reported values for the heats of combustion are the arithmetic mean of three measurements.

4.4 Rheological Measurements and Mechanical Properties

4.4.1 Viscosity Measurements

The viscosity measurements of copolymer samples were performed with a MCR 501 rheometer from Anton Paar. The viscosities of liquid polymer samples were measured in dependence of the shear rate ranging from $1\,s^{-1}$ to $1000\,s^{-1}$ at 20 °C, 40 °C and 60 °C. All samples showed an approximately constant viscosity over the whole range of applied shear rates, thus showing Newtonian characteristics. All presented viscosity values were measured at a shear rate of $10\,s^{-1}$. The process viscosities during propellant formulation experiments were measured with a Brookfield DV-III Ultra rheometer.

4.4.2 Shore A Hardness

Shore A hardness of cured propellant samples were measured with a Bareiss HPEII durometer. Each sample was measured 5 times at different regions. The result is presented as the arithmetic mean of the five measurements. The used durometer is shown in Figure 4.1. Shore A hardness was always measured on tensile test specimen after the finished tensile test.

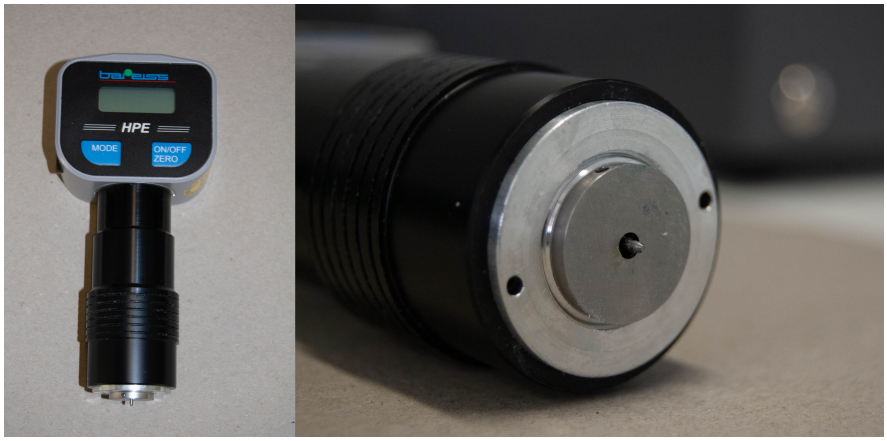

Figure 4.1 Bareiss HPEII durometer used for the Shore A hardness measurements.

4.4.3 Tensile Testing

Mechanical properties of the prepared propellants were characterized using a ZWICK UPM 1476 tensile test machine (Figure 4.2). Tensile test specimen were investigated in uniaxial tensile tests at 20 °C and −40 °C under atmospheric pressure. The samples were kept at the respective temperature at least for 10 min to ensure thermal equilibration, which is especially critical for the low-temperature measurements. The exact dimensions of the used casting molds for curing are presented in Figure 4.3. Stress, strain and E-modulus were determined applying a pre-load of 0.25 N and a crosshead speed of

Figure 4.2 Zwick UPM 1476 tensile test machine at Fraunhofer ICT. Setup in a thermo-chamber, which can be operated in a temperature range between −40 °C and 60 °C.

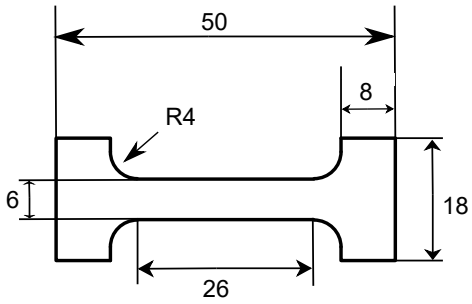

Figure 4.3 Dimensions of the casting molds for cast-cure preparation of tensile test specimen in mm.

50 mm/min. The actual dimensions of the specimen were manually measured for each sample prior to the measurements. Each measurement was repeated using three different samples, average values are presented.

4.5 Sensitivity Measurements

4.5.1 Sensitivity Towards Impact

Sensitivity towards impact was measured with a BAM drophammer according to NATO STANAG 4489 [119]. The presented values are the minimum impact energy that caused at least one positive result in six independent measurements. A positive result is indicated by acoustic and/or optical effects. Classifications according to the 'UN Recommendations on the Transport of Dangerous Goods' are [120]:

- >40 Nm: Insensitive
- 35 Nm to 40 Nm: Less sensitive
- 4 Nm to 35 Nm: Sensitive
- <4 Nm: Very sensitive

4.5.2 Sensitivity Towards Friction

Sensitivity towards friction was measured by using a BAM friction tester according to NATO STANAG 4487 [121]. The presented values are the minimum pin strain that caused at least one positive experimental result in six independent measurements. A positive result is indicated by acoustic and/or optical effects. Classifications according to the 'UN Recommendations on the Transport of Dangerous Goods' are [120]:

- >360 N: Insensitive
- Approximately 360 N: Less sensitive
- 80 N to 360 N: Sensitive
- 10 N to 80 N: Very sensitive
- <10 N: Extremely sensitive

4.6 Calculations

4.6.1 Oxygen Balance

The oxygen balance Ω is defined as the amount of oxygen in weight percent that is remaining after oxidation of all hydrogen, carbon or metals in the sample to H_2O, CO_2 and metal oxides [7]. If there is an excess of oxygen that can be released after the combustion reaction, the compound has to be considered to have 'positive' oxygen balance. If the amount of available oxygen is not sufficient for a complete oxidation reaction, the deficient amount of oxygen needed to complete the oxidation reaction is reported with a negative oxygen balance [26]. All presented oxygen balances in wt. % are calculated referring to CO_2 using the following equation for a compound with the empirical formula $C_aH_bN_cO_d$ and a molecular mass M (g/mol):

$$\Omega_{CO_2} = \frac{(d - 2a - \frac{b}{2}) \cdot 16.0\,\mathrm{g/mol}}{M} \cdot 100 \tag{4.3}$$

4.6.2 Enthalpy of Formation

Enthalpies of formation were determined according to the literature [122]. The heats of combustion that were measured by bomb calorimetry were converted into the standard molar enthalpies of combustion ($\Delta_c H_m^0$) by using the equations:

$$\Delta_c H_m^0 = \Delta_c U + \Delta n RT \tag{4.4}$$

$$\Delta n = \Delta n_\mathrm{i}(\text{products, g}) - \Delta n_\mathrm{i}(\text{educts, g}) \tag{4.5}$$

The following ideal combustion reaction was assumed for the respective polymer repeating unit:

$$C_aH_bN_cO_d + \left(a + \frac{b}{4} - \frac{d}{2}\right) O_2 \longrightarrow a\,CO_2 + \frac{b}{2}\,H_2O + \frac{c}{2}\,N_2 \tag{4.6}$$

$\Delta_f H_m^0$ was always calculated at 298.15 K using the Hess' law:

$$\Delta_f H_m^0 = a\Delta_f H_m^0(CO_2) + \frac{1}{2}\Delta_f H_m^0(H_2O) - \Delta_c H_m^0 \tag{4.7}$$

Literature values used for the calculations:

- $\Delta_f H_m^0$ (CO_2 (g)) = −394 kJ/mol [123]
- $\Delta_f H_m^0$ (H_2O (g)) = −242 kJ/mol [123]

5 Synthesis and Characterization of Glycidyl Azide Copolymers

Abstract This chapter deals with the synthesis and characterization of novel glycidyl azide copolymers with nonpolar *n*-alkyl side chains acting as internal plasticizers. Epichlorohydrin and *n*-alkyl substituted oxiranes were polymerized via cationic ring-opening polymerization using BF_3xTHF as a catalyst and 1,4-butanediol (BDO) as an initiator leading to polyepichlorohydrin (PECH) copolymers. Structures of the resulting polymers were confirmed by IR and NMR spectroscopy, the molecular weight distributions were analyzed by GPC. Azidations that were carried out as a subsequent synthesis step by using a mixture of sodium azide (NaN_3) and dimethyl sulfoxide (DMSO), delivered the desired glycidyl azide copolymers by nucleophilic substitution of the chlorine groups. Quantitative conversion was checked by spectroscopic methods (IR/NMR). The introduced *n*-alkyl side chains (methyl to dodecyl moiety) showed the desired plasticizing effects by lowering the glass transition temperatures (T_g) and viscosities depending on the side chain length and molecular composition. P($GA_{0.75}$-*co*-$EpO_{0.25}$) is a copolymer consisting of glycidyl azide (GA) and 1,2-epoxyoctane (EpO) units. It was identified as the most promising copolymer for further investigations based on the analysis results. DSC and TGA measurements showed a thermal stability comparable to the reference compound glycidyl azide polymer (GAP). A decreased sensitivity towards mechanical stimuli compared to GAP was measured by BAM drop hammer and friction tests. Based on bomb calorimetric measurements, the heat of formation was calculated as an input parameter for further evaluation using thermodynamic computer codes, which will be discussed in the following chapters.

5.1 Introduction

In 1956, Szwarc reported on the concept of living polymerization that had a great impact on modern macromolecular chemistry and is still important nowadays [124, 125]. The term 'living' describes the characteristics of growing chain ends to maintain their

reactivity even after complete monomer consumption due to the absence of termination and transfer reactions over time. Due to this outstanding reaction control, living polymerizations offer the possibility to synthesize well defined telechelic polymers with narrow molecular weight distributions. Since these path breaking publications, a lot of work in the field of organic synthesis has been performed to develop procedures leading to such well defined polymers. To date, a variety of different living and controlled polymerization techniques have been published and extensively reviewed including anionic polymerization, radical polymerization, cationic polymerization and ring-opening polymerization [126–132].

Polyepichlorohydrin (PECH) with a number average weight (M_n) between 1000 g/mol and 4000 g/mol is the precursor of glycidyl azide polymer (GAP) as discussed in chapter 3.3. It is commonly synthesized by a controlled cationic ring-opening polymerization (CROP) of epichlorohydrin. In general, the anionic ring-opening polymerization of oxiranes provides a better control over the molecular weight distribution but can usually not be utilized for epichlorohydrin. Reasons are the electrophilicity of the chloromethyl group and the highly nucleophilic species that are used in conventional anionic polymerization techniques. Nevertheless, Carlotti et al. published a living anionic polymerization of epichlorohydrin by utilizing a weakly nucleophilic combination of triisobutylaluminum [i-Bu_3Al] and tetraoctylammonium bromide [$NOct_4Br$] leading to the successful synthesis of high molecular weight PECH up to 100 000 g/mol [133].

It is important to note that the microstructure and properties of PECH, obtained by controlled ring-opening polymerization, strongly depends on the type of the used initiator. The glycidyl azide copolymers presented in this work were synthesized via cationic copolymerization. An overview about the cationic ring-opening polymerization of cyclic ethers is therefore presented in this section, particularly of epichlorohydrin using different types of initiators and catalysts. In general, the historical development of low-molecular weight PECH is strongly driven by the intention of using GAP as a binder for solid propellants. This is the reason why the polymer topics PECH and GAP are strongly entangled, especially in the US patent literature.

5.1.1 Cationic Ring-Opening Polymerization of Cyclic Ethers

The synthesis of polyethers via cationic ring-opening polymerization is limited to monomers that have enough ring strain to be readily opened. This includes particularly derivatives of ethylene oxide (EO), oxetane and THF, in which THF is the most intensively studied monomer [127]. In general, different initiator systems are established

in the literature including Brønsted acids, Lewis acids and alkyl esters of strong organic acids like sulfonic acid [134].

There are two different mechanisms that are discussed for the cationic ring-opening polymerization of cyclic ethers. The first mechanism involves a tertiary oxonium ion located at the growing chain end, which adds to a monomer molecule by S_N2 or S_N1 mechanism depending on the stability of the acyclic cationic species. In case of non-substituted cyclic ethers, which are without stabilizing neighbor groups, the S_N2 mechanism is usually predominant. This approach is discussed in the literature as the activated chain end mechanism (ACE) (Figure 5.1) [19].

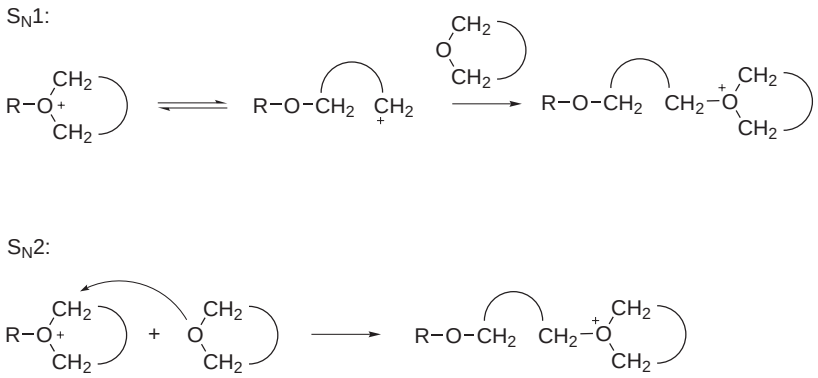

Figure 5.1 Cationic ring-opening polymerization involving the active chain end (ACE) mechanism with S_N1 or S_N2 characteristics, depending on the monomer structure.

Due to the relatively high nucleophilicity of the main chain oxygen atoms, oligomers can be formed by backbiting reactions with the electrophilic propagating chain end species that are predominantly involved in the activated chain end mechanism [135]. An additional side reaction is the ring elimination that can occur subsequently to the backbiting process leading to macrocycles (Figure 5.2). The occurrence of these side reactions depends on the relative rates of the propagation compared to the backbiting process, that are mostly determined by the relative nucleophilicity of the heteroatom in a monomer molecule or in the polymer backbone unit, as well as steric factors [127].

The structure and amount of the formed by-products, is strongly depended on the utilized monomers and initiator systems. The polymerization of THF for example, proceeds with negligible oligomeric by-products because the backbiting and intramolecular chain transfer reactions are slow compared to the chain propagation [136]. In contrast, cyclic oligomers can be formed in high amounts during the polymerization of cyclic oxiranes or even become the major product under certain synthesis conditions [136]. The predominating by-product is dependent on the molecular structure of the monomer. For instance, the cylic dimer 1,4-dioxane is almost exclusively formed in

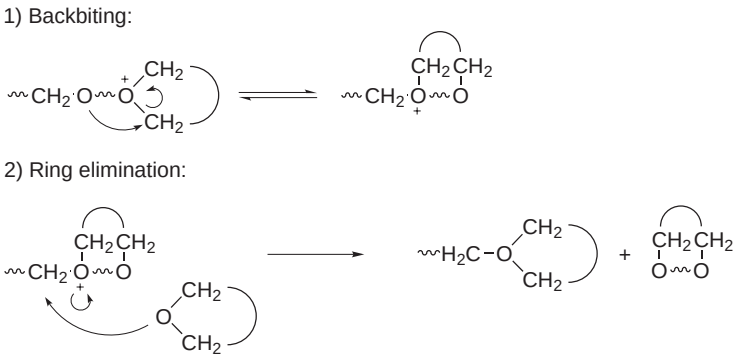

Figure 5.2 Possible side reactions in the cationic ring-opening polymerization of heterocyclic monomers. Depending on the molecular structure of the utilized monomer, cyclization can become predominant under conditions where the activated chain end (ACE) mechanism is favored over the activated monomer mechanism (AMM).

the polymerization of ethylene oxide (EO), while in the CROP of substituted oxiranes like propylene oxide (PO) or epichlorohydrin (ECH), trimers or tetramers can also be formed in significant amounts [127].

When the cationic ring-opening polymerization of cyclic ethers is carried out in the presence of alcohols, the mechanism of the chain propagation changes. In contrast to the described ACE mechanism, which involves a nucleophilic attack of the monomer molecule on the propagating chain end, the so called 'activated monomer mechanism' (AMM) is based on a nucleophilic attack of a hydroxyl-terminated chain end on a protonated monomer molecule (Figure 5.3). The hydroxyl groups of a polyol act as an initiator for this polymerization reaction. For the synthesis of well-defined telechelic polyethers, conditions should be applied where the AMM becomes predominant in comparison to the activated chain end mechanism (ACE). Since there are no electrophilic chain ends involved, the AMM proceeds without backbiting side reactions [137]. The rate of AMM propagation depends on the concentration of hydroxyl end groups and activated monomers, while the rate of ACE propagation is proportional only to the concentration of non-protonated monomers [19]. To increase the participation of AMM propagation, the instantaneous concentration of non-protonated monomers should therefore be kept as low as possible. This means for the practical work that the addition of monomers to the reaction mixture has to be slower than the rate of monomer consumption in order to run the synthesis under monomer starving conditions. By favoring the AMM approach, the occurrence of cyclic oligomers that are formed by backbiting can be reduced but not completely eliminated. Apart from the polymerization of epichlorohydrin and related structures with additional electrophilic centers, the anionic ring-opening methods are therefore mostly preferred over the cationic variations. They generally provide better

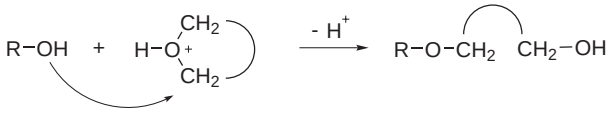

Figure 5.3 Cationic ring-opening polymerization of cylic ethers: Propagation via activated monomer mechanism (AMM).

control in the preparation of well-defined copolymers and enable lower polydispersity indices compared to to cationic ring-opening polymerizations.

Another approach for the CROP of cyclic ethers was recently discussed in the literature for the polymerization of oxetanes, making use of 1,4-dioxane as a reaction solvent. The oxygen nucleophilicity in 1,4-dioxane is higher compared to the nucleophilicity of oxygen atoms in the polymer backbone. Dioxane is therefore usable as an end-capping agent, causing dormant chain ends with a lower reactivity, and prevents the backbiting side reactions. With this modification, it was possible to synthesize well-defined poly(oxetanes) with molecular weights up to 150 000 g/mol. However, a significant incorporation of the 1,4-dioxane was observed due to copolymerization reactions [138].

5.1.2 Synthesis of Polyepichlorohydrin (PECH)

Some functionalized oxiranes like epichlorohydrin (ECH) can be readily polymerized by cationic and ionic-coordinative ring-opening polymerization due to their relatively high ring strain involved in the three membered ring. Depending on the nature of utilized initiator systems and synthesis conditions, different types of polymers can be obtained. Three categories of polyoxirane products can be classified according to their microstructures [139]:

1. Linear polymers with a high molecular mass ($M_n > 100\,000$ g/mol).
2. Cylic oligomers: Predominantly formed under conditions where ACE propagation is favored.
3. Linear telechelic oligomers with low molecular mass ($M_n < 4000$ g/mol): Predominantly formed under conditions where AMM propagation is favored.

After a first evidence of epichlorohydrin polymerization products in 1936 [140], Baggett (1959) [141] and Ishida (1960) [142] were the first to report the synthesis of solid high molecular weight polyepichlorohydrin by using $FeCl_3$ complexes as catalysts. Later in the early 1960s, Vandenberg developed an industrial process for the manufacturing of oil resistant PECH elastomers using alkylaluminum catalysts [143–146]. They are sold in large quantities under the trademarks HERCLOR® and HYDRIN® [147].

Depending on the specific synthesis conditions and procedures, amorphous atactic PECH ($T_g \approx -20\,°C$) or crystalline isotactic PECH (m.p. $\approx 120\,°C$) can be synthesized by using the Vandenberg process [147, 148]. Vandenberg was also the first to claim the idea of synthesizing glycidyl azide polymer (GAP) and copolymers thereof but with a high molecular weight that is not suitable for the formulation of polyurethane based propellant binders [51].

The suitable molecular weight range of PECH as a precursor for GAP is ranging from 1000 g/mol to 4000 g/mol and is therefore belonging to the third polyoxirane category, mentioned above. Between the 1970s and early 1980s, it was discovered that in the presence of proton donating species like water or alcohols, linear polyethers with a low molecular weight can be synthesized with low fractions of oligomeric by-products [149, 150]. Until that, attempts with cationic catalysts virtually caused exclusive formation of low molecular weight cycles with a size depending on the utilized monomers and applied synthesis conditions [139, 151]. Cyclic impurities are not involved in the cross-linking cure process because of missing functional chain ends and are therefore undesirable in polymers for propellant binders.

Okamoto developed a method for the synthesis of polyepihalohydrins using trialkyl oxonium salts like triethyloxonium hexafluorophosphate (TEOP) in the presence of water or ethylene glycol [152, 153]. Later on, two initiator systems based on $SnCl_4$ and BF_3 respectively became predominant for the synthesis of PECH and its copolymers in the literature. Frankel et al. prepared linear PECH for the synthesis of GAP by using BF_3 as a catalyst [50]. A synthesis procedure using $SnCl_4$ was patented by 3M and became the basis for the later 3M GAP patents [52, 154]. 1991, Biedron et al. published a cationic ring-opening polymerization of epichlorohydrin leading to PECH almost free of cyclic oligomers up to a molecular weight of $M_n \approx 2500\,g/mol$ by using

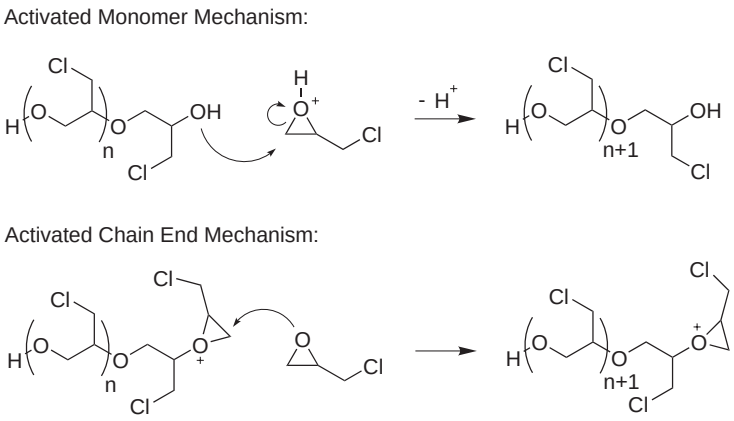

Figure 5.4 Competing mechanisms in the cationic ring-opening polymerization of epichlorohydrin.

BF_3 as a catalyst and several diols as initiators (Figure 5.4) [155]. In this article, the activated monomer mechanism (AMM) is applied for the synthesis of telechelic polyepichlorohydrin diols.

Francis et al. compared PECH synthesized by using $SnCl_4$ and BF_3 initiator systems in presence of 1,4-butanediol concerning their molecular weights and microstructures. It turned out, that the hydroxyl content of PECH prepared by using a BF_3 complex is higher than that of PECH samples synthesized using $SnCl_4$. The achieved number average weight (M_n) was also higher when BF_3 was used as catalyst. NMR investigations showed that there is a significant influence of the catalyst on the microstructure of the polymer chains. PECH prepared by using BF_3 contains a higher content of secondary hydroxyl groups (91.3 %) than PECH prepared by using the stannic chloride catalyst (83.3 %) (Table 5.1) [156].

Table 5.1 Comparison of PECH samples prepared by different initiator systems [156].

Sample	Catalyst	[M]/[I]	M_n [g/mol]	PDI	Eq. Weight [meq/g]
PECH I	BF_3	50:1	2070	-	0.83
PECH II	$SnCl_4$	240:1	1239	3.55	0.69
PECH III	$SnCl_4$	200:1	1045	2.82	0.76

5.2 Experimental Part

5.2.1 Materials

Dichloromethane (DCM) was refluxed over P_2O_5 for 4 hours, distilled and stored over 4 Å molecular sieves. All oxiranes were purchased from Sigma-Aldrich, distilled over CaH_2 and stored under nitrogen atmosphere over 4 Å molecular sieves in a fridge. 1,4-Butanediol was purchased from Sigma-Aldrich, stored over 4 Å molecular sieves and used without further purification. BF_3xTHF was purchased from Sigma-Aldrich and stored under nitrogen in a fridge. Water content is crucial for cationic ring-opening polymerization and has therefore been determined by Karl Fischer titration for each monomer as well as for 1,4-butanediol and the polymerization solvent DCM prior to the experiments. Specific distillation data and water content for each reagent after distillation is presented in Table 5.2. Sodium azide $\geq$ 99.0 % was purchased from Dynamit Nobel GmbH and used without further purification. DMSO synthesis grade was purchased from Merck and used as received. GAP (Lot 06S12) was purchased from Eurenco and used as received.

Table 5.2 Distillation data and water content of polymerization chemicals.

Chemical	CAS	p [mbar]	T_B [a] [°C]	Water cont. [b] [ppm]
Dichloromethane (DCM)	75-09-2	1013	39	0.006
1,4-Butanediol [c] (BDO)	110-63-4	–	–	0.077
Epichlorohydrin (ECH)	106-89-8	150	61	0.042
Propylene oxide [c] (PO)	75-56-9	–	–	0.017
Butylene oxide (BO)	106-88-7	1013	65	0.022
1,2-Epoxyhexane (EpH)	1436-34-6	100	59	0.013
1,2-Epoxyoctane (EpO)	2984-50-1	60	88	0.019
1,2-Epoxydodecane (EpD)	2855-19-8	10	130	0.020
1,2-Epoxytetradecane [c] (EpT)	3234-28-4	–	–	0.037

[a] Measured boiling point.
[b] Determined by Karl Fischer titration.
[c] Not distilled, used as received.

5.2.2 Ring-Opening Polymerizations

General Synthesis Procedure 1 (GP1): Copolymerization

To a stirred mixture of 1,4-butanediol (BDO) and dichloromethane (DCM), BF_3xTHF was added under nitrogen atmosphere. The resulting emulsion was stirred for 15 min at 20 °C. A solution consisting of epichlorohydrin (ECH), the respective *n*-alkyl oxirane and DCM was added at 10 °C with a constant dosing rate of approximately 0.20 ml/min using a dosing pump. After complete addition, the resulting clear viscous solution was stirred at 10 °C for 12 h. DCM was added to dilute the mixture and distilled water was added for quenching the reaction. Then saturated $NaHCO_3$ solution was added and stirring was continued for additional 15 min. The organic layer was separated and washed three times with distilled water. Neutralization was checked with a pH paper. After drying over $MgSO_4$ and filtration, the solvent was evaporated at a maximum temperature of 80 °C under reduced pressure.

PECH (1) [155, 156]

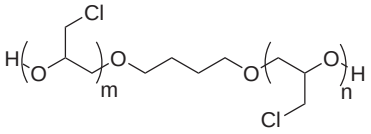

To a stirred mixture of 1,4-butanediol (BDO) (2.20 ml, 24.9 mmol) and dichloromethane (DCM) (7 ml), BF_3xTHF (0.23 ml, 2.1 mmol) was added under nitrogen atmosphere.

The resulting emulsion was stirred for 15 min at 20 °C. A solution consisting of epichlorohydrin (58.66 ml, 750 mmol) and DCM (30 ml) was added at 10 °C with a constant dosing rate of approximately 0.20 ml/min using a dosing pump. After complete addition, the resulting clear viscous solution was stirred at 10 °C for 12 h. 60 ml of DCM was added to dilute the mixture and 25 ml distilled water was added for quenching the reaction. Then 25 ml of saturated $NaHCO_3$ solution was added and stirred for additional 15 min. The organic layer was separated and washed three times with distilled water. Neutralization was checked with a pH paper. After drying over $MgSO_4$ and filtration, the solvent was evaporated at a maximum temperature of 80 °C under reduced pressure. The product was obtained as a clear colorless viscous liquid with a yield of 92 %.

GPC: M_w = 3835 g/mol, M_n = 2530 g/mol, M_p = 3048 g/mol, PDI = 1.52. T_g = −34.4 °C. TGA = 337.9 °C. IR (ATR): $\tilde{\nu}$ [cm^{-1}] = 3467 (w, br), 2917 (m), 1100 (s), 744 (s). ^{1}H NMR (400 MHz, $CDCl_3$): Repeating units δ : 4.05 − 3.36 (br, m, polymer backbone, CH_2Cl). ^{13}C NMR (100 MHz, $CDCl_3$): Repeating units δ : 79.7 − 79.0 (RO*C*HCH$_2$R), 71.9 − 69.3 (ROCH*C*H$_2$R), 45.8 − 43.4 (R*C*H$_2$Cl). Anal. calcd. for $C_3H_5Cl_1O$: C 38.95, H 5.45; Found: C 39.01, H 5.49.

P(ECH$_{0.74}$-*co*-PO$_{0.26}$) (2)

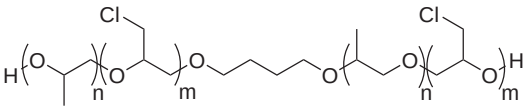

P(ECH$_{0.74}$-*co*-PO$_{0.26}$) with [M]/[I] = 30 was synthesized following the procedure described in GP1. A stirred mixture consisting of BF_3xTHF (0.22 ml, 2.0 mmol), BDO (2.39 ml, 27.0 mmol) and DCM (5 ml) was used as the initiator solution. A mixture of ECH (46.92 ml, 600 mmol) and 1,2-propylene oxide (PO) (14.00 ml, 200 mmol) in DCM (30 ml) was added at 10 °C with a dosing rate of 0.16 ml/min. The product was obtained as a clear colorless viscous liquid with a yield of 94 %.

GPC: M_w = 3625 g/mol, M_n = 1879 g/mol, M_p = 3615 g/mol, PDI = 1.93. T_g = −47.1 °C. TGA = 324.1 °C. IR (ATR): $\tilde{\nu}$ [cm^{-1}] = 3453 (w, br), 2917 (m), 1094 (s), 744 (s). ^{1}H NMR (400 MHz, $CDCl_3$): Repeating units δ : 4.06 − 3.25 (br, m, polymer backbone, CH_2Cl), 1.77 − 0.98 (br, m, CH_3). ^{13}C NMR (100 MHz, $CDCl_3$): Repeating units δ : 79.8 − 68.0 (polymer backbone), 46.1 − 42.3 (R*C*H$_2$Cl), 18.1 − 16.0 (*C*H$_3$). Anal. calcd. for $C_3H_{5.25}Cl_{0.75}O$: C 42.94, H 6.31; Found: C 42.75, H 6.35.

P(ECH$_{0.75}$-*co*-BO$_{0.25}$) (3)

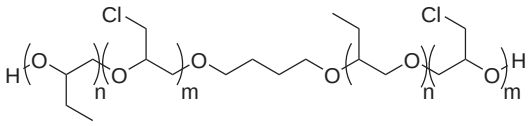

P(ECH$_{0.75}$-*co*-BO$_{0.25}$) with [M]/[I] = 30 was synthesized following the procedure described in GP1. A stirred mixture consisting of BF_3xTHF (0.19 ml, 1.7 mmol), BDO (2.03 ml, 23.0 mmol) and DCM (5 ml) was used as the initiator solution. A mixture of ECH (39.89 ml, 510 mmol) and 1,2-butylene oxide (BO) (14.79 ml, 170 mmol) in DCM (28 ml) was added at 10 °C with a dosing rate of 0.17 ml/min. The product was obtained as a clear colorless viscous liquid with a yield of 93 %.

GPC: M_w = 2932 g/mol, M_n = 1674 g/mol, M_p = 2723 g/mol, PDI = 1.75. T_g = −44.2 °C. TGA = 324.5 °C. IR (ATR): $\tilde{\nu}$ [cm^{-1}] = 3456 (w, br), 2921 (m), 1093 (s), 744 (s). ^{1}H NMR (400 MHz, $CDCl_3$): Repeating units δ : 4.03 − 3.27 (br, m, polymer backbone, CH_2Cl), 1.74 − 0.85 (br, m, CH_2CH_3). ^{13}C NMR (100 MHz, $CDCl_3$): Repeating units δ : 81.2 − 68.7 (polymer backbone), 45.9 − 43.1 (RCH_2Cl), 27.0 − 9.8 (CH_2CH_3). Anal. calcd. for $C_{3.25}H_{5.75}Cl_{0.75}O$: C 44.66, H 6.63; Found: C 44.27, H 6.67.

P(ECH-*co*-EpH) Copolymers (4) – (8)

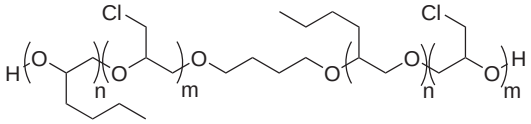

Spectroscopic information for copolymers (4) – (8) is presented combined. They only differ in the molecular compositions, thus showing identical signal patterns in NMR and IR measurements but with different integrals. IR (ATR): $\tilde{\nu}$ [cm^{-1}] = 3451 (w, br), 2929 (m), 1097 (s), 745 (s). ^{1}H NMR (400 MHz, $CDCl_3$): Repeating units δ : 4.02 − 3.32 (br, m, polymer backbone, CH_2Cl), 1.70 − 1.20 (br, m, C_3H_6), 0.97 − 0.82 (br, t, CH_3). ^{13}C NMR (100 MHz, $CDCl_3$): Repeating units δ : 79.9 − 68.7 (polymer backbone), 46.1 − 43.1 (RCH_2Cl), 32.3 − 13.9 (C_4H_9).

P(ECH$_{0.73}$-*co*-EpH$_{0.27}$) (4) P(ECH$_{0.73}$-*co*-EpH$_{0.27}$) with [M]/[I] = 50 was synthesized following the procedure described in GP1. A stirred mixture consisting of BF_3xTHF (0.11 ml, 1.0 mmol), BDO (0.71 ml, 8.0 mmol) and DCM (5 ml) was used as the initiator solution. A mixture of ECH (23.46 ml, 300 mmol) and 1,2-epoxyhexane (EpH) (12.05 ml,

100 mmol) in DCM (18 ml) was added at 10 °C with a dosing rate of 0.19 ml/min. The product was obtained as a clear colorless viscous liquid with a yield of 98 %.

GPC: M_w = 4182 g/mol, M_n = 1856 g/mol, M_p = 4600 g/mol, PDI = 2.25. T_g = −45.2 °C. TGA = 323.3 °C. Anal. calcd. for $C_{3.75}H_{6.75}Cl_{0.75}O$: C 47.70, H 7.21; Found: C 48.08, H 7.17.

P(ECH$_{0.74}$-*co*-EpH$_{0.26}$) (5) P(ECH$_{0.74}$-*co*-EpH$_{0.26}$) with [M]/[I] = 40 was synthesized following the procedure described in GP1. A stirred mixture consisting of BF_3xTHF (0.11 ml, 1.0 mmol), BDO (0.88 ml, 10.0 mmol) and DCM (5 ml) was used as the initiator solution. A mixture of ECH (23.46 ml, 300 mmol) and 1,2-epoxyhexane (EpH) (12.05 ml, 100 mmol) in DCM (18 ml) was added at 10 °C with a dosing rate of 0.20 ml/min. The product was obtained as a clear colorless viscous liquid with a yield of 93 %.

GPC: M_w = 3625 g/mol, M_n = 1879 g/mol, M_p = 3615 g/mol, PDI = 1.93. T_g = −47.1 °C. TGA = 324.1 °C. Anal. calcd. for $C_{3.75}H_{6.75}Cl_{0.75}O$: C 47.70, H 7.21; Found: C 47.35, H 7.20.

P(ECH$_{0.74}$-*co*-EpH$_{0.26}$) (6) P(ECH$_{0.74}$-*co*-EpH$_{0.26}$) with [M]/[I] = 30 was synthesized following the procedure described in GP1. A stirred mixture consisting of BF_3xTHF (0.17 ml, 1.5 mmol), BDO (1.79 ml, 20.3 mmol) and DCM (5 ml) was used as the initiator solution. A mixture of ECH (35.19 ml, 450 mmol) and 1,2-epoxyhexane (EpH) (18.08 ml, 150 mmol) in DCM (29 ml) was added at 10 °C with a dosing rate of 0.20 ml/min. The product was obtained as a clear colorless viscous liquid with a yield of 94 %.

GPC: M_w = 3341 g/mol, M_n = 1982 g/mol, M_p = 2854 g/mol, PDI = 1.69. T_g = −46.5 °C. TGA = 313.8 °C. Anal. calcd. for $C_{3.75}H_{6.75}Cl_{0.75}O$: C 47.70, H 7.21; Found: C 47.59, H 7.35.

P(ECH$_{0.74}$-*co*-EpH$_{0.26}$) (7) P(ECH$_{0.74}$-*co*-EpH$_{0.26}$) with [M]/[I] = 20 was synthesized following the procedure described in GP1. A stirred mixture consisting of BF_3xTHF (0.22 ml, 2.0 mmol), BDO (1.77 ml, 20.0 mmol) and DCM (5 ml) was used as the initiator solution. A mixture of ECH (23.46 ml, 300 mmol) and 1,2-epoxyhexane (EpH) (12.05 ml, 100 mmol) in DCM (18 ml) was added at 10 °C with a dosing rate of 0.20 ml/min. The product was obtained as a clear colorless viscous liquid with a yield of 92 %.

GPC: M_w = 2469 g/mol, M_n = 1452 g/mol, M_p = 2095 g/mol, PDI = 1.70. T_g = −48.7 °C. TGA = 321.7 °C. Anal. calcd. for $C_{3.75}H_{6.75}Cl_{0.75}O$: C 47.70, H 7.21; Found: C 47.86, H 7.19.

P(ECH$_{0.73}$-*co*-EpH$_{0.27}$) (8) P(ECH$_{0.73}$-*co*-EpH$_{0.27}$) with [M]/[I] = 10 was synthesized following the procedure described in GP1. A stirred mixture consisting of BF_3xTHF (0.33 ml, 3.0 mmol), BDO (3.53 ml, 40.0 mmol) and DCM (5 ml) was used as the initiator solution. A mixture of ECH (23.46 ml, 300 mmol) and 1,2-epoxyhexane (EpH) (12.05 ml, 100 mmol) in DCM (18 ml) was added at 10 °C with a dosing rate of 0.20 ml/min. The product was obtained as a clear colorless viscous liquid with a yield of 89 %.

GPC: M_w = 1349 g/mol, M_n = 1016 g/mol, M_p = 1218 g/mol, PDI = 1.33. T_g = −52.1 °C. TGA = 314.0 °C. Anal. calcd. for $C_{3.75}H_{6.75}Cl_{0.75}O$: C 47.70, H 7.21; Found: C 48.23, H 7.34.

P(ECH-*co*-EpO) Copolymers (9) – (12)

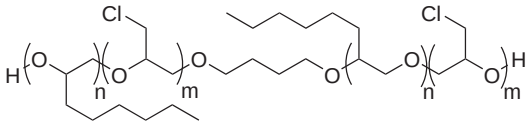

Spectroscopic information for copolymers (9) – (12) is presented combined. They only differ in the molecular compositions, thus showing identical signal patterns in NMR and IR measurements but with different integrals. IR (ATR): $\tilde{\nu}$ [cm^{-1}] = 3450 (w, br), 2926 (m), 1106 (s), 746 (s). ^{1}H NMR (400 MHz, $CDCl_3$): Repeating units δ : 4.01 − 3.30 (br, m, polymer backbone, CH_2Cl), 1.71 − 1.17 (br, m, C_5H_{10}), 0.94 − 0.81 (br, t, CH_3). ^{13}C NMR (100 MHz, $CDCl_3$): Repeating units δ : 80.3 − 69.1 (polymer backbone), 46.2 − 42.9 (RCH$_2$Cl), 32.8 − 13.7 (C_6H$_{13}$).

P(ECH$_{0.89}$-*co*-EpO$_{0.11}$) (9) P(ECH$_{0.89}$-*co*-EpO$_{0.11}$) with [M]/[I] = 30 was synthesized following the procedure described in GP1. A stirred mixture consisting of BF_3xTHF (0.20 ml, 1.8 mmol), BDO (1.33 ml, 15.0 mmol) and DCM (5 ml) was used as the initiator solution. A mixture of ECH (31.28 ml, 400 mmol) and 1,2-epoxyoctane (EpO) (6.88 ml, 45 mmol) in DCM (19 ml) was added at 10 °C with a dosing rate of 0.19 ml/min. The product was obtained as a clear colorless viscous liquid with a yield of 93 %.

GPC: M_w = 2677 g/mol, M_n = 1598 g/mol, M_p = 2448 g/mol, PDI = 1.68. T_g = −42.3 °C. TGA = 338.3 °C. Anal. calcd. for $C_{3.5}H_{6.1}Cl_{0.9}O$: C 43.75, H 6.40; Found: C 44.06, H 6.63.

P(ECH$_{0.75}$-*co*-EpO$_{0.25}$) (10) P(ECH$_{0.75}$-*co*-EpO$_{0.25}$) with [M]/[I] = 30 was synthesized following the procedure described in GP1. A stirred mixture consisting of BF_3xTHF

(0.17 ml, 1.5 mmol), BDO (1.79 ml, 20.3 mmol) and DCM (5 ml) was used as the initiator solution. A mixture of ECH (35.19 ml, 450 mmol) and 1,2-epoxyoctane (EpO) (22.92 ml, 150 mmol) in DCM (30 ml) was added at 10 °C with a dosing rate of 0.21 ml/min. The product was obtained as a clear colorless viscous liquid with a yield of 91 %.

GPC: M_w = 3593 g/mol, M_n = 1874 g/mol, M_p = 3638 g/mol, PDI = 1.92. T_g = −52.2 °C. TGA = 318.7 °C. Anal. calcd. for $C_{4.25}H_{7.75}Cl_{0.75}O$: C 50.32, H 7.70; Found: C 50.19, H 7.72.

P(ECH$_{0.63}$-*co*-EpO$_{0.37}$) (11) P(ECH$_{0.63}$-*co*-EpO$_{0.37}$) with [M]/[I] = 30 was synthesized following the procedure described in GP1. A stirred mixture consisting of BF_3xTHF (0.17 ml, 1.5 mmol), BDO (1.15 ml, 13.0 mmol) and DCM (5 ml) was used as the initiator solution. A mixture of ECH (19.55 ml, 250 mmol) and 1,2-epoxyoctane (EpO) (20.63 ml, 135 mmol) in DCM (19 ml) was added at 10 °C with a dosing rate of 0.22 ml/min. The product was obtained as a clear colorless viscous liquid with a yield of 93 %.

GPC: M_w = 2343 g/mol, M_n = 1407 g/mol, M_p = 2434 g/mol, PDI = 1.67. T_g = −58.5 °C. TGA = 324.7 °C. Anal. calcd. for $C_{4.75}H_{8.85}Cl_{0.65}O$: C 54.33, H 8.49; Found: C 52.82, H 8.56.

P(ECH$_{0.47}$-*co*-EpO$_{0.53}$) (12) P(ECH$_{0.47}$-*co*-EpO$_{0.53}$) with [M]/[I] = 30 was synthesized following the procedure described in GP1. A stirred mixture consisting of BF_3xTHF (0.17 ml, 1.5 mmol), BDO (1.19 ml, 13.5 mmol) and DCM (5 ml) was used as the initiator solution. A mixture of ECH (15.64 ml, 200 mmol) and 1,2-epoxyoctane (EpO) (30.56 ml, 200 mmol) in DCM (20 ml) was added at 10 °C with a dosing rate of 0.24 ml/min. The product was obtained as a clear colorless viscous liquid with a yield of 84 %.

GPC: M_w = 3067 g/mol, M_n = 1624 g/mol, M_p = 3224 g/mol, PDI = 1.89. T_g = −64.9 °C. TGA = 333.7 °C. Anal. calcd. for $C_{5.5}H_{10.5}Cl_{0.5}O$: C 59.86, H 9.59; Found: C 59.70, H 10.09.

P(ECH$_{0.73}$-*co*-EpD$_{0.27}$) (13)

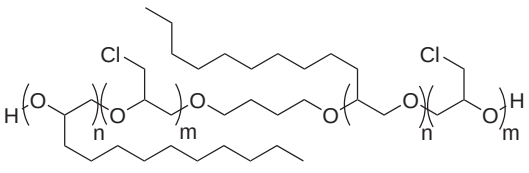

P($ECH_{0.73}$-*co*-$EpD_{0.27}$) with [M]/[I] = 30 was synthesized following the procedure described in GP1. A stirred mixture consisting of BF_3xTHF (0.17 ml, 1.5 mmol), BDO (1.79 ml, 20.3 mmol) and DCM (5 ml) was used as the initiator solution. A mixture of ECH (35.19 ml, 450 mmol) and 1,2-epoxydodecane (EpD) (32.76 ml, 150 mmol) in DCM (33 ml) was added at 10 °C with a dosing rate of 0.24 ml/min. The product was obtained as a clear colorless viscous liquid with a yield of 90 %.

GPC: M_w = 4261 g/mol, M_n = 2216 g/mol, M_p = 4365 g/mol, PDI = 1.92. T_g = −56.1 °C. TGA = 331.2 °C. IR (ATR): $\tilde{\nu}$ [cm^{-1}] = 3457 (w, br), 2923 (m), 1107 (s), 747 (s). ^{1}H NMR (400 MHz, $CDCl_3$): Repeating units δ : 4.02 − 3.33 (br, m, polymer backbone, CH_2Cl), 1.67 − 1.16 (br, m, C_9H_{18}), 0.92 − 0.82 (br, t, CH_3). ^{13}C NMR (100 MHz, $CDCl_3$): Repeating units δ : 80.1 − 69.2 (polymer backbone), 45.8 − 43.3 (R*C*H_2Cl), 32.4 − 14.1 ($C_{10}H_{21}$). Anal. calcd. for $C_{5.25}H_{9.75}Cl_{0.75}O$: C 54.61, H 8.51; Found: C 55.03, H 8.58.

P($ECH_{0.75}$-*co*-$EpT_{0.25}$) (14)

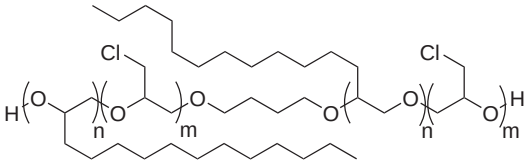

P($ECH_{0.75}$-*co*-$EpT_{0.25}$) with [M]/[I] = 30 was synthesized following the procedure described in GP1. A stirred mixture consisting of BF_3xTHF (0.11 ml, 1.0 mmol), BDO (0.64 ml, 7.3 mmol) and DCM (5 ml) was used as the initiator solution. A mixture of ECH (12.90 ml, 165 mmol) and 1,2-epoxytetradecane (EpT) (13.91 ml, 55 mmol) in DCM (13 ml) was added at 10 °C with a dosing rate of 0.22 ml/min. The product was obtained as a clear colorless viscous liquid with a yield of 94 %.

GPC: M_w = 3474 g/mol, M_n = 2168 g/mol, M_p = 3337 g/mol, PDI = 1.60. TGA = 334.1 °C. IR (ATR): $\tilde{\nu}$ [cm^{-1}] = 3453 (w, br), 22922 (m), 1105 (s), 747 (s). ^{1}H NMR (400 MHz, $CDCl_3$): Repeating units δ : 4.01 − 3.29 (br, m, polymer backbone, CH_2Cl), 1.68 − 1.14 (br, m, $C_{11}H_{22}$), 0.93 − 0.82 (br, t, CH_3). ^{13}C NMR (100 MHz, $CDCl_3$): Repeating units δ : 80.0 − 69.3 (polymer backbone), 45.8 − 43.4 (R*C*H_2Cl), 32.5 − 14.1 ($C_{12}H_{25}$). Anal. calcd. for $C_{5.75}H_{10.75}Cl_{0.75}O$: C 56.39, H 8.85; Found: C 55.44, H 9.05.

P(EpO) (15)

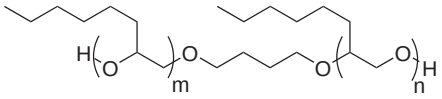

P(EpO) with [M]/[I] = 30 was synthesized following the procedure described in GP1. A stirred mixture consisting of BF_3xTHF (0.17 ml, 1.5 mmol), BDO (0.72 ml, 8.2 mmol) and DCM (5 ml) was used as the initiator solution. A mixture of 1,2-epoxyoctane (EpO) (38.20 ml, 250 mmol) in DCM (18 ml) was added at 10 °C with a dosing rate of 0.26 ml/min. The product was obtained as a clear colorless viscous liquid with a yield of 97 %.

GPC: M_w = 3719 g/mol, M_n = 2612 g/mol, M_p = 4119 g/mol, PDI = 1.42. T_g = −72.9 °C. TGA = 341.6 °C. IR (ATR): $\tilde{\nu}$ [cm^{-1}] = 3466 (w, br), 2924 (m), 1109 (s). ^{1}H NMR (400 MHz, $CDCl_3$): Repeating units δ : 3.79 − 3.11 (br, m, polymer backbone), 1.70 − 1.16 (br, m, C_5H_{10}), 0.96 − 0.79 (br, t, CH_3). ^{13}C NMR (100 MHz, $CDCl_3$): Repeating units δ : 80.1 − 69.6 (polymer backbone), 33.8 − 14.0 (C_6H_{13}). Anal. calcd. for $C_8H_{16}O$: C 74.95, H 15.58; Found: C 73.64, H 13.06.

5.2.3 Azidations

General Procedure 2 (GP2): Azidation

The respective halogenated precursor polymer **1**–**14** was dissolved in DMSO in a round bottom flask equipped with a condenser and a magnetic stirrer. The solution was heated up to 100 °C and sodium azide (NaN_3) was slowly added to the reaction mixture. Stirring at 100 °C was continued until IR spectroscopy showed complete conversion (≈ 48 h). After completion of the reaction, the mixture was cooled down to room temperature and EtOAC together with distilled water was added. The organic layer was separated and washed three times with distilled water. After drying over $MgSO_4$ and filtration, the solvent was evaporated using a rotary evaporator. Drying was continued under reduced pressure (3 mbar) for 8 h at 80 °C to remove last residues of solvent.

GAP (16) [50]

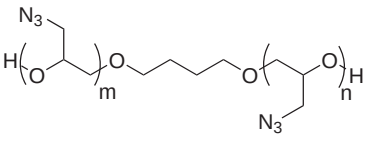

GAP was synthesized following the procedure described in GP2, using PECH **1** (55.39 g), NaN_3 (46.70 g, 718 mmol) and 150 ml DMSO. The product was obtained as a clear yellow viscous liquid (55.04 g).

GPC: M_w = 4234 g/mol, M_n = 2896 g/mol, M_p = 3373 g/mol, PDI = 1.46. T_g = −50.7 °C. T_d = 218.8 °C. TGA = 235.6 °C. ρ = 1.280 g/cm^3. OH-Value = 37.97 mg/g KOH. Eq. Weight = 1478 g/mol. IR (ATR): $\tilde{\nu}$ [cm^{-1}] = 3450 (w, br), 2923 (m), 2089 (s), 1108 (s). ^{1}H NMR (400 MHz, $CDCl_3$): Repeating units δ : 4.00 − 3.08 (br, m, polymer backbone, CH_2N$_3$). ^{13}C NMR (100 MHz, $CDCl_3$): Repeating units δ : 79.4 − 69.4 (polymer backbone), 53.3 − 51.4 (*C*H$_2$N$_3$). Anal. calcd. for $C_3H_5N_3O$: C 36.36, H 5.09, N 42.41; Found: C 36.62, H 5.27, N 40.46.

P(GA$_{0.73}$-*co*-PO$_{0.27}$) (17)

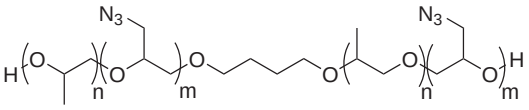

P(GA$_{0.73}$-*co*-PO$_{0.27}$) was synthesized following the procedure described in GP2, using P(ECH$_{0.74}$-*co*-PO$_{0.26}$) **2** (55.80 g), NaN_3 (38.02 g, 585 mmol) and 150 ml DMSO. The product was obtained as a clear yellow viscous liquid (55.58 g).

GPC: M_w = 3822 g/mol, M_n = 2081 g/mol, M_p = 3928 g/mol, PDI = 1.84. T_g = −52.6 °C. T_d = 219.3 °C. TGA = 239.8 °C. ρ = 1.229 g/cm^3. OH-Value = 50.52 mg/g KOH. Eq. Weight = 1111 g/mol. IR (ATR): $\tilde{\nu}$ [cm^{-1}] = 3454 (w, br), 2923 (m), 2091 (s), 1101 (s). ^{1}H NMR (400 MHz, $CDCl_3$): Repeating units δ : 4.01 − 2.88 (br, m, polymer backbone, CH_2N$_3$), 1.77 − 1.03 (br, m, CH_3). ^{13}C NMR (100 MHz, $CDCl_3$): Repeating units δ : 79.6 − 68.3 (polymer backbone), 53.6 − 51.2 (R*C*H$_2$N$_3$), 18.3 − 16.5 (*C*H$_3$). Anal. calcd. for $C_3H_{5.25}N_{2.25}O$: C 40.56, H 5.96, N 35.48; Found: C 40.36, H 6.12, N 33.90.

P(GA$_{0.74}$-*co*-BO$_{0.26}$) (18)

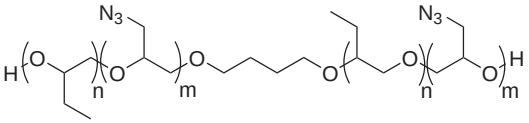

P(GA$_{0.74}$-*co*-BO$_{0.26}$) was synthesized following the procedure described in GP2, using P(ECH$_{0.75}$-*co*-BO$_{0.25}$) **3** (49.30 g), NaN_3 (32.29 g, 497 mmol) and 150 ml DMSO. The product was obtained as a clear yellow viscous liquid (49.06 g).

GPC: M_w = 3593 g/mol, M_n = 1908 g/mol, M_p = 3030 g/mol, PDI = 1.80. T_g = −54.0 °C. T_d = 218.9 °C. TGA = 235.3 °C. ρ = 1.210 g/cm^3. OH-Value = 47.18 mg/g KOH. Eq. Weight = 1189 g/mol. IR (ATR): $\tilde{\nu}$ [cm^{-1}] = 3458 (w, br), 2925 (m), 2092 (s), 1093 (s). ^{1}H NMR (400 MHz, $CDCl_3$): Repeating units δ : 4.01 − 2.87 (br, m, polymer backbone, CH_2N$_3$), 1.80 − 0.84 (CH_2CH_3). ^{13}C NMR (100 MHz, $CDCl_3$): Repeating units δ : 81.4 − 68.9 (polymer backbone), 53.5 − 51.5 (RCH_2N$_3$), 27.1 − 9.6 (CH_2CH_3). Anal. calcd. for $C_{3.25}H_{5.75}N_{2.25}O$: C 42.27, H 6.28, N 34.13; Found: C 42.27, H 6.35, N 32.62.

P(GA-*co*-EpH) Copolymers (19) – (23)

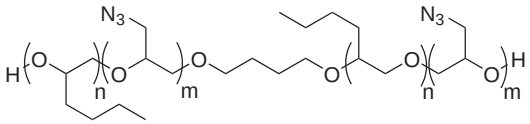

Spectroscopic information for copolymers (19) – (23) is presented combined. They only differ in the molecular compositions, thus showing identical signal patterns in NMR and IR measurements but with different integrals. IR (ATR): $\tilde{\nu}$ [cm^{-1}] = 3453 (w, br), 2929 (m), 2093 (s), 1102 (s). ^{1}H NMR (400 MHz, $CDCl_3$): Repeating units δ : 3.94 − 3.16 (br, m, polymer backbone, CH_2N$_3$), 1.83 − 1.19 (br, m, C_3H_6), 1.01 − 0.79 (br, t, CH_3). ^{13}C NMR (100 MHz, $CDCl_3$): Repeating units δ : 80.1 − 69.2 (polymer backbone), 53.6 − 51.5 (RCH_2N$_3$), 32.5 − 13.8 (C_4H$_9$).

P(GA$_{0.72}$-*co*-EpH$_{0.28}$) (19) P(GA$_{0.72}$-*co*-EpH$_{0.28}$) was synthesized following the procedure described in GP2, using P(ECH$_{0.73}$-*co*-EpH$_{0.27}$) **4** (26.96 g), NaN_3 (16.39 g, 252 mmol) and 100 ml DMSO. The product was obtained as a clear yellow viscous liquid (25.80 g).

GPC: M_w = 4427 g/mol, M_n = 2020 g/mol, M_p = 4811 g/mol, PDI = 2.19. T_g = −56.6 °C. T_d = 219.1 °C. TGA = 235.2 °C. ρ = 1.165 g/cm^3. OH-Value = 36.29 mg/g KOH. Eq. Weight = 1546 g/mol. Anal. calcd. for $C_{3.75}H_{6.75}N_{2.25}O$: C 45.33, H 6.85, N 31.72; Found: C 45.82, H 6.92, N 29.97.

P(GA$_{0.75}$-*co*-EpH$_{0.25}$) (20) P(GA$_{0.75}$-*co*-EpH$_{0.25}$) was synthesized following the procedure described in GP2, using P(ECH$_{0.74}$-*co*-EpH$_{0.26}$) **5** (26.52 g), NaN_3 (16.05 g, 247 mmol) and 100 ml DMSO. The product was obtained as a clear yellow viscous liquid (23.27 g).

GPC: M_w = 3586 g/mol, M_n = 1872 g/mol, M_p = 3383 g/mol, PDI = 1.92. T_g = −56.9 °C. T_d = 218.7 °C. TGA = 234.7 °C. ρ = 1.175 g/cm^3. OH-Value = 47.96 mg/g KOH. Eq. Weight = 1170 g/mol. Anal. calcd. for $C_{3.75}H_{6.75}N_{2.25}O$: C 45.33, H 6.85, N 31.72; Found: C 45.04, H 6.82, N 30.55.

P(GA$_{0.73}$-*co*-EpH$_{0.27}$) (21) P(GA$_{0.73}$-*co*-EpH$_{0.27}$) was synthesized following the procedure described in GP2, using P(ECH$_{0.74}$-*co*-EpH$_{0.26}$) **6** (47.00 g), NaN_3 (28.57 g, 439 mmol) and 150 ml DMSO. The product was obtained as a clear yellow viscous liquid (42.63 g).

GPC: M_w = 3574 g/mol, M_n = 1928 g/mol, M_p = 3360 g/mol, PDI = 1.85. T_g = −56.8 °C. T_d = 218.8 °C. TGA = 236.5 °C. ρ = 1.174 g/cm^3. OH-Value = 47.24 mg/g KOH. Eq. Weight = 1188 g/mol. Anal. calcd. for $C_{3.75}H_{6.75}N_{2.25}O$: C 45.33, H 6.85, N 31.72; Found: C 45.11, H 6.86, N 30.36.

P(GA$_{0.74}$-*co*-EpH$_{0.26}$) (22) P(GA$_{0.74}$-*co*-EpH$_{0.26}$) was synthesized following the procedure described in GP2, using P(ECH$_{0.74}$-*co*-EpH$_{0.26}$) **7** (29.26 g), NaN_3 (17.30 g, 266 mmol) and 100 ml DMSO. The product was obtained as a clear yellow viscous liquid (28.07 g).

GPC: M_w = 2653 g/mol, M_n = 1664 g/mol, M_p = 2223 g/mol, PDI = 1.59. T_g = −57.8 °C. T_d = 219.3 °C. TGA = 234.5 °C. ρ = 1.168 g/cm^3. OH-Value = 62.28 mg/g KOH. Eq. Weight = 901 g/mol. Anal. calcd. for $C_{3.75}H_{6.75}N_{2.25}O$: C 45.33, H 6.85, N 31.72; Found: C 45.65, H 6.90, N 29.71.

P(GA$_{0.73}$-*co*-EpH$_{0.27}$) (23) P(GA$_{0.73}$-*co*-EpH$_{0.27}$) was synthesized following the procedure described in GP2, using P(ECH$_{0.73}$-*co*-EpH$_{0.27}$) **8** (28.39 g), NaN_3 (16.06 g, 247 mmol) and 100 ml DMSO. The product was obtained as a clear yellow viscous liquid (27.92 g).

GPC: M_w = 1416 g/mol, M_n = 1087 g/mol, M_p = 1295 g/mol, PDI = 1.30. T_g = −60.3 °C. T_d = 218.5 °C. TGA = 234.3 °C. ρ = 1.160 g/cm^3. OH-Value = 102.38 mg/g KOH. Eq. Weight = 548 g/mol. Anal. calcd. for $C_{3.75}H_{6.75}N_{2.25}O$: C 45.33, H 6.85, N 31.72; Found: C 45.56, H 7.06, N 27.78.

P(GA-*co*-EpO) Copolymers (24) – (26)

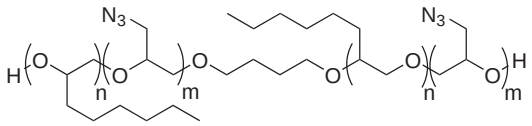

Spectroscopic information for copolymers (24) – (26) is presented combined. They only differ in the molecular compositions, thus showing identical signal patterns in NMR and IR measurements but with different integrals. IR (ATR): $\tilde{\nu}$ [cm^{-1}] = 3454 (w, br), 2926 (m), 2093 (s), 1108 (s). ^{1}H NMR (400 MHz, $CDCl_3$): Repeating units $\delta : 3.99 - 3.08$ (br, m, polymer backbone, CH_2N$_3$), $1.72 - 1.19$ (br, m, C$_5H_{10}$), $0.96 - 0.81$ (br, t, CH_3). ^{13}C NMR (100 MHz, $CDCl_3$): Repeating units $\delta : 80.1 - 69.1$ (polymer backbone), $53.7 - 51.4$ (RCH$_2$N$_3$), $33.0 - 14.0$ (C_6H$_{13}$).

P(GA$_{0.89}$-*co*-EpO$_{0.11}$) (24) P(GA$_{0.89}$-*co*-EpO$_{0.11}$) was synthesized following the procedure described in GP2, using P(ECH$_{0.89}$-*co*-EpO$_{0.11}$) **9** (34.81 g), NaN_3 (20.00 g, 308 mmol) and 100 ml DMSO. The product was obtained as a clear yellow viscous liquid (35.60 g).

GPC: M_w = 3113 g/mol, M_n = 1800 g/mol, M_p = 2696 g/mol, PDI = 1.73. T_g = −54.6 °C. T_d = 218.8 °C. TGA = 238.4 °C. ρ = 1.080 g/cm^3. OH-Value = 54.19 mg/g KOH. Eq. Weight = 1035 g/mol. Anal. calcd. for $C_{3.5}H_{6.1}N_{2.7}O$: C 41.21, H 6.03, N 37.08; Found: C 41.73, H 6.28, N 35.90.

P(GA$_{0.74}$-*co*-EpO$_{0.26}$) (25) P(GA$_{0.74}$-*co*-EpO$_{0.26}$) was synthesized following the procedure described in GP2, using P(ECH$_{0.75}$-*co*-EpO$_{0.25}$) **10** (49.52 g), NaN_3 (28.56 g, 439 mmol) and 150 ml DMSO. The product was obtained as a clear yellow viscous liquid (47.70 g).

GPC: M_w = 3924 g/mol, M_n = 1972 g/mol, M_p = 3839 g/mol, PDI = 1.90. T_g = −60.5 °C. T_d = 219.4 °C. TGA = 239.3 °C. ρ = 1.140 g/cm^3. OH-Value = 40.19 mg/g KOH. Eq. Weight = 1396 g/mol. Anal. calcd. for $C_{4.25}H_{7.75}N_{2.25}O$: C 47.99, H 7.34, N 29.63; Found: C 47.55, H 7.42, N 28.45.

P(GA$_{0.63}$-*co*-EpO$_{0.37}$) (26) P(GA$_{0.63}$-*co*-EpO$_{0.37}$) was synthesized following the procedure described in GP2, using P(ECH$_{0.63}$-*co*-EpO$_{0.37}$) **11** (29.50 g), NaN_3 (21.06 g, 324 mmol) and 120 ml DMSO. The product was obtained as a clear yellow viscous liquid (27.39 g).

GPC: M_w = 2585 g/mol, M_n = 1553 g/mol, M_p = 2515 g/mol, PDI = 1.66. T_g = −63.4 °C. T_d = 218.7 °C. TGA = 244.5 °C. ρ = 1.098 g/cm^3. OH-Value = 64.26 mg/g KOH. Eq. Weight = 873 g/mol. Anal. calcd. for $C_{4.75}H_{8.85}N_{1.95}O$: C 52.21, H 8.16, N 24.99; Found: C 51.93, H 8.50, N 23.16.

P(GA$_{0.47}$-*co*-EpO$_{0.53}$) (27) P(GA$_{0.47}$-*co*-EpO$_{0.53}$) was synthesized following the procedure described in GP2, using P(ECH$_{0.47}$-*co*-EpO$_{0.53}$) **12** (29.49 g), NaN_3 (15.46 g, 238 mmol) and 120 ml DMSO. The product was obtained as a clear yellow viscous liquid (25.69 g).

GPC: M_w = 3347 g/mol, M_n = 1831 g/mol, M_p = 3291 g/mol, PDI = 1.83. T_g = −66.6 °C. T_d = 221.3 °C. TGA = 245.7 °C. ρ = 1.038 g/cm^3. OH-Value = 58.18 mg/g KOH. Eq. Weight = 964 g/mol. Anal. calcd. for $C_{5.5}H_{10.5}N_{1.5}O$: C 58.13, H 9.31, N 18.49; Found: C 58.49, H 9.83, N 16.26.

P(GA$_{0.73}$-*co*-EpD$_{0.27}$) (28)

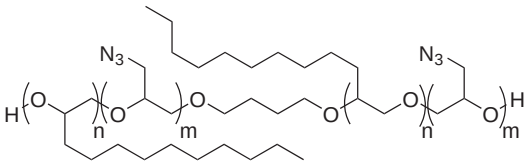

P(GA$_{0.73}$-*co*-EpD$_{0.27}$) was synthesized following the procedure described in GP2, using P(ECH$_{0.73}$-*co*-EpD$_{0.27}$) **13** (55.84 g), NaN_3 (27.92 g, 430 mmol) and 150 ml DMSO. The product was obtained as a clear yellow viscous liquid (54.26 g).

GPC: M_w = 4475 g/mol, M_n = 2308 g/mol, M_p = 4266 g/mol, PDI = 1.94. T_g = −61.7 °C. T_d = 219.5 °C. TGA = 242.9 °C. ρ = 1.091 g/cm^3. OH-Value = 38.56 mg/g KOH. Eq. Weight = 1455 g/mol. IR (ATR): $\tilde{\nu}$ [cm^{-1}] = 3453 (w, br), 2923 (m), 2095 (s), 1112 (s). ^{1}H NMR (400 MHz, $CDCl_3$): Repeating units δ : 4.00 − 3.05 (br, m, polymer backbone, CH_2N$_3$), 1.71 − 1.17 (br, m , C_9H_{18}), 0.96 − 0.78 (br, t, CH_3). ^{13}C NMR (100 MHz, $CDCl_3$): Repeating units δ : 80.1 − 69.2 (polymer backbone), 53.8 − 51.6 (R*C*H$_2$N$_3$), 33.1 − 13.7 ($C_{10}H_{21}$). Anal. calcd. for $C_{5.25}H_{9.75}N_{2.25}O$: C 52.38, H 8.16, N 26.18; Found: C 52.60, H 8.34, N 24.41.

P(GA$_{0.75}$-*co*-EpT$_{0.25}$) (29)

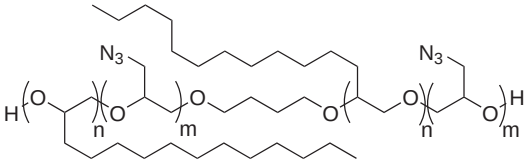

P(GA$_{0.75}$-*co*-EpT$_{0.25}$) was synthesized following the procedure described in GP2, using P(ECH$_{0.75}$-*co*-EpT$_{0.25}$) **14** (16.51 g), NaN_3 (15.00 g, 231 mmol) and 75 ml DMSO. The product was obtained as a clear yellow viscous liquid (15.88 g).

GPC: M_w = 3328 g/mol, M_n = 2014 g/mol, M_p = 3289 g/mol, PDI = 1.65. T_d = 218.3 °C. TGA = 243.8 °C. $\rho = 1.217\,g/cm^3$. OH-Value = 52.15 mg/g KOH. Eq. Weight = 1076 g/mol. IR (ATR): $\tilde{\nu}$ [cm^{-1}] = 3456 (w, br), 2922 (m), 2095 (s), 1113 (s). ^{1}H NMR (400 MHz, $CDCl_3$): Repeating units $\delta : 4.00 - 3.11$ (br, m, polymer backbone, CH_2N$_3$), $1.72 - 1.06$ (br, m, C$_{11}H_{22}$), $0.98 - 0.76$ (br, t, CH_3). ^{13}C NMR (100 MHz, $CDCl_3$): Repeating units $\delta : 80.0 - 69.2$ (polymer backbone), $53.4 - 51.7$ (RCH_2N_3), $32.4 - 14.2$ ($C_{12}H_{25}$). Anal. calcd. for $C_{5.75}H_{10.75}N_{2.25}O$: C 54.21, H 8.50, N 24.74; Found: C 54.05, H 8.68, N 24.22.

5.3 Results and Discussion: Synthesis and Characterization

5.3.1 Synthesis and Characterization of P(GA-*co*-EpH) Copolymers

The synthesis of glycidyl azide (GA) copolymers is usually a two-step process. First, a copolymerization of epichlorohydrin (ECH) and the selected comonomers is carried out to form polyepichlorohydrin (PECH) copolymers, which are sometimes referred as the halogen precursor of the respective GA copolymer. A subsequent azidation results in the azido copolymer by nucleophilic substitution of the chlorine groups.

The first step in the evaluation of *n*-alkyl chains as internal plasticizers for glycidyl azide copolymers was therefore the investigation, whether an already established initiator system will deliver appropriate results for the copolymerization of ECH and *n*-alkyl substituted oxiranes. 1,2-epoxyhexane (EpH), a monomer with a moderate *n*-alkyl side chain length of four carbon atoms (*n*-butyl moiety), was chosen for the first synthesis experiments (Figure 5.5). Different [Monomer]/[Initiator] ([M]/[I]) ratios ranging from

[M]/[I] = 10 to [M]/[I] = 50 were investigated to evaluate the properties of copolymers with different molecular weights. The aim was to find the most suitable synthesis parameters for further copolymerization studies with respect to promising energetic binder prepolymers.

The polymerization of ECH leading to PECH with a number average weight of approximately $M_n \approx 2000\,\mathrm{g/mol}$ is typically performed via controlled cationic ring-opening polymerization (CROP) using lewis acids as a catalyst and a diol compound as an initiator molecule to yield telechelic hydroxyl-terminated polymers. The lewis acids BF_3 and $SnCl_4$ are reported in the literature as the most widely used cationic catalysts for this polymerization reaction [156].

It was decided to use BF_3xTHF for the synthesis of the novel copolymers based on ECH and *n*-alkyl substituted oxiranes, since BF_3 is known as an effective catalyst for the polymerization of various cyclic ethers and to deliver higher molecular weights in the synthesis of PECH [136, 156]. Furthermore, BF_3 polymerized polyepichlorohydrin showed a higher hydroxyl content thus providing a higher functionality of the polymer [156]. A higher functionality can be beneficial for the mechanical properties of resulting binder networks due to a higher degree of cross-linking and ist therefore clearly desirable. 1,4-Butanediol (BDO) was chosen as the diol initiator as Biedron et al. stated that less cyclic oligomers were formed during the polymerization of epichlorohydrin when BDO was used instead of ethylene glycol (EG) which is also a commonly utilized initiator for this reaction [155]. The overall two-step strategy for the synthesis of glycidyl azide copolymers with incorporated EpH units is outlined in Figure 5.5.

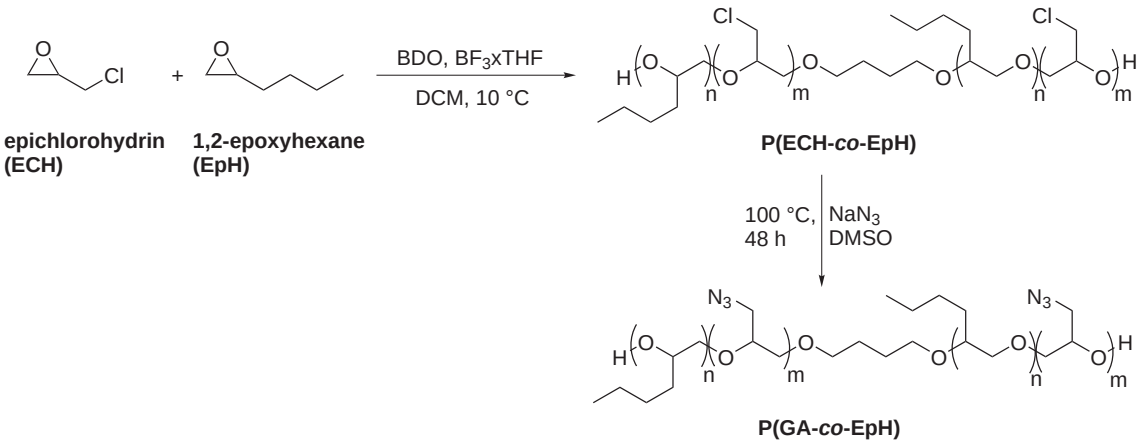

Figure 5.5 Synthesis of P(GA-*co*-EpH) copolymers via cationic ring-opening polymerization followed by a subsequent azidation procedure.

By application of the activated monomer mechanism (AMM) approach, a significant reduction of backbiting can be achieved due to the absence of active species at the

growing chain ends that occur in an active chain end (ACE) propagation reaction (Chapter 5.1). Kinetic studies showed that the contribution of the ACE mechanism can be limited when the ratio [OH]/[Monomer] is kept high during the reaction by choosing suitable reaction conditions [157]. Therefore, the monomer solutions consisting of epichlorohydrin (75 mol %) and 1,2-epoxyhexane (25 mol %) in DCM were added slowly to the initiator solution with a feed rate of approximately 1.5 mmol/min by using a dosing pump. The initial ratio between terminal hydroxyl groups (from BDO) and catalyst [OH]/[BF_3xTHF] was kept at 30 for all experiments. Table 5.3 summarizes the experimental parameters of the performed polymerizations. The copolymers were obtained in good yields (> 85 %) as clear and colorless, viscous liquids. For comparison, the polyepichlorohydrin (PECH) homopolymer was also synthesized according to the same procedure delivering the expected product in comparably good yield.

Table 5.3 Parameters for the synthesis of P(ECH-*co*-EpH) copolymers with varying [M]/[I] ratios. The reactions were initiated with BF_3xTHF and BDO at a ratio of [OH]/[Cat.] ≈ 30.

No.	Composition [a]	[ECH]/[EpH] [b]	[M]/[I]	Feed Rate [mmol/min]	Yield
1	PECH	100	30	1.44	92 %
4	P($ECH_{0.73}$-*co*-$EpH_{0.27}$)	75:25	50	1.42	89 %
5	P($ECH_{0.74}$-*co*-$EpH_{0.26}$)	75:25	40	1.49	93 %
6	P($ECH_{0.74}$-*co*-$EpH_{0.26}$)	75:25	30	1.47	94 %
7	P($ECH_{0.74}$-*co*-$EpH_{0.26}$)	75:25	20	1.49	92 %
8	P($ECH_{0.73}$-*co*-$EpH_{0.27}$)	75:25	10	1.49	89 %

[a] Real composition calculated by ^{1}H NMR spectroscopy.
[b] Theoretical composition in mol %.

The process temperature was recorded online during the entire reaction, to get a better understanding about the thermal characteristics of this reaction which is crucial for future scale-up experiments. Figure 5.6 presents the temperature measurement of copolymerization experiment **5** as an example, all other performed copolymerizations showed almost identical temperature profiles. All polymerizations were performed using a 250 ml double-jacket reactor, which was operated at 10 °C jacket-temperature. 11 °C were measured inside the initiator solution (process temperature) before the monomer feeding was started. Shortly after the monomer dosing was started during the synthesis of copolymer **5**, the temperature showed a slow increase to 12.5 °C for the first 40 min before reaching a sharp temperature peak of 23.5 °C ($\Delta_{max}T = 12.5$ K) (Figure 5.6). This observed induction period confirms the results of Kim et al., where the homopolymerization of epichlorohydrin was investigated using online temperature

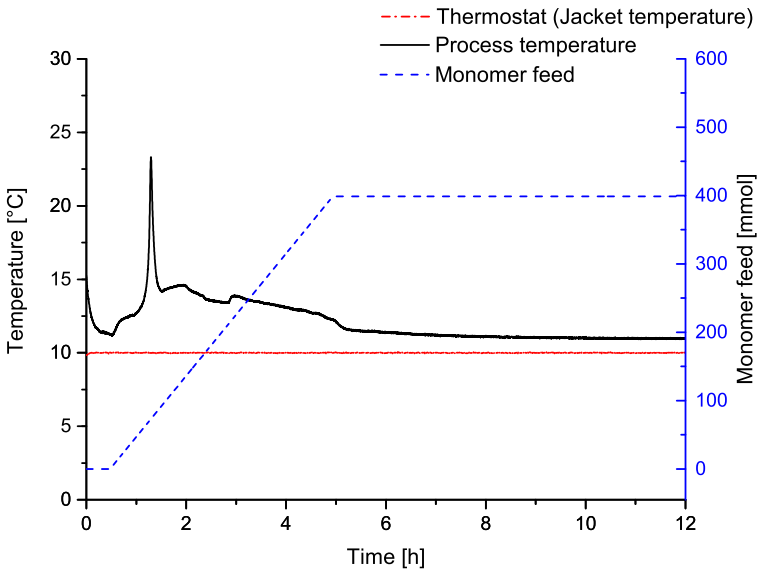

Figure 5.6 Online temperature measurement of Exp. **5**. The red line shows the internal temperature of the thermostat, which was set to 10 °C for the entire experiment. The black line shows the temperature that was measured inside of the reactor (reaction temperature). The blue dotted line shows the monomer feed, which was kept at a constant value by using a dosing pump.

monitoring [69]. The existence of such an induction period causes an accumulation of monomers that can react in an uncontrolled thermally accelerated polymerization. Kim et al. explained the induction phenomenon by the aggregation of 1,4-butanediol (BDO) with the catalyst BF_3 at the beginning of the monomer addition. Aggregated initiators are supposed to be less reactive than non-aggregated ones [68, 69]. This induction period is supposed to have a negative influence on the product properties. Accumulated unreacted monomers could cause the formation of cyclic oligomers by favoring ACE propagation in an uncontrolled reaction. This can lead to a higher polydispersity (PDI) and a lower hydroxyl functionality of the final product which is undesirable for the propellant manufacturing process.

To determine the molecular weight distributions of the synthesized copolymers, gel permeation chromatography (GPC) was performed. The resulting GPC curves are presented in Figure 5.7. Detailed data including the number average molecular weights M_n and polydispersity indices are listed in Table 5.4. Additional GPC data including M_w and M_p can be found in the experimental section for each respective copolymer. The experiments showed that copolymers with M_n ranging from 1000 g/mol to 2000 g/mol were successfully synthesized with a moderate polydispersity ranging from 1.33 to 2.25. As shown in Figure 5.7, a broadening can be noticed for higher [M]/[I] ratios than

Table 5.4 GPC data on the molecular weight distributions of synthesized P(ECH-*co*-EpH) copolymers with different [M]/[I] ratios **1**, **4**–**8**.

No.	Composition [a]	[M]/[I]	M_n [th.] [g/mol]	M_n [b] [g/mol]	PDI [c]
1	PECH	30	2877	2530	1.52
4	P($ECH_{0.73}$-*co*-$EpH_{0.27}$)	50	4812	1856	2.25
5	P($ECH_{0.74}$-*co*-$EpH_{0.26}$)	40	3867	1879	1.93
6	P($ECH_{0.74}$-*co*-$EpH_{0.26}$)	30	2888	1808	1.81
7	P($ECH_{0.74}$-*co*-$EpH_{0.26}$)	20	1979	1452	1.70
8	P($ECH_{0.73}$-*co*-$EpH_{0.27}$)	10	1034	1016	1.33

[a] Real composition calculated by ^{1}H NMR spectroscopy.
[b] Determined by GPC (THF, PS standard).
[c] PDI = M_w/M_n

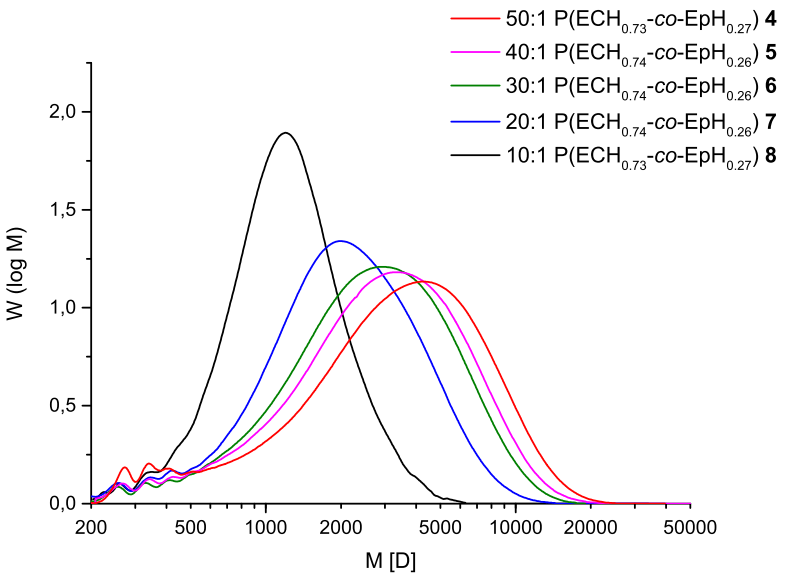

Figure 5.7 GPC graphs of P(ECH-*co*-EpH) copolymers with different [M]/[I] ratios ranging from 10:1 to 50:1.

20:1, which was expected as a similar trend of the PDI was reported in the literature for the synthesis of polyepichlorohydrin using BF_3 under comparable conditions [155]. Nevertheless, the shoulder peaks at lower molecular weights are negligible even for a higher ratio like [M]/[I] = 50. The GPC measurements therefore confirm that a low amount of oligomers was formed as byproducts and can be considered as a good result for a cationic copolymerization. The difference between M_n [th.] and M_n increases with the [M]/[I] ratio, similar to results of the PECH homopolymerization experiments using the BF_3 initiator system [155]. To obtain a good GPC resolution especially at the lower molecular weight ranges, a column set with pore sizes from 50 Å to 105 Å was

used. The calibration was carried out using polystyrene standards to ensure a good comparability because most of the literature discussing polyepichlorohydrin and GAP reported PS standards as a reference for their GPC investigations. Noor et al. reported that polyether calibration standards are supposed to deliver molecular weights closer to the theoretical expected values and could therefore be an interesting alternative for further studies [158].

IR spectroscopy provided a first confirmation of the assumed copolymer structure (Figure 5.8). The most important signals of the synthesized epichlorohydrin copolymers **4**–**8** are the C-Cl stretching vibration at 745 cm^{-1} (s) and the absorbance at 1190 cm^{-1} (s) associated with the C-O-C polyether linkage. For a more comprehensive structure

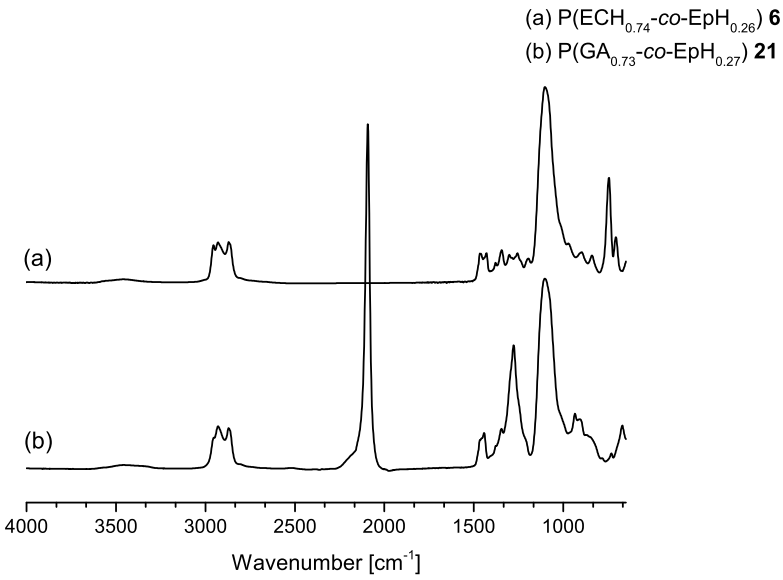

Figure 5.8 IR spectra of the halogen precusor P($ECH_{0.74}$-*co*-$EpH_{0.26}$) **6** and the corresponding azidated copolymer P($GA_{0.73}$-*co*-$EpH_{0.27}$) **21**.

information, NMR spectroscopy was applied. The molecular structure of the synthesized PECH **1** (M_n = 2530 g/mol) was confirmed by a comparison with literature spectral data [156]. The ^{1}H NMR of P($ECH_{0.74}$-*co*-$EpH_{0.26}$) **6** is presented as an example for the synthesized copolymers in Figure 5.9. The assumed structure was confirmed for all synthesized copolymers. A triplet can be observed at 0.84 ppm for the $-CH_3$ group of the *n*-butyl side chain, while between 1.16 ppm and 1.65 ppm three broadened signals appear caused by the methylene units. The overlapped signals of the polyether backbone together with the chloromethyl units show a broadened signal ranging from 3.18 ppm to 3.97 ppm, which was likewise observed for the pure PECH homopolymer [156]. ^{1}H NMR spectroscopy was also used to calculate the ratio ECH/EpH of the incorporated

monomers by an integral comparison of the signals of the *n*-butyl side chains with the signals caused by the polyether backbone together with the chloromethyl side chains. The calculated values for all polyepichlorohydrin copolymers **1**, **4**–**8** are summarized in Table 5.4 and showed values close to the theoretically targeted composition of 75:25.

The synthesized polymers **1**, **4**–**8** were azidated in a subsequent reaction using 1.2 eq NaN_3 in DMSO at 100 °C (Figure 5.5). Nucleophilic substitution of the chlorine groups delivered the desired energetic azido copolymers. Table 5.5 lists the synthesized azido polymers **16**, **19**–**23** together with the incorporated monomer composition, molecular weights and polydispersity indices. IR spectroscopy was used for monitoring the reaction and to check the quantitative conversion before the reaction was quenched.

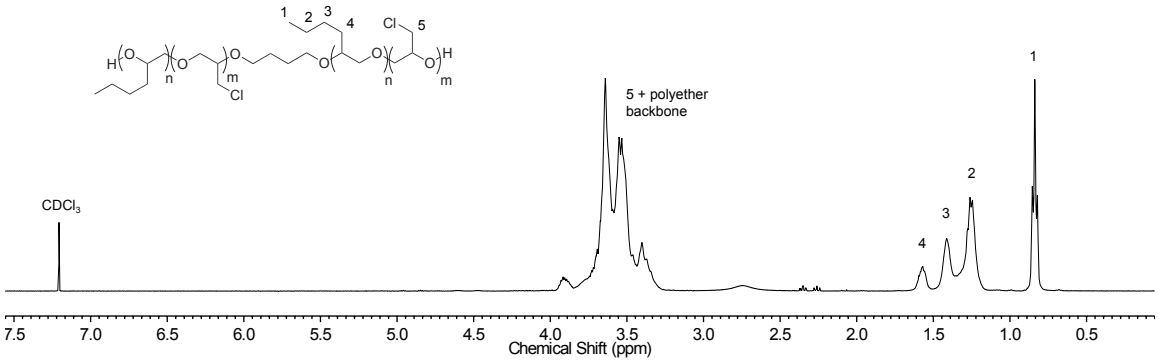

Figure 5.9 ^{1}H NMR spectrum of P($ECH_{0.74}$-*co*-$EpH_{0.26}$) No. **6**. Calculation of the molecular composition of the synthesized copolymers was performed by comparing the integrals of the main chain protons (5 and polyether backbone) with the integrals of the side chain protons (1–4).

Table 5.5 Data about the molecular weight distributions of synthesized GAP **16** and P(GA-*co*-EpH) copolymers with different [M]/[I] ratios ranging from [M]/[I] = 10 to [M]/[I] = 50 **19**–**23**.

No.	Composition [a]	[M]/[I]	M_n [b] [g/mol]	PDI [c]
16	GAP	30	2896	1.46
19	P($GA_{0.72}$-*co*-$EpH_{0.28}$)	50	2020	2.19
20	P($GA_{0.75}$-*co*-$EpH_{0.25}$)	40	1872	1.92
21	P($GA_{0.73}$-*co*-$EpH_{0.27}$)	30	1928	1.85
22	P($GA_{0.74}$-*co*-$EpH_{0.26}$)	20	1664	1.59
23	P($GA_{0.73}$-*co*-$EpH_{0.27}$)	10	1087	1.30

[a] Real composition calculated by ^{1}H NMR spectroscopy.
[b] Determined by GPC (THF, PS standard).
[c] PDI = M_w/M_n

IR spectra of the halogen precursor P($ECH_{0.74}$-*co*-$EpH_{0.26}$) **6** and of the azido-polymer P($GA_{0.73}$-*co*-$EpH_{0.27}$) **21** are shown in Figure 5.8 as a representative example. The complete disappearance of the signal at 745 cm^{-1} (s) indicates the complete substitution of chlorine (−Cl) by azido groups ($-N_3$). The azido signal can be observed at 2100 cm^{-1} (s). The molecular structure as well as the completeness of the azidation was also checked by comparing the ^{13}C NMR spectra of the halogenated precursor polymers **1**, **4**–**8** with the corresponding azido polymers **16**, **19**–**23**. An example is shown in Figure 5.10 for P($ECH_{0.74}$-*co*-$EpH_{0.26}$) **6** and P($GA_{0.73}$-*co*-$EpH_{0.27}$) **21**. The signals of the *n*-butyl side chain appear in the range of 10 ppm to 30 ppm for the halogen precursor as well as for the corresponding azido copolymer, whereas the signals of the polyether backbone are ranging from 65 ppm to 78 ppm. The signal of the $-CH_2Cl$ chloromethylene unit (43.4 ppm to 45.6 ppm) completely disappeared after azidation, which indicates quantitative substitution of the chlorine groups by azido groups. After successful azidation, the molecular weight distribution shifted as expected to slightly higher values because the molecular weight of the functional group in the side chains

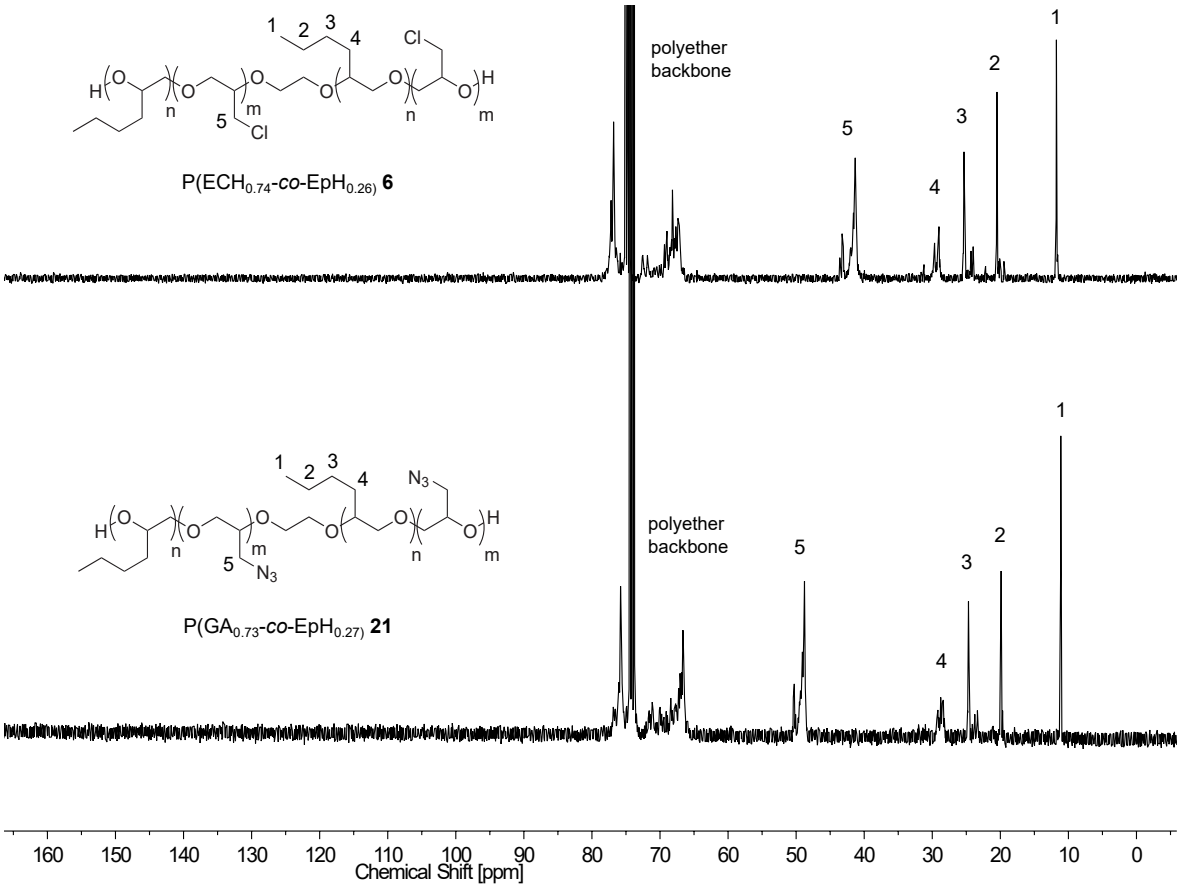

Figure 5.10 ^{13}C NMR spectra of the copolymers P($ECH_{0.74}$-*co*-$EpH_{0.26}$) **6** and P($GA_{0.73}$-*co*-$EpH_{0.27}$) **21**.

increased. The molecular weight distributions of the copolymers were analyzed by GPC, the resulting data are summarized in Table 5.5. The respective GPC curves of the synthesized P(GA-*co*-EpH) copolymers **19**–**23** are presented as an overlay in Appendix A.1.1.

Glass Transition Temperatures

Glass transition temperatures (T_g) of all synthesized polymers were determined by DSC applying a heating rate (HR) of 10 K/min. The obtained values are stated in the experimental section. In comparison to the polyepichlorohydrin (PECH) homopolymer, the incorporation of the comonomer 1,2-epoxyhexane (EpH) leads to a significant decrease of the T_g. For the synthesized PECH ([M]/[I] = 30) a value of $T_g = -34.4\,°C$ was determined. Concerning comonomer sample **6**, which consists of approximately 75 mol % ECH and 25 mol % EpH ([M]/[I] = 30), the T_g decreases to $-46.5\,°C$ ($\Delta T_g = 13\,K$). The substitution of the chlorine groups leading to the corresponding energetic azido polymers causes a further T_g drop, since the azido group itself has a plasticizing effect compared to the chlorine group [92]. For the selected reference, commercial GAP (Lot 06S12), a T_g of $-48.7\,°C$ was determined by DSC. The measurement of copolymer P($GA_{0.73}$-*co*-$EpH_{0.27}$) **21** shows a glass transition at $-56.8\,°C$. The curves of both measurements are presented as an overlay in Figure 5.11. The incorporation of EpH

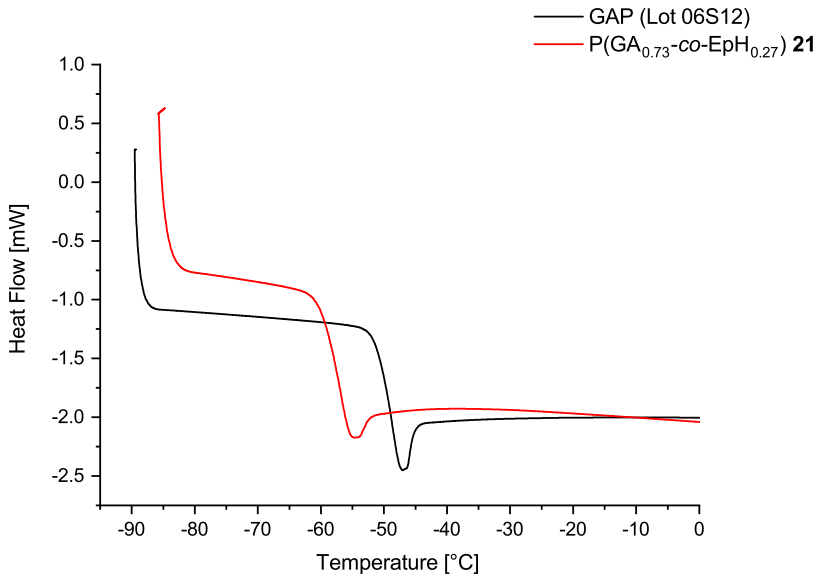

Figure 5.11 DSC curves of P($GA_{0.73}$-*co*-$EpH_{0.27}$) **21** and GAP (Lot 06S12). Pendant *n*-butyl side chains act as internal plasticizer by lowering the glass transition temperature (T_g) (HR = 10 K/min).

with *n*-butyl side chains into the GAP polyether backbone chains clearly shows the desired plasticizing effect by lowering the T_g compared to the GAP homopolymer. By decreasing the [M]/[I] ratio, the glass transition temperature of the azido copolymer likewise decreases down to −60.3 °C at a [M]/[I] ratio of 10:1. This copolymer may be also suitable for the synthesis of an energetic plasticizer comparable to GAP-A, which is an azido-terminated GAP with a low-molecular weight [57].

Viscosity and Density

The viscosity of energetic prepolymers is an important parameter for the processibility of propellants. Viscosity measurements at 20 °C, 40 °C, and 60 °C were therefore performed in dependence of the shear rate. Figure 5.12 presents the results of P($GA_{0.73}$-*co*-$EpH_{0.27}$) **21** in comparison to GAP (Lot 06S12). Both polymers show the behavior of a Newtonian fluid at all measured temperatures over the whole range of applied shear rates ($10^1\,s^{-1}$ to $10^3\,s^{-1}$). The viscosity of **21** is significantly lower compared to the viscosity of GAP, which is along with the lowered glass transition temperature a proof for the plasticizing effect of the nonpolar *n*-butyl side chains. Viscosity values of the presented measurements at a shear rate of $10^1\,s^{-1}$ are listed in Table 5.6. A reduced viscosity is desirable since the liquid prepolymers can exhibit better processing at lower temperatures and provide the possibility of achieving higher filler contents.

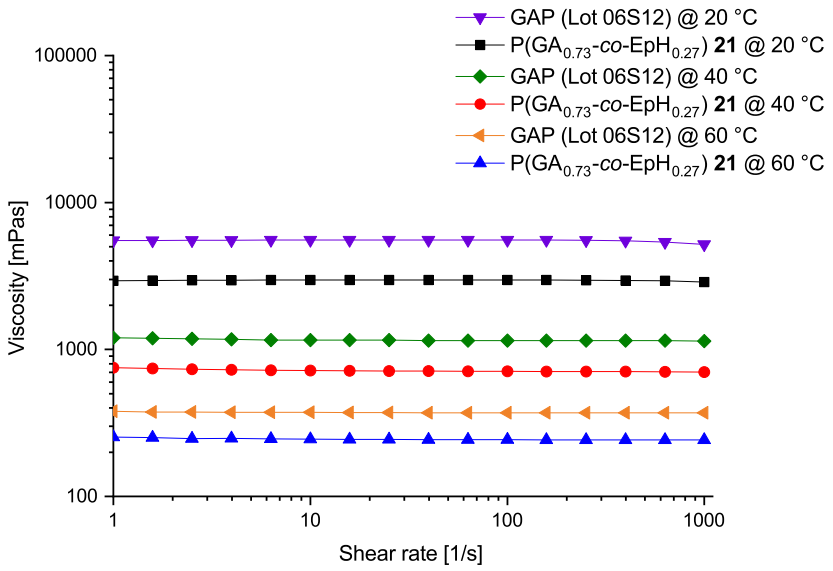

Figure 5.12 Viscosity measurements of GAP (Lot 06S12) and synthesized P($GA_{0.73}$-*co*-$EpH_{0.27}$) **21** in dependence of the shear rate at three different temperatures (20 °C, 40 °C, 60 °C).

Viscosity measurement data of all other synthesized P(GA-*co*-EpH) copolymers **19**–**23** are summarized in Appendix A.1.2.

The density of P($GA_{0.73}$-*co*-$EpH_{0.27}$) **21** was determined using a He gas pycnometer following the procedure described in DIN 66137-2 [115] at 20 °C and compared to GAP (Lot 06S12). The results of the measurements are presented in Table 5.6. The measured density of GAP (Lot 06S12) was consistent with literature reported values of GAP [26]. All density data of the other synthesized P(GA-*co*-EpH) copolymers **19**–**23** are presented in the experimental section. The copolymer density is slightly reduced compared to the GAP homopolymer since the side chains act like a spacer between the backbone chains. By the introduction of *n*-butyl chains, the sterical hindrance compared to the chloromethyl side chains is significantly increased.

Table 5.6 Viscosity and density measurements of GAP (Lot 06S12) and P($GA_{0.73}$-*co*-$EpH_{0.27}$) **21**.

No.	Composition [a]	η [b] [mPas] @ 20 °C	η [b] [mPas] @ 40 °C	η [b] [mPas] @ 60 °C	ρ [c] [g/cm³]
–	GAP (Lot 06S12)	5550	1160	373	1.284
21	P($GA_{0.73}$-*co*-$EpH_{0.27}$)	2970	719	245	1.174

[a] Calculated by ^{1}H NMR spectroscopy.
[b] Measured at a shear rate of 10^1 1/s.
[c] Measured at 20 °C.

End Group Analysis

The polyether end groups were determined by classical titration method following the procedure described in DIN 53240-2 [116]. The hydroxyl groups were acetylated with acetic anhydride followed by titration of the excess reagent with KOH solution. Results are presented in Table 5.7. Determination of the end groups is crucial for the manufacturing of propellants because the respective equivalent weight is needed for the calculation of the binder mixture. The OH-Value increases with lower M_n values from **19** to **23** because shorter chains have a higher content of free hydroxyl chain ends per gram. Because of the same reason, the equivalent weight decreases along with M_n. As expected, samples with a M_n of approximately 1900 g/mol to 2000 g/mol **20, 21** have comparable equivalent weights as the commercial GAP (Lot 06S12), which shows an M_n in the same molecular weight range. This is preferable since already gained results in curing studies with GAP can be easier applied on a new energetic binder prepolymer when it provides a similar equivalent weight.

Table 5.7 Results of end group analysis performed by classical titration method for various synthesized P(GA-*co*-EpH) polymers **19**–**23**.

No.	Composition [a]	OH-Value [b] [mg KOH/g]	Equivalent Weight [b] [g/mol]	M_n [c] [g/mol]
–	GAP (Lot 06S12)	46.33	1211	1904
19	P($GA_{0.72}$-*co*-$EpH_{0.28}$)	36.29	1546	2020
20	P($GA_{0.75}$-*co*-$EpH_{0.25}$)	47.96	1170	1872
21	P($GA_{0.73}$-*co*-$EpH_{0.27}$)	47.24	1188	1928
22	P($GA_{0.74}$-*co*-$EpH_{0.26}$)	62.28	901	1664
23	P($GA_{0.73}$-*co*-$EpH_{0.27}$)	102.38	548	1087

[a] Real composition calculated by ^{1}H NMR spectroscopy.
[b] Determined by titration.
[c] Determined by GPC (THF, PS standard).

5.3.2 Variation of the *n*-Alkyl Side Chain Length

The synthesis and characterization of P(GA-*co*-EpH) copolymers with different molecular weights confirmed that the incorporation of nonpolar *n*-alkyl side chains effects the properties of the resulting glycidyl azide copolymers by decreasing the glass transition temperatures (T_g) and viscosities. The synthesis parameters were varied regarding the ratio between monomers and initiator. P($GA_{0.73}$-*co*-$EpH_{0.27}$) **21** with a [M]/[I] ratio of 30 showed the most interesting properties by having a T_g of −56.8 °C, a decreased viscosity compared to GAP and an equivalent weight close to commercial GAP.

A further evaluation of commercially available *n*-alkyl oxiranes with different chain lengths was realized in the following experiments in order to investigate the influence of the *n*-alkyl chain length on the copolymer properties. As the introduction of non-energetic alkyl side chains will lower the nitrogen content and thus the overall energy level of the polymer ($\Delta_f H^0$), the aim is to find the best trade-off between nitrogen content and low-temperature properties for the specific application of the copolymer. Based on market availability and price, a selection of comonomers with *n*-alkyl side chains ranging from C1 (methyl moiety) to C12 (dodecyl moiety) was investigated. The selected monomers are:

- Propylene oxide (PO): methyl moiety (C1)
- Butylene oxide (BO): ethyl moiety (C2)
- 1,2-Epoxyhexane (EpH): butyl moiety (C4)
- 1,2-Epoxyoctane (EpO): hexyl moiety (C6)

- 1,2-Epoxydodecane (EpD): decyl moiety (C10)
- 1,2-Epoxytetradecane (EpT): dodecyl moiety (C12)

For the evaluation of the influence of the *n*-alkyl side chain length, a molecular comonomer composition of 75 mol % glycidyl azide (GA) units and 25 mol % *n*-alkyl oxirane units was targeted for all synthesized samples by preparing the monomer feed solution in the appropriate ratio. The aim of setting the composition to a fixed value was to focus specifically on the impact of the *n*-alkyl side chain length and to eliminate the influence of different molecular compositions as far as possible. An amount of 25 mol % *n*-alkyl oxirane units was considered to be sufficient enough, to show the plasticizing effects and to provide the possibility to distinguish between the impact of different chain lengths. Based on the results of the previous section, a [M]/[I] ratio of 30 was selected for the copolymerization studies. The synthesis of all copolymers was performed according to the synthesis parameters which were determined in the previous chapter. Cationic ring-opening polymerization using BF_3xTHF and 1,4-butanediol was applied for the synthesis of the respective polyepichlorohydrin copolymers **2**–**3**, **10**, **13**–**14** (Figure 5.13). Details about synthesis, structural information and the molecular weight distributions of those halogenated precursors can be found in the experimental section. GPC curves are presented as an overlay in Appendix A.1.1.

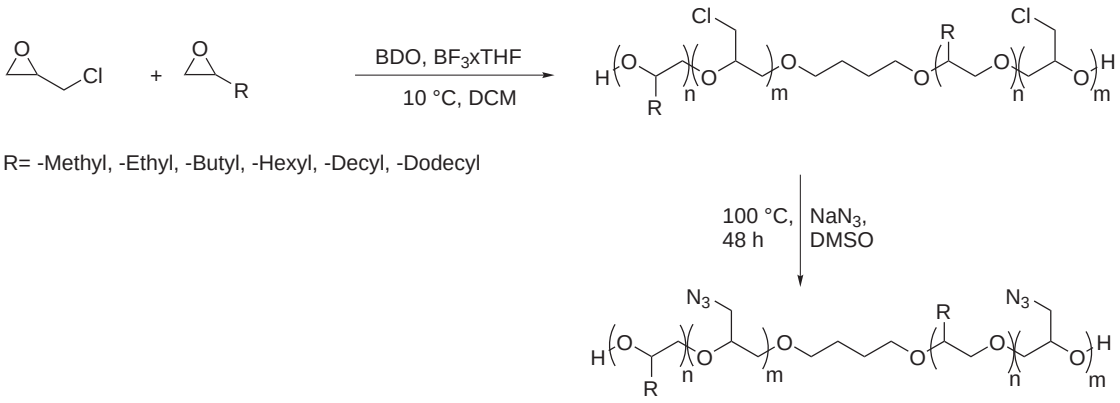

Figure 5.13 Synthesis of glycidyl azide copolymers with *n*-alkyl side chains that have different chain lengths ranging from C1 (methyl moiety) to C12 (dodecyl moiety).

The subsequent azidation using sodium azide in DMSO delivered the completely azidated target molecules, which were checked by IR and NMR spectroscopy as discussed before for the P(GA-*co*-EpH) copolymers (Figure 5.13). Table 5.8 presents the data of synthesized azido copolymers **17**–**18**, **21**, **25**, **28**–**29** together with details about their molecular composition and molecular weight averages.

The GPC graphs of the synthesized azido-copolymers are shown as an overlay in Figure 5.14. Compared to the already discussed P($GA_{0.73}$-*co*-$EpH_{0.27}$) **21** copolymer with [M]/[I] = 30, no significant broadening of the distribution could be noticed by incorporating longer side chains. In fact, the copolymer with the highest alkyl side chain length showed the narrowest distribution with a PDI of 1.65, which is slightly lower compared to the other copolymers. In comparison, the pure GAP

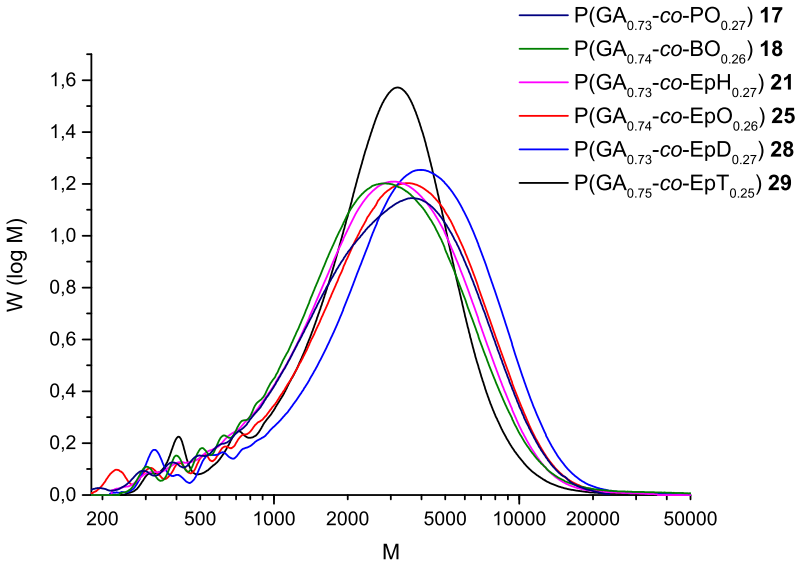

Figure 5.14 GPC graphs of synthesized glycidyl azide copolyethers with nonpolar *n*-alkyl side chains. The molecular compositions between glycidyl azide (GA) and *n*-alkyl oxirane units are approximately 75:25. For further details see Table 5.8.

Table 5.8 Characterization of synthesized azido copolymers ([M]/[I] = 30) with varying *n*-alkyl side chain length between C1 and C12. The targeted molecular composition between glycidyl azide and *n*-alkyl oxirane units was 75:25.

No.	Composition [a]	Moiety	C Chain Length	M_n [b] [g/mol]	PDI [c]
17	P($GA_{0.73}$-*co*-$PO_{0.27}$)	-Methyl	1	2081	1.84
18	P($GA_{0.74}$-*co*-$BO_{0.26}$)	-Ethyl	2	1908	1.80
21	P($GA_{0.73}$-*co*-$EpH_{0.27}$)	-Buthyl	4	1928	1.85
25	P($GA_{0.74}$-*co*-$EpO_{0.26}$)	-Hexyl	6	1972	1.90
28	P($GA_{0.73}$-*co*-$EpD_{0.27}$)	-Decyl	10	2308	1.94
29	P($GA_{0.75}$-*co*-$EpT_{0.25}$)	-Dodecyl	12	2014	1.65

[a] Real composition calculated by ^{1}H NMR spectroscopy.
[b] Determined by GPC (THF, PS standard).
[c] PDI = M_w/M_n

homopolymer was synthesized with a PDI of 1.46 by applying the same synthesis procedure (Table 5.5). The structures and molecular compositions were analyzed by spectroscopic methods as presented in the previous section for the P(GA-*co*-EpH) copolymers. Detailed information can be found in the experimental section. The targeted molecular compositions of 75 mol % GA units and 25 mol % *n*-alkyl substituted units were approximately reached, the actual compositions can be found in Table 5.8. Based on the discussed analytical results, the developed synthesis procedure can be considered as suitable for the selected copolymer systems.

Glass Transition Temperatures and Nitrogen Content

The incorporation of *n*-butyl side chains showed a plasticizing effect by lowering the glass transition temperature of the copolymers in comparison to the pure GAP homopolymer as discussed for P(GA-*co*-EpH) copolymers. Therefore, the synthesized azido copolymers with varying alkyl side chain lengths as well as their respective halogen precursors were analyzed by DSC to gather information about the influence of the side chain length on the low-temperature properties of the copolymers. Detailed results can be found in the experimental section.

The measurements confirmed that the glass transition temperatures of the copolymers shifted to lower values when the lengths of the alkyl side chain were increased (Figure 5.15). This was expected, since plasticizers with a higher chain length are usually supposed to be more effective in decreasing T_g by lowering intra-/ and intermolecular forces between the polar polyether backbones [97]. Because of the nonavailability / high costs of the monomers, polymers with C3, C5, C7-C9 side chains were not synthesized, but the glass transition temperature of the respective copolymers can be estimated by the calculated polynomial fitting curves:

$$T_g = -4.14323x + 0.20537x^2 - 34.92143 \quad \text{(halogen precursors)} \tag{5.1}$$

$$T_g = -2.66285x + 0.14143x^2 - 49.21304 \quad \text{(azido copolyethers)} \tag{5.2}$$

The pure GAP homopolymer is represented in Figure 5.15 with 'Side Chain Length' = 0 for no additional pendant alkyl moieties. A sample of the commercial GAP (Lot 06S12) from Eurenco was taken for the reference measurements. The glass transition temperature (T_g) decreased from −48.7 °C (GAP (Lot 06S12)) to −61.7 °C for P($GA_{0.73}$-*co*-$EpD_{0.27}$) **28** with a C10 *n*-alkyl moiety. The T_g curves of the azido-polymers showed in general a lower slope than curves of the halogen-precursors (Figure 5.15). This is caused by the fact that the azido group itself has a plasticizing effect compared to the

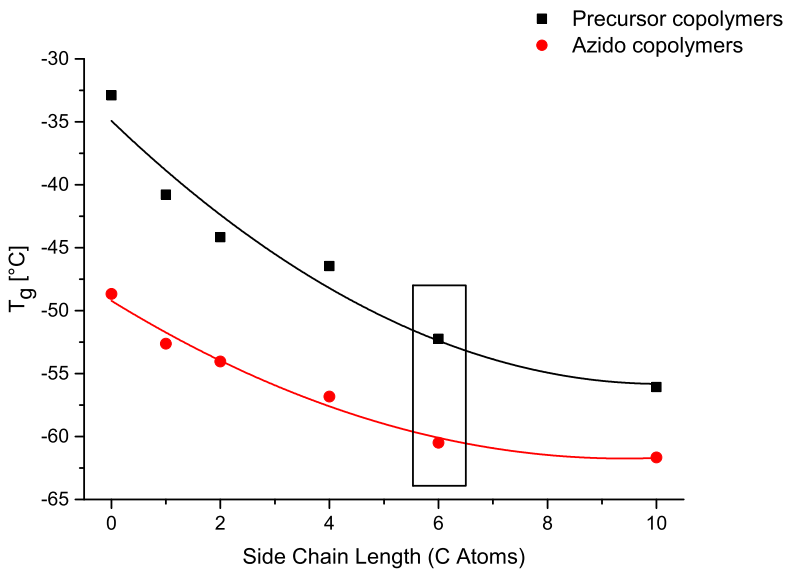

Figure 5.15 Relation between the glass transition temperature (T_g) of synthesized copolymers and the *n*-alkyl side chain length. Upper curve (black line) presents the T_g values of the halogen-precursors and the lower curve (red line) the respective energetic azido-copolymers.

chloromethyl moiety [92]. Therefore, the incorporation of nonpolar side chains will have a lower effect for the glycidyl azide (GA) copolymers than for the PECH copolymers.

At a *n*-alkyl chain length of C12 (dodecyl moiety), side chain crystallization occured by showing an additional melting point at −12.8 °C for P($GA_{0.75}$-*co*-$EpT_{0.25}$) **29** as shown in Figure 5.16. This is clearly undesired, because an effective binder material for composite propellants should not show semi-crystalline behavior that could lead to brittleness of propellant formulations when they are applied at low temperatures. The comonomer 1,2-epoxytetradecane (EpT) is therefore unsuitable for the use in energetic binder systems and was not further investigated.

The comonomer 1,2-epoxyoctane (EpO) with a hexyl moiety (C6) was considered as the most promising candidate for further studies concerning the DSC results. The next step to 1,2-epoxydodecane (EpD) C10 leads only to a small decrease of T_g (ΔT_g = −1.2 K) but also to a further undesirable decrease of the nitrogen content which was determined by elemental analysis (Figure 5.17). P($GA_{0.74}$-*co*-$EpO_{0.26}$) **25** has a nitrogen content of 28.45 wt %, which indicates a higher energy content compared to P($GA_{0.73}$-*co*-$EpD_{0.27}$) **28** with a nitrogen content of 24.41 wt %. Compared to the copolymer based on 1,2-epoxyhexane (EpH) with the same [M]/[I] ratio and molecular composition, P($GA_{0.74}$-*co*-$EpO_{0.26}$) **25** has the strong benefit of an approximately 4 K lower T_g. Detailed data of the elemental analysis are presented in the experimental section for

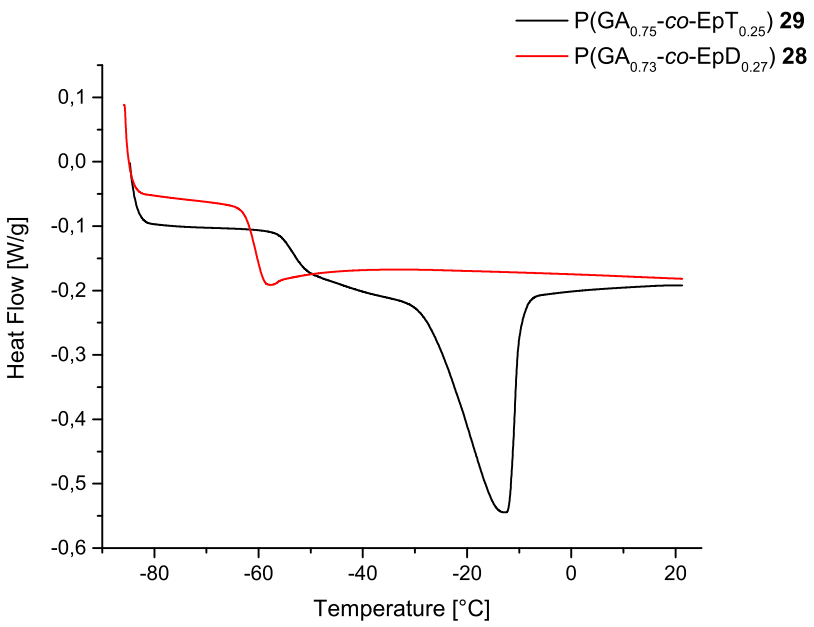

Figure 5.16 DSC measurements: Comparison between P($GA_{0.73}$-*co*-$EpD_{0.27}$) **28** showing the glass transition at −61.7 °C and P($GA_{0.75}$-*co*-$EpT_{0.25}$) **29** exhibiting an additional melting point at −12.8 °C.

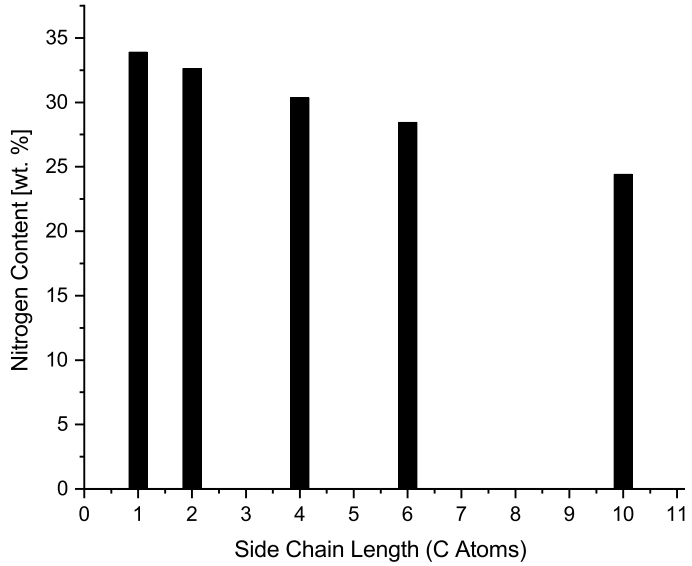

Figure 5.17 Nitrogen contents of synthesized copolymers with *n*-alkyl moieties, ranging from C1 (methyl) to C10 (decyl), determined by elemental analysis.

all synthesized azido-polymers. By considering the trade-off between T_g and nitrogen content, the comonomer 1,2-epoxyoctane (EpO) was selected for further studies. It represents the best compromise among the investigated comonomers regarding the positive influence on low-temperature properties compared to the linked energy loss.

Viscosity and Density

Viscosity measurements of the *n*-alkyl substituted glycidyl azide copolymers **17**–**29** were performed in dependence of the shear rate at 20 °C, 40 °C and 60 °C. The results are summarized in Table 5.9. Each sample showed a constant viscosity over the whole range of applied shear rates, thus showing the characteristic of a Newtonian fluid like GAP. The viscosity of the synthesized azido-copolymers **17**–**29** at a shear rate of $10\,s^{-1}$ is plotted in dependence of the temperature in Figure 5.18. The viscosity of all samples is decreasing with increasing temperature. The highest viscosity differences between samples with different side chain length were obtained at 20 °C. When the temperature was increased from 20 °C to higher values, the effect became smaller. A general trend of decreasing viscosity with increasing side chain length was observed, which was expected. The pure GAP polymer exhibited the highest viscosities at all three temperatures, while the copolymer with the longest side chain length P($GA_{0.75}$-*co*-$EpT_{0.25}$) **29** showed

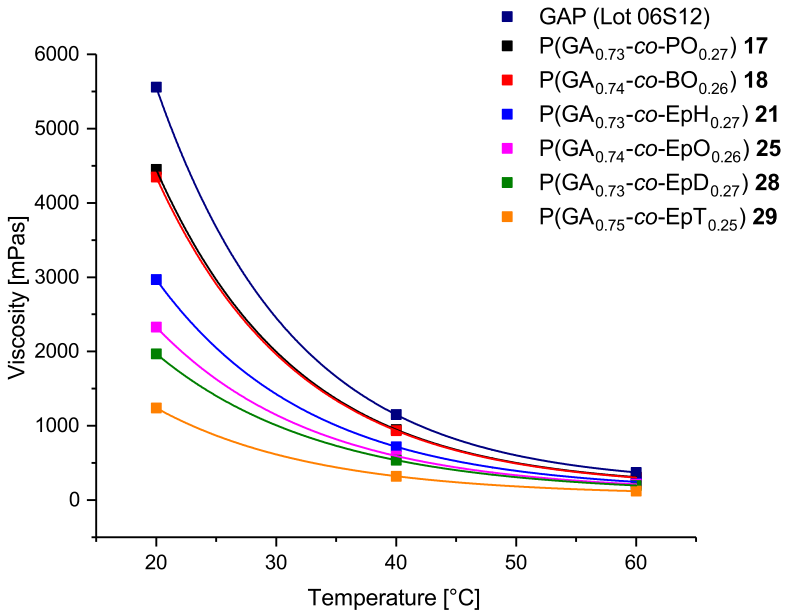

Figure 5.18 Relation between temperature and viscosity for synthesized glycidyl azide copolymers with different *n*-alkyl side chain lengths in comparison to GAP (Lot 06S12).

the lowest viscosity values. Lowered viscosities are beneficial for the processing of propellants not only because higher filler contents can be achieved, but also because the processing at lower temperatures provides improvement concerning safety when working with energetic materials (in this case oxidizers). If the viscosity of the prepolymer is too high, propellant processing temperatures often have to be increased up to 60 °C. Another benefit of processing at lower temperatures is a decreased shrinkage of the material after the curing process which leads to reduced strain in the propellant.

Table 5.9 Viscosity and density data of synthesized glycidyl azide copolymers ([M]/[I] = 30) with varying *n*-alkyl side chain length.

No.	Composition [a]	η [b] [mPas] @ 20 °C	η [b] [mPas] @ 40 °C	η [b] [mPas] @ 60 °C	ρ [c] [g/cm^3]
—	GAP (Lot 06S12)	5560	1150	373	1.284
17	P(GA$_{0.73}$-*co*-PO$_{0.27}$)	4450	949	309	1.229
18	P(GA$_{0.74}$-*co*-BO$_{0.26}$)	4350	936	303	1.210
21	P(GA$_{0.73}$-*co*-EpH$_{0.27}$)	2970	719	245	1.174
25	P(GA$_{0.74}$-*co*-EpO$_{0.26}$)	2330	594	213	1.140
28	P(GA$_{0.73}$-*co*-EpD$_{0.27}$)	1970	538	197	1.091
29	P(GA$_{0.75}$-*co*-EpT$_{0.25}$)	1240	322	120	1.217

[a] Real composition calculated by ^{1}H NMR spectroscopy.
[b] Measured at a shear rate of 10 s^{-1}.
[c] Measured at 20 °C.

The densities of the synthesized azido copolymers **17**–**29** are lower in comparison to GAP. The introduced nonpolar n-alkyl chains lower the intermolecular forces between the polymer backbone chains which is supposed to be reasonable for the increase of the measured densities. With an increasing *n*-alkyl side chain length, a decreasing trend in the density can be noticed. This was expected, since higher chain lengths will cause an enlarged sterical hindrance of the substituents which reduces the intermolecular forces and therefore the density of the material. A little discontinuity can be noticed for P(GA$_{0.75}$-*co*-EpT$_{0.25}$) **29**. It shows the highest density in comparison to the other synthesized copolymers but still a lower one than GAP. This might be caused by the partial crystallinity of the copolymer, which was identified in the DSC measurements (Figure 5.16).

End Group Analysis

The end groups of the synthesized *n*-alkyl substituted glycidyl azide copolymers were determined by titration method as discussed in the previous section. The results of the measurements are summarized in Table 5.10. The obtained equivalent weights are close to each other as expected, because each synthesis was performed with the same [M]/[I] ratio delivering polymers with a number average molecular weight in a relatively narrow range. The equivalent of commercial GAP (Lot 06S12) was determined using the same procedure to be 1211 g/mol. The synthesized copolymers showed equivalent weights very close to GAP, they are therefore supposed to be suitable for cast-cure applications with curing systems that are already established for GAP.

Table 5.10 Data of end group analysis for various synthesized glycidyl azide copolymers. The samples show equivalent weight values in the same range as the commercial GAP sample.

No.	Composition [a]	OH-Value [b] [mg KOH/g]	Equivalent Weight [b] [g/mol]
-	GAP (Lot 06S12)	46.33	1211
17	P($GA_{0.73}$-*co*-$PO_{0.27}$)	50.52	1111
18	P($GA_{0.74}$-*co*-$BO_{0.26}$)	47.18	1189
21	P($GA_{0.73}$-*co*-$EpH_{0.27}$)	47.24	1188
25	P($GA_{0.74}$-*co*-$EpO_{0.26}$)	40.19	1396
28	P($GA_{0.73}$-*co*-$EpD_{0.27}$)	38.56	1455
29	P($GA_{0.75}$-*co*-$EpT_{0.25}$)	52.15	1076

[a] Real composition calculated by ^{1}H NMR spectroscopy.
[b] Determined by titration.
[c] Determined by GPC (THF, PS standard).

5.3.3 P(GA-*co*-EpO) Copolymers: Influence of the Molecular Composition on the Copolymer Properties

Considering the nitrogen content, viscosity and glass transition temperature of the synthesized copolymers with varying *n*-alkyl side chain lengths, 1,2-epoxyoctane (EpO) was identified as the most interesting comonomer. The molecular composition P($GA_{0.74}$-*co*-$EpO_{0.26}$) **25** showed a promising compromise between improved low-temperature properties and decreasing nitrogen content. Furthermore it provided low viscosity values and an equivalent weight close to commercial GAP, which indicates good processibility in propellant cast-cure processes. An aim of this study was to provide a copolymer system, where the molecular compositions can be adjusted over the whole possible range

depending on the requirements in the specific application. To investigate the influence of the ratio between glycidyl azide (GA) units and 1,2-epoxyhexane (EpO) units on the copolymer properties, different molecular compositions of P(GA-*co*-EpO) copolymers were synthesized. It was also necessary to check if there is an additional melting point due to phase separation phenomena at a certain comonomer concentration as observed for P($GA_{0.75}$-*co*-$EpT_{0.25}$) **29** in the previous section. The P(GA-*co*-EpO) copolymer with the most interesting properties should be selected for further evaluation in scale-up and formulation experiments.

Four different P(GA-*co*-EpO) copolymers ranging from 10 mol % to 50 mol % EpO comonomer content as well as the pure P(EpO) homopolymer were synthesized and characterized. The [M]/[I] ratio was set to 30 for all experiments. The copolymerization of ECH and EpO was performed via cationic copolymerization using BF_3xTHF and BDO as established for the former copolymers (Figure 5.19). The polyepichlorohydrin copolymers **9**–**12** were obtained in good yields as clear colorless viscous liquids. Details about the characterization of the halogenated precursors can be found in the experimental section. The P(EpO) homopolymer **15** was also isolated in a good yield of 97 %. The subsequent azidation procedure using NaN_3 and DMSO at 100 °C delivered the *n*-hexyl substituted glycidyl azide copolymers **24**–**27** (Figure 5.19). The results of the synthesis experiments are summarized in Table 5.11. GAP (0 % comonomer) and P(EpO) (100 % comonomer) can be considered as the boundaries of the GA/EpO copolymer system. The actual molecular compositions were determined by ^{1}H NMR and were very close to the theoretically targeted values (Table 5.11).

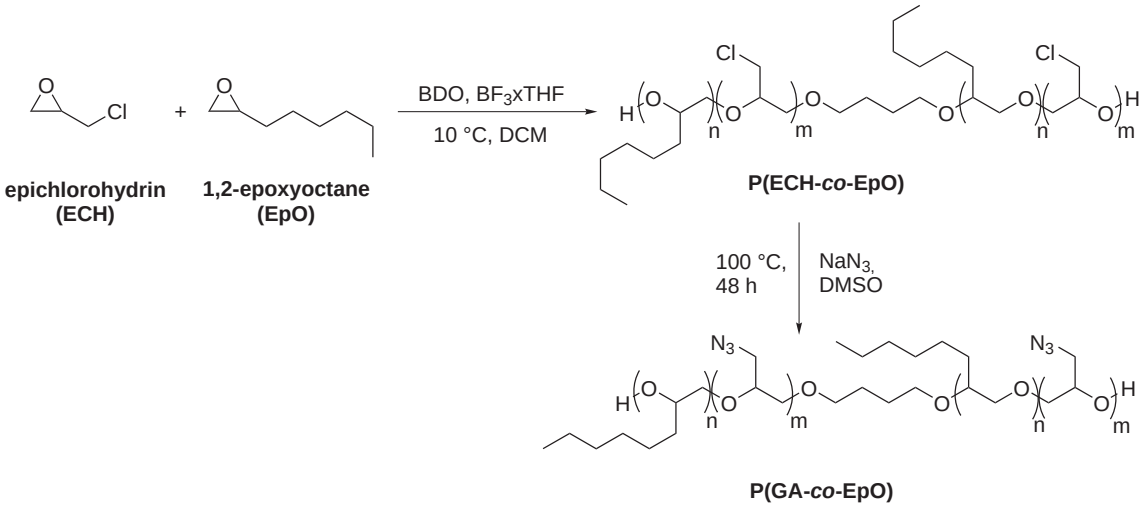

Figure 5.19 Synthesis of P(GA-*co*-EpO) copolymers. P(ECH-*co*-EpO) copolymers were synthesized via cationic ring-opening polymerization and azidated by a subsequent synthesis step.

The molecular weight distributions of the synthesized P(GA-*co*-EpO) copolymers were determined by GPC. The obtained curves are presented as an overlay in Figure 5.20. The results are also summarized in Table 5.11. The GPC curves of the respective PECH precursor copolymers can be found in Appendix A.1.1. The distributions are monomodal over the whole range from 10 mol % EpO content to the pure homopolymer P(EpO) which showed the most narrow distribution in this experimental series with a PDI of 1.42. The shoulder peaks are still small even for a 50:50 composition of the comonomers. The utilized synthesis can therefore be considered as suitable for the chosen copolymer system, providing the possibility to vary the comonomer content

Table 5.11 Detailed data about the molecular weight distributions of synthesized P(EpO) **15** and P(GA-*co*-EpO) copolymers **24**–**27** with different molecular compositions.

No.	Composition [a]	[M]/[I] (th.)	M_n [b] [g/mol]	PDI [c]
15	P(EpO)	30	2612	1.42
24	P($GA_{0.89}$-*co*-$EpO_{0.11}$)	30	1800	1.73
25	P($GA_{0.74}$-*co*-$EpO_{0.26}$)	30	1972	1.90
26	P($GA_{0.63}$-*co*-$EpO_{0.37}$)	30	1553	1.66
27	P($GA_{0.47}$-*co*-$EpO_{0.53}$)	30	1831	1.83

[a] Real composition calculated by ^{1}H NMR spectroscopy.
[b] Determined by GPC (THF, PS standard).
[c] PDI = M_w/M_n

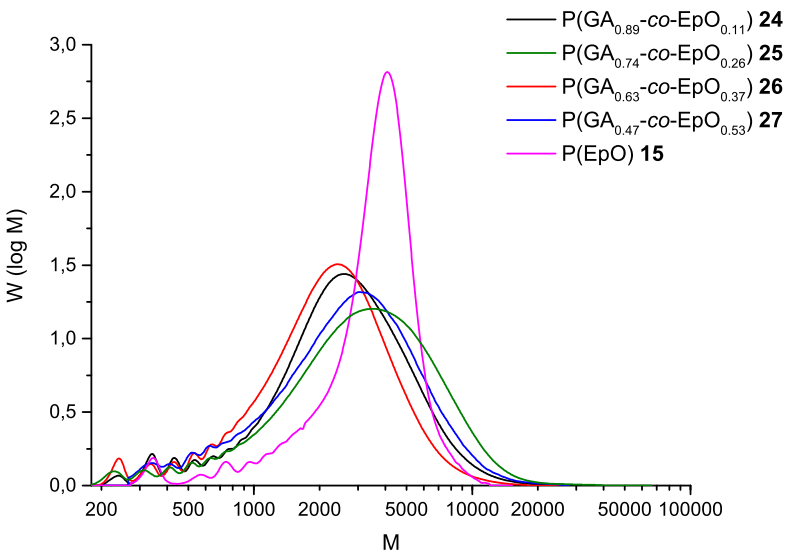

Figure 5.20 GPC curves of synthesized P(GA-*co*-EpO) copolymers with different molecular compositions and P(EpO).

depending on the desired properties of the copolymer and the specific application scenario of the binder.

Glass Transition Temperatures

The influence of the molecular composition on the low-temperature properties of the synthesized P(GA-*co*-EpO) copolymers **24**–**27** was investigated by DSC. The results of the measurements are presented in Figure 5.21. Further detailed information can be found in the experimental section. By increasing the amount of 1,2-epoxyoctane (EpO) that is incorporated in the polymer backbone, the glass transition temperature (T_g) is lowered. For the commercial GAP (Lot 06S12) homopolymer from Eurenco, a T_g of $-48.7\,°C$ was measured and for the pure P(EpO) homopolymer a value of $T_g = -72.9\,°C$ was determined. This is supposed to be the lowest possible value that can be achieved for P(GA-*co*-EpO) copolymers in the targeted M_n range of approximately $2000\,g/mol$. The decrease of the glass transition temperature between those two limiting values can be expressed by a simple exponential regression fit (5.3) that is given below. By applying this fitting curve, the T_g can be estimated approximately for all possible molecular compositions.

$$T_g = -75.60603 + 26.6856 \cdot e^{-0.02243x} \tag{5.3}$$

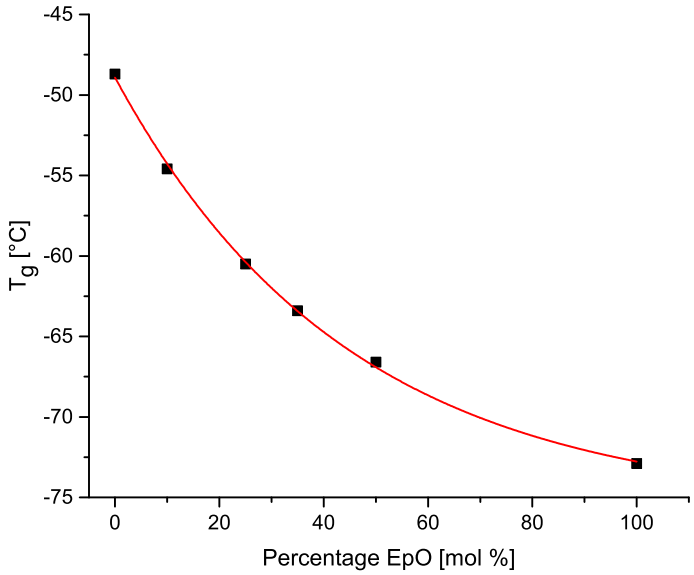

Figure 5.21 Influence of the molecular composition on the glass transition temperature (T_g) of P(GA-*co*-EpO) copolymers.

Viscosity and Density

The analysis of *n*-alkyl substituted glycidyl azide copolymers showed a decreased viscosity compared to GAP. Viscosity measurements in dependence of the shear rate at different temperatures (20 °C, 40 °C, 60 °C) were therefore performed for all synthesized P(GA-*co*-EpO) samples to investigate the influence of the molecular composition on the viscosity of the respective copolymers. The results are summarized in Table 5.12

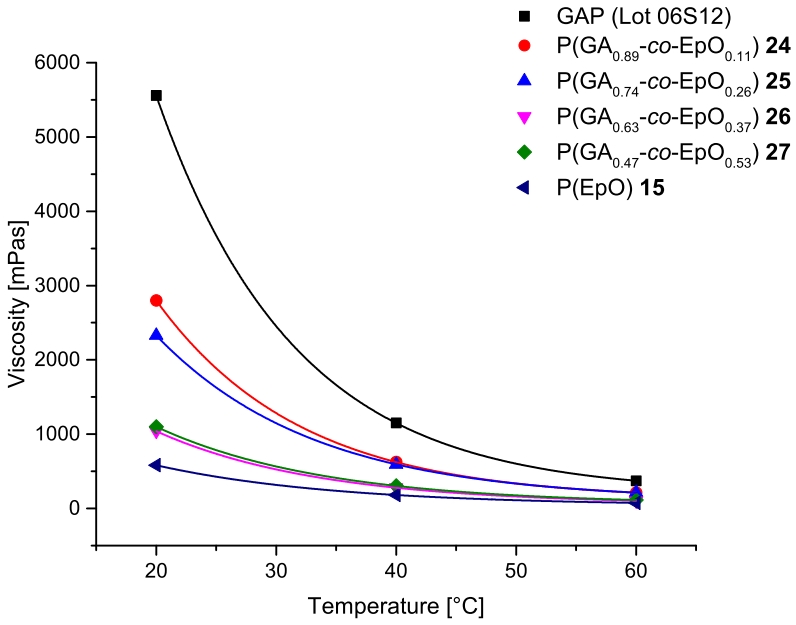

Figure 5.22 Influence of the molecular composition of various P(GA-*co*-EpO) copolymers on the viscosity. Measurements were performed for 20 °C, 40 °C, 60 °C. Values are presented for a shear rate of $10\,s^{-1}$.

Table 5.12 Viscosity and density measurements of synthesized P(GA-*co*-EpO) copolymers ([M]/[I] = 30) with various molecular compositions.

No.	Composition [a]	η [b] [mPas] @ 20 °C	η [b] [mPas] @ 40 °C	η [b] [mPas] @ 60 °C	ρ [c] [g/cm^3]
—	GAP (Lot 06S12)	5560	1150	373	1.284
24	P($GA_{0.89}$-*co*-$EpO_{0.11}$)	2800	624	212	1.080
25	P($GA_{0.74}$-*co*-$EpO_{0.26}$)	2330	594	213	1.140
26	P($GA_{0.63}$-*co*-$EpO_{0.37}$)	1040	279	104	1.098
27	P($GA_{0.47}$-*co*-$EpO_{0.53}$)	1100	304	114	1.038
15	P(EpO)	582	181	75	0.913

[a] Real composition calculated by ^{1}H NMR spectroscopy.
[b] Measured at a shear rate of $10\,s^{-1}$.
[c] Measured at 20 °C.

and visualized as an overlay in Figure 5.22. The commercial GAP (Lot 06S12) showed by far the highest viscosity of 5560 mPas at 20 °C. The synthesized copolymers showed reduced viscosities over the whole range of investigated temperatures compared to GAP. Especially at 20 °C, huge differences between the viscosity values can be noticed. At 60 °C, the differences became merely small but the possibility of shifting the propellant mixing process to lower temperatures provides clear advantages as already discussed in the previous section. Therefore, the synthesized copolymers clearly provide a better processability compared to GAP.

The measured densities are in a range between 1.038 g/cm^3 and 1.140 g/cm^3 and did not follow a clear trend for the increasing content of *n*-hexyl substituted units. Compared to the pure GAP homopolymer with a density of 1.284 g/cm^3 (Table 5.9) all P(GA-*co*-EpO) copolymers exhibit a significantly reduced density which is explainable by the introduction of bulky substituents that have a higher sterical hindrance.

End Group Analysis

All results of the end group measurements are summarized in Table 5.13. The experiments showed a high variance in the hydroxyl values and equivalent weights. This may be caused by different amounts of oligomers that were formed in the polymerization reaction. Especially cyclic oligomers are a problem, because they can not contribute to the acetylation reaction due to the missing free hydroxyl chain ends and will therefore affect the measurement. Nevertheless, all synthesized copolymers exhibited equivalent weights in a range that are suitable for the isocyanate based curing systems in a range of 873 g/mol to 1396 g/mol. Already gained experiences in established GAP curing systems can be easier transferred to a new binder when the equivalent weights are close to each other. P($GA_{0.74}$-*co*-$EpO_{0.26}$) **25** is therefore particularly suitable.

Table 5.13 Data of end group analysis of P(GA-*co*-EpO) copolymers with different molecular compositions.

No.	Composition [a]	OH-Value [b] [mg KOH/g]	Equivalent Weight [b] [g/mol]
-	GAP (Lot 06S12)	46.33	1211
24	P($GA_{0.89}$-*co*-$EpO_{0.11}$)	54.19	1035
25	P($GA_{0.74}$-*co*-$EpO_{0.26}$)	40.19	1396
26	P($GA_{0.63}$-*co*-$EpO_{0.37}$)	64.26	873
27	P($GA_{0.47}$-*co*-$EpO_{0.53}$)	58.18	964

[a] Real composition calculated by ^{1}H NMR spectroscopy.
[b] Determined by titration.

5.4 Results and Discussion: Decomposition and Energetic Properties

Based on the obtained physicochemical data of novel synthesized *n*-alkyl substituted glycidyl azide copolymers, P(GA-*co*-EpO) copolymers were identified as the most suitable prepolymers for further evaluation in propellant formulation experiments, especially the molecular composition P($GA_{0.74}$-*co*-$EpO_{0.26}$) **25**. This copolymer showed low viscosity and a low glass transition temperature, while still providing a nitrogen content of 28.45 wt. % (Table 5.14). The investigations concerning decomposition behavior and energetic properties were performed for all P(GA-*co*-EpO) copolymers. A special focus was on the sample **25** with a molecular composition of approximately 75:25 (GA/EpO). The decomposition of the halogenated precursor polymers P(ECH-*co*-EpO) is also briefly discussed.

5.4.1 Decomposition of Precursors

Thermogravimetric analysis of the halogenated precursor copolymers showed a typical one-step degradation of the non-energetic polymer backbone at approximately 320 °C. An example is shown as an overlay of TGA measurements of P($ECH_{0.75}$-*co*-$EpO_{0.25}$) **10**

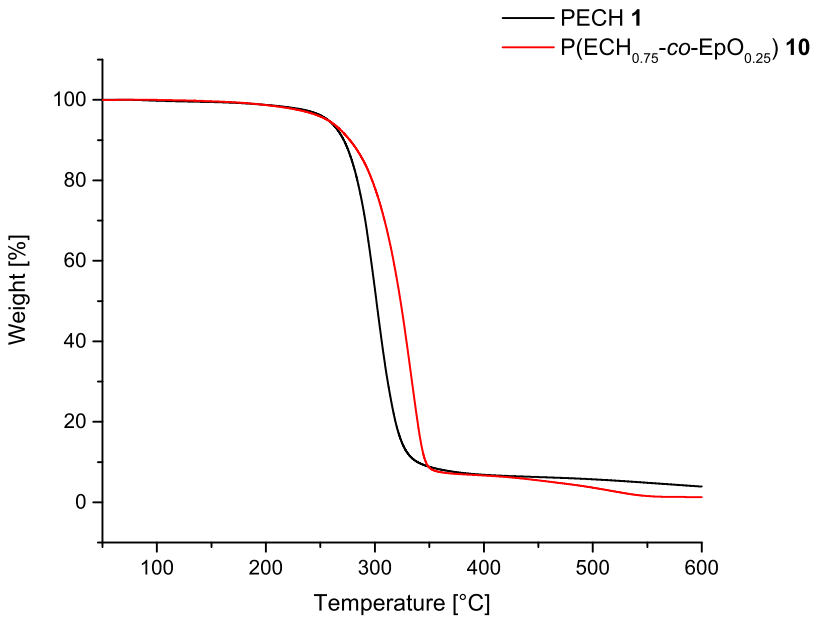

Figure 5.23 TGA curve of P($ECH_{0.75}$-*co*-$EpO_{0.25}$) **10** in comparison to the PECH **1** homopolymer. Both polymer samples exhibited a similar thermal stability up to 250 °C (HR = 5 K/min).

and PECH **1** in Figure 5.23. In comparison to PECH **1**, the copolymer **10** exhibited the same thermal stability up to 250 °C followed by a sharp weight loss at 318.7 °C. The degradation of the polymer backbone is finished at around 550 °C and a solid residue of 1.5 % of the initial weight was determined. All other synthesized halogen precursors showed a similar decomposition profile, the complete TGA data are presented in the experimental section for the respective copolymers.

5.4.2 Decomposition of Azido Polymers

Beside a low viscosity and low glass transition temperature, good thermal stability is an important characteristic of an energetic binder. As a first step to investigate the thermal stability, thermogravimetric analysis (TGA) and high temperature differential scanning calorimetry (DSC) experiments were performed.

The results of TGA and DSC measurements for the synthesized copolymer P($GA_{0.74}$-*co*-$EpO_{0.26}$) **25** is presented as an overlay in Figure 5.24. The TGA curve shows a two-step degradation process. The first drop in the curve, which corresponds to the major weight loss step, coincides with the exothermic decomposition peak of the DSC curve. This decomposition step is caused by the exothermic scission of the azido group forming molecular nitrogen which is typical for azido-based energetic polyethers [159]. The second step at around 320 °C is caused by the decomposition of the polyether

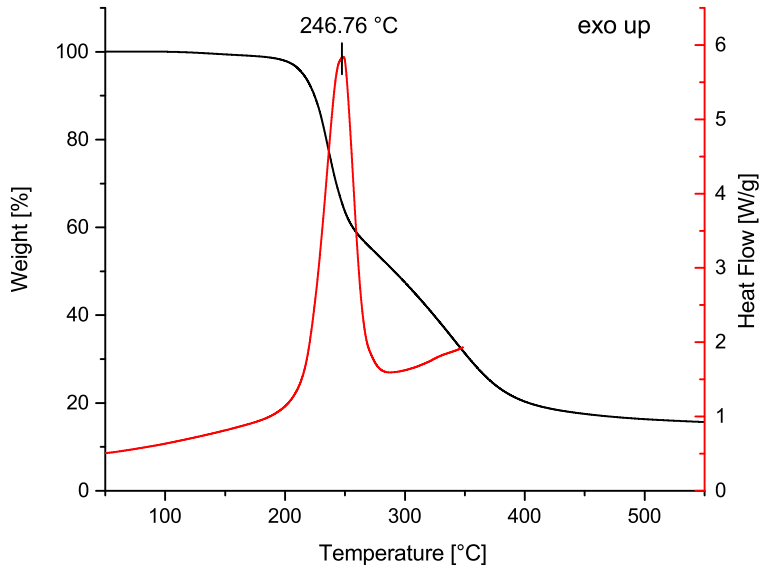

Figure 5.24 TGA and DSC curves of P($GA_{0.74}$-*co*-$EpO_{0.26}$) **25** (HR = 5 K/min).

backbone similar to the halogenated precursor polymers as discussed before. By reaching 350 °C to 400 °C, the decomposition is almost finished and a solid residue below 20 wt. % was measured in the TGA. The DSC curve shows a single exothermic peak, starting at $T_{\mathrm{Dec}} = 219.4\,°\mathrm{C}$ (onset value) with a peak maximum at 247 °C, which is caused as stated by the azido group decomposition forming molecular nitrogen N_2.

Detailed data on the TGA and DSC measurements for the P(GA-*co*-EpO) copolymers are summarized and compared to commercial GAP (Lot 06S12) in Table 5.14. The enthalpy of the first decomposition step depends on the number of azido groups in the polymer and is therefore proportional to the nitrogen content, which is decreasing with an increasing content of nonpolar plasticizing 1,2-epoxyoctane (EpO) units (Figure 5.25). Therefore, all synthesized copolymers showed a lower enthalpy of decomposition compared to GAP (Lot 06S12). With decreasing nitrogen content, the decomposition enthalpy is lowered from a value of 2430 J/g for the GAP (Lot 06S12) homopolymer to 933 J/g for the copolymer composition ($GA_{0.47}$-*co*-$EpO_{0.53}$) **27**. The pure P(EpO) homopolymer was also analyzed by DSC and showed no decomposition peak up to 350 °C, which was expected as it contains no azido groups that could decompose. The DSC curves of these measurements are presented as an overlay in Figure 5.26. The decomposition temperatures (T_{Dec}) were in a range of 218.7 °C to 221.3 °C (onset) and showed no significant variation for the analyzed copolymers, meaning that they have a similar thermal stability.

The thermal decomposition mechanism of glycidyl azide polymers was intensively studied in the literature [12] showing that the decomposition of azido polymers starts by the exothermic scission of the azido ($-N_3$) bond. The measured heat release (DSC)

Table 5.14 Results of DSC and elemental analysis experiments for P(GA-*co*-EpO) copolymers with different molecular compositions.

No.	Composition [a]	TGA [b] [°C]	T_{Dec} [c] [°C]	ΔH_{Dec} [d] [J/g]	N [e] [wt. %]
—	GAP (Lot 06S12)	238.1	218.8	2430	41.89
24	P($GA_{0.89}$-*co*-$EpO_{0.11}$)	238.4	218.8	1957	35.90
25	P($GA_{0.74}$-*co*-$EpO_{0.26}$)	239.3	219.4	1661	28.45
26	P($GA_{0.63}$-*co*-$EpO_{0.37}$)	244.5	218.7	1324	23.16
27	P($GA_{0.47}$-*co*-$EpO_{0.53}$)	245.7	221.3	933	16.26
15	P(EpO)	341.6	–	–	0.00

[a] Real composition calculated by ^{1}H NMR spectroscopy.
[b] Decomposition temperature determined by TGA (inflection point).
[c] Decomposition temperature determined by DSC (onset value) up to 350 °C.
[d] Decomposition enthalpy determined by DSC.
[e] Determined by elemental analysis.

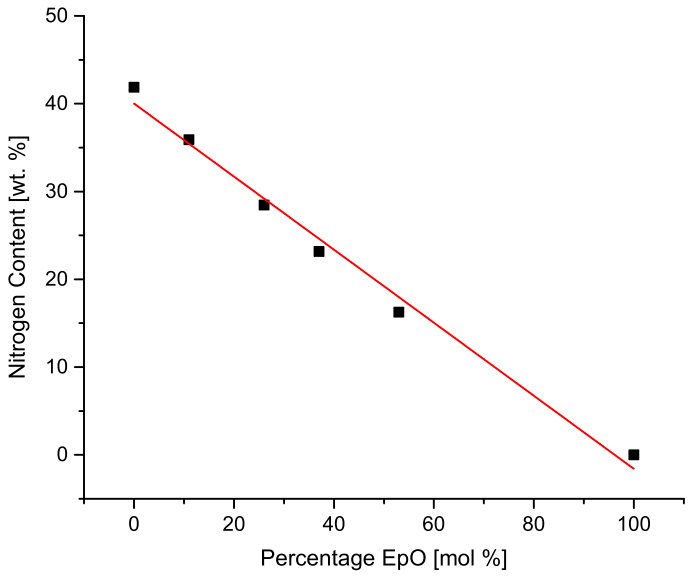

Figure 5.25 Measured nitrogen content of synthesized P(GA-*co*-EpO) copolymers in relation to the amount of EpO units. Detailed data are presented in Table 5.14.

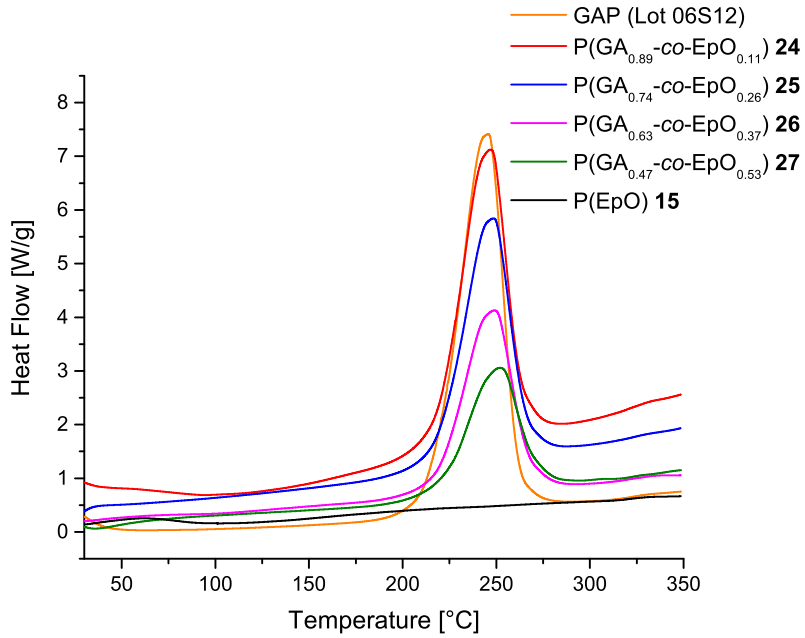

Figure 5.26 DSC curves for P(GA-*co*-EpO) copolymers with different molecular composition showing a decreasing heat flow at decomposition when the percentage of nonenergetic *n*-hexyl substituted units is increased.

derives from the elimination of molecular nitrogen by forming polymeric imines and acrylonitriles (Figure 5.27). When the polymer is further heated to higher temperatures, degradation of the backbone continues. The main decomposition products that can be detected in the gas phase contain besides other species: N_2, CO, HCN, NH_3, CH_2O, CH_4, C_2H_2 and low molecular weight oligomers of the polymer [12, 160].

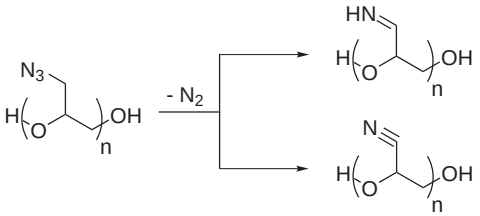

Figure 5.27 The thermal decomposition mechanism of glycidyl azide polymers [160]. Figure reproduced from [12].

Compared to GAP, the copolymers showed the same decomposition behavior with a similar decomposition temperature but a reduced enthalpy of decomposition [79, 161]. Therefore, the synthesized P(GA-*co*-EpO) copolymers can be considered to have the same thermal stability as GAP. Further thermoanalytical information about the other synthesized glycidyl azide copolymers discussed in the previous paragraphs together with their elemental analysis can be found in the experimental section.

5.4.3 Enthalpy of Formation

For the theoretical evaluation of a propellant formulation using thermodynamic computer codes like the ICT thermodynamic code or EXPLO5, an investigation of the energetic properties of the synthesized copolymer is necessary. Precise substance data about density and heat of formation are needed as an direct input for these computer codes [162].

Calculations concerning the enthalpies of formation were performed for GAP (Lot 06S12) in comparison to copolymer P($GA_{0.74}$-*co*-EpO_{26}) **25**, which was evaluated in the previous subsections to be the most suitable candidate for scale-up and formulation experiments concerning viscosity, glass transition temperature and nitrogen content. The enthalpies of formation were calculated at 298.15 K by applying the Hess thermochemical cycle, according to the literature [122]. First, the energies of combustion ($\Delta_c U$) were determined via bomb calorimetric measurements using an IKA C2000 basic bomb calorimeter following the procedure described in DIN 51900-2 [118]. The arithmetic mean value of three bomb calorimetric measurements were used for the subsequent

calculations. The combustion energies were converted to molar enthalpies of combustion ($\Delta_c H_m^0$):

$$\Delta_c H_m^0 = \Delta_c U + \Delta n RT \tag{5.4}$$

$$\Delta n = \Delta n_{\mathrm{i}}(\text{products, g}) - \Delta n_{\mathrm{i}}(\text{educts, g}) \tag{5.5}$$

For the calculations of $\Delta_f H_m^0$, the following combustion reactions were assumed:

GAP: $C_3H_5N_3O$ (s) + 3.75 O_2 (g) $\longrightarrow$ 3 CO_2 (g) + 2.5 H_2O (l) + 1.5 N_2 (g)
25: $C_{4.25}H_{7.75}N_{2.25}O$ (s) + 5.69 O_2 (g) $\longrightarrow$ 4.25 CO_2 (g) + 3.875 H_2O (l) + 1.125 N_2 (g)

Applying the literature reported enthalpies of formation of H_2O (l) (−286 kJ/mol) [123, 163] and CO_2 (g) (−394 kJ/mol) [123, 163], the enthalpies of formation ($\Delta_f H_m^0$) for the copolymer P($GA_{0.74}$-*co*-$EpO_{0.26}$) **25** and for GAP (Lot 06S12) were calculated by using the Hess thermochemical cycle leading to the following equation assuming the composition $C_aH_bN_cO_d$:

$$\Delta_f H_m^0\,(\text{copolymer}) = a\Delta_f H_m^0\,(CO_2) + 0.5b\Delta_f H_m^0\,(H_2O) - \Delta_c H_m^0\,(\text{copolymer}) \tag{5.6}$$

Results of the calculations are summarized in Table 5.15. The synthesized copolymer **25** showed a reduced enthalpy of formation in comparison to the commercial GAP sample which was expected as the nitrogen content is lowered by the incorporation of nonpolar *n*-hexyl side chains. Elemental analysis of both samples showed that copolymer **25** has a nitrogen content of 28.45 wt. % which is 13.44 wt. % lower than the nitrogen content of

Table 5.15 Energetic properties of the synthesized copolymer **25** in comparison to the commercial sample GAP (Lot 06S12).

	GAP (Lot 06S12)	P($GA_{0.74}$-*co*-$EpO_{0.26}$) **25**
Formula RU [a]	$C_3H_5N_3O$	$C_{4.25}H_{7.75}N_{2.25}O$
FW RU [a] [g/mol]	99.09	106.37
Elemental analysis	C35.34 H5.78 N41.89	C47.55 H7.42 N28.45
$-\Delta_c U$ [b] [J g^{-1}]	20312	26236
$-\Delta_c H_m^0$ [kJ mol^{-1}]	2011	2792
$\Delta_f H_m^0$ [kJ mol^{-1}]	114	9
$\Delta_f H^0$ [kJ g^{-1}]	1.15	0.08
Oxygen Balance Ω [%]	−121	−171
Sensitivity towards impact [J]	7.9 [26]	30.0
Sensitivity towards friction [N]	>360 [26]	>360

[a] Repeating unit
[b] Determined by bomb calorimetry.

the GAP sample. The obtained enthalpy of formation of 1.15 kJ/g for GAP (Lot 06S12) is close to already literature reported values. Diaz et al. stated 1.15 kJ/g for $\Delta_f H^0$ [162], Frankel et al. a slightly higher value of 1.17 kJ/g [18] and in Meyers encyclopedia of explosives a slightly higher value of 1.42 kJ/g was reported [26]. Results of calculations for the other P(GA-*co*-EpO) compositions can be found in Appendix A.1.3.

5.4.4 Sensitivity Towards Mechanical Stimuli

For the application as a component of solid propellant binders, the sensitivity of energetic prepolymers against mechanical stimuli is an important parameter. Therefore, sensitivity against impact and friction were measured and compared to literature reported data of GAP. The measurements were performed using a BAM drop hammer and friction tester according to the routines described in DIN EN 13631-4 [164] and DIN EN 13631-3 [165] respectively. The results are also presented in Table 5.15. As expected, the sensitivity against impact decreases with a decreasing nitrogen content from GAP to the synthesized copolymer P($GA_{0.74}$-*co*-$EpO_{0.26}$) **25**. Decreased sensitivity is very beneficial for the formulation of insensitive propellant mixtures and provides a clear advantage in terms of safety.

5.5 Conclusions

The scope of this chapter was the synthesis and characterization of novel glycidyl azide copolymers with nonpolar side chains that act as an internal plasticizer to provide energetic polymers with improved low-temperature properties compared to GAP. Based on commercial availability and pricing, six different oxiranes were selected that are substituted with *n*-alkyl groups having a chain length between C1 (-methyl moiety) and C12 (-dodecyl moiety). They were evaluated as comonomers for *n*-alkyl substituted glycidyl azide copolymers.

The targeted copolymers were synthesized via cationic ring-opening polymerization using BF_3xTHF as a catalyst and 1,4-butanediol as an initiator followed by a subsequent azidation leading to glycidyl azide copolymers with different *n*-alkyl side chain lengths (Figure 5.28). These copolymers were obtained as clear yellow, viscous liquids and were extensively evaluated using different characterization methods with respect to their use as prepolymers for energetic binder systems in composite solid propellants.

The introduction of nonpolar *n*-alkyl side chains showed the desired internal plasticizing effect by lowering the glass transition temperature (T_g) and the viscosity, depending on the side chain length of the comonomer and the molecular composition. Based on

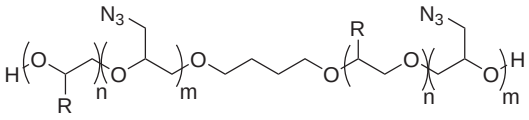

R= -Methyl, -Ethyl, -Butyl, -Hexyl, -Decyl, -Dodecyl

Figure 5.28 Molecular structures of synthesized *n*-alkyl substituted glycidyl azide copolymers.

the analysis results, P($GA_{0.74}$-*co*-$EpO_{0.26}$) **25** was selected as the most suitable prepolymer for further evaluation in scale-up and formulation experiments. DSC and TGA measurements showed a thermal stability and decomposition behavior similar to GAP, with the difference of a lower decomposition enthalpy and a lower heat of formation. This is a consequence of the azido group substitution with non-energetic alkyl groups leading to a lower nitrogen content. Likewise, the sensitivity towards mechanical stimuli (friction and impact) is lower compared to the reference compound GAP, which is a clear advantage in terms of safety concerning the manufacturing of insensitive ammunition. End group analysis revealed equivalent weights close to commercial available GAP, meaning that the already established curing procedures based on isocyanates can be readily transferred to the novel energetic copolymer with improved low-temperature

Table 5.16 Analysis summary of P($GA_{0.74}$-*co*-$EpO_{0.26}$) **25** in comparison to commercial GAP (Lot 06S12).

	GAP (Lot 06S12)	P($GA_{0.74}$-*co*-$EpO_{0.26}$) **25**
Formula RU [a]	$C_3H_5N_3O$	$C_{4.25}H_{7.75}N_{2.25}O$
FW RU [a] [g/mol]	99.09	106.37
Elemental analysis	C35.34 H5.78 N41.89	C47.55 H7.42 N28.45
M_n [g/mol]	2507	1972
Equivalent weight [g/mol]	1211	1397
T_g [°C]	−48.7	−60.5
Viscosity η [b] [mPas]	5560	2330
Density [g/cm^3]	1.284	1.140
T_{Dec} [c] [°C]	217.0	219.4
$\Delta_f H^0_m$ [kJ/mol]	114	9
$\Delta_f H^0$ [kJ/g]	1.15	0.08
Oxygen Balance Ω [%]	−121	−171
Sensitivity towards impact [J]	7.9 [26]	30.0
Sensitivity towards friction [N]	>360 [26]	>360

[a] Repeating unit
[b] Measured at 20 °C, 10 s^{-1}.
[c] Decomposition temperature determined by DSC (onset value).

properties. Table 5.16 summarizes the analysis results of P($GA_{0.74}$-*co*-$EpO_{0.26}$) **25** in comparison to the commercial GAP (Lot 06S12) provided by Eurenco Bofors. Scale-up experiments and the theoretical and practical evaluation of P($GA_{0.74}$-*co*-$EpO_{0.26}$) **25** in composite model propellant formulations will be discussed in the following chapters.

6 Scale-Up Experiments

Abstract This chapter describes the scale-up experiments performed for the synthesis of P($GA_{0.75}$-*co*-$EpO_{0.25}$) to provide enough material for further studies. For an evaluation in composite model propellant formulations, an estimated amount of at least 500 g was required. Batch size of the polymerization was therefore increased to 100 g and repeated multiple times. The reproducibility of the polymerization step was investigated by analysis of the several lots of P($ECH_{0.75}$-*co*-$EpO_{0.25}$) that were synthesized according to the same synthesis procedure. The process showed high reproducibility concerning the molecular composition, molecular weight distribution and material properties like glass transition temperature or density. The individual P($ECH_{0.75}$-*co*-$EpO_{0.25}$) lots were combined to yield two different homogeneous batches that were separately azidated by using a NaN_3/DMSO mixture in a subsequently following synthesis step. The two obtained lots of P($GA_{0.75}$-*co*-$EpO_{0.25}$), with a total mass of 775.75 g, were analyzed and compared to each other. Both batches showed very similar properties and were considered to be suitable for the formulation experiments described in the next chapter.

6.1 Experimental Part

6.1.1 Materials

Dichloromethane (DCM) was refluxed over P_2O_5 for 4 hours, distilled and stored over 4 Å molecular sieves. 1,4-Butanediol was purchased from Sigma-Aldrich, stored over 4 Å molecular sieves and used without further purification. BF_3xTHF was purchased from Sigma-Aldrich and stored under nitrogen in a fridge. 1,2-Epoxyoctane was purchased from Chemical Point (purity >97 % (GC) as stated in the data sheet), distilled over CaH_2 and stored under nitrogen atmosphere over 4 Å molecular sieves in a fridge. Water content is crucial for cationic ring-opening polymerization and was therefore determined by Karl Fischer titration for each reagent and the polymerization solvent DCM pior to the experiments. Specific distillation data and water contents are presented in Table 6.1. Sodium azide $\geq$ 99.0 % was purchased from Dynamit Nobel and used without further

purification. DMSO synthesis grade was purchased from Merck and used as received. GAP (Lot 06S12) was purchased from Eurenco Bofors.

Table 6.1 Distillation data and water content of polymerization chemicals.

Chemical	CAS Number	p [mbar]	T_B [a] [°C]	Water content [b] [ppm]
Dichloromethane	75-09-2	1013	39	0.012
1,4-Butanediol [c]	110-63-4	–	–	0.045
Epichlorohydrin	106-89-8	150	61	0.042
1,2-Epoxyoctan	2984-50-1	60	88	0.049

[a] Measured boiling point.
[b] Determined by Karl Fischer titration.
[c] Not distilled, used as received.

6.1.2 Synthesis of P(ECH-*co*-EpO) Copolymers

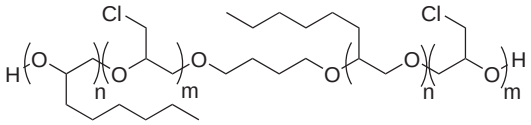

General Procedure 3 (GP3): Copolymerization In order to keep contamination with moisture as low as possible, the apparatus was evaporated to 5 mbar and flushed with dry nitrogen at 100 °C three times in cycles prior to the synthesis procedures. To a stirred mixture of 1,4-butanediol (BDO) (3.22 ml, 36.5 mmol) and dichloromethane (DCM) (7.0 ml), BF_3xTHF (0.50 ml, 4.5 mmol) was added under nitrogen atmosphere. The resulting emulsion was stirred for 15 min at 20 °C. A solution consisting of epichlorohydrin (ECH) (63.35 ml, 810 mmol), 1,2-epoxyoctane (EpO) (41.26 ml, 270 mmol) and DCM (40 ml) was added at 10 °C with a constant dosing rate of approximately 0.20 ml/min. After complete addition, the resulting clear viscous solution was stirred at 10 °C for 12 h. 100 ml of DCM was added to dilute the mixture and 30 ml distilled water was added for quenching the reaction. Then 40 ml of saturated $NaHCO_3$ solution was added and stirred for additional 15 min. The organic layer was separated and washed three times with distilled water. Neutralization was checked by pH paper. After drying over $MgSO_4$ and filtration, the solvent was evaporated at a maximum temperature of 80 °C under reduced pressure.

IR (ATR): $\tilde{\nu}$ [cm^{-1}] = 3450 (w, br), 2926 (m), 1106 (s), 746 (s). ^{1}H NMR (400 MHz, $CDCl_3$): Repeating units $\delta = 4.01 - 3.30$ (br, m, polymer backbone, CH_2Cl), $1.71 - 1.17$ (br, m, C_5H_{10}), $0.94 - 0.81$ (br, t, CH_3) ppm. ^{13}C NMR (100 MHz, $CDCl_3$): Repeating units $\delta = 80.3 - 69.1$ (polymer backbone), $46.2 - 42.9$ (RCH$_2$Cl), $32.8 - 13.7$ (C_6H$_{13}$) ppm.

P(ECH$_{0.74}$-*co*-EpO$_{0.26}$) Lot P1 Yield: 108.04 g; 96 % GPC: $M_w = 3424$ g/mol, $M_n = 1894$ g/mol, $M_p = 3205$ g/mol, PDI = 1.81. $T_g = -52.9$ °C. TGA = 314.9 °C.

P(ECH$_{0.74}$-*co*-EpO$_{0.26}$) Lot P2 Yield: 109.33 g; 97 % GPC: $M_w = 3553$ g/mol, $M_n = 1918$ g/mol, $M_p = 3537$ g/mol, PDI = 1.85. $T_g = -50.5$ °C. TGA = 333.6 °C.

P(ECH$_{0.75}$-*co*-EpO$_{0.25}$) Lot P3 Yield: 106.52 g; 94 % GPC: $M_w = 3618$ g/mol, $M_n = 1956$ g/mol, $M_p = 3582$ g/mol, PDI = 1.85. $T_g = -51.8$ °C. TGA = 331.8 °C.

P(ECH$_{0.74}$-*co*-EpO$_{0.26}$) Lot P4 Yield: 108.43 g; 96 % GPC: $M_w = 3708$ g/mol, $M_n = 2007$ g/mol, $M_p = 3801$ g/mol, PDI = 1.85. $T_g = -49.4$ °C. TGA = 334.3 °C.

P(ECH$_{0.73}$-*co*-EpO$_{0.27}$) Lot P5 Yield: 106.18 g; 94 % GPC: $M_w = 3138$ g/mol, $M_n = 1866$ g/mol, $M_p = 2814$ g/mol, PDI = 1.68. $T_g = -53.1$ °C. TGA = 327.5 °C.

P(ECH$_{0.75}$-*co*-EpO$_{0.25}$) Lot P6 Yield: 108.55 g; 96 % GPC: $M_w = 3419$ g/mol, $M_n = 1711$ g/mol, $M_p = 3185$ g/mol, PDI = 2.00. $T_g = -49.9$ °C. TGA = 323.1 °C.

P(ECH$_{0.75}$-*co*-EpO$_{0.25}$) Lot P7 Yield: 107.29 g; 95 % GPC: $M_w = 3526$ g/mol, $M_n = 1996$ g/mol, $M_p = 3416$ g/mol, PDI = 1.77. $T_g = -51.8$ °C. TGA = 302.5 °C.

P(ECH$_{0.74}$-*co*-EpO$_{0.26}$) Lot P8 Yield: 94.50 g; 84 % GPC: $M_w = 3456$ g/mol, $M_n = 1843$ g/mol, $M_p = 3328$ g/mol, PDI = 1.87. $T_g = -53.4$ °C. TGA = 303.8 °C.

P(ECH$_{0.74}$-*co*-EpO$_{0.26}$) Lot P9 Yield: 109.31 g; 97 % GPC: $M_w = 3439$ g/mol, $M_n = 1938$ g/mol, $M_p = 3124$ g/mol, PDI = 1.78. $T_g = -51.1$ °C. TGA = 306.4 °C.

6.1.3 Synthesis of P(GA-*co*-EpO) Copolymers

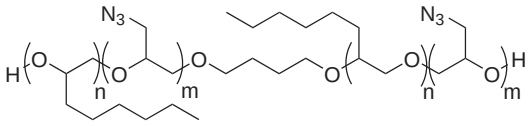

General Procedure 4 (GP4): Azidation The halogenated precursor polymer P(ECH-*co*-EpO) was dissolved in DMSO in a 3 L double-jacket reactor equipped with a thermostat and a KPG stirrer. The solution was heated up to 100 °C and sodium azide (NaN_3) was slowly added to the reaction mixture. Stirring at 100 °C was continued until IR spectroscopy showed complete conversion. After completion of the reaction, the mixture was cooled down to room temperature and EtOAC (1000 ml) together with distilled water (1000 ml) was added. The organic layer was separated and washed three times with distilled water. After drying over $MgSO_4$ and filtration, the solvent was evaporated using a rotary evaporator. Drying was continued under reduced pressure (3 mbar) for 8 h at 80 °C to remove last residues of solvent.

IR (ATR): $\tilde{\nu}$ [cm^{-1}] = 3454 (w, br), 2926 (m), 2093 (s), 1108 (s). ^{1}H NMR (400 MHz, $CDCl_3$): Repeating units $\delta = 3.99 - 3.08$ (br, m, polymer backbone, CH_2N_3), $1.72 - 1.19$ (br, m, C_5H_{10}), $0.96 - 0.81$ (br, t, CH_3) ppm. ^{13}C NMR (100 MHz, $CDCl_3$): Repeating units $\delta = 80.1 - 69.1$ (polymer backbone), $53.7 - 51.4$ (RCH$_2$N$_3$), $33.0 - 14.0$ (C_6H_{13}) ppm.

P(GA$_{0.75}$-*co*-EpO$_{0.25}$) Lot CAP1 P(GA$_{0.75}$-*co*-EpO$_{0.25}$) Lot CAP1 was synthesized following the procedure described in GP4 using P(ECH-*co*-EpO) Lots P1–P5 (total mass 485.69 g), NaN_3 (302.67 g, 4656 mmol) and DMSO (1494 ml). The product was obtained as a clear yellow viscous liquid (479.46 g).

GPC: M_w = 4122 g/mol, M_n = 2170 g/mol, M_p = 4332 g/mol, PDI = 1.90. T_g = −58.3 °C. T_d = 219.1 °C. TGA = 218.9 °C. ρ = 1.141 g/cm^3. OH-Value = 54.1 mg/g KOH. Eq. Weight = 1038 g/mol. Anal. calcd. for $C_{4.25}H_{7.75}N_{2.25}O$: C47.99 , H7.34 , N29.63; Found: C47.33 , H7.56 , N28.88.

P(GA$_{0.74}$-*co*-EpO$_{0.26}$) Lot CAP2 P(GA$_{0.74}$-*co*-EpO$_0$.26) Lot CAP2 was synthesized following the procedure described in GP4 using P(ECH-*co*-EpO) Lots P6–P9 (total mass 327.00 g), NaN_3 (201.00 g, 3092 mmol) and DMSO (1000 ml). The product was obtained as a clear yellow viscous liquid (296.29 g).

GPC: M_w = 3617 g/mol, M_n = 2228 g/mol, M_p = 3105 g/mol, PDI = 1.62. T_g = −57.8 °C. T_d = 221.2 °C. TGA = 242.0 °C. ρ = 1.147 g/cm^3. OH-Value = 50.8 mg/g KOH. Eq. Weight = 1106 g/mol. Anal. calcd. for $C_{4.25}H_{7.75}N_{2.25}O$: C47.99 , H7.34 , N29.63; Found: C47.84 , H7.53 , N29.40.

6.2 Results and Discussion

Various *n*-alkyl substituted glycidyl azide copolymers have been evaluated in Chapter 5. The novel copolymer P($GA_{0.74}$-*co*-$EpO_{0.26}$) **25** turned out to be the most interesting prepolymer for further studies in formulation experiments. These studies required sufficient amounts of copolymer material. An amount of at least 500 g copolymer was estimated for a first evaluation in binary polymer-plasticizer mixtures and model composite propellant formulations. The scale-up experiments that were necessary to obtain enough substance for the desired experiments are presented in this chapter. The batch size of the polymerization procedure delivering the halogenated precursor copolymer P($ECH_{0.75}$-*co*-$EpO_{0.25}$) was increased to 100 g. Several copolymer batches **P1**–**P9** were synthesized and combined to two master batches, which were azidated in a second synthesis step to deliver two different lots of P($GA_{0.75}$-*co*-$EpO_{0.25}$) (Lot **CAP1** and **CAP2**). The properties of the azido copolymers were compared to each other to ensure a similar product quality which is necessary in order to provide comparable results in the formulation experiments.

Concerning cationic ring-opening polymerizations, the reproducibility of the reaction is often challenging. In contrast to anionic ring-opening polymerization that strictly proceeds under living conditions, cationic ring-opening polymerizations exhibit only a 'quasi-living' character because of different side reactions that can occur (Chapter 5.1). The elaborated synthesis of P($ECH_{0.75}$-*co*-$EpO_{0.25}$) copolymer was therefore repeated several times (Figure 6.1). The respective product properties like the molecular weight

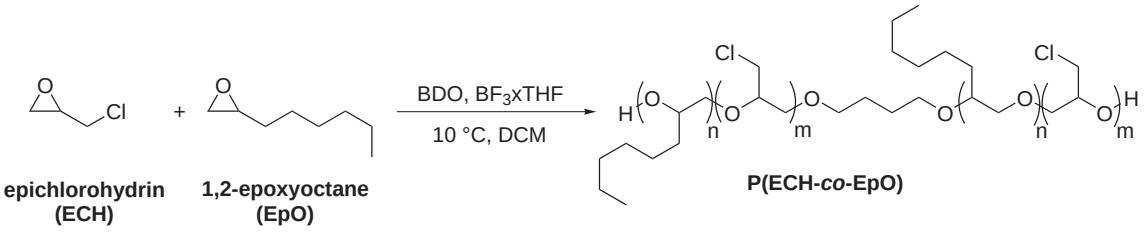

Figure 6.1 Synthesis of P($ECH_{0.75}$-*co*-$EpO_{0.25}$) in multiple batches **P1**–**P9**. After individual analysis of each batch, they were later combined to two different master batches that were used in a subsequent azidation step for the synthesis of P($GA_{0.75}$-*co*-$EpO_{0.25}$) (Lot **CAP1** and **CAP2**).

distributions, molecular compositions and glass transition temperatures (T_g) were analyzed and compared between the individual batches to assess the reproducibility of the polymerization step.

All presented polymerization experiments were performed in a 250 ml double-jacket reactor connected to a HiTec Zang reaction automation system (Figure 6.2). This

Figure 6.2 Setup for polymerization scale-up experiments. A 250 ml double-jacket reactor with magnetic stirring coupling was connected to a HiTec Zang reaction automation system.

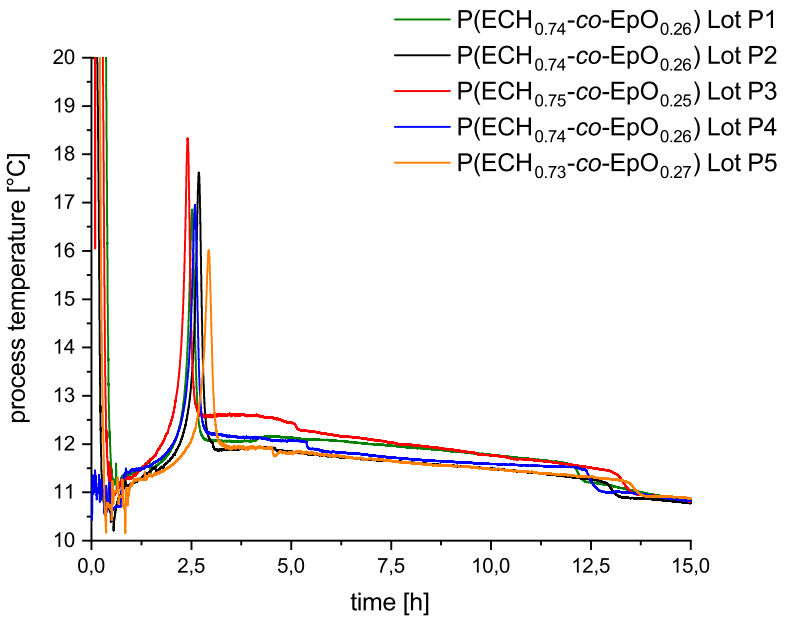

Figure 6.3 Temperature monitoring during the synthesis of the P($ECH_{0.75}$-*co*-$EpO_{0.25}$) polymerization lots **P1**–**P5**.

experimental setup provides the possibility of online temperature monitoring and repeatable dosing of the monomer solution together with an adjustable temperature control. The reaction temperature was monitored by using a Pt100 probe that was connected to the automation system to check if the reaction proceeds consistently in different polymerization batches. The recorded temperature profiles of polymerization batches **P1**–**P5** are presented as an overlay in Figure 6.3. Polymerization batches **P6**–**P9** were unfortunately not monitored due to problems with the temperature probe. The temperature profiles of the reactions **P1**–**P5** appeared to be very similar but differed slightly in the height of the signals after the induction period, which was discussed in the former chapter. These differences might be caused by small variations concerning the stirring of the initiator solution. The initial volume of the reaction bulk is very low (approx. 5 ml) compared to the end volume (approx. 200 ml). Effective stirring using the KPG stirrer, especially at the beginning of the reaction, is hard to implement because the size dimension of the stirrer was designed as a compromise to provide the most effective stirring possible over the whole range of increasing reaction volumina. The products were obtained as clear colorless viscous liquids as described in the former experiments. No discoloration of the substances were noticed. The results of the polymerizations are summarized in Table 6.2. The molecular compositions were calculated by ^{1}H NMR spectroscopy and showed values close to the theoretical composition, which was targeted

Table 6.2 Glass transition temperatures and molecular weight distributions of synthesized P($ECH_{0.75}$-*co*-$EpO_{0.25}$) lots **P1**–**P9**.

No.	Composition [a]	[M]/[I]	M_n [b] [g/mol]	M_p [b] [g/mol]	PDI [c]	T_g [d] [°C]
Lot P1	P($ECH_{0.74}$-*co*-$EpH_{0.26}$)	30	1894	3205	1.81	−52.9
Lot P2	P($ECH_{0.74}$-*co*-$EpH_{0.26}$)	30	1918	3537	1.85	−50.5
Lot P3	P($ECH_{0.75}$-*co*-$EpH_{0.25}$)	30	1956	3582	1.85	−51.8
Lot P4	P($ECH_{0.74}$-*co*-$EpH_{0.26}$)	30	2007	3801	1.85	−49.4
Lot P5	P($ECH_{0.73}$-*co*-$EpH_{0.27}$)	30	1866	2814	1.68	−53.1
Lot P6	P($ECH_{0.75}$-*co*-$EpH_{0.25}$)	30	1711	3185	2.00	−49.9
Lot P7	P($ECH_{0.75}$-*co*-$EpH_{0.25}$)	30	1996	3416	1.77	−51.8
Lot P8	P($ECH_{0.74}$-*co*-$EpH_{0.26}$)	30	1843	3328	1.87	−53.4
Lot P9	P($ECH_{0.74}$-*co*-$EpH_{0.26}$)	30	1938	3124	1.78	−51.1
Arithmetic mean $\bar{x}$		-	1903	3332	1.83	−51.5
Standard deviation s		-	91	292	0.09	1.5

[a] Real composition calculated by ^{1}H NMR spectroscopy.
[b] Determined by GPC (THF, PS standard).
[c] PDI = M_w/M_n
[d] Determined by DSC (HR 10 °C min^{-1}).

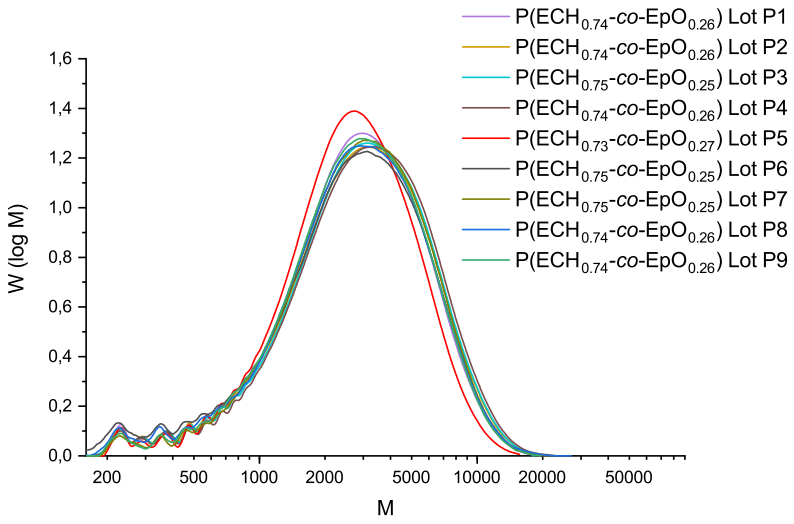

Figure 6.4 Molecular weight distributions of synthesized P($ECH_{0.75}$-*co*-$EpO_{0.25}$) lots **P1**–**P9**.

at 75 mol % : 25 mol %. The molecular weight distributions of P(ECH-*co*-EpO) lots **P1**–**P9** that were determined by GPC measurements, are presented as an overlay in Figure 6.4. They showed a monomodal curve with a high reproducibility. The molecular distributions turned out to be narrow with a PDI of 1.83 ± 0.09 and a number average molecular weight of 1903 ± 91 g/mol. Lot **P5** can be considered as an outlier, because the stirrer was accidentally set to a lower stirring speed compared to the other lots. Nevertheless, the molecular weight distribution was decided to be close enough to the others to use the copolymer **P5** in a combined batch and was therefore also included in the calculation of mean values $\overline{x}$ and standard deviations s as presented in Table 6.2. The glass transition temperatures were determined by DSC measurements and showed a range of $-53.4\,°C$ to $-49.4\,°C$ with an arithmetic mean value of $-51.5 \pm 1.5\,°C$.

After individual analysis of the copolymerization lots **P1**–**P9**, they were combined to two different batches. The lots **P1**–**P5** were combined to deliver the homogeneous batch **CP1** and the lots **P6**–**P9** were combined to yield the homogeneous batch **CP2**.

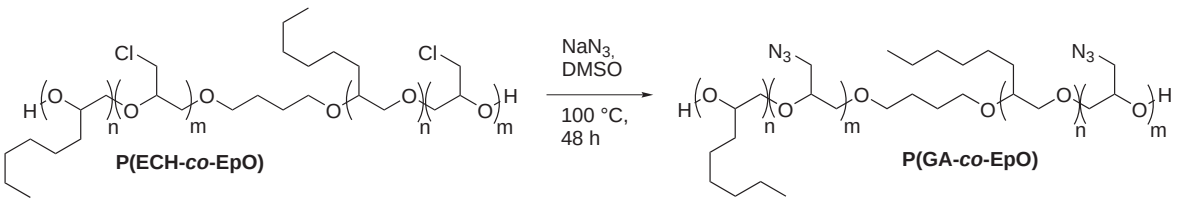

Figure 6.5 Synthesis of P($GA_{0.75}$-*co*-$EpO_{0.25}$) (**CAP1**, **CAP2**) by azidation of P($ECH_{0.75}$-*co*-$EpO_{0.25}$) (**P1**–**P9**) using a NaN_3 / DMSO mixture at 100 °C.

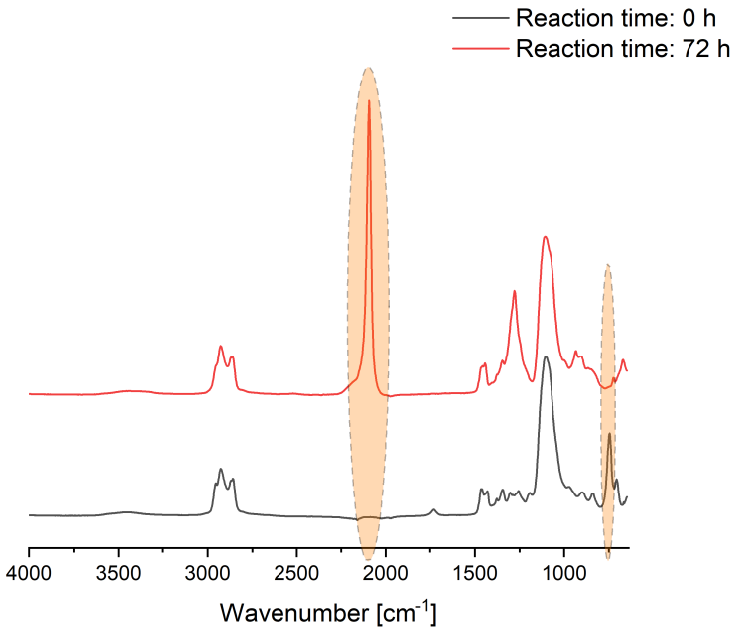

Figure 6.6 IR spectroscopy was used to monitor the azidation reaction of experiment **CAP1** and **CAP1**. The graph shows the monitoring of **CAP1** as an example. Spectrum confirmed complete conversion after 72 h due to missing chloromethyl signal at wavenumer 745 cm^{-1}.

Figure 6.7 Azidation setup for experiments **CAP1** and **CAP2**. 3 L double-jacket reactor equipped with KPG stirrer connected to a Huber unistat. Left picture was taken during the reaction, the right picture shows the phase separation during the first extracting step after quenching.

Both combined batches (lot **CP1** and **CP2**) were azidated individually using the azidation procedure that was established in the previous experiments (Figure 6.5). The prepolymer was dissolved in DMSO and treated with sodium azide at 100 °C until full conversion could be confirmed by IR spectroscopy. The reaction monitoring using IR of experiment **CAP1** is presented as an example in Figure 6.6. At the wavenumer 2100 cm^{-1} the appearance of an azido signal was observed, while the signal intensity of the chloromethyl group at 745 cm^{-1} decreased over time until the signal disappeared once the reaction was finished. The setup used for this reaction was a 3 L double-jacket reactor equipped with KPG stirrer and a Huber unistat (Figure 6.7). Two separate P(GA-*co*-EpO) lots **CAP1** and **CAP2** were obtained and characterized. Table 6.3 shows the corresponding analysis data concerning MWD and molecular compositions.

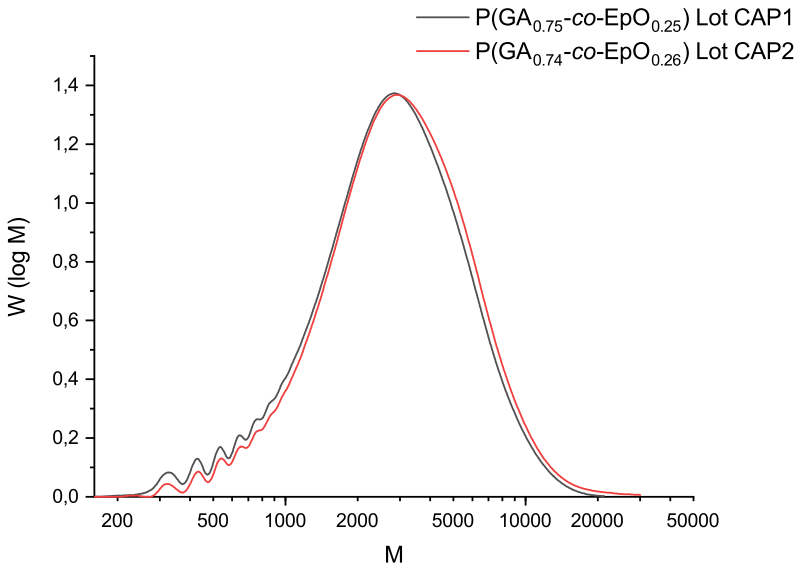

Figure 6.8 GPC curves of synthesized P($GA_{0.75}$-*co*-$EpO_{0.25}$) batches **CAP1** and **CAP2**. Both copolymers showed a narrow distribution with similar characteristics.

Table 6.3 Experimental data of P(GA-*co*-EpO) lots **CAP1** and **CAP2**. The combined P(ECH-*co*-EpO) batches **CP1** and **CP2** were used as reagents.

Exp. No.	Educt batch	Composition [a]	M_n [b] [g/mol]	PDI [c]
CAP1	CP1 (P1–P5)	P($GA_{0.75}$-*co*-$EpH_{0.25}$)	2228	1.90
CAP2	CP2 (P6–P9)	P($GA_{0.74}$-*co*-$EpH_{0.26}$)	2170	1.62

[a] Real composition calculated by ^{1}H NMR spectroscopy.
[b] Determined by GPC (THF, PS standard).
[c] PDI = M_w/M_n

The first synthesized lot **CAP1** was obtained with a mass of 479.46 g. The second synthesized lot **CAP2** was obtained with a mass of 296.29 g. In total, 775.75 g of P($GA_{0.75}$-*co*-$EpO_{0.25}$) copolymer was prepared in these experiments. The respective curves of the GPC measurements are presented in Figure 6.8. Both GPC curves showed a narrow distribution and close characteristics especially in the range of lower molecular weights. The established synthesis procedure can therefore be considered to provide a good reproducibility concerning the molecular weight distribution of the products. The molecular composition was checked by ^{1}H NMR spectroscopy. The ratio between GA and EpO units was close to the targeted value of 75:25 for both copolymers. Further structural information obtained by spectroscopy can be found in the experimental section.

Table 6.4 Analytical data of the scaled up P($GA_{0.75}$-*co*-$EpO_{0.25}$) lots **CAP1** and **CAP2**. Both batches are highly comparable concerning their material properties, indicating a good reproducibility of the synthesis procedure.

	Lot CAP1	Lot CAP2
Composition	P($GA_{0.75}$-*co*-$EpO_{0.25}$)	P($GA_{0.74}$-*co*-$EpO_{0.26}$)
Lot size [g]	479.46	296.29
Elemental analysis	C47.33 H7.56 N28.88	C47.84 H7.53 N29.40
M_n [g/mol]	2170	2228
Equiv. weight [g/mol]	1038	1106
T_g [°C]	−58.3	−57.8
Viscosity η [a] [mPas]	2090	2190
Density [g/cm^3]	1.141	1.147
T_{Dec} [b] [°C]	219.1	221.2
ΔH_{Dec} [c] [J/g]	1642	1619

[a] Measured at 20 °C, 10 s^{-1}.
[b] Decomposition temperature determined by DSC (onset value).
[c] Decomposition enthalpy determined by DSC.

Beside the molecular structure and molecular weight distribution, further analyses concerning viscosity, T_g and density were carried out for both synthesized copolymer lots. The results are summarized and compared to each other in Table 6.4. The glass transition temperatures were determined by DSC measurements. P($GA_{0.75}$-*co*-$EpO_{0.25}$) **CAP1** showed a T_g of −58.3 °C, the second batch P($GA_{0.76}$-*co*-$EpO_{0.24}$) **CAP2** a slightly higher value of −57.8 °C. The deviation can be considered as negligible and within the range of a typical error of DSC measurements. The viscosities of both copolymers were also measured and compared. At 20 °C and a shear rate of 10 s^{-1}, **CAP1** showed a viscosity of 2090 mPas and **CAP2** showed a value of 2190 mPas. The densities were

determined by He pycnometry and the obtained values of 1.141 g/cm^3 for lot **CAP1** and 1.147 g/cm^3 for lot **CAP2** are also very close to each other. Energetic properties were characterized by elemental analysis, thermal analysis and bomb calorimetric measurements. The results are summarized in Table 6.4. Elemental analysis revealed a nitrogen content of 28.88 wt. % for lot **CAP1** and 29.40 wt. % for lot **CAP2**. DSC and TGA experiments were performed for both lots in order to compare the decomposition behavior of the material. The results are presented in Figure 6.9 for lot **CAP1** as an example. The results for lot **CAP2** can be found in Appendix A.2.1. Both samples of P($GA_{0.75}$-*co*-$EpO_{0.25}$) showed a thermal stability similar to GAP as already pointed out in the previous experiments (Chapter 5). The decomposition temperatures were determined as the DSC onset values (T_{Dec}) at 219.1 °C (**CAP1**) and 221.2 °C (**CAP2**), respectively.

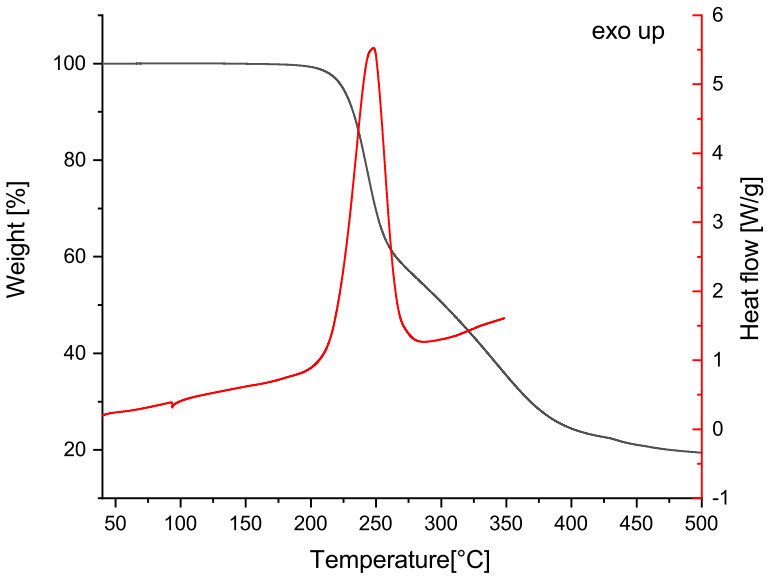

Figure 6.9 Overlay of TGA and DSC curves of P($GA_{0.75}$-*co*-$EpO_{0.25}$) **CAP1** (HR = 5 K/min).

6.3 Conclusions

The aim of the presented work in this chapter was the scale-up of the P($GA_{0.75}$-*co*-$EpO_{0.25}$) copolymer synthesis to deliver enough material for a first evaluation of the novel energetic azido-prepolymer in binary polymer-plasticizer mixtures and model composite propellants. A minimum amount of 500 g copolymer was required for these experimental

series. The main issue of the synthesis of P($GA_{0.75}$-*co*-$EpO_{0.25}$) is the reproducibility of the polymerization step. The cationic copolymerization of epichlorohydrin and 1,2-epoxyoctane was therefore scaled-up to 100 g batches and repeated multiple times to investigate the reproducibility of the product properties. The obtained P($ECH_{0.75}$-*co*-$EpO_{0.25}$) copolymers were analyzed by using IR and NMR spectroscopy for structural information and GPC measurements to determine the molecular weight distribution. ^{1}H NMR spectroscopy confirmed that the theoretical targeted composition of 75:25 was achieved for all samples. The determined molecular weight distributions were quite narrow with a PDI of 1.83 ± 0.09 and exhibited a number average molecular weight (M_n) of 1903 ± 91 g/mol. Taking the analysis results into account, the established polymerization process showed good reproducibility.

The nine synthesized lots of P($ECH_{0.75}$-*co*-$EpO_{0.25}$) were combined yielding two separate homogeneous batches. Both batches were azidated to obtain two lots of P($GA_{0.75}$-*co*-$EpO_{0.25}$) (**CAP1** and **CAP2**) with a total mass of 775.75 g. A comparison between both lots showed very similar properties indicating a reproducible synthesis procedure of the energetic azido-copolymer.

7 Formulation Studies

Abstract This chapter describes the work performed on the application of the novel P($GA_{0.75}$-*co*-$EpO_{0.25}$) copolymer in ammonium dinitramide (ADN) composite propellant formulations. An evaluation using the ICT thermodynamic code was carried out to investigate the theoretical performance of propellant binders based on the novel copolymer in comparison to conventional energetic binders based on GAP. Binary mixtures consisting of the energetic prepolymer and several commercially available plasticizers were also produced in different compositions in order to find the most suitable copolymer-plasticizer system for further studies. The properties of the respective mixtures were investigated by using DSC and viscosity measurements. Based on the analytical results, DOA turned out to be the most promising plasticizer for the binder system. For a first evaluation of the novel glycidyl azide copolymer in a model composite propellant, different formulations based on the green oxidizer ADN were manufactured and compared to the analogous GAP formulations. The experiments confirmed that the formulations based on the novel copolymer P($GA_{0.75}$-*co*-$EpO_{0.25}$) exhibit lower process viscosities and lower glass transition temperatures compared to the corresponding GAP formulations. The characterization results indicate an improved processibility of the slurry and better low-temperature properties of the cured propellant.

7.1 Introduction

7.1.1 The Solid Rocket Motor

While liquid rocket propellants are able to reach the highest performances, solid rocket motors (SRM) have the major advantage of a relatively simple setup, easy handling and application as well as a high reliability. The construction of SRMs is based on fewer moving parts compared to liquid propellant engines, which makes them less service intensive [8]. These features make SRMs the favored propulsion system for tactical missiles and space launchers, for example the Ariane IV/V boosters. SRMs are basically built by a uniform propellant grain enclosed in a casing that acts as the burning chamber (Figure 7.1). The chamber pressures of modern solid motors are typically between

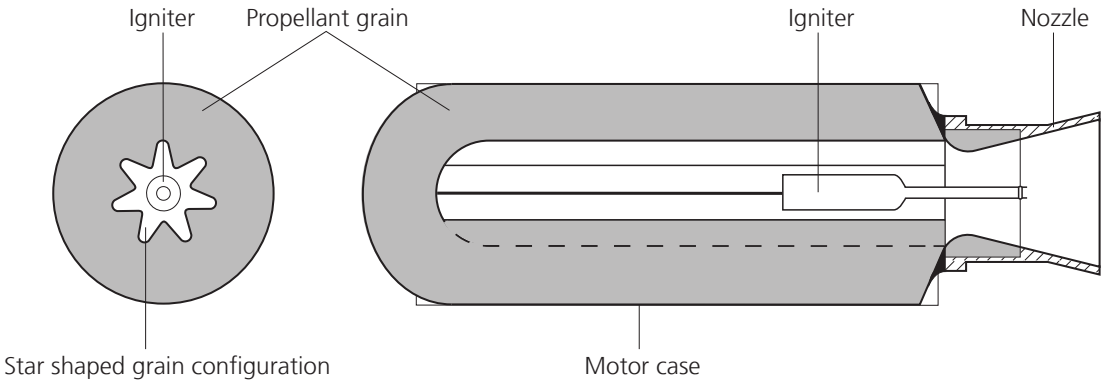

Figure 7.1 Simplified construction of a solid propellant motor. The depicted grain is case-bonded and exhibits a star-shaped configuration.

5 MPa and 10 MPa. They are especially suitable for high thrusts over a short period of time [166]. While discussing the advantages of solid propellants, it is important to emphasize their limits like the restricted thrust control which is predominantly determined by the complex grain geometry. The grain can be considered as the solid body of the cured propellant which accounts for 80 % to 94 % of the total motor mass [8]. Solid propellant grains can be devided into two main categories: free-standing grains (cartridge loaded) and case-bonded grains that are directly bound to the motor case. Typical grain configurations are end burner, internal burning tubes, segmented tubes, internal star or multiperforated. By selecting the grain geometry, the thrust over time characteristics can be effectively adjusted. For example, for a neutral burning grain the burning surface has to stay approximately constant, while for regressive burning characteristics the burning surface decreases during the combustion process. The maximum thrust of an end-burner is determined by the diameter of the grain, the defined propellant mixture and the chamber pressure. Internal burning tubes or star shaped geometries have the advantage of higher combustion surfaces, which can provide high thrusts for limited burning periods [5]. The following subsections describe the basic components and manufacturing processes of composite propellant grains.

7.1.2 Essential Components of Solid Rocket Propellants

Modern composite propellants consist of three major components [167]:

- A solid oxidizer delivering the necessary oxygen for the combustion reaction.

- A fuel, usually a metal like aluminum that acts as a reducing agent and increases the combustion temperature and performance.
- A binder, which is a polymeric organic substance that acts as an elastic matrix for the solid filler particles and as a fuel.

Oxidizer

Composite rocket propellants are characterized by a high percentage of solid crystalline oxidizer particles, which are the major component with a total amount up to 70 wt. % of the formulation or even higher [8]. Ammonium perchlorate (AP) is the most widely used oxidizer in modern high performance composite propellants to-date (Figure 7.2). The compound exhibits a high positive oxygen balance of 34.04 % and a high density of 1.96 g/cm^3 [26]. The excellent energetic properties, low price and high stability raised AP as the standard oxidizer in military applications and space launchers. Beside the mentioned outstanding properties, AP has two major disadvantages. First, the perchlorate anion ClO_4^- is toxic by causing thyroid disorders which is a severe problem for regions with highly contaminated environment [168]. The second problem is the formation of HCl that is released during the combustion. This may lead to substantial contribution to acid rain and ozone depletion by taking into account that for example the Ariane 5 booster produces 270 t of HCl at full conversion [169]. Im military applications, the HCl plume of missiles can be easily detected as a rocket signature. This can cause severe tactical drawbacks [170].

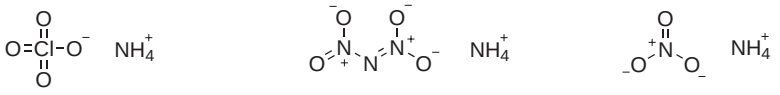

Figure 7.2 Oxidizers used in solid rocket motors (SRM) for space launchers and military applications.

Ammonium dinitramide (ADN) was developed in 1971 at the Zelinsky Institute in the former USSR as a halogen-free oxidizer, intended to overcome the drawbacks of AP [171]. The soviet technology was strictly classified and unknown to the western world until the end of the 1980s. The remarkable properties of ADN are its high energy content and signature free combustion forming products with relatively low toxicity [172]. ADN is therefore considered as a very promising 'green' oxidizer and potential AP replacement. FOI in Sweden developed a large-scale synthesis method for ADN in the 1990s, the material is nowadays commercially available from Eurenco Bofors [173]. ADN is a white

solid with a high positive oxygen balance of 25.79 %, a density of 1.81 g/cm^3 and a melting point of 93 °C [169]. Thermodynamic calculations showed that ADN based solid propellants are able to achieve higher performances compared to conventional AP based composites. By replacing AP in the widely used AP/Al/HTPB formulation with ADN, the specific impulse can be increased by 5 s to 10 s while the combustion chamber temperature is decreased [174]. Furthermore, ADN/GAP formulations have the potential to increase the performance of minimum smoke propellants by 10 % to 15 % compared to conventional double-base propellants [175]. Published results are discussing ADN formulations using GAP based binder material because of good compatibility, performance improvement and promising ballistic performance [169]. The high solubility of ADN in polar solvents provides the possibility of applying ADN as a component within liquid propellants. Due to these special properties, ADN is not only a promising green replacement for AP but also for the widely used monergol hydrazine. A viable formulation was developed by the Swedish Space Corporation (SSC) and FOI, consisting of ADN, methanol, ammonia and water. The mixture is known under the name LMP-103S. Compared to hydrazine it has the advantage of a higher density and exceeds the specific impulse of hydrazine by 6 % while being less toxic [169]. Despite promising properties, ADN propellants are still an objective of many ongoing R&D projects, barely managing the transition to real applications. Reasons are the moderate thermal stability of ADN, its highly hygroscopic behavior and compatibility problems with already established binders, plasticizers and curing systems.

Ammonium nitrate (AN) is known as one of the most important chemicals in the agriculture but can also be applied as an oxidizer for composite propellants. Compared to perchlorates, AN has to be considered as a relatively low-performance oxidizer. However, it found applications due to its low-cost production and the smokeless combustion exhibiting a comparatively low-toxicity plume [8]. One of the biggest drawbacks of AN are phase transitions between different polymorphic states that occur at atmospheric pressure below the melting point. This problem is countered by using additives like NiO or KNO_3 that change the transition temperatures. The product containing such additives can be used as an oxidizer for solid propellants and is called phase-stabilized ammonium nitrate (PSAN) [7]. Further information about green oxidizers is excellently reviewed in the literature [172, 176].

Metal Fuel

By adding metal fuels, the performance of composite propellants can be significantly improved. Different substances including alkali metals, alkaline earth metals, aluminum

(Al) and boron (B) have been evaluated regarding their capability as metals fuels for composite propellants [8, 177]. Aluminum turned out to be the most widely used fuel in composite propellants, usually with a content of around 14 wt. % to 20 wt. % in the formulation. It increases the heat of combustion, the density of the formulation and the combustion temperature. The specific impulse (I_{sp}) can therefore be increased by 15 s to 30 s compared to non-metalized formulations [6].

Beryllium (Be) raised attention because of featuring a higher combustion temperature than Al but is limited to specific applications since very toxic products are formed during combustion [5]. Boron (B) is a material with a very high energy density but some drawbacks limit the applicability. Under the typical thermodynamic conditions of the combustion chamber, B is very hard to burn quantitatively because of its relatively low vapor pressure and the formation of passivation layers. Furthermore, by favoring the formation of suboxides instead of B_2O_3 under combustion conditions, the energetic advantage over aluminum is drastically decreased in real SRMs. An exception are applications where extraordinary oxygen-rich environments can be realized in the combustion chamber (ramjets) [5, 177].

Metal hydrides like AlH_3 (alane) and BeH_2 are also discussed as attractive fuels because of a high thermal release during combustion and a rich source of hydrogen. The high reactivity and the complicated manufacturing of stable materials that provide sufficient shelf live in solid propellant compositions, prevents a practical application so far [6].

Binder

An overview about the history of binders for SRMs and energetic polymers in general is presented in Chapter 3. This section is focused on the application of the binder in formulations of composite propellants. The binder forms the matrix where the solid particles and liquid additives are embedded. The rubber-like organic polymers are not only responsible for retaining the structure and shape of the propellant grain, but also serve as a fuel in the combustion process. The binder has a strong influence on the mechanical properties, burning rate and aging properties, which are crucial for the motor reliability [8].

Modern composite propellant binders are usually made from a liquid prepolymer that is crosslinked by using a suitable curing agent, sometimes also referred as cross-linking agent, to form a three-dimensional polymeric network. Depending on the functional end-groups of the prepolymer, different curing agents can be used. The most common examples for end groups are carboxyl groups (e.g. CTPB) and hydroxyl

groups (e.g. HTPB). Prepolymers with carboxyl end groups are usually cured with epoxide or aziridine based curing agents, while prepolymers with hydroxyl groups usually require isocyanate based curing systems to form polyurethanes [177]. Sometimes three functional cross-linkers like trimethylolpropane (TMP) are necessary to increase the functionality of the prepolymer which results in a higher degree of crosslinking. Various types of isyocanates can be used as crosslinkers, differing in their reactivity, which depends on their steric and electronic structure. Examples of commonly used isocyanates in the manufacturing of propellant binders are presented in Figure 7.3. Also very common are aliphatic polyisocyanates, for example Desmodur N100, which is a biuret of hexamethylene-1,6-diisocyanate (HDI). The curing of hydroxyl-terminated

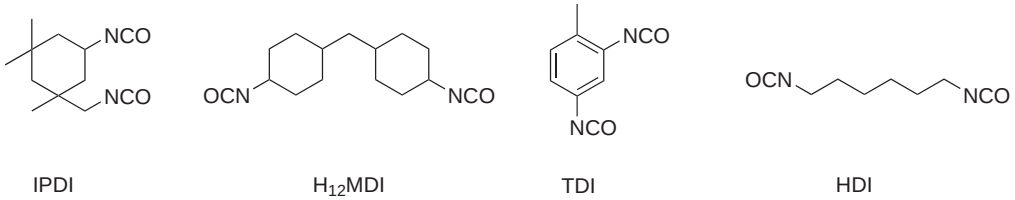

Figure 7.3 Common types of di-functional isoycanates being used for the curing of prepolymers.

prepolymers by formation of polyurethane linkages belongs to the class of step-growth polymerization reactions (Figure 7.4). In general, isocyanates are a very reactive functional group. They readily react with water, alcohols, amines and in the presence of a strong base even with themselves to form isocyanurates. Therefore, the curing reaction of propellants has to be strictly carried out under exclusion of moisture. In case of contamination with humidity, the polymerization reaction is terminated under the formation of CO_2 (Figure 7.5). This leads to voids in the polyurethane matrix, which has tremendous negative influence on the mechanical properties of the propellant grain and the combustion properties [38]. Because of superior properties concerning chemical and thermal stability and versatile processability, polyurethane based binder systems evolved to the most widely used binders for composite propellants. Their alternating hard- and softblock structure are a key feature, which provides very good mechanical properties over a wide range of temperatures [178].

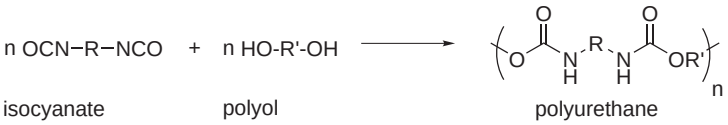

Figure 7.4 Curing of hydroxyl-terminated prepolymers with isocyanates to form an elastomeric polyurethane binder network [23].

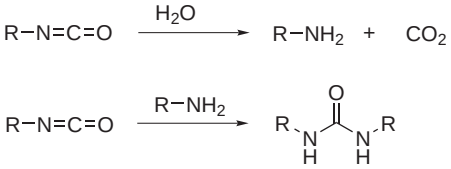

Figure 7.5 Reaction of isocyanates with water. Formation of CO_2 leads to unwanted voids in the binder matrix. The released amine will react with isocyanates to form urea derivatives [178].

The required time for curing depends on the chosen components, catalysts and applied temperature in the cast-cure process. These factors also affect the pot-life of the mixture which is the time where the formulation can still be processed before the viscosity becomes too high. Depending on the formulation, curing catalysts are sometimes required to enable complete curing in an appropriate time frame. Typical catalysts for the synthesis of polyurethanes are tertiary amines, organometallics and carboxylic acid salts. While amine catalysts primarily tend to catalyse the isocyanate-water reaction, organometallic catalysts are known to catalyse the polyol-isocyanate reaction in particular. Carboxylic acid catalysts are used to catalyse the trimerisation reaction in the production of isocyanurate foams [178]. Organometallics based on tin and other transition metals play an important role as catalysts in the manufacturing of propellant binders [177]. Dibutyltin dilaurate (DBTDL, D22) was found to be an effective curing catalyst for GAP and Desmodur N100. A reaction rate enhancement of factor 23 was achieved by applying a concentration of 50 ppm DTBTDL [179]. The proposed reaction mechanism starts with the alcoholysis of the tin complex forming a tin alkoxide which reacts with an isocyanate group to a N-coordinated tin compound. A following transfer of the alkoxide anion to the coordinated isocyanate affords N-stannylurethane which undergoes alcoholysis to form the urethane linkage [180].

Multifunctional dipolarophiles were recently investigated as an isocyanate-free curing system for GAP by exploiting the 1,3-dipolar azido groups which can be considered as an alternative curing site (Figure 7.6) [181–184]. Compounds bearing terminal dipolarophilic functional groups can readily react with the azido group in a 1,3-dipolar cycloaddition. The special case of alkines reacting with azido derivatives leading to

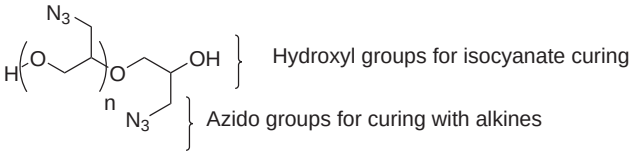

Figure 7.6 Multiple curing sites of glycidyl azide polymer (GAP).

triazoles is known as the Huisgen reaction (Figure 7.7) [185]. The products of this reaction are always obtained as a mixture of the 1,5- and 1,4- structural isomer. In contrast to the isocyanate curing reaction, no additional catalysts are needed for the cycloaddition to complete under typical propellant processing conditions. The reaction rate is determined by the electron deficiency at the alkine group, which is caused by electron withdrawing groups in the molecular structure. With activated alkines, the curing will take place in a temperature range of 35 °C to 50 °C [12]. Compared to the polyurethane synthesis, the isocyanate-free approach is less sensitive to moisture but exhibits the drawback of substantial by increasing the glass-transition temperature of the material due to the formation of the rigid triazole cross-linked structure. GAP curing using alkines is discussed in the literature as a promising isocyanate-free alternative, since ADN showed sometimes compatibility issues with isocyanates [184].

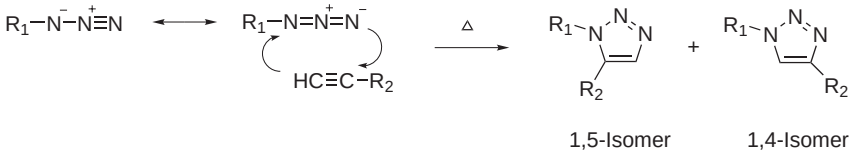

Figure 7.7 GAP curing using dipolarophiles: 1,3-Dipolar cycloaddition of an alkine with the azido group of GAP.

Plasticizer

Plasticizers are used as an additive to improve low-temperature properties and the mechanical characteristics of the propellant grain. They are extensively discussed in Chapter 3.4.

Additives

Solid propellants often contain several additives that are used in small amounts to optimize the characteristics of the formulation. The most important additives are burning-rate modifiers, stabilizers and bonding agents. Inorganic compounds like iron oxide are used as burning-rate modifiers to accelerate or decelerate the combustion reaction and to adjust the pressure exponent, which plays an important role for the pressure dependency of the burning rate. Organometallic compounds like ferrocene derivates were also identified as effective agents for accelerating the combustion [177].

Bonding agents were developed to improve the adhesion between the solid oxidizer particles and the binder network. As a result, tensile strength and effective strain of the propellant grain can be significantly improved [6]. In AP propellants, highly polar amine

compounds turned out to be very effective bonding agents. They undergo a cation exchange reaction at the particle surface and bind to the oxidizer grain. Functional groups of the bonding agent molecule react with the binder matrix in a crosslinking reaction, therefore strengthen the bonding between oxidizer and binder [186, 187]. Further information about additives can be found in the literature [6].

7.1.3 Processing of Composite Propellants

The manufacturing of composite propellants by cast-curing involves several steps. Starting with the mixing operations followed by molding, curing and finishing with analysis and quality control. The propellant slurry is prepared by mixing oxidizer particles, metal fuels and additional additives in a polymerizable liquid prepolymer followed by addition of the curing agents. The grain size distributions of the oxidizer particles have a tremendous influence on the castability of the propellant slurry as well as on the burn-rate characteristics and mechanical properties of the cured propellant [188]. The mixing for full-scale SRMs is usually performed in large kneaders, while small-scale ballistic evaluation motors or strand burners in R&D projects are often processed in other devices like small centrifugal mixers in order to safe time and material. The whole procedure is sensitive to humidity and should therefore be carried out in air conditioned laboratories trying to avoid contamination with moisture. After the components are homogeneously dispersed, the propellant slurry is casted into the motor case around a mandrel, which determines the specific grain geometry. The casting has to be performed under reduced pressure to prevent void formation. The subsequent

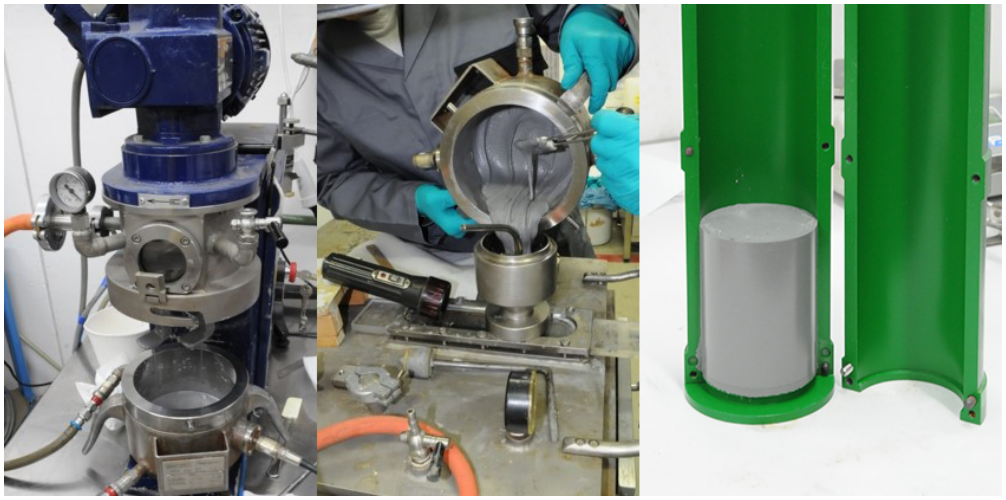

Figure 7.8 Processing of a small-scale propellant grain (end burner $\approx 350\,\mathrm{g}$) at Fraunhofer ICT. From left to right: mixing, casting and the final cured propellant grain.

curing reaction of prepolymer and curing agents builts the cross-linked elastic matrix. The complete curing process is usually performed at moderate temperatures up to 60 °C, to obtain the final propellant grain, which can weigh up to several thousand kg depending on the application [167, 189]. Figure 7.8 illustrates a composite propellant cast-cure process performed at Fraunhofer ICT.

7.2 Theoretical Evaluation

7.2.1 Methods

The ballistic performances were calculated using the ICT thermodynamic computer code [190] and the ICT thermochemical database [191]. The calculations were performed for a chamber pressure of 7 MPa, assuming an expansion ratio of 70:1. Additives such as bonding agents, curing agents, burn rate modifiers and plasticizers were not taken into account in the calculations because their contribution dependents highly on the specific formulation.

Calculations using the ICT code can be performed under hypothesis of frozen or shifting chemical equilibrium. In the frozen equilibrium method it is assumed, that the equilibrium is fixed at the exit of the chamber (before the nozzle) and remains constant during the expansion process, meaning that the composition of the products at the nozzle exit is identical to the composition inside the chamber. In contrast, the shifting equilibrium model assumes a continuous local equilibrium that shifts throughout the nozzle depending on the changing pressure and temperature conditions. The frozen equilibrium method typically predicts a slightly lower performance than the shifting equilibrium method. The shifting equilibrium method tends to overestimate by a few percent, while the real performance will be somewhere between both boundary conditions [8]. The I_{sp} and I_{spv} values in this thesis were obtained according to the shifting equilibrium model if not otherwise stated.

7.2.2 Metalized Composites

The goal of aluminized ammonium dinitramide (ADN) formulations is to obtain high performance composite propellants with a focus on outperforming conventional composites, which are usually based on the oxidizer ammonium perchlorate (AP). To study the potential performance of the synthesized copolymer in such propellants, calculations were performed for ADN composites containing 18 wt. % aluminum (Al) as the metal fuel. The results of the I_{sp} calculations are presented for a varying ADN content in

Figure 7.9. The widely used AP/Al/HTPB system with an Al content of 18 wt. % was used as a reference for the performed calculations.

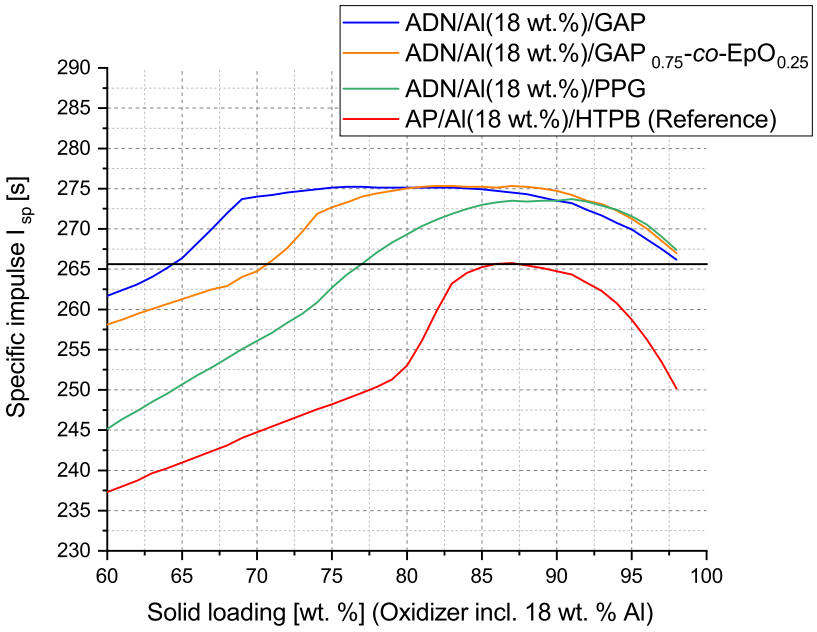

Figure 7.9 Calculations of I_{sp} for metalized ADN propellants containing 18 wt. % Al. The influence of different polyether binder materials is compared to a conventional AP/Al/HTPB system.

The theoretical performance of P($GA_{0.75}$-*co*-$EpO_{0.25}$) based formulations was between GAP and polyproylene glycol (PPG), which was selected as a completely nonenergetic reference polyether. GAP based formulations showed a significant better performance, especially at lower oxidizer contents under 75 wt. % filler level. This was expected, because of the higher nitrogen content of GAP compared to the copolymer. Due to the substitution of azidomethyl groups by nonenergetic *n*-hexyl side chains, the energy that can be released during the combustion process is decreased. By increasing the oxidizer content of the formulation, more oxidizer is present for the oxidation of the additional carbon that is bound in the *n*-hexyl side chains of P($GA_{0.75}$-*co*-$EpO_{0.25}$). This enhances the specific impulse of the respective mixture. The calculated performance of the formulations based on the copolymer therefore converges at a certain threshold of approximately 80 wt. % solid loading (incl. 18 wt. % Al) to the performance of the GAP based formulations.

Table 7.1 summarizes all calculated values for formulations containing 86 wt. % solid fillers (incl. 18 wt. % Al). This specific formulation was selected as an example, because it provides the maximum specific impulse I_{sp} of the AP/Al/HTPB composite with 265.8 s and is therefore a suitable benchmark. The formulation based on the

Table 7.1 Results of thermodynamic calculations performed with the ICT code for different aluminized propellant formulations.

	AP/Al/HTPB 68/18/14	ADN/Al/P($GA_{0.75}$-*co*-$EpO_{0.25}$) 68/18/14	ADN/Al/GAP 68/18/14
ρ [g/cm^3]	1.777	1.771	1.817
Ω [%]	–37.30	–22.42	–15.42
T_c [K]	3388.9	3692.0	3801.0
I_{sp} [s]	265.8	275.2	274.7
I_{spv} [Ns/dm^3]	4633	4780	4896

copolymer P($GA_{0.75}$-*co*-$EpO_{0.25}$) exceeds the performance of AP/Al/HTPB by 9.4 s and is approximately equal to the I_{sp} of ADN/Al/GAP. A difference can be noticed by comparing the volume specific impulse (I_{spv}) of both formulations. The formulation based on the copolymer showed a predicted I_{spv} of 4780 Ns/dm^3 which is 116 Ns/dm^3 lower than for the analogous GAP formulation. This is caused by the slightly higher theoretical density of 1.817 g/cm^3 calculated for the GAP formulation. Nevertheless, the formulation based on the novel copolymer P($GA_{0.75}$-*co*-$EpO_{0.25}$) is able to outperform the classical AP/Al/HTPB reference by 147 Ns/dm^3.

7.2.3 Non-Metalized Composites

Metalized composite propellant formulations are designed to deliver maximum performance but have the disadvantage of primary smoke production by the combustion of aluminum to form Al_2O_3, which can be detected in the exhaust jet. To prevent smoke formation, which can be detected during military operations, signature reduced propellants are desirable. A reduction of the signature may be more important than the loss of propellant performance, depending on the specific operation scenario. Pure ADN propellant formulations, free of any metal fuel additives, were therefore also evaluated using the ICT thermodynamic code. Calculations of ADN formulations based on the novel copolymer P($GA_{0.75}$-*co*-$EpO_{0.25}$) were compared to GAP and the inert polyether PPG. A propellant based on AP/HTPB was selected as the reference for the performed calculations. All results are presented as an overlay in Figure 7.10 for oxidizer contents ranging from 50 wt. % to 95 wt. %. Especially at low oxidizer amounts under 75 wt. %, the formulations based on the P($GA_{0.75}$-*co*-$EpO_{0.25}$) copolymer lacks of performance by exhibiting a significantly lower I_{sp} compared to GAP. The performance of GAP and the copolymer converge as discussed for the metalized propellants, when reaching higher oxidizer contents. The same I_{sp} is reached at approximately 83 wt. % ADN content.

83 wt. % is a solid filler content, which is considered as still processable, depending on quality and available grain sizes of the ADN prills. As a specific example, calculations for non-metalized formulations with an ADN content of 80 wt. % are summarized in Table 7.2. The ADN formulation based on the copolymer shows a slightly decreased I_{sp} of 258.21 s compared to the analogues GAP formulation (which is comparable to AP/Al/HTPB) but a significantly increased performance to the conventional AP/HTPB formulation.

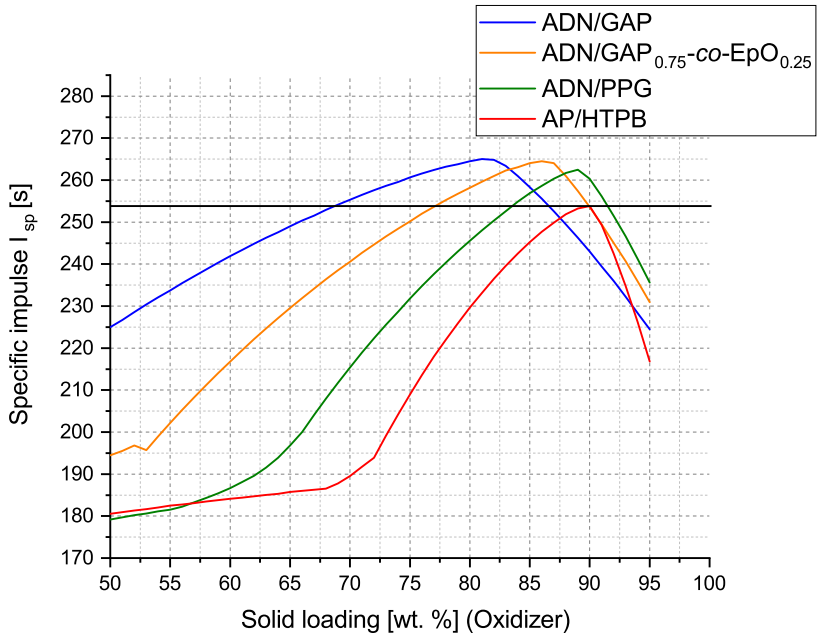

Figure 7.10 Calculated I_{sp} values for non-metalized ADN propellants, aimed to reduce the combustion signature.

Table 7.2 Results of thermodynamic calculations performed with the ICT Code for non metalized ADN propellants at an oxidizer content of 80 wt. %.

	AP/HTPB	ADN/P($GA_{0.75}$-*co*-$EpO_{0.25}$)	ADN/GAP
ρ [g/cm^3]	1.611	1.621	1.676
Ω [%]	–36.30	–13.58	–3.58
T_c [K]	2332.4	2952.1	3102.6
I_{sp} [s]	229.7	258.2	264.5
I_{spv} [Ns/dm^3]	3629	4106	4350

7.2.4 Conclusions

Calculations using the ICT thermodynamic code were carried out to evaluate the influence of nonergetic *n*-hexyl side chains of P($GA_{0.75}$-*co*-$EpO_{0.25}$) on the performance of ADN composite propellants in comparison to formulations based on GAP and PPG. The results confirmed that the substitution of azidomethyl groups by *n*-alkyl side chains clearly has a negative influence on the energetic properties by exhibiting decreased specific impulses I_{sp}, especially at low oxidizer contents. The formulations based on the novel copolymer still delivered much higher performances compared to formulations based on completely non-energetic alternatives like PPG or HTPB. By increasing the oxidizer content to reasonable values above 70 wt. % ADN, the I_{sp} values of the GAP and copolymer based formulations slowly converges. The loss of enthalpy of formation, which is caused by the introduction of the *n*-hexyl side chains may therefore be balanced by a sufficient amount of oxidizer in the formulation. The calculated ADN/P($GA_{0.75}$-*co*-$EpO_{0.25}$) propellants were clearly able to outperform conventional composites based on AP and AP/Al and can compete with GAP-based formulations.

7.3 Binary Polymer-Plasticizer Mixtures

P($GA_{0.74}$-*co*-$EpO_{0.26}$) Lot **CAP2** was synthesized as an energetic prepolymer for composite propellant formulations with a T_g of approximately −58 °C (Chapter 5). This can be considered as a significant improvement compared to the pure GAP homopolymer with a T_g of −45 °C [18]. During the propellant curing process using isocyanates, the glass transition temperature increases by roughly 10 K, depending on the respective prepolymer and curing system. This explains why GAP formulations usually need remarkable amounts of external plasticizer to meet the service temperature requirements. The minimum service temperature can be down at −54 °C depending on the propellant application scenario [16, 17]. Because the T_g of the propellant binder must fall below the specified minimum service temperature, external plasticizers may still be required when using the novel copolymer instead of GAP though notably lower amounts are targeted to avoid problems with plasticizer migration phenomena. A theoretical evaluation of common and widely available plasticizers was therefore performed, followed by the formulation and investigation of binary copolymer/plasticizer mixtures in order to find a promising copolymer/plasticizer system.

Similar to prepolymers, plasticizers can be divided into two separate groups: energetic plasticizers and non-energetic plasticizers. Though the energetic plasticizers have the superior attribute to deliver additional energy, hence in general a propellant with a

higher performance, they have the disadvantage of higher freezing points compared to non-energetic plasticizers (Table 7.3). In final cured propellant mixtures, adipates like DOA or phthalates are typically the most effective in lowering the T_g and are therefore widely used. The aim of the following propellant formulation experiments was to obtain propellants with the lowest possible glass transition temperature. Therefore non-energetic plasticizers were used while performance was not the main priority. An overview on literature reported data discussing common plasticizers is presented in Table 7.3.

Table 7.3 Literature reported data on common energetic and inert plasticizers.

Energetic plasticizer	Formula	M [g/mol]	Ω [%]	ρ [g/cm^3]	FRP [°C]	ΔH_f^0 [kJ/mol]
BuNENA [192]	$C_6H_{13}N_3O_5$	207.19	–104.25	1.22	–9	–192.47
NG [192]	$C_3H_5N_3O_9$	227.1	3.5	1.599	13.2/2.2	–370.97
EGDN [192]	$C_2H_4N_2O_6$	152.1	0.0	1.48	–22	–242.98
TMETN [192]	$C_5H_9O_9N_3$	255.1	–34.5	1.460	–15	–443.72
BTTN [192]	$C_4H_7N_3O_9$	241.1	–16.6	1.474	–27	–285.46
TEGDN [192]	$C_6H_{12}N_2O_8$	240.0	–66.6	1.335	–	–606.65
BDNPA/F [191]	$C_{7.5}H_{13}N_4O_{10}$	319.21	–57.64	1.39	–15	–620.03
DNDA-57 [191]	$C_{36}H_{92}N_{40}O_{40}$	1725.37	–72.33	1.345	–7 to –10	–576.14
Inert plasticizer	**Formula**	**M [g/mol]**	**Ω [%]**	**ρ [g/cm^3]**	**FRP [°C]**	**ΔH_f^0 [kJ/mol]**
DOA [191]	$C_{22}H_{42}O_4$	370.56	–263.37	0.925	–67.8	–1215.03
DOS [191]	$C_{26}H_{50}O_4$	426.68	–273.73	0.913	–67	–1334.70
Triacetin [191]	$C_9H_{14}O_6$	218.21	–139.31	1.160	–78	–1291.18
TOTM [94]	$C_{33}H_{54}O_6$	546.78	–254.6	0.987	–38	–
DINP [94]	$C_{26}H_{42}O_4$	418.62	–263.7	0.974	–	–
DINCH [94]	$C_{26}H_{48}O_4$	424.7	–271.3	0.942	–	–
GPO [193]	$C_{24}H_{38}O_4$	390.56	–258.1	0.983	<–67.2	–

7.3.1 Materials

Prepolymer - GAP (Lot 06S12)

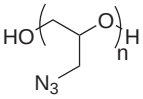

GAP Lot 06S12 was purchased from Eurenco. The following analysis data was stated in the provided datasheet:

$M_w = 2075\,\mathrm{g/mol}$, $M_n = 1904\,\mathrm{g/mol}$, PDI = 1.09. Eq. Weight = 1220 g/mol.

Prepolymer - P(GA$_{0.74}$-*co*-EpO$_{0.26}$) (Lot CAP2)

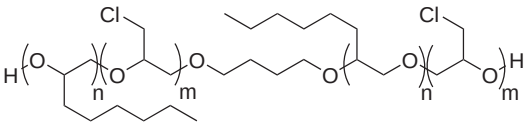

P(GA$_{0.74}$-*co*-EpO$_{0.26}$) Lot CAP2 was synthesized as described in Chapter 6. Analysis results:

$M_w = 3617\,\mathrm{g/mol}$, $M_n = 2228\,\mathrm{g/mol}$, PDI = 1.62. Eq. Weight = 1106 g/mol.

Oxsoft GPO

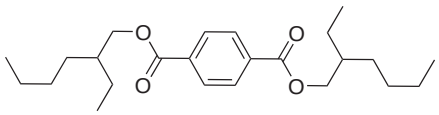

Di-(2-ethylhexyl)-1,4-benzenedicarboxylate (GPO) was received from Oxea. The plasticizer is suitable in cases where environmentally critical phthalate-based products need to be replaced. It can be used as a direct replacement for DOP (dioctyl phthalate) and also for other general purpose phthalates like DINP (diisononyl phthalate). Specifications as stated in the product datasheet:

Empirical formula: $C_{24}H_{38}O_4$. $M = 390.6\,\mathrm{g/mol}$. Density at 20 °C = $0.983\,\mathrm{g/cm^3}$. FRP at 1013 hPa < −67.2 °C. Viscosity at 25 °C = 63.0 mPas.

Palatinol TOTM

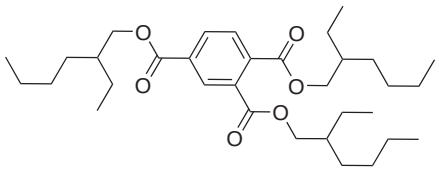

Tri-(2-ethylhexyl) trimellitate (TOTM) was received from BASF. It is primarily used as a branched monomeric plasticizer for vinyl homopolymers and copolymers thereof. TOTM is claimed to have a very low migration tendency and is therefore suitable for applications where low volatility is required [194]. TOTM is discussed in the literature

as a potential replacement for toxic phthalates [97]. Specifications as stated in the product datasheet:

Empirical formula: $C_{33}H_{54}O_6$. $M = 546.0\,\mathrm{g/mol}$. Density at 25 °C =0.984 g/cm^3. Viscosity at 20 °C: 332 mPas. No data available for FRP.

DOS

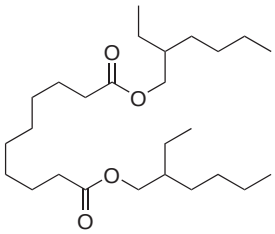

Di-(2-ethylhexyl) sebacate (DOS, DEHS, Edenol 888) was received from Silbermann GmbH & Co. KG. DOS is a plasticizer that is used for cellulose, nitrocellulose, PVA and PVC. It is known to have a low volatility and to be insoluble in water. Furthermore, DOS is characterized by a low freezing point [97]. Specifications as stated in the product datasheet:

Empirical formula: $C_{26}H_{50}O_4$. $M = 426.68\,\mathrm{g/mol}$. Density at 20 °C = 0.91 g/cm^3. FRP at 1013 hPa = −67 °C. Viscosity at 20 °C =19 mPas to 23 mPas.

Oxsoft DOA

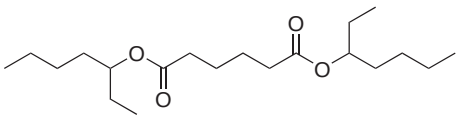

Di-(2-ethylhexyl) adipate (DOA, DEHA) was received from Oxea. DOA is a highly efficient plasticizer delivering products with excellent low-temperature flexibility and low brittle points. These characteristics lead to wide application particularly in PVC products but it is also utilized in food-contact applications [195]. Specifications as stated in the product datasheet:

Empirical formula: $C_{22}H_{42}O_4$. $M = 370.6\,\mathrm{g/mol}$. Density at 20 °C = 0.925 g/cm^3, FRP at 1013 hPa = −68 °C. Viscosity at 20 °C =13.7 mPas.

DINP

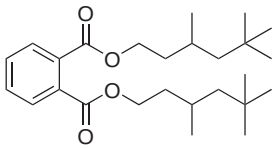

Diisononyl phthalate (DINP, Palatinol N) was received from BASF. DINP is a versatile plasticizer, which is used for PVC products and provides very good low-temperature performance. It also exhibits a low volatility [196]. Specifications as stated in the product datasheet:

Empirical formula: $C_{26}H_{42}O_4$. $M = 418.6\,\mathrm{g/mol}$. Density at 20 °C: $0.970\,\mathrm{g/cm^3}$. Viscosity at 20 °C: 82 mPas. No data available for FRP.

Hexamoll DINCH

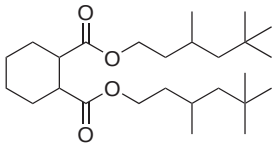

Diisononyl-1,2-cyclohexanedicarboxylic acid (DINCH) was received from BASF. The compound is synthesized by catalytic hydrogenation of diisononyl phthalate and was introduced as a replacement for the hazardous diethylhexyl phthalate (DEHP). DINCH is known to have an excellent toxicological profile, low migration rate and is specially intended for the use in applications that involve human contact [197].

Empirical formula: $C_{25}H_{48}O_4$. $M = 424.7\,\mathrm{g/mol}$. Density at 25 °C: $0.952\,\mathrm{g/cm^3}$. Viscosity at 20 °C: 52 mPas. No data available for FRP.

Triacetin

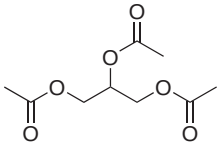

Glycerin triacetate (Triacetin, TA) was received from Merck KGaA. Triacetin is a clear colorless liquid, which is used for plasticization of synthetic rubbers and cellulose derivatives. It is also required in large scale for medical applications and as a food additive (E1518) [198]. Specifications as stated in the product datasheet:

Empirical formula: $C_9H_{14}O_6$. $M = 218.23\,\mathrm{g/mol}$. Density at 20 °C = $1.16\,\mathrm{g/cm^3}$. FRP at 1013 hPa = −78 °C. Viscosity at 20 °C =23 mPas.

7.3.2 Experimental Part

The binary polymer-plasticizer mixtures were prepared at 40 °C by weighing the substances in the stated weight fractions in a vial. Each mixture was prepared in 1.00 g sample. The mixing was performed manually with a spatula followed by treatment with a vortex mixer for 1 min. The produced mixtures were kept at room temperature for at least 7 d prior to any analysis in order to check potential phase separations. Mixtures that stayed homogeneous were analyzed by low-temperature DSC experiments and viscosity measurements in dependence of the shear-rate at 20 °C, 40 °C and 60 °C.

7.3.3 Results and Discussion

Binary mixtures of the copolymer P($GA_{0.74}$-*co*-$EpO_{0.26}$) **CAP2** and the selected non-energetic plasticzers (Table 7.4) were prepared in different weight fractions and analyzed. The results were compared to analogous GAP formulations concerning miscibility, T_g and viscosity, searching for the most suitable polymer/plasticizer system for further binder studies. DOS and DOA were selected as common representatives of the adipate and sebacate plasticizer family that is known to have excellent plasticizing properties in HTPB and PVC mixtures. Triacetin was selected as a very common inert plasticizer that is used in the rubber and also food industry. Though known to be very effective plasticizers in synthetics, small molecular weight phthalates like DBP are under REACH regulation and therefore no alternative for future research. Because of being less toxic, DINP was selected as a potential phthalate candidate that is not regulated yet. The compounds H-DINCH, GPO and TOTM are all discussed as potential replacements for DBP, hence they were evaluated in this work. Further details about the substances can be found in the materials section.

Miscibility Studies

The selected plasticizers were mixed with GAP Lot 06S12 and P($GA_{0.74}$-*co*-$EpO_{0.26}$) **CAP2** in weight fractions between 5 wt. % and 75 wt. % plasticizer content. Table 7.4 summarizes the results of the miscibility studies, further detailed information can be found in Appendix A.3.1. All prepared mixtures with P($GA_{0.74}$-*co*-$EpO_{0.26}$) **CAP2** showed no phase separation, which indicates good compatibility. In contrast, the GAP mixtures showed phase separation depending on the respective plasticizer and their weight fraction. Triacetin (TA) turned out to be the only investigated plasticizer, which showed miscibility with GAP over the whole range of applied weight fraction. In the literature, DOA is sometimes referred as compatible with GAP, which could not be

reproduced in this study [199, 200]. The GAP/DOA system showed phase separation at a DOA content above 15 wt. %. Furthermore, no significant influence of DOA on the T_g of the mixture was found by DSC experiments (Appendix A.3.1). Most of the common used inert plasticizers have a highly nonpolar structure compared to the polar polyether backbone of GAP, which should be responsible for the compatibility problems with nonpolar plasticizers like DOA or phthalates. The introduction of nonpolar *n*-hexyl chains lowers the polarity of the substance, thus increasing the interaction between prepolymer and plasticizer. Compared to GAP, a better compatibility of the

Table 7.4 Miscibility studies of GAP and P($GA_{0.74}$-*co*-$EpO_{0.26}$) **CAP2** with various non-energetic plasticizers ranging from 5 wt. % up to 75 wt. % plasticizer content. Partially miscible means at a certain plasticizer concentration phase separation occurs. Further details can be found in Appendix A.3.1.

Plasticizer	GAP	P(GA-*co*-EpO)
DOA	partially miscible	miscible
H-DINCH	not miscible	miscible
GPO	partially miscible	miscible
TOTM	not miscible	miscible
DINP	partially miscible	miscible
Triacetin	miscible	miscible

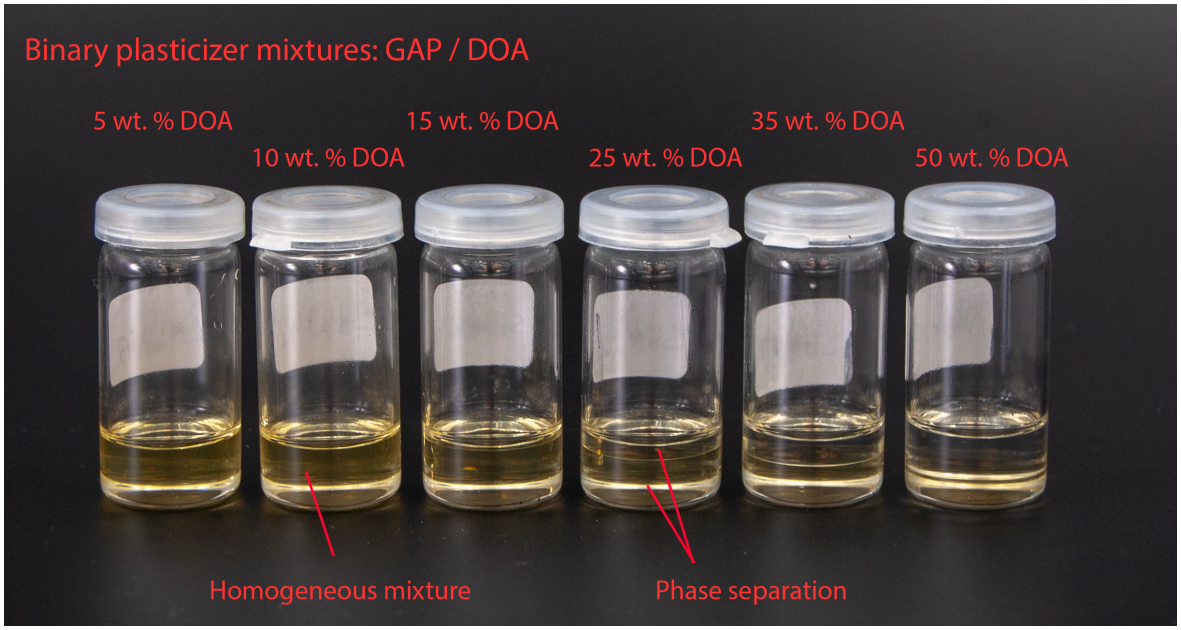

Figure 7.11 Binary mixtures of DOA and GAP ranging from 5 wt. % to 50 wt. % DOA content. The mixtures show phase separation within several hours when DOA percentages over 15 wt. % are used.

energetic prepolymer P($GA_{0.74}$-*co*-$EpO_{0.26}$) **CAP2** with common inert plasticizers can therefore be achieved. An example for partial miscibility is presented in Figure 7.11 for the GAP/DOA system. Up to 10 wt. % DOA content, the mixture appeared to be homogeneous even after weeks. In contrast, mixtures between 15 wt. % and 50 wt. % DOA content showed separation by exhibiting two distinct phases, almost immediately after finishing of the mixing. The lower, slightly yellow phase was the DOA saturated GAP phase and the upper one the DOA phase itself.

Glass Transition Temperatures of Binary Mixtures

For a more quantitative analysis, all homogeneous mixtures were investigated by low-temperature DSC measurements to determine their glass transition temperatures (T_g). Detailed information about the results can be found in Appendix A.3.1. By increasing the weight fraction of the plasticizer, the T_g can be lowered, with an efficiency depending on the specific type of the plasticizer. For the calculation of the T_g of a single-phase binary polymer/plasticizer system in Kelvin, the common Fox equation [201] can be used:

$$\frac{1}{T_g} = \frac{w_1}{T_{g1}} + \frac{w_2}{T_{g2}} \tag{7.1}$$

In this equation, w_1 is the weight fraction of the polymer and w_2 the weight fraction of the plasticizer. The equation gives a rough estimation, when only the glass transition temperatures of the pure substances are known. The interaction between polymer and plasticizer is not covered by this model. Jenckel and Heusch [202] introduced an equation based on the well-known Gordon Taylor equation [203] for modeling the T_g of binary polymer/plasticizer systems, considering also the molecular interactions:

$$T_g = w_1 T_{g1} + w_2 T_{g2} - K w_1 w_2 \tag{7.2}$$

This equation has already been used successfully in the literature to describe uncured mixtures of prepolymers with energetic plasticizers [93, 204, 205]. K can be considered as an interaction parameter, which characterizes the solvent quality of the plasticizer [206] and correlates with the free volume of the molecule [205]. The parameter K can therefore be calculated and used to benchmark the different investigated plasticizers in their ability to decrease the T_g in binary mixtures with P($GA_{0.74}$-*co*-$EpO_{0.26}$) **CAP2**. The interaction parameter K was calculated using the Levenberg-Marquardt algorithm implemented in the Origin 2018 © software (damped least squares DLS method). K was calculated for all plasticizers of the investigated mixtures, in order to find the most

effective for binders based on the copolymer. The results are summarized in Table 7.5. The related curves are presented as an overlay in Figure 7.12. DOA showed the most dominant effect by decreasing the T_g even at low plasticizer levels and is superior to all other investigated plasticizers. GPO showed a K parameter close to zero, which indicates little to none interaction between polymer and plasticizer. This leads to an almost linear regression curve. Triacetin (TA) showed an interesting behavior by exhibiting the second highest K value. The associated curve is characterized by having a high slope at lower plasticizer contents but the T_g of the pure substance is too high for a good overall performance. The results of the investigations with the copolymer can hardly be compared with GAP since GAP showed no miscibility with most of the investigated plasticizers. TA was the only GAP-compatible plasticizer, the calculated K parameter was therefore also added in Table 7.5. When comparing the different compositions of TA with GAP and P($GA_{0.74}$-*co*-$EpO_{0.26}$) **CAP2**, the mixtures based on the copolymer always show the lower T_g values, because of the superior low-temperature behavior of the copolymer itself. Detailed data about these experiments can be found in Appendix A.3.1.

Table 7.5 Calculated K parameters for binary polymer-plasticizer systems using the Jenckel Heusch equation. P($GA_{0.74}$-*co*-$EpO_{0.26}$) **CAP2** is compared to commercial GAP Lot 06S12, which was only compatible with Triacetin.

Plasticizer	Polymer	T_g [°C] ($w_1 = 0$)	T_g [°C] ($w_2 = 0.25$)	K [Kelvin]
DOA	P($GA_{0.74}$-*co*-$EpO_{0.26}$)	–105.5	–75.2	31.69 ± 1.14
Triacetin	P($GA_{0.74}$-*co*-$EpO_{0.26}$)	–69.8	–64.1	16.56 ± 0.44
DINP	P($GA_{0.74}$-*co*-$EpO_{0.26}$)	–78.5	–63.3	5.24 ± 0.87
GPO	P($GA_{0.74}$-*co*-$EpO_{0.26}$)	–83.3	–64.1	5.17 ± 1.74
DINCH	P($GA_{0.74}$-*co*-$EpO_{0.26}$)	–89.1	–66.1	2.68 ± 1.29
TOTM	P($GA_{0.74}$-*co*-$EpO_{0.26}$)	–78.8	–62.6	0.29 ± 0.99
Triacetin	GAP (Lot 06S12)	–69.8	–56.8	14.70 ± 0.66

The binary polymer-plasticizer system P($GA_{0.74}$-*co*-$EpO_{0.26}$) **CAP2** / DOA was the most effective polymer plasticizer system found in the experiments. The curve calculated with the Jenckel Heusch equation is plotted and compared to results based on the Fox equation (Figure 7.13). Especially for higher plasticizer contents above 15 wt. %, the model based on the Jenckel Heusch equation appears to be more accurate. For the case $K = 0$, meaning zero interaction, the term reduces to $T_g = w_1 T_{g1} + w_2 T_{g2}$ delivering a linear model for the pure dilution effect. Taking the results of the DSC experiments and its commercial availability into account, DOA was considered as a very promising plasticizer for binder developments based on the novel copolymer.

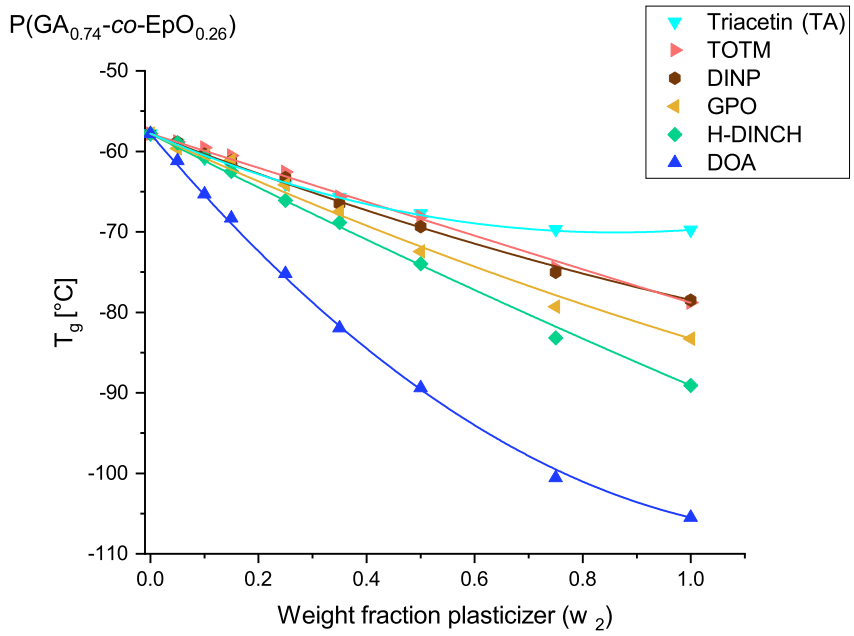

Figure 7.12 Glass transition temperatures of binary mixtures consisting of the prepolymer P($GA_{0.74}$-*co*-$EpO_{0.26}$) **CAP2** with common nonenergetic plasticizers. The curves are fitted using the Jenckel Heusch equation.

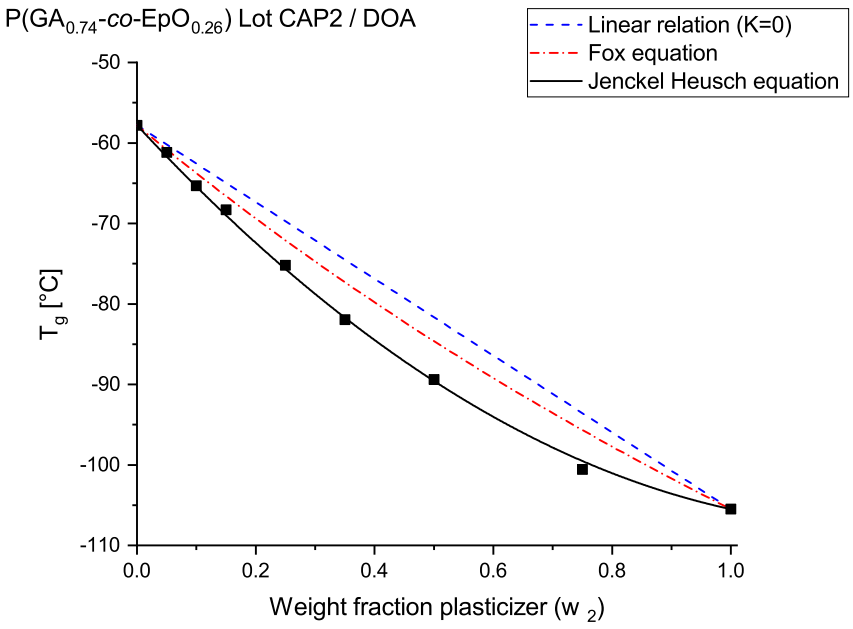

Figure 7.13 Evaluation of DOA as a plasticizer for binders based on the novel copolymer P($GA_{0.74}$-*co*-$EpO_{0.26}$) **CAP2**.

Viscosities of Binary Mixtures

Beside of lowering the T_g, reducing the viscosity is a second major indicator for the efficiency of an external plasticizer. The mixtures with 25 wt. % plasticizer content were therefore investigated concerning their rheology. The viscosity measurements at 20 °C, 40 °C and 60 °C are summarized in Figure 7.14. Further detailed information can be found in Appendix A.3.1.

The pure P($GA_{0.74}$-*co*-$EpO_{0.26}$) **CAP2** sample exhibited a viscosity of 2190 mPas at 20 °C. All tested samples showed a significant reduction of viscosity compared to the pure copolymer. Similar to the low-temperature DSC experiments, DOA showed an outstanding interaction with the copolymer by reducing the viscosity from 2190 mPas (0 wt. %DOA) to 406 mPas (25 wt. % DOA) at room temperature.

As the DOA based copolymer-plasticizer system showed the most interesting properties in the screening measurements, further studies were carried out by measuring the viscosity in dependence of the plasticizer content and temperature in order to obtain a more comprehensive characterization. Samples with DOA weight fractions from 0 wt. % to 100 wt. % were measured, the results are presented in Figure 7.15. Further information about the measurements can be found in Appendix A.3.1. The viscosity of the samples showed an exponential decrease with an increasing amount of DOA.

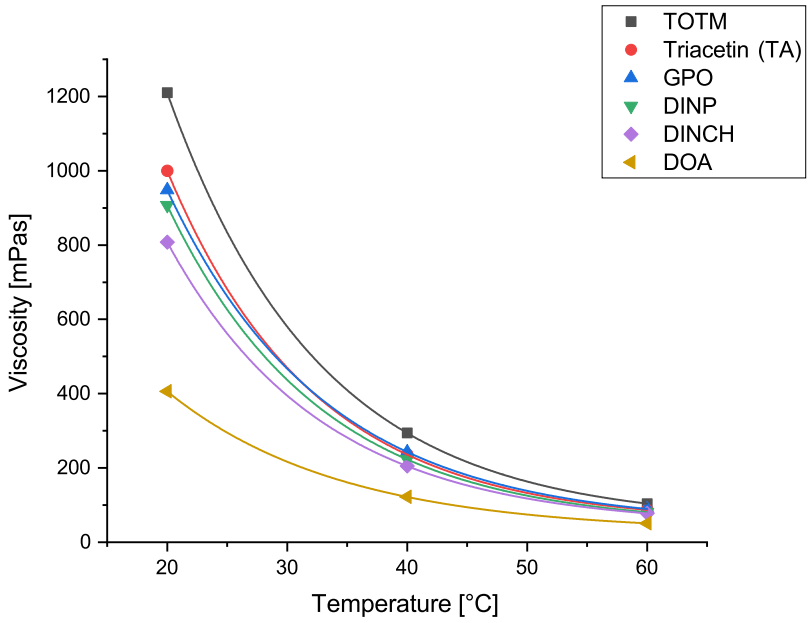

Figure 7.14 Viscosity measurements of various binary mixtures consisting of P($GA_{0.74}$-*co*-$EpO_{0.26}$) **CAP2** with a content of 25 wt. % non-energetic plasticizer. All samples were measured at 20 °C, 40 °C and 60 °C at a shear rate of 10 s^{-1}.

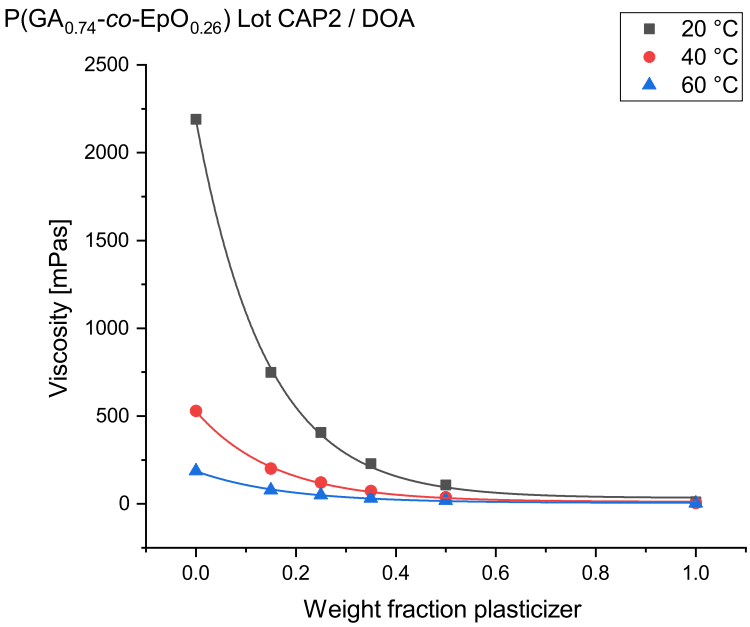

Figure 7.15 Characterization of the binary system P($GA_{0.74}$-*co*-$EpO_{0.26}$) **CAP2** / DOA by viscosity measurements. Weight fractions are ranging from 0 wt. % to 100 wt. % plasticizer content. All samples were measured at 20 °C, 40 °C and 60 °C at a shear rate of 10 s^{-1}.

Especially at temperatures close to room temperature, the viscosity can be substantially reduced. For example, the 15 wt. % mixture showed a reduction by 1441 mPas at 20 °C compared to the pure unplasticized sample. When the temperature was increased from 20 °C to 60 °C, the influence of the external plasticizer decreased resulting in a lower slope of the curve. This is reasonable because the temperature has a significant impact on the viscosity of the copolymer itself, which was discussed in Chapter 5. Having a low viscosity at temperatures close to room temperature is very desirable. By setting a low process temperature, safety and pot-life of the formulation can be increased. High process temperatures are often required when the viscosities of prepolymer and curing agents set a limit to the solid filler content and therefore to the performance of the propellant formulation.

7.3.4 Conclusions

Binary mixtures of P($GA_{0.74}$-*co*-$EpO_{0.26}$) **CAP2** and various non-energetic plasticizers were prepared and characterized in order to find the most suitable plasticizer for further formulation experiments. The pure GAP homopolymer turned out to be incompatible with the tested commercial non-energetic plasticizers. Miscibility studies showed phase

separation in all cases (except for TA) even at low plasticizer contents. This is caused by the nonpolar nature of the plasticizers compared to the polar polyether backbone of GAP. By incorporating nonpolar *n*-alkyl side chains, the overall polarity of the corresponding copolymer is decreased, which results in good compatibility of the tested mixtures even at concentrations up to 75 wt. % non-energetic plasticizer. The screening of the selected mixtures by low-temperature DSC and rheological measurements revealed that DOA showed the most promising properties by substantially lowering the glass transition temperature and the viscosity of the copolymer-plasticizer system even at low weight fractions. DOA was therefore selected as a suitable plasticizer for the following propellant formulation experiments.

7.4 Formulation and Characterization of ADN Composite Propellants

7.4.1 Materials

ADN (Oxidizer)

The ADN prills used in this work were purchased from Eurenco Bofors or prepared at Fraunhofer ICT according to procedures published in the literature [207–209]. Two prill types with different grain sizes were used:

- Lot 1 with a grain size of $d_{0.5} = 285\,\mu m$
- Lot 2 with a grain size of $d_{0.5} = 58\,\mu m$

Literature reported data on ADN [190]:
Empirical formula: $H_4N_4O_4$. $M = 124.06\,g/mol$. $\rho = 1.812\,g/cm^3$. $\Omega = 25.79\,\%$. $\Delta_f H_m^0 = -149.79\,kJ/mol$. State of aggregation: solid.

HMX (Gas Generating Component)

HMX was purchased from Chemring Nobel and used as a small grain size fraction with $d_{0.5} = 5\,\mu m$. A small grain size particle fraction was selected to ensure a good processability of the propellant formulation. ADN prills with similar grain size were not available and therefore substituted by HMX. HMX will lower the overall performance of the propellant but it was only used in a small percentages in the investigated formulations (Table 7.6 and Table 7.7).

Literature reported data on HMX [190]:

Empirical formula: $C_4H_8N_8O_8$. $M = 296.16\,\mathrm{g/mol}$. $\rho = 1.91\,\mathrm{g/cm^3}$. $\Omega = -21.61\,\%$. $\Delta_f H_m^0 = 84.01\,\mathrm{kJ/mol}$. State of aggregation: solid.

P(GA$_{0.75}$-*co*-EpO$_{0.25}$) (Energetic Prepolymer)

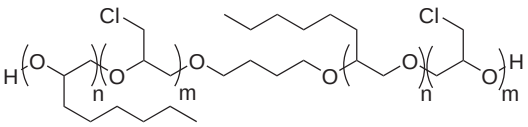

The copolymer P(GA$_{0.75}$-*co*-EpO$_{0.25}$) **CAP1** was synthesized according to the procedure described in Chapter 6.

Analysis results:

GPC: $M_w = 4122\,\mathrm{g/mol}$, $M_n = 2170\,\mathrm{g/mol}$, $M_p = 4332\,\mathrm{g/mol}$, PDI = 1.90. $T_g = -58.3\,^\circ\mathrm{C}$. $T_d = 219.1\,^\circ\mathrm{C}$. TGA = 218.9 °C. $\rho = 1.141\,\mathrm{g/cm^3}$. OH-Value = 54.1 mg/g KOH. Eq. Weight = 1038 g/mol. $\Delta_f H_m^0 = 8.83\,\mathrm{kJ/mol}$. State of aggregation: liquid.

GAP 06S15 (Energetic Prepolymer)

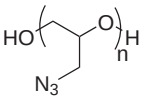

GAP Lot 06S15 was purchased from Eurenco with the following analysis stated in the provided datasheet:

$M_w = 1986\,\mathrm{g/mol}$, $M_n = 1794\,\mathrm{g/mol}$, PDI = 1.10. Eq. Weight = 1250 g/mol.

Literature reported data on GAP [190]:

$\rho = 1.29\,\mathrm{g/cm^3}$. $\Omega = -121.10\,\%$. $\Delta_f H_m^0 = 113.97\,\mathrm{kJ/mol}$. State of aggregation: liquid.

Oxsoft DOA (Plasticizer)

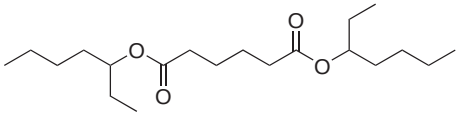

Di-(2-ethylhexyl) adipate (DOA, DEHA) was received from Oxea. Specifications as stated in the product datasheet:

Empirical formula: $C_{22}H_{42}O_4$. $M = 370.57\,\mathrm{g/mol}$. Density at 20 °C = $0.925\,\mathrm{g/cm^3}$. FRP at 1013 hPa = −68 °C. Viscosity at 20 °C =13.7 mPas.

Literature reported on DOA [190]:

Empirical formula: $C_{22}H_{42}O_4$. $M = 370.57\,\mathrm{g/mol}$. $\rho = 0.925\,\mathrm{g/cm^3}$. $\Omega = -263.37\,\%$. $\Delta_f H_m^0 = -1215.03\,\mathrm{kJ/mol}$. State of aggregation: liquid.

Desmodur N100 (Curing Agent)

Desmodur N100 was supplied by Covestro and is an aliphatic tri-functional isocyanate based curing agent. N100 is a colorless, viscous liquid. Specifications as stated in the product data sheet [210]:

NCO content: $22.0 \pm 0.3\,\%$. Viscosity at 23 °C: $10\,000 \pm 2000$ mPas. HDI content: $\leq 0.5\,\%$, $\rho = 1.14\,\mathrm{g/cm^3}$. Eq. Weight: 191.

Baymedix AP501 (Curing Agent)

Baymedix AP501 was supplied by Covestro and is an aliphatic difunctional isocyanate curing agents based on hexamethylene diisocyanate (HDI). It is a colorless, viscous liquid. Specifications as stated in the product data sheet [211]:

NCO content: 12.3 % to 13.3 %. Viscosity at 23 °C: 4000 mPas. HDI content: $\leq 0.39\,\%$. Eq. Weight: 328.

DBTDL (Curing Catalyst)

Dibutyltin dilaurate (DBTDL, D22) was used as a curing catalyst with a concentration of 100 ppm in each formulation.

7.4.2 Experimental Part

Mixing Device

A planetary centrifugal mixer (Thinky Mixer ARV-310) was used for the processing of the propellants [212] (Figure 7.16). In contrast to kneaders, this kind of mixer allows processing at small scales between 30 g to 100 g propellant batch size. The planetary centrifugal vacuum mixer is designed for mixing and deaeration of various kinds of liquid, slurry, paste and powder materials. The working principle is based

on two simultaneous movements, thus enabling a mixing procedure with shear forces. Beside the possibility of processing smaller batches, the planetary mixer has the advantage of reducing processing time and avoiding intensive cleaning procedures after the experiment compared to conventional kneaders. Nevertheless, it is important to consider the drawbacks like reproducibility issues especially at high solid filler contents and the missing possibility of precise temperature control, which has to be adjusted by setting the correct RPM and mixing time based on empirical findings.

Figure 7.16 Mixing principle of the Thinky Mixer ARV-310. Device is operated safely under remote control [212].

Preparation of Propellant Samples

Catalyst (DBTDL, D22) and the respective prepolymer were weighted in a beaker and mixed at 1600 rpm for 20 s using the above described Thinky Mixer ARV-310. When the formulation contained plasticizer, it was added as the second ingredient, again followed by mixing at 1600 rpm for 20 s. HMX (5 μ) as a lubricating grain was added as the first solid filler substance followed by mixing at 1600 rpm under vacuum ($\approx$ 10 kPa) for 30 s. ADN was added as the second solid filler substance in two portions each followed by mixing at 1600 rpm under vacuum ($\approx$ 10 kPa) for 30 s. Temperature was checked after each mixing cycle under the precaution of not exceeding 40 °C. The maximum measured temperature was 37 °C. The prepared homogeneous propellant slurry was kept at RT for 20 min until reaching a temperature of 25 °C. The curing agents were added as the last ingredients followed by a final mixing cycle at 1600 rpm under vacuum ($\approx$ 10 kPa) for 55 s. The prepared homogeneous slurry was immediately casted in the test specimen molds followed by multiple degassing (Figure 7.17). Before casting the propellant, the viscosity was measured by using a Brookfield DV-III ultra rheometer. Finally, the samples were cured at 40 °C for 6 d (Figure 7.18).

Figure 7.17 Propellant slurry after addition of all ingredients (left). Casting process of the propellant slurry into the molds for tensile test specimen (right).

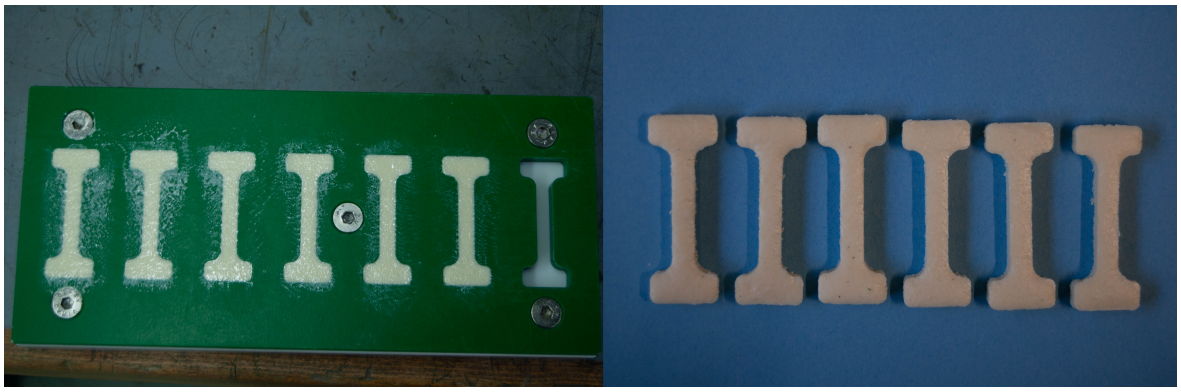

Figure 7.18 Tensile test specimen before (left) and after demolding (right).

7.4.3 Results and Discussion

Four different model propellant compositions (**ADNP1**–**ADNP4**) were selected to study the influence of the novel copolymer P($GA_{0.75}$-*co*-$EpO_{0.25}$) on the propellant properties, with a special focus on the low-temperature properties. Ammonium dinitramide (ADN) was chosen as the oxidizer with a total filler content of 70 wt. % including 11 wt. % HMX (5 µm). HMX was used as a lubricating grain to provide good processibility in the mixing process, because ADN was not available in small grain size distributions. A combination of trifunctional (Desmodur N100) and difunctional (Baymedix AP501) isocyanates was used as curing agent, based on research experience at Fraunhofer ICT concerning GAP propellants. A total R_f value of 0.97 ([NCO]/[OH] ratio) was applied for all formulations. It is important to emphasize that this study was aimed to do a preliminary qualitative comparison between GAP and the novel copolymer P($GA_{0.75}$-*co*-$EpO_{0.25}$). This study is not a comprehensive development of a novel propellant formulation, which would be beyond the scope of this work. Dibutyltin dilaurate (DBTDL, D22) was used as a curing catalyst in each propellant formulation. Two

different types of propellant formulations were prepared. One without a plasticizer, the other one containing a small amount of DOA (4.5 wt. %) as an external plasticizer, which was selected in the previous section as a suitable plasticizer for improving the low-temperature properties. Table 7.6 and Table 7.7 present a summary of the prepared propellant compositions and details about T_g and viscosity measurements. **ADNP1** and **ADNP2** label the formulations based on the copolymer, whereas **ADNP3** and **ADNP4** describe the formulations containing GAP as the binder prepolymer.

Table 7.6 Selected ADN propellant formulations based on the novel synthesized prepolymer P($GA_{0.75}$-*co*-$EpO_{0.25}$) **CAP1**.

Formulation	ADNP1	ADNP2
Oxidizer [a] [wt. %]	70	70
Prepolymer (P($GA_{0.75}$-*co*-$EpO_{0.25}$) **CAP1**) [wt. %]	25.51	21.47
Curing Agent 1 (N100) [wt. %]	3.99	3.57
Curing Agent 2 (AP501) [wt. %]	0.51	0.46
Plasticizer (DOA) [wt. %]	–	4.50
Catalyst (DBTDL) [wt. %]	0.0125	0.0125
Viscosity [b] [Pas]	160	101
T_g [c] [°C]	–43	–61

[a] ADN incl. 11 wt. % HMX (5 µm).
[b] Measured by a Brookfield DV-III rheometer after last mixing cycle.
[c] Determined by DSC after curing (HR = 10 K/min).

Table 7.7 Selected ADN propellant formulations based on the prepolymer GAP (Lot 06S15).

Formulation	ADNP3	ADNP4
Oxidizer [a] [wt. %]	70	70
Prepolymer (GAP Lot 06S15) [wt. %]	25.87	22.06
Curing Agent 1 (N100) [wt. %]	3.66	3.05
Curing Agent 2 (AP501) [wt. %]	0.47	0.39
Plasticizer (DOA) [wt. %]	–	4.50
Catalyst (DBTDL) [wt. %]	0.0125	0.0125
Viscosity [b] [Pas]	230	170
T_g [c] [°C]	–35	–40

[a] ADN incl. 11 wt. % HMX (5 µm).
[b] Measured by a Brookfield DV-III rheometer after last mixing cycle.
[c] Determined by DSC after curing (HR = 10 K/min).

Processibility and Glass Transition Temperatures

After the final mixing cycle according to the procedure described in the experimental section, the viscosity was measured using a Brookfield rheometer prior to the casting operation. The results give a good indication about the processibility of the respective propellant formulation. The mixtures based on the novel copolymer P($GA_{0.75}$-*co*-$EpO_{0.25}$) **ADNP1**, **ADNP2** showed significant lower process viscosities and excellent properties during the casting process. The formulation **ADNP2** containing an additional amount of 4.5 wt. % DOA showed the lowest measured viscosity of 101 Pas (Table 7.7). The reduced viscosities compared to the analogues GAP formulations **ADNP3**, **ADNP4** indicate that higher oxidizer contents can be achieved. This is beneficial for a future propellant development aiming at enhanced performances as described in section 7.2 on thermodynamic calculations.

Thermal analysis of the cured propellant formulations by DSC was carried out to gain a first insight into the low-temperature behavior of the samples. The results are summarized as a bar plot in Figure 7.19, the determined T_g values can be found in Table 7.6 and Table 7.7. The propellants based on the copolymer showed a significant reduction of the T_g compared to the analogous GAP formulations. The T_g of the formulation based on P($GA_{0.75}$-*co*-$EpO_{0.25}$) without plasticizer **ADNP1** is still 3 °C lower than the GAP formulation **ADNP4**, which contains 4.5 wt. % DOA. By adding 4.5 wt. % DOA to the formulation based on P($GA_{0.75}$-*co*-$EpO_{0.25}$) **ADNP1**, it was

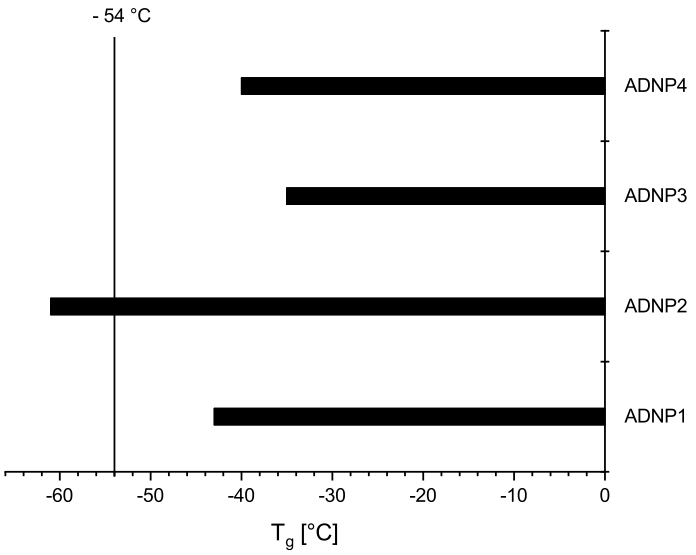

Figure 7.19 Glass transition temperatures (T_g) of cured ADN propellant samples **ADNP1**–**ADNP4** determined by DSC (HR = 10 K/min).

possile to decrease the T_g down to −61 °C. This confirms the results of the experiments of binary mixtures that indicated good interaction between the copolymer and DOA. A T_g of −61 °C can be considered as an excellent result and is 7 K below the benchmark that was set to −54 °C concerning NATO standards [16, 17].

Mechanical Properties

The prepared specimen **ADNP1**–**ADNP4** were investigated by mechanical analysis for a first evaluation of composite propellants based on the novel copolymer P($GA_{0.75}$-*co*-$EpO_{0.25}$). Stress (σ_{max}, σ_{break}), elongation (ϵ_{max}, ϵ_{break}) and E modulus (E) were measured by an uniaxial tensile test, which was performed with a pre-load of 0.25 N and a testing speed of 50 mm/min (Figure 7.20). The aim of these experiments was to characterize the influence of the internal plasticized copolymer on the mechanical properties of cured propellant specimen in comparison to analogous GAP formulations. Two separate experimental series were performed. The first experiments were carried out at room temperature comparing the mechanical properties of all four prepared formulations. The most promising samples were selected and tested at a decreased

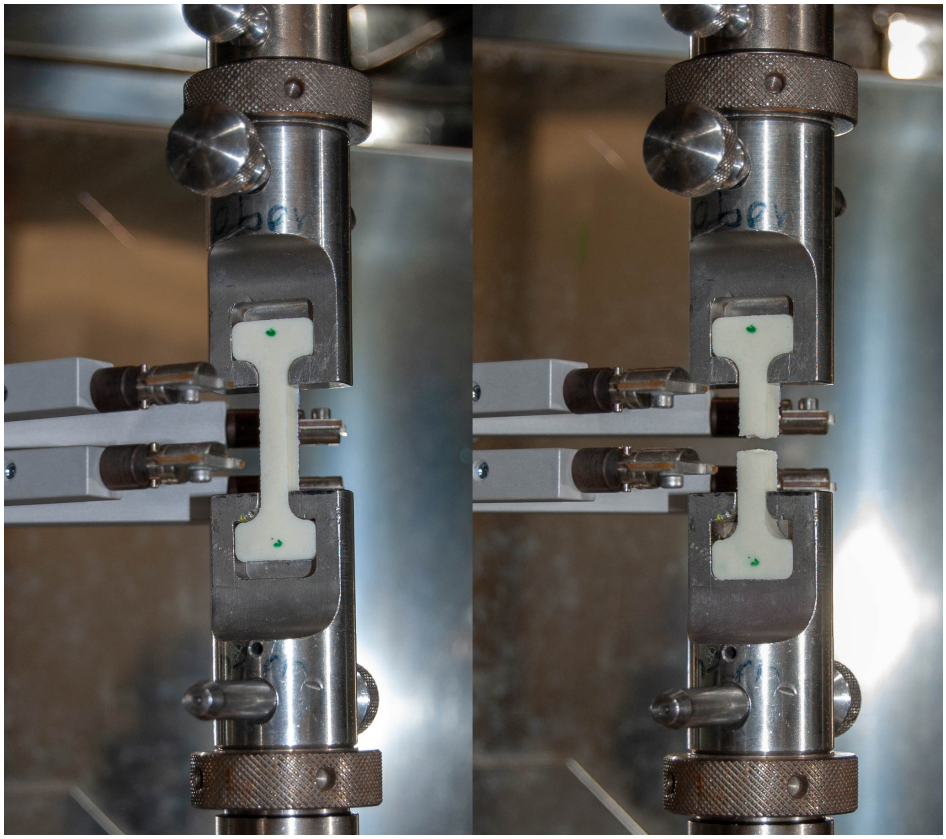

Figure 7.20 Setup of the tensile tests (here shown for an **ADNP1** specimen). Left: Before tensile test. Right: Torn specimen after finished experiment.

temperature of −40 °C in order to investigate the low-temperature properties of the respective formulations. Table 7.8 presents a summary of a publication of Stacer et al. dealing with the optimization of mechanical properties of composite propellants [92]. The parameters give a good estimation of the desirable characteristics of a potential propellant formulation. Another guideline was published by Shusser, who recommends design goals for solid propellants. Tensile strengths should be ≥ 0.7 MPa, elongation ≥ 50 %, and E modulus approximately at 3 MPa [6].

Table 7.8 Ideal mechanical properties of solid propellants depending on the operational purpose, according to Stacer [92].

	Space Launcher	Tactical Air-to-Air
E [MPa]	2–6	2–6
σ_{max} [MPa]	> 0.7	> 0.7
ϵ_{max} [%]	> 45	> 30

The results of the tensile tests at room temperature are summarized in Table 7.9. Three specimen of each formulation were tested. A representative curve of each experimental series was selected and is presented as an overlay in Figure 7.21. Further detailed information about the experiments can be found in Appendix A.3.2. By replacing GAP with P($GA_{0.75}$-*co*-$EpO_{0.25}$), the E modulus average slightly decreased from 8.07 MPa (**ADNP3**) to 7.17 MPa (**ADNP1**) because of the internal plasticizing effect of the pendant *n*-hexyl chains of the copolymer. The E modulus of both samples appear to be slightly too high concerning the literature reported requirements by Stacer and Shusser. The plasticizing effect was also noticed by a slight decrease of the tensile strengths σ_{max} of the samples. Compared to the requirements for an ideal propellant by Stacer et al., the maximum tensile strengths of the samples are slightly too low, since

Table 7.9 Mechanical properties of the formulations **ADNP1**–**ADNP4** at 20 °C as arithmetic mean values.

	ADNP1	ADNP2	ADNP3	ADNP4
E [MPa]	7.17	3.58	8.07	6.98
σ_{max} [MPa]	0.61	0.33	0.69	0.48
ϵ_{max} [%]	22.76	19.02	32.86	18.77
σ_{break} [MPa]	0.57	0.29	0.66	0.46
ϵ_{break} [%]	27.70	22.73	38.07	21.73
Shore A	72.2	63.8	62.4	50.3

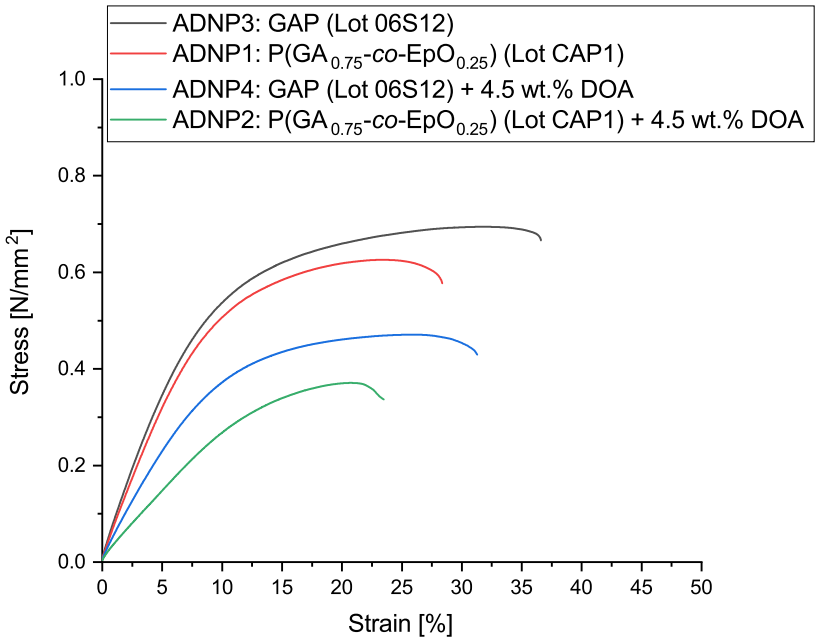

Figure 7.21 Result of tensile tests of **ADNP1**–**ADNP4** formulations at 20 °C. A representative curve was selected for each formulation. Detailed informations about all measurements can be found in Appendix A.3.2.

they did not exceed the 0.7 MPa threshold. The maximum elongation ϵ_{max} of the GAP based propellant sample **ADNP3** was sufficient according to Stacer by exceeding 30 %. The analogous copolymer formulation **ADNP1** showed a lower average of 27.70 % and stays therefore behind the requirements. The reduced maximum elongation may be caused by inadequate bonding between the ADN prills and binder matrix. The use of a suitable bonding agent is expected to improve the characteristics significantly. By adding 4.5 wt. % DOA as an external plasticizer to the formulations (**ADNP2**, **ADNP4**), the stiffness of the binder matrix as characterized by E modulus and maximum tensile strength σ_{max} furthermore decreased. By adding a plasticizer it would normally be expected that the maximum elongation ϵ_{max} should increase but ϵ_{max} actually decreased slightly (Table 7.9). This could again be explained by interaction problems between ADN prills and binder matrix that has to be improved by ADN compatible bonding agents. The research for a suitable ADN bonding agent is still an ongoing process in literature to-date and is not part of this study.

For the low-temperature measurements, the formulations based on P($GA_{0.75}$-*co*-$EpO_{0.25}$) (**ADNP2**) and GAP (**ADNP4**) containing 4.5 wt. % DOA as an external plasticizer were selected because of the promising results of the DSC experiments performed prior to the tensile tests (Figure 7.19). The propellant sample **ADNP2** showed a glass transition of −61 °C in DSC experiments and was therefore decided to

be suitable for an investigation of the mechanical properties at lower temperatures. The analogous GAP formulation **ADNP4** was selected as a reference. Tensile tests of the specimen were carried out at −40 °C, using the Zwick machine operated in an adjustable climatic chamber. The results of the experiments are summarized in Table 7.10, further detailed information can be found in Appendix A.3.2. As presented in Figure 7.22, the sample **ADNP2** based on the copolymer still showed elastomeric properties at −40 °C tough the binder network stiffness was drastically increased compared to the experiments at room temperature. The E modulus increased to 185.70 MPa and the sample showed a higher tensile strength of $\sigma_{max} = 2.46$, while the maximum elongation was decreased to 9.33 %. In contrast, the reference GAP formulation **ADNP4** was clearly operated below the T_g of the binder matrix as it showed no more elastic

Table 7.10 Result of tensile tests of the formulations **ADNP2** and **ADNP4** at −40 °C as arithmetic mean values.

	ADNP2	ADNP4
E [MPa]	185.70	2278.63
σ_{max} [MPa]	2.46	4.12
ϵ_{max} [%]	7.46	0.38
σ_{break} [MPa]	2.20	4.12
ϵ_{break} [%]	9.33	0.38

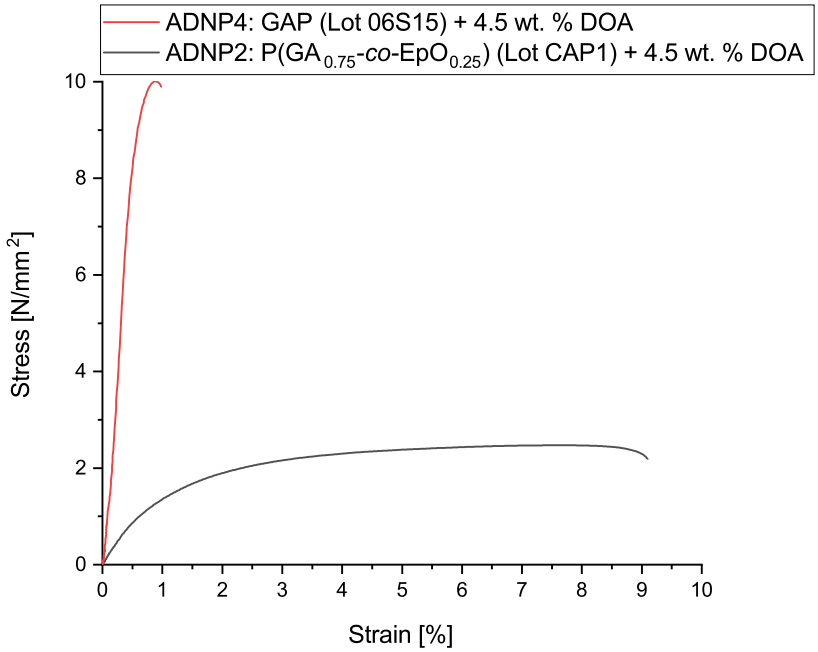

Figure 7.22 Result of tensile tests of **ADNP2** and **ADNP4** at −40 °C. Detailed informations about all measurements can be found in Appendix A.3.2.

behavior (Figure 7.22). Only for the presented curve a reasonable E modulus could be calculated, the other experiments can be found in Appendix A.3.2. The binder based on the copolymer P($GA_{0.75}$-*co*-$EpO_{0.25}$) exhibited significant improved low-temperature properties compared to the GAP binder. The influence of the *n*-alkyl substituted side chains as internal plasticizers was therefore also confirmed for cured propellant samples.

Sensitivity

The sensitivity of a composite propellant grain towards mechanical stimuli is an important parameter concerning the manufacturing, transport, storage and handling of missile systems. It was therefore necessary to check whether replacing GAP by the copolymer P($GA_{0.75}$-*co*-$EpO_{0.25}$) would have a negative influence on sensitivities. Therefore, all four formulations **ADNP1**–**ADNP4** were tested regarding their sensitivities towards impact and friction. The results are presented in Table 7.11.

Table 7.11 Results of sensitivity measurements against friction and impact for cured propellant formulations **ADNP1**–**ADNP4**.

	ADNP1	ADNP2	ADNP3	ADNP4
Friction Sensitivity [N]	240	160	168	160
Impact Sensitivity [Nm]	4.0	5.5	3.0	5.5

The replacement of GAP with the copolymer P($GA_{0.75}$-*co*-$EpO_{0.25}$) caused no negative influence on the sensitivities, which was expected because of the lower nitrogen content of the copolymer. **ADNP1**, which is the formulation based on P($GA_{0.75}$-*co*-$EpO_{0.25}$) without external plasticizer content, showed a slightly decreased sensitivity compared to the analogous GAP formulation **ADNP3**. The ADN propellant samples **ADNP2** and **ADNP4**, containing 4.5 wt. % DOA, showed basically the same sensitivity, which was decreased compared to **ADNP1** and **ADNP3**. This is caused by the additional amount of non-energetic plasticizer, which decreased the content of energetic components in the mixture.

7.4.4 Conclusions

ADN model propellants with an oxidizer content of 70 wt. % were prepared in a cast-cure process in order to evaluate the influence of P($GA_{0.75}$-*co*-$EpO_{0.25}$) on the material properties of cured propellant samples. Two different types were investigated. The first type was based on the binder matrix without plasticizer (**ADNP1**), while the second type (**ADNP2**) contained 4.5 wt. % DOA as an external plasticizer for a further

improvement of the low-temperature properties. The analogous propellants using GAP binders (**ADNP3**, **ADNP4**) were prepared as reference samples.

The formulations based on the copolymer P($GA_{0.75}$-*co*-$EpO_{0.25}$) (**ADNP1**, **ADNP2**) showed excellent processibility in the mixing and casting process, by exhibiting decreased viscosity values compared to the GAP reference mixtures. DSC measurements confirmed significantly decreased glass transition temperatures (T_g) of the formulations with binders based on the copolymer compared to the GAP propellants. It was possible to reach a T_g of −61 °C by addition of only 4.5 wt. % DOA (**ADNP2**), which is below the selected benchmark of −54 °C. The results confirmed a good interaction of the polymer-plasticizer system that was already investigated for binary mixtures in the previous section.

In order to study the influence of the copolymer on the mechanical properties, tensile tests were performed at 20 °C and −40 °C. The propellant specimen based on P($GA_{0.75}$-*co*-$EpO_{0.25}$) (**ADNP1**, **ADNP2**) showed reduced E modulus and lower tensile strengths compared to the GAP formulations (**ADNP3**, **ADNP4**), thus providing a softer binder matrix. This was expected because of the plasticizing effect of the *n*-hexyl side chains of the copolymer. The formulations containing 4.5 wt. % DOA (**ADNP2**, **ADNP4**) were selected for further investigations. The experiments at −40 °C confirmed the influence of the copolymer on the T_g of the binder matrix. While the GAP formulation (**ADNP4**) showed almost no elastic properties, the copolymer samples (**ADNP2**) still exhibited a reasonable elongation of $\epsilon_{break} \approx 9\,\%$, confirming the improved low-temperature properties of the binder based on the novel copolymer P($GA_{0.75}$-*co*-$EpO_{0.25}$).

8 Summary and Outlook

The aim of this thesis was the synthesis and characterization of novel energetic copolymers, suitable for application as binders in composite rocket propellants. The copolymers should exhibit improved low-temperature properties compared to the reference compound glycidyl azide polymer (GAP), which is currently one of the most prominent literature-published energetic polymers. Despite promising properties, GAP suffers from a high glass transition temperature (T_g). Composite propellants based on GAP binders therefore usually require high amounts of external plasticizers to avoid brittleness at low-temperature operation conditions and to meet the established NATO standards. By the synthesis of novel energetic glycidyl azide copolymers with improved low-temperature properties, a reduction of the required amounts of external plasticizers was targeted in order to minimize the problems that are linked with plasticizer migration phenomena. Nonpolar *n*-alkyl side chains were identified as suitable internal plasticizers for glycidyl azide copolymers. Internal plasticizers are bonded to the molecular structure of the polymer chains, which prevents migration processes to the surface of the propellant grain over time.

The developed synthesis of *n*-alkyl-substituted glycidyl azide copolymers started with the cationic copolymerization of epichlorohydrin (ECH) and *n*-alkyl-substituted oxiranes, using the lewis acid BF_3 as a catalyst and 1,4-butanediol as an initiator (Figure 8.1).

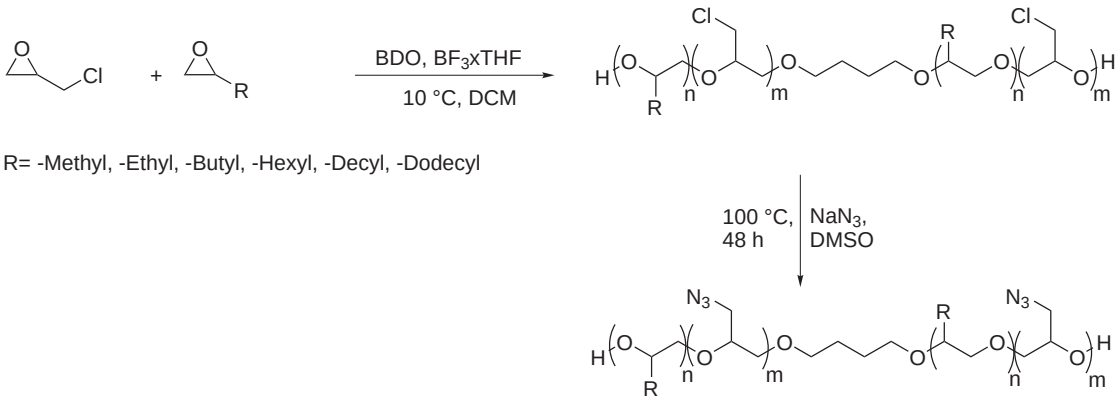

Figure 8.1 Synthesis of *n*-alkyl-substituted glycidyl azide copolymers for energetic composite propellant binders following a two-step procedure.

The resulting polyepichlorohydrin copolymers were azidated in a subsequent synthesis step using a mixture of sodium azide (NaN_3) and DMSO. The nucleophilic substitution delivered the desired *n*-alkyl-substituted glycidyl azide copolymers in good yields as clear yellow viscous liquids. All synthesized copolymers were analyzed with respect to their application as prepolymers for energetic binder systems. Due to the plasticizing effect of the nonpolar side chains T_g was reduced and the decreased viscosity of the copolymers indicated improved processability in propellant cast-cure processes. The exact properties were dependent on the specific type of comonomer and the selected molecular composition. In a small-scale synthesis screening, copolymers with different *n*-alkyl side chain lengths between C1 (methyl moiety) and C12 (dodecyl moiety) were synthesized and characterized. The comonomer 1,2-epoxyoctane (EpO, hexyl moiety) had the most promising influence in the respective copolymers and was therefore selected for further studies. The molecular composition of glycidyl azide (GA) and EpO units was varied between 0 % and 100 % comonomer percentage, searching for an appropriate trade-off between improved low-temperature properties and sufficient energy content. Based on the analysis results, P($GA_{0.74}$-*co*-$EpO_{0.26}$) **25** was selected as a candidate for further evaluation in model propellant formulations. The copolymer exhibited interesting properties such as a T_g of −60.5 °C, suitable energetic properties,

Table 8.1 Analysis summary of P($GA_{0.74}$-*co*-$EpO_{0.26}$) **25** in comparison to a commercial GAP (Lot 06S12) sample from Eurenco Bofors.

	GAP (Lot 06S12)	P($GA_{0.74}$-*co*-$EpO_{0.26}$) **25**
Formula RU [a]	$C_3H_5N_3O$	$C_{4.25}H_{7.75}N_{2.25}O$
FW RU [a] [g/mol]	99.09	106.37
Elemental analysis	C35.34 H5.78 N41.89	C47.55 H7.42 N28.45
M_n [g/mol]	2507	1972
Equivalent weight [g/mol]	1211	1397
T_g [°C]	−48.7	−60.5
Viscosity η [b] [mPas]	5560	2330
Density [g/cm^3]	1.284	1.140
T_{Dec} [c] [°C]	217.0	219.4
$\Delta_f H_m^0$ [kJ/mol]	114	9
$\Delta_f H^0$ [kJ/g]	1.15	0.08
Oxygen Balance Ω	−121 %	−171 %
Sensitivity towards impact [J]	7.9 [26]	30.0
Sensitivity towards friction [N]	>360 [26]	>360

[a] Repeating unit
[b] Measured at 20 °C, 10 s^{-1}.
[c] Decomposition temperature determined by DSC (onset value).

low sensitivity to mechanical stimuli and a low viscosity. The most important properties of the synthesized copolymer P($GA_{0.74}$-*co*-$EpO_{0.26}$) **25** are summarized and compared to a commercial sample of GAP (Lot 06S12) purchased from Eurenco Bofors in Table 8.1.

For an evaluation of a novel energetic copolymer in propellant formulations, larger amounts of the material were required. A minimum amount of 500 g copolymer was estimated for the investigation of binary polymer-plasticizer mixtures and model composite propellant samples. The key issue of the P($GA_{0.74}$-*co*-$EpO_{0.26}$) **25** synthesis is the reproducibility of the polymerization step, because cationic ring-opening polymerizations are known to exhibit side reactions by the formation of unwanted low-molecular impurities. The copolymerization of ECH and EpO was therefore scaled-up to a 100 g batch size and repeated several times to investigate the reproducibility, considering the product properties. The molecular weight distributions were quite narrow with a PDI of 1.83 ± 0.09, indicating a good reproducibility and a molecular weight of $M_n = 1903 \pm 91$ g/mol (Figure 8.2). The consecutively synthesized lots of P($ECH_{0.75}$-*co*-$EpO_{0.25}$) (**P1**–**P9**) were combined to master batches and azidated to deliver two separate lots of P($GA_{0.75}$-*co*-$EpO_{0.25}$) (**CAP1**, **CAP2**) with a total amount of 775.75 g copolymer, which was used in subsequent propellant formulation studies.

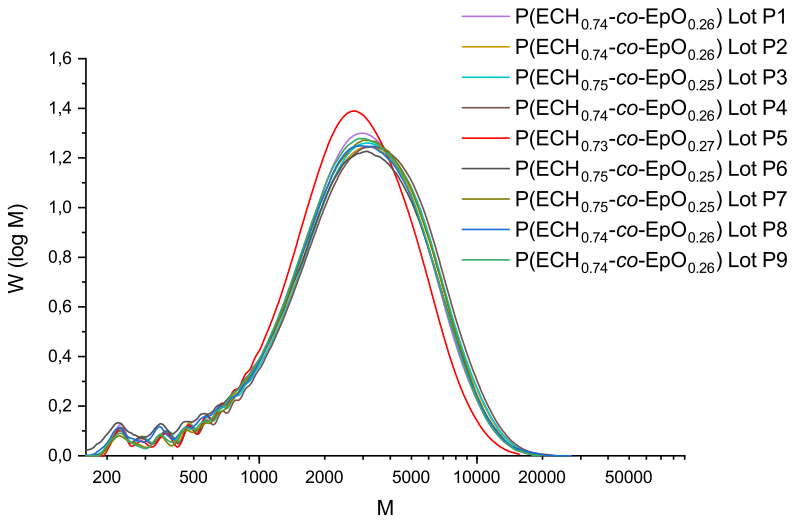

Figure 8.2 Synthesis of P($ECH_{0.75}$-*co*-$EpO_{0.25}$) in multiple batches (**P1**–**P9**). The polymerization showed good reproducibility. **P5** can be considered as an outlier, because of an incorrect stirrer speed setting.

The last part of the thesis was dedicated to the evaluation of the influence of the novel copolymer on the material properties of cured composite model propellant specimen. First, calculations using the ICT thermodynamic code were carried out to study the

performances that can be expected by propellants with binders consisting of the novel copolymer. Metalized and non-metalized ADN composites based on P($GA_{0.75}$-*co*-$EpO_{0.25}$) were examined in comparison to analogous formulations based on GAP and the inert prepolymer polypropylene glycol (PPG) as reference systems. It was found that the formulations based on P($GA_{0.75}$-*co*-$EpO_{0.25}$) exhibited specific impulses (I_{sp}) between the GAP and PPG mixtures. By stepwise increasing the oxidizer content to a reasonable value over 70 wt. %, the performance of the copolymer and GAP-based formulations slowly converged. The loss of energy caused by the introduction of non-energetic *n*-hexyl side chains can therefore be balanced by selecting an adequate amount of oxidizer. A comparison of the P($GA_{0.75}$-*co*-$EpO_{0.25}$)/ADN composites to conventional ammonium perchlorate (AP) propellants showed significant improvements concerning both I_{sp} and I_{spv}.

Despite the improved low-temperature properties of the copolymer, the use of external plasticizers in small amounts may be necessary depending on the operation purpose. Binary mixtures of P($GA_{0.75}$-*co*-$EpO_{0.25}$) with various commercial plasticizers in different weight fractions were therefore prepared and characterized by DSC experiments and viscosity measurements. The copolymer showed improved compatibility to various types of plasticizers compared to GAP. The incorporation of *n*-hexyl chains lowered the overall polarity of the copolymer, thus improving the interaction between the copolymer and plasticizers which was evaluated by miscibility studies and by the calculation of interaction parameters according to Jenckel-Heusch. The screening revealed dioctyl adipate (DOA) as the most efficient plasticizer for further formulation studies.

Finally, ADN model propellants (**ADNP1**–**ADNP4**) with an oxidizer content of 70 wt. % were prepared in a cast-cure process in order to evaluate the influence of P($GA_{0.75}$-*co*-$EpO_{0.25}$) on cured propellants in comparison to analogous GAP reference samples, with a special focus on the low-temperature properties (Figure 8.3). The copolymer showed excellent processability due to decreased process viscosities compared to the GAP reference mixtures. DSC measurements of the cured propellant samples containing P($GA_{0.75}$-*co*-$EpO_{0.25}$) confirmed significantly decreased T_g values compared to the GAP-based propellants. It was possible to achieve a T_g of −61 °C by addition of only 4.5 wt. % DOA. Tensile tests of the prepared propellant samples were performed at 20 °C and −40 °C. The propellant specimen based on P($GA_{0.75}$-*co*-$EpO_{0.25}$) (**ADNP1**, **ADNP2**) showed reduced E modulus and lower tensile strengths compared to the GAP formulations (**ADNP3**, **ADNP4**) due to the softer binder matrix caused by the internal plasticizing effect of the nonpolar side chains. The formulations containing 4.5 wt. % DOA (**ADNP2**, **ADNP4**) were qualified for low-temperature measurements due to their low T_g values. The tensile tests at −40 °C confirmed the improved low-temperature

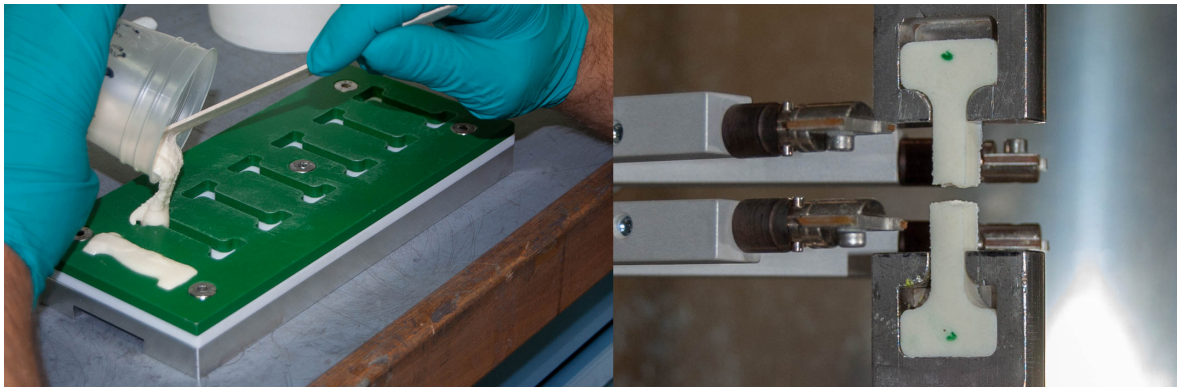

Figure 8.3 Cast-cure processing of ADN composite propellant samples (left). Analysis of mechanical properties by tensile tests (right).

properties of the binder based on P($GA_{0.75}$-*co*-$EpO_{0.25}$). While the GAP-based samples showed no more elastic properties, the propellant specimen based on the copolymer still exhibited a considerable elongation at break.

The work presented in this thesis offers a building block-like selection of copolymers, which can be used as energetic binders for composite propellants. By adjusting the type of comonomer and the individual molecular composition, copolymers with variable properties and energy contents can be synthesized for specific applications. In upcoming work, a further investigation of the performance and influences of such copolymers in propellant formulations will be carried out. This includes the optimization of oxidizer content and curing systems but also details about additives such as burn-rate modifiers, stabilizers and bonding agents. Beside the optimization of mechanical properties, analysis of stability and combustion processes is also necessary. The energetic polymer may also be suitable for application in space launchers [213], as recently considered in the EU project GRAIL [214].

Appendix

A.1 Synthesis and Characterization of Glycidyl Azide Copolymers

A.1.1 GPC Data of Synthesized Copolymers

GPC curves of P(GA-*co*-EpH) copolymers

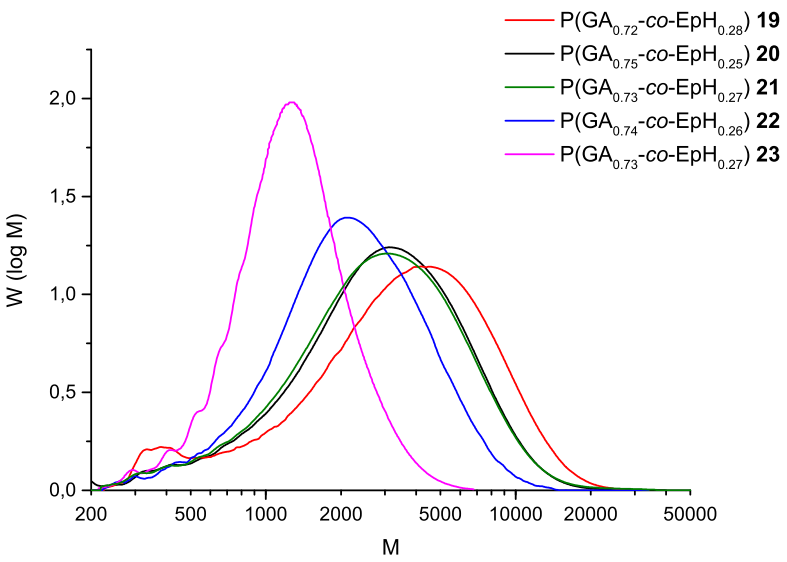

Figure A.1 GPC curves of synthesized P(GA-*co*-EpH) copolymers **19**–**23** with different [M]/[I] ratios and a molecular composition of approx. 75:25.

GPC curves of ECH-copolymers with varying *n*-alkyl side chain lengths

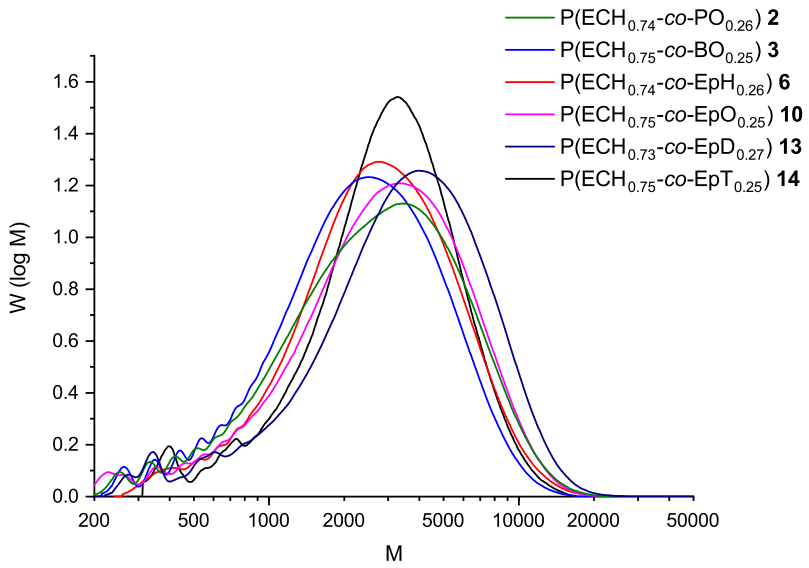

Figure A.2 GPC curves of various PECH copolymers with nonpolar *n*-alkyl side chains **2**–**3**, **6**, **10**, **13**–**14**.

GPC curves of P(ECH-*co*-EpO) copolymers

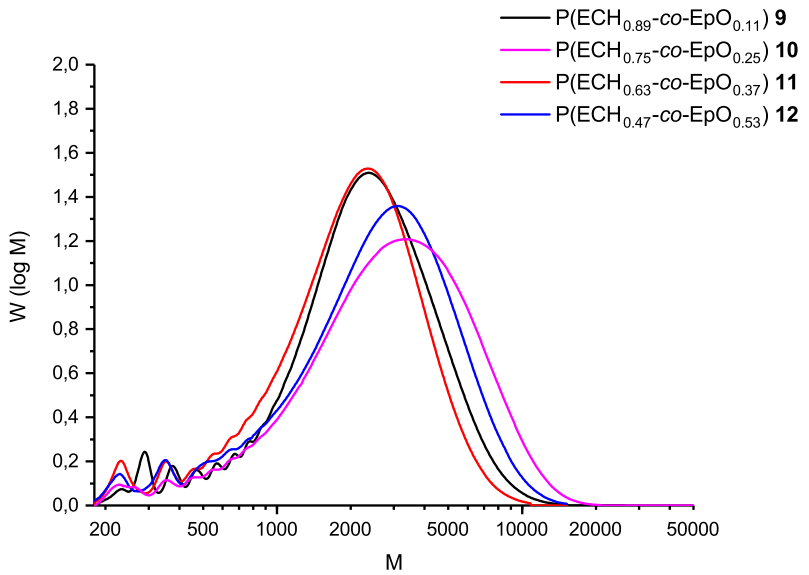

Figure A.3 GPC curves of synthesized P(ECH-*co*-EpO) copolymers **9**–**12** with different molecular compositions.

A.1.2 Viscosity Measurements

Viscosities of P(GA-*co*-EpH) copolymers

Table A.1 Viscosity measurements of P(GA-*co*-EpH) copolymers **19**–**23**.

No.	Composition [a]	[M]/[I]	η [b] [mPas] @ 20 °C	η [b] [mPas] @ 40 °C	η [b] [mPas] @ 60 °C
19	P($GA_{0.72}$-*co*-$EpH_{0.28}$)	50	3660	873	296
20	P($GA_{0.75}$-*co*-$EpH_{0.25}$)	40	3030	731	249
21	P($GA_{0.73}$-*co*-$EpH_{0.27}$)	30	2970	719	245
22	P($GA_{0.74}$-*co*-$EpH_{0.26}$)	20	2050	507	175
23	P($GA_{0.73}$-*co*-$EpH_{0.27}$)	10	980	248	89

[a] Real composition calculated by ^{1}H NMR spectroscopy.
[b] Measured at a shear rate of $10\,s^{-1}$.

A.1.3 Enthalpy of Formation of P(GA-*co*-EpO) Copolymers

Calculation of the enthalpy of formation ($\Delta_f H^0$) was performed for the synthesized P(GA-*co*-EpO) copolymers with varying molecular compositions as described in Chapter 5.4.3. The selected compositions are:

- P($GA_{0.89}$-*co*-$EpO_{0.11}$) **24**: Molecular composition approximated as 90:10 for the formula of the repeating unit.
- P($GA_{0.74}$-*co*-$EpO_{0.26}$) **25**: Molecular composition approximated as 75:25 for the formula of the repeating unit.
- P($GA_{0.63}$-*co*-$EpO_{0.37}$) **26**: Molecular composition approximated as 65:35 for the formula of the repeating unit.
- P($GA_{0.47}$-*co*-$EpO_{0.53}$) **27**: Molecular composition approximated as 50:50 for the formula of the repeating unit.

Based on the repeating unit formula for the respective copolymer (Table A.2), the following combustion reactions were assumed:

24: $C_{3.5}H_{6.1}N_{2.7}O\,(s) + 4.525\,O_2\,(g) \longrightarrow 3.5\,CO_2\,(g) + 3.050\,H_2O\,(l) + 1.350\,N_2\,(g)$
25: $C_{4.25}H_{7.75}N_{2.25}O\,(s) + 5.69\,O_2\,(g) \longrightarrow 4.250\,CO_2\,(g) + 3.875\,H_2O\,(l) + 1.125\,N_2\,(g)$
26: $C_{4.75}H_{8.85}N_{1.95}O\,(s) + 6.463\,O_2\,(g) \longrightarrow 4.750\,CO_2\,(g) + 4.425\,H_2O\,(l) + 0.975\,N_2\,(g)$
27: $C_{5.5}H_{10.5}N_{1.5}O\,(s) + 7.625\,O_2\,(g) \longrightarrow 5.5\,CO_2\,(g) + 5.25\,H_2O\,(l) + 0.75\,N_2\,(g)$

The calculated enthalpies of formation are summarized in Table A.2.

Table A.2 Energetic properties of synthesized P(GA-*co*-EpO) copolymers **24**–**27**.

	24	**25**	**26**	**27**
Formula RU [a]	$C_{3.5}H_{6.1}N_{2.7}O$	$C_{4.25}H_{7.75}N_{2.25}O$	$C_{4.75}H_{8.85}N_{1.95}O$	$C_{5.5}H_{10.5}N_{1.5}O$
FW RU [a] [g/mol]	102.01	106.37	109.29	113.65
$-\Delta_c U$ [J g^{-1}]	22892	26236	28474	31550
$-\Delta_c H_m^0$ [kJ mol^{-1}]	2334	2792	3114	3589
$\Delta_f H_m^0$ [kJ mol^{-1}]	83	9	–23	–79
$\Delta_f H^0$ [kJ g^{-1}]	0.81	0.08	–0.21	-0.70
Oxygen Balance Ω [%]	−142	–171	–189	–214

[a] Repeating unit

A.2 Scale-Up Experiments

A.2.1 Thermal Analysis

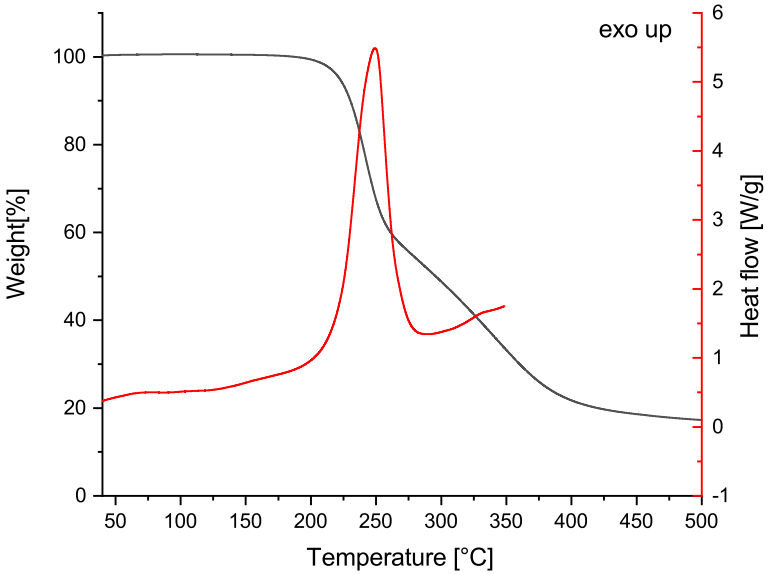

Figure A.4 Overlay of TGA and DSC curves of P($GA_{0.74}$-*co*-$EpO_{0.26}$) **CAP2** (HR = 5 K/min).

A.3 Formulation Studies

A.3.1 Characterization of Binary Polymer-Plasticizer Mixtures

Glass Transition Temperatures of Binary Mixtures

Table A.3 T_g data of binary mixtures consisting of P($GA_{0.74}$-*co*-$EpO_{0.26}$) **CAP2** and common non-energetic plasticizers. The values were determined by low-temperature DSC measurements (HR = 10 K/min).

T_g Mixture [°C]	5 wt. %	10 wt. %	15 wt. %	25 wt. %	35 wt. %	50 wt. %	75 wt. %
DOA	– 61.2	–65.3	–68.3	–75.2	–82.0	–89.4	–93.7
H-DINCH	–59.0	–60.7	–62.5	–66.1	–68.9	–74.0	–83.2
GPO	–59.6	–60.6	–61.1	–64.2	–67.5	–72.5	–79.3
TOTM	–58.8	–59.6	–60.5	–62.6	–65.7	–68.1	–74.5
DINP	–58.9	–60.3	–61.2	–63.3	–66.5	–69.4	–75.0
Triacetin	–59.0	–60.8	–62.0	–64.1	–65.7	–67.7	–69.7

Table A.4 T_g data of binary mixtures consisting of GAP (Lot 06S12) and common non-energetic plasticizers. The values were determined by low-temperature DSC measurements (HR = 10 K/min).

T_g Mixture [°C]	5 wt. %	10 wt. %	15 wt. %	25 wt. %	35 wt. %	50 wt. %	75 wt. %
DOA	–52.2	–53.0	–53.0	n.m.	n.m.	n.m.	n.m.
H-DINCH	n.m.	n.m.	n.m.	n.m.	n.m.	n.m.	n.m.
GPO	n.m.	n.m.	n.m.	n.m.	n.m.	n.m.	n.m.
TOTM	n.m.	n.m.	n.m.	n.m.	n.m.	n.m.	n.m.
DINP	n.m.	n.m.	n.m.	n.m.	n.m.	n.m.	n.m.
Triacetin	–50.6	–52.5	–54.0	–56.8	–59.6	–62.5	–67.4

n.m.: The mixture showed phase separation. DSC experiments were therefore not performed.

Viscosity Measurements of Binary Mixtures

Table A.5 Viscosity measurements of various binary polymer-plasticizer mixtures at 20 °C, 40 °C and 60 °C.

Polymer ($x_1 = 0.75$)	Plasticizer ($x_2 = 0.25$)	η [a] [mPas] @ 20 °C	η [a] [mPas] @ 40 °C	η [a] [mPas] @ 60 °C
P($GA_{0.74}$-*co*-$EpO_{0.26}$)	DOS	472	137	56
P($GA_{0.74}$-*co*-$EpO_{0.26}$)	DOA	406	122	51
P($GA_{0.74}$-*co*-$EpO_{0.26}$)	H-DINCH	808	205	78
P($GA_{0.74}$-*co*-$EpO_{0.26}$)	GPO	948	243	90
P($GA_{0.74}$-*co*-$EpO_{0.26}$)	TOTM	1210	294	104
P($GA_{0.74}$-*co*-$EpO_{0.26}$)	DINP	907	223	81
P($GA_{0.74}$-*co*-$EpO_{0.26}$)	Triacetin	550	143	56
GAP (Lot 06S12)	Triacetin	1000	236	87

[a] Measured at a shear rate of $10\,s^{-1}$.

Table A.6 Viscosity measurements of P($GA_{0.74}$-*co*-$EpO_{0.26}$) **CAP2** / DOA mixtures ranging from 0 wt. % to 100 wt. % plasticizer content.

P($GA_{0.74}$-*co*-$EpO_{0.26}$) x_1	DOA x_2	η [a] [mPas] @ 20 °C	η [a] [mPas] @ 40 °C	η [a] [mPas] @ 60 °C
1.00	0.00	2190	529	187
0.85	0.15	749	202	79
0.75	0.25	406	122	51
0.50	0.50	108	39	19
0.00	1.00	11	5	3

[a] Measured at a shear rate of $10\,s^{-1}$.

A.3.2 Tensile Tests

Tensile Tests of ADNP1 at 20 °C

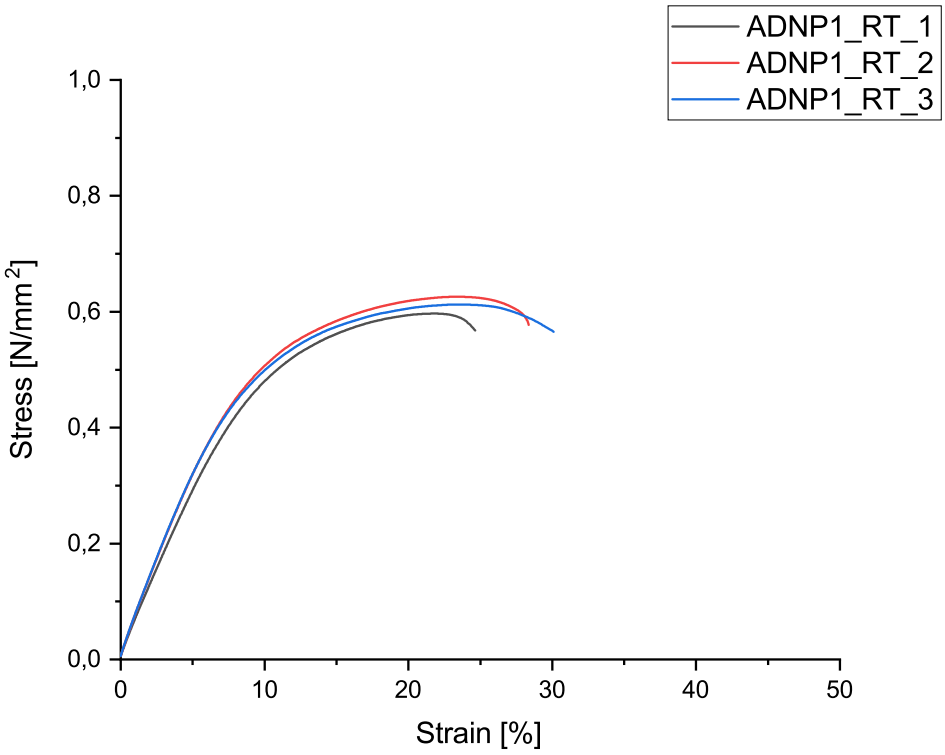

Figure A.5 Tensile tests of propellant sample **ADNP1** at 20 °C.

Table A.7 Tensile tests of propellant sample **ADNP1** at 20 °C.

Sample	F_m [N]	σ_m [MPa]	ϵ_m [%]	σ_b [MPa]	ϵ_m [%]	E [MPa]
ADNP1_RT_1	22.13	0.60	21.83	0.57	24.65	6.67
ADNP1_RT_2	22.87	0.63	23.25	0.58	28.36	7.42
ADNP1_RT_3	22.49	0.61	23.19	0.57	30.09	7.42
$\overline{x}$	22.50	0.61	22.76	0.57	27.70	7.17

Tensile Tests of ADNP2 at 20 °C

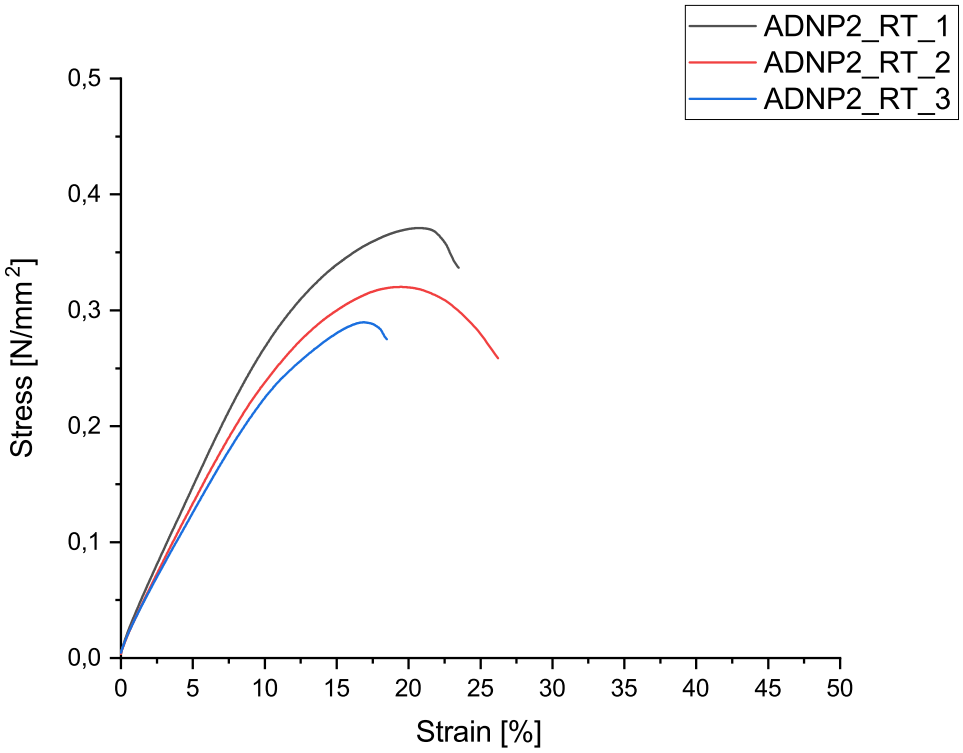

Figure A.6 Tensile tests of propellant sample **ADNP2** at 20 °C.

Table A.8 Tensile tests of propellant sample **ADNP2** at 20 °C.

Sample	F_m [N]	σ_m [MPa]	ϵ_m [%]	σ_b [MPa]	ϵ_m [%]	E [MPa]
ADNP2_RT_1	12.42	0.37	20.72	0.34	23.47	3.91
ADNP2_RT_2	10.64	0.32	19.43	0.26	26.21	3.40
ADNP2_RT_3	10.05	0.29	16.90	0.27	18.50	3.44
$\overline{x}$	11.04	0.33	19.02	0.29	22.73	3.58

Tensile Tests of ADNP3 at 20 °C

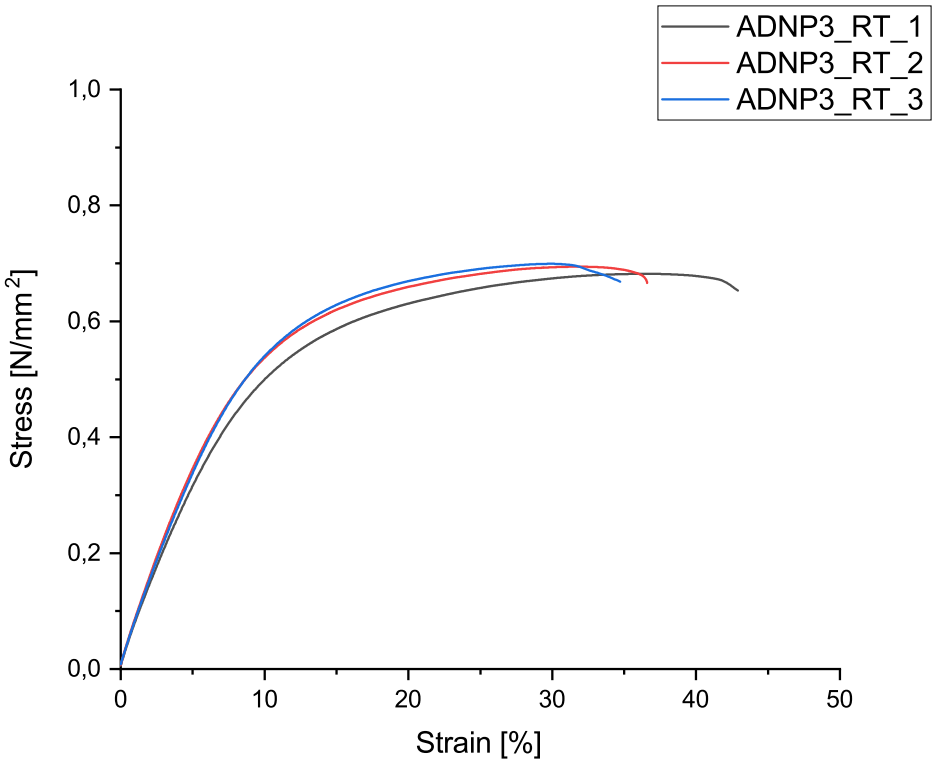

Figure A.7 Tensile tests of propellant sample **ADNP3** at 20 °C.

Table A.9 Tensile tests of propellant sample **ADNP3** at 20 °C.

Sample	F_m [N]	σ_m [MPa]	ϵ_m [%]	σ_b [MPa]	ϵ_m [%]	E [MPa]
ADNP3_RT_1	24.71	0.68	36.76	0.65	42.90	7.89
ADNP3_RT_2	25.11	0.69	31.94	0.67	36.60	8.38
ADNP3_RT_3	25.13	0.70	29.87	0.67	34.73	7.95
$\overline{x}$	24.98	0.69	32.86	0.66	38.07	8.07

Tensile Tests of ADNP4 at 20 °C

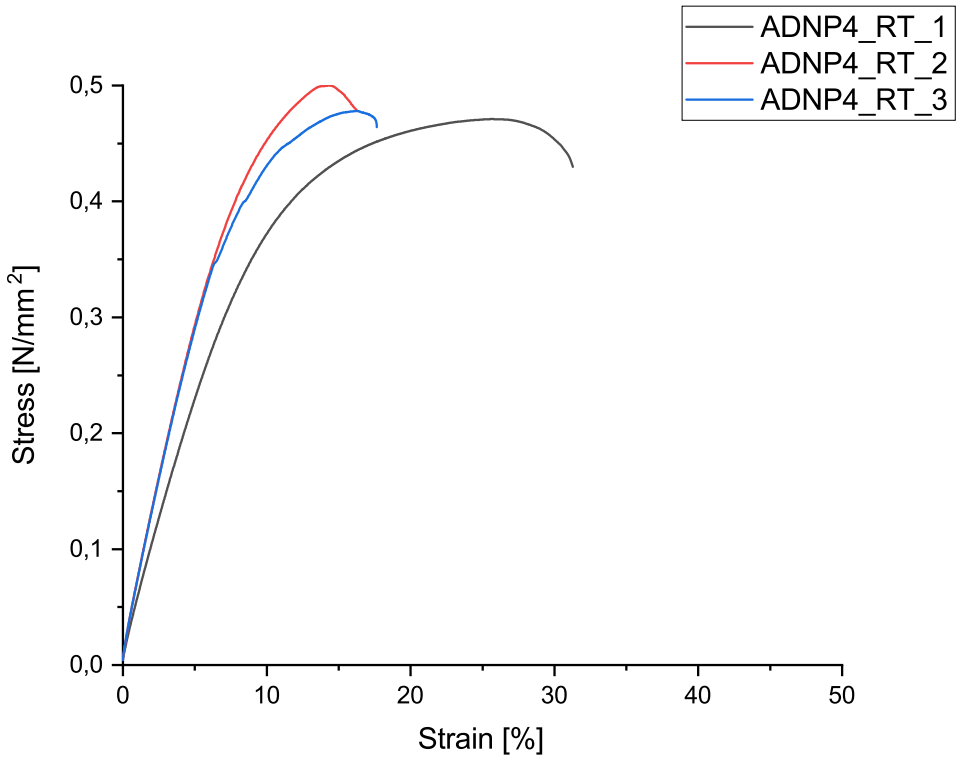

Figure A.8 Tensile tests of propellant sample **ADNP4** at 20 °C.

Table A.10 Tensile tests of propellant sample **ADNP4** at 20 °C.

Sample	F_m [N]	σ_m [MPa]	ϵ_m [%]	σ_b [MPa]	ϵ_m [%]	E [MPa]
ADNP4_RT_1	16.75	0.47	25.67	0.43	31.28	5.87
ADNP4_RT_2	17.49	0.50	14.34	0.48	16.28	7.57
ADNP4_RT_3	16.50	0.48	16.29	0.46	17.64	7.49
$\overline{x}$	16.91	0.48	18.77	0.46	21.73	6.98

Tensile Tests of ADNP2 at −40°C

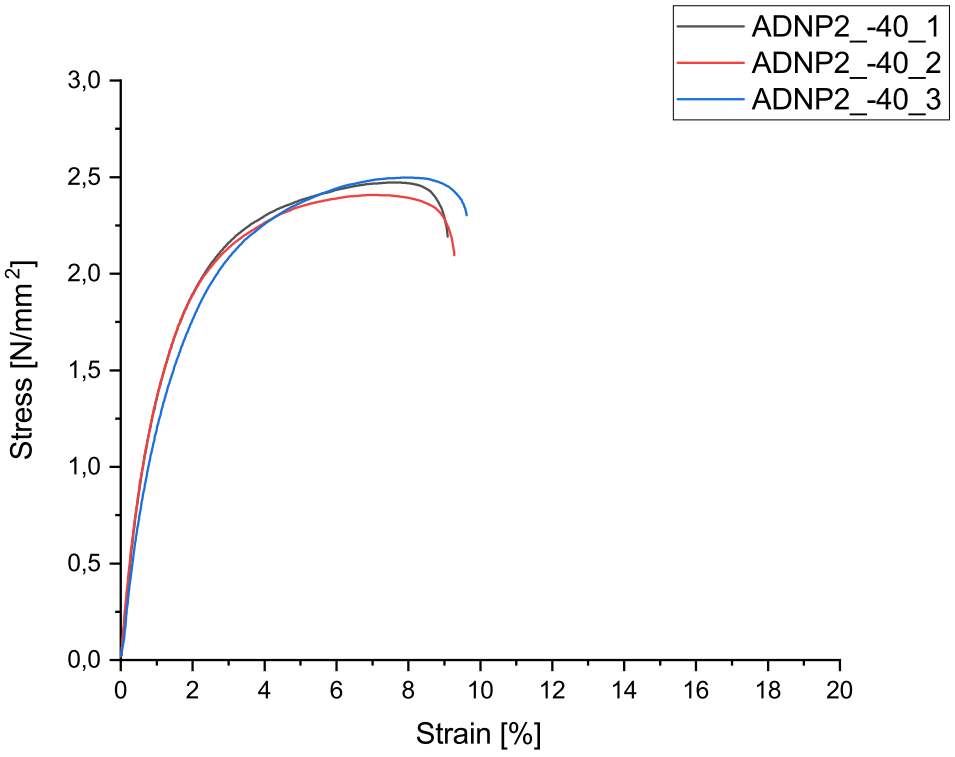

Figure A.9 Tensile tests of propellant sample **ADNP2** at −40 °C.

Table A.11 Tensile tests of propellant sample **ADNP2** at −40 °C.

Sample	F_m [N]	σ_m [MPa]	ϵ_m [%]	σ_b [MPa]	ϵ_m [%]	E [MPa]
ADNP2_-40_1	92.45	2.47	7.50	2.19	9.10	182.10
ADNP2_-40_2	81.52	2.41	6.91	2.10	9.28	192.80
ADNP2_-40_3	84.72	2.50	7.96	2.30	9.62	182.19
$\overline{x}$	86.23	2.46	7.46	2.20	9.33	185.70

Tensile Tests of ADNP4 at −40°C

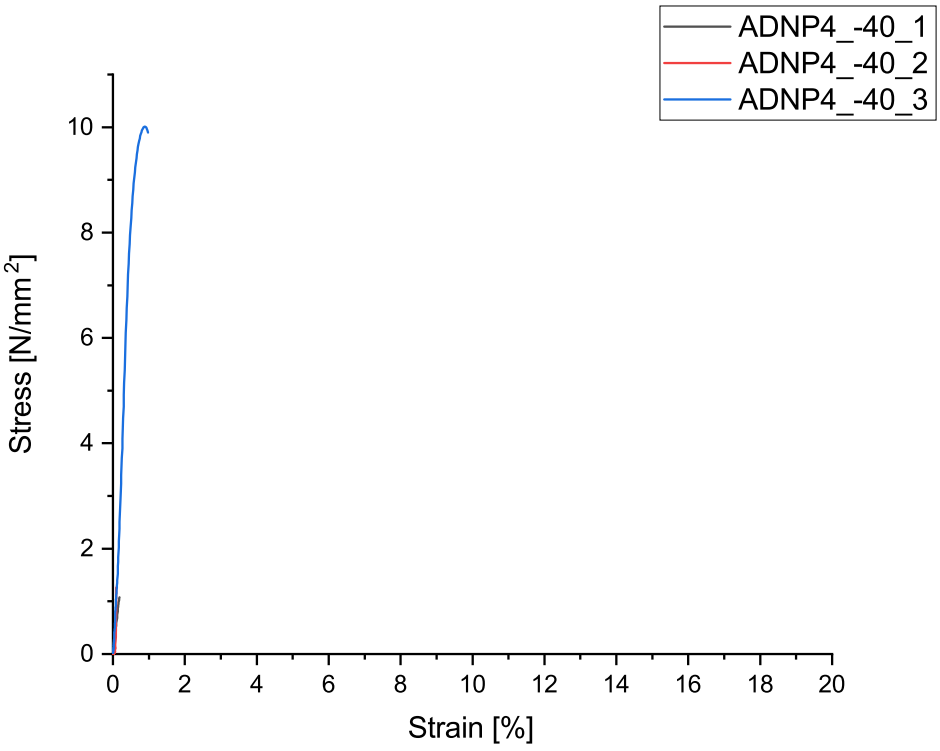

Figure A.10 Tensile tests of propellant sample **ADNP4** at −40 °C.

Table A.12 Tensile tests of propellant sample **ADNP4** at −40 °C.

Sample	F_m [N]	σ_m [MPa]	ϵ_m [%]	σ_b [MPa]	ϵ_m [%]	E [MPa]
ADNP4_-40_1	37.47	1.07	0.18	1.07	0.18	–
ADNP4_-40_2	41.40	1.26	0.09	1.26	0.09	–
ADNP4_-40_3	346.63	10.01	0.88	10.01	0.88	2278.63
$\overline{x}$	–	–	–	–	–	–

The samples of propellant formulation **ADNP4** showed no more elastic property at −40 °C, therefore no average values were calculated. For the result section, ADNP4_-40_3 was selected as the representative test result because it was the only one where a resonable E modulus could be calculated.

List of Publications

Full Papers

1. M. Hübner, S. Hafner, N. Barsan, U. Weimar, The Influence of Pt Doping on the Sensing and Conduction Mechanism of SnO_2 Based Thick Film Sensors, *Procedia Eng.* **2011**, *25*, 104–107.

2. S. Hafner, V. A. Hartdegen, M. S. Hofmayer, T. M. Klapötke, Potential Energetic Plasticizers on the Basis of 2,2-Dinitropropane-1,3-diol and 2,2-Bis(azidomethyl)-propane-1,3-diol, *Propellants, Explos., Pyrotech.* **2016**, *41*, 806–813.

3. A. B. Bellan, S. Hafner, V. A. Hartdegen, T. M. Klapötke, Polyurethanes Based on 2,2-Dinitropropane-1,3-diol and 2,2-Bis(azidomethyl)propane-1,3-diol as Potential Energetic Binders, *J. Appl. Polym. Sci.* **2016**, 43991.

4. M. Nörrlinger, S. Hafner, T. Ziegler, Synthesis and NMR-studies of malonyl-linked Glycoconjugates of *N*-(2-Aminoethyl)glycine. Building Blocks for the Construction of Combinatorial Glycopeptide Libraries, *Beilstein J. Org. Chem.* **2016**, *12*, 1939–1948.

5. S. Hafner, T. Keicher, T. M. Klapötke, Copolymers based on GAP and 1,2-Epoxyhexane as Promising Prepolymers for Energetic Binder Systems, *Propellants, Explos., Pyrotech.* **2018**, *43*, 126–135.

6. V. Gettwert, V. Weiser, C. Tagliabue, S. Hafner, S. Fischer, Environment-Friendly Composite Propellant Based on Ammonium Dinitramide, *Int. J. Energ. Mater. Chem. Propul.* **2019**, *18*, 31–49.

Selected Conference Contributions

1. T. Keicher, S. Hafner, H. Krause, H. Östmark, M. Kölhed, P. Krumlinde, EXPEDIA - A New EU Project Aiming to Reduce Threats from Homemade Explosives, 10th Future Security Conference, September 15–17, **2015**, Berlin.

2. S. Hafner, T. Keicher, T. M. Klapötke, Poly(ECH-*co*-1,2-Epoxyhexane)diol - A promising precursor for an energetic azido polymer for cast-cure processing, 47th International Annual Conference of the Fraunhofer ICT, June 28–July 1, **2016**, Karlsruhe.

3. S. Hafner, T. Keicher, T. M. Klapötke, Synthesis of P(GAP-*co*-EpH) - An Energetic Copolyether Suitable for Cast-Cure Applications, 48th International Annual Conference of ICT, June 27–30 , **2017**, Karlsruhe.

4. S. Hafner, T. Keicher, Synthese neuer energetischer Copolymere für die Formulierung von Festtreibstoffen, Angewandte Forschung für Verteidigung und Sicherheit in Deutschland, February 20–22, **2018**, Bonn.

5. S. Hafner, T. Keicher, T. M. Klapötke, Internal Plasticized Gycidyl Azide Polyethers for Solid Propellant Binders, DEA-A-65-GE-1060, April 16-19, **2018**, Fraunhofer EMI, Freiburg.

6. S. Hafner, T. Keicher, T. M. Klapötke, Internal Plasticized Gycidyl Azide Copolymers for Solid Propellant Binders, 11th International Symposium on Special Topics in Chemical Propulsion & Energetic Materials, September 09–13, **2018**, Stuttgart.

References

[1] T. Urbański, *Chemistry and Technology of Explosives*, *Vol. 3*, Pergamon Press, Oxford, **1985**.

[2] W. von Braun, F. J. Ordway, *Raketen: Vom Feuerpfeil zum Raumtransporter*, Pfriemer, München, **1979**.

[3] T. L. Davis, *The Chemistry of Powder and Explosives*, Wiley & Sons, Hoboken, New Jersey, **1943**.

[4] M. S. Cohen, Advanced Binders for Solid Propellants - A Review in *Advanced Propellant Chemistry*, (Ed.: R. T. Holzmann), Advances in Chemistry 54, American Chemical Society, Washington, D. C., **1966**, pp. 93–107.

[5] H. W. Köhler, *Feststoffraketenantriebe I: Einführung und Grundlagen*, Girardet, Essen, **1972**.

[6] M. Shusser, Composite Rocket Propellants in *Wiley encyclopedia of composites*, (Eds.: L. Nicolais, S. M. Lee), Wiley & Sons, Hoboken, New Jersey, **2011**, pp. 527–544.

[7] J. P. Agrawal, *High Energy Materials: Propellants, Explosives and Pyrotechnics*, Wiley-VCH, Weinheim, **2010**.

[8] G. P. Sutton, O. Biblarz, *Rocket Propulsion Elements*, 8th ed., Wiley & Sons, Hoboken, New Jersey, **2010**.

[9] K. Klager, J. M. Wrightson, Recent Advances in Solid Propellant Binder Chemistry in *Mechanics and Chemistry of Solid Propellants*, (Eds.: A. C. Eringen, H. Liebowitz, S. L. Koh), Pergamon Press, **1967**, pp. 47–74.

[10] G. Da Silva, S. C. Rufino, K. Iha, An Overview of the Technological Progress in Propellants Using Hydroxyl-Terminated Polybutadiene as Binder During 2002–2012, *J. Aerosp. Technol. Manag.* **2013**, *5*, 267–278.

[11] S. Chaturvedi, P. N. Dave, Solid propellants: AP/HTPB composite propellants, *Arabian J. Chem.* **2015**, in press.

[12] H. G. Ang, S. Pisharath, *Energetic polymers: Binders and plasticizers for enhancing performance*, Wiley-VCH, Weinheim, **2012**.

[13] GAP-5527 Polyol: Product data sheet, 3M, http://www.machichemicals.com/pdf/3M_GAP-5527.pdf (visited on 05/08/2019).

[14] GAP Diol: Product Information Data Sheet, Eurenco Bofors, https://www.eurenco.com/content/explosives/defence-security/oxidizers-energetic-polymers/gap-diol/ (visited on 05/03/2019).

[15] A. N. Nazare, S. N. Asthana, H. Singh, Glycidyl Azide Polymer (GAP) - An Energetic Component of Advanced Solid Rocket Propellants: A Review, *J. Energ. Mater.* **1992**, *10*, 43–63.

[16] NATO Standardization Office, NATO STANAG 2895: Extreme Climatic Conditions and Derived Conditions for Use in Defining Design/Test Criteria for NATO Forces Materiel, **1990**.

[17] NATO Standardization Office, NATO AECTP-200: Environmental Conditions, **2009**.

[18] M. B. Frankel, L. R. Grant, J. E. Flanagan, Historical Development of Glycidyl Azide Polymer, *J. Propul. Power* **1992**, *8*, 560–563.

[19] P. Kubisa, S. Penczek, Cationic activated monomer polymerization of heterocyclic monomers, *Prog. Polym. Sci.* **1999**, *24*, 1409–1437.

[20] C. E. Rehberg, W. A. Faucette, C. H. Fisher, Preparation and Properties of Secondary and Branched-Chain Alkyl Acrylates, *J. Am. Chem. Soc.* **1944**, *66*, 1723–1724.

[21] S. R. Jain, Solid Propellant Binders, *J. Sci. Ind. Res.* **2002**, *61*, 899–911.

[22] W. F. Arendale, Chemistry of Propellants Based on Chemically Crosslinked Binders in *Propellants Manufacture, Hazards, and Testing*, (Eds.: C. Boyars, K. Klager), Advances in Chemistry 88, American Chemical Society, Washington, D. C., **1969**, pp. 67–83.

[23] M. A. Daniel, Polyurethane Binder Systems for Polymer Bonded Explosives, Report DSTO-GD-0492, DSTO Weapons Systems Division, Edinburgh South Australia, Australia, **2006**.

[24] F. J. Hendel, Review of Solid Propellants for Space Exploration, Technical Memorandum No. 33-254, Jet Propulsion Laboratory, Pasadena, California, **1965**.

[25] B. D. Dunn, *Materials and Processes: For Spacecraft and High Reliability Applications*, Springer International Publishing, Basel, **2016**.

[26] R. Meyer, A. Homburg, J. Köhler, *Explosives*, 6th ed., Wiley-VCH, Weinheim, **2007**.

[27] N. C. Paul, R. W. Millar, P. Golding, *US Patent*, 5145974, **1992**.

[28] J. P. Agrawal, Recent Trends in High-Energy Materials, *Prog. Energy Combust. Sci.* **1998**, *24*, 1–30.

[29] H. J. Desai, A. V. Cunliffe, T. Lewis, R. W. Millar, N. C. Paul, M. J. Stewart, A. J. Amass, Synthesis of narrow molecular weight α, ω-hydroxy telechelic poly(glycidyl nitrate) and estimation of theoretical heat of explosion, *Polymer* **1996**, *37*, 3471–3476.

[30] M. E. Colclough, N. C. Paul, Nitrated Hydroxy-Terminated Polybutadiene: Synthesis and Properties in *Nitration*, (Eds.: L. F. Albright, R. V. C. Carr, R. J. Schmitt), ACS Symposium Series 623, American Chemical Society, Washington, D.C., **1996**, pp. 97–103.

[31] A. Arber, G. Bagg, E. Colclough, H. Desai, R. Millar, N. Paul, A. J. Sanderson, M. J. Stewart in Proceedings of the 21st International Annual Conference of ICT, Karlsruhe, Germany, Fraunhofer ICT, **1990**.

[32] U. C. Durgapal, P. K. Dutta, S. C. Mishra, J. Pant, Investigations on Polyvinyl Nitrate as a High Energetic Material, *Propellants Explos. Pyrotech.* **1995**, *20*, 64–69.

[33] S. Gayathri, S. Reshmi, Nitrato Functionalized Polymers for High Energy Propellants and Explosives: Recent Advances, *Polym. Adv. Technol.* **2017**, *28*, 1539–1550.

[34] G. E. Manser, R. M. Hajik, *US Patent*, 5214166, **1993**.

[35] P. Golding, R. W. Millar, N. C. Paul, D. H. Richards, Preparation of Di- and Polynitrates by Ring-Opening Nitration of Oxetanes by Dinitrogen Pentoxide (N_2O_5), *Tetrahedron* **1993**, *49*, 7051–7062.

[36] G. E. Manser, *US Patent*, 4483978, **1984**.

[37] M. E. Colclough, H. Desai, R. W. Millar, N. C. Paul, M. J. Stewart, P. Golding, Energetic Polymers as Binders in Composite Propellants and Explosives, *Polym. Adv. Technol.* **1994**, *5*, 554–560.

[38] A. Provatas, Energetic Polymers and Plasticisers for Explosive Formulations – A Review of Recent Advances, Report DSTO-TR-0966, DSTO Aeronautical and Maritime Research Laboratory, Melbourne Victoria, Australia, **2000**.

[39] G. E. Manser, *US Patent*, 4393199, **1983**.

[40] R. F. Stockel, P. C. Valenti, *US Patent*, 4031110, **1977**.

[41] R. A. Earl, J. S. Elmslie, *US Patent*, 4450762, **1981**.

[42] K. E. Hardenstine, G. V. S. Henderson, L. H. Sperling, C. J. Murphy, G. E. Manser, Crystallization Behavior of Poly(3,3-*bis* ethoxymethyl oxetane) and Poly(3,3-*bis* azidomethyl oxetane), *J. Polym. Sci. Polym. Phys. Ed.* **1985**, *23*, 1597–1609.

[43] T. Miyazaki, N. Kubota, Energetics of BAMO, *Propellants Explos. Pyrotech.* **1992**, *17*, 5–9.

[44] G. E. Manser, R. S. Miller, *US Patent*, 5210153, **1993**.

[45] Y.-L. Liu, G.-H. Hsiue, Y.-S. Chiu, Studies on the Polymerization Mechanism of 3-Nitratomethyl-3'-Methyloxetane and 3-Azidomethyl-3'-Methyloxetane and the Synthesis of Their Respective Triblock Copolymers with Tetrahydrofuran, *J. Polym. Sci. Part A: Polym. Chem.* **1995**, *33*, 1607–1613.

[46] M. A. H. Talukder, Ring-Opening Polymerization of Oxetanes by Cationic Initiators: Polymerization of 3-Azidomethyl-3-Methyloxetane with Bis(chlorodimethylsilyl)benzene/Silver Hexafluoroantimonate Initiating System, *Makromol. Chem. Macromol. Symp.* **1991**, *42/43*, 501–511.

[47] J. D. Ingham, W. L. Petty, J. P. L. Nichols, The Addition of Azide Ion to Epoxides, **1956**, *21*, 373–375.

[48] R. A. Earl, *US Patent*, 4486351, **1984**.

[49] E. Ahad, *European Patent*, 0274213B1, **1988**.

[50] M. B. Frankel, J. E. Flanagan, *US Patent*, 4268450, **1981**.

[51] E. J. Vandenberg, *US Patent*, 3645917, **1972**.

[52] B. Johannessen, *US Patent*, 4879419, **1989**.

[53] M. B. Frankel, E. F. Witucki, *US Patent*, 4379894, **1983**.

[54] B. Gaur, B. Lochab, V. Choudhary, I. K. Varma, Azido Polymers – Energetic Binders for Solid Rocket Propellants, *J. Macromol. Sci. Part C: Polym. Rev.* **2003**, *43*, 505–545.

[55] R. I. Wagner, *US Patent*, 5055600, **1991**.

[56] E. Ahad, *US Patent*, 4891438, **1990**.

[57] G. Ampleman, *US Patent*, 5124463, **1992**.

[58] E. R. Wilson, M. B. Frankel, *US Patent*, 4781861, **1988**.

[59] E. Ahad, *US Patent*, 4882395, **1989**.

[60] E. Ahad, *US Patent*, 5191034, **1993**.

[61] E. Ahad, *US Patent*, 5130381, **1992**.

[62] E. Ahad, *US Patent*, 5605975, **1997**.

[63] G. Ampleman, *US Patent*, 5256804, **1993**.

[64] Y. M. Mohan, K. M. Raju, Synthesis and Characterization of Low Molecular Weight Azido Polymers as High Energetic Plasticizers, *Int. J. Polym. Anal. Charact.* **2005**, *9*, 289–304.

[65] Y. Murali Mohan, K. Mohana Raju, B. Sreedhar, Synthesis and Characterization of Glycidyl Azide Polymer with Enhanced Azide Content, *Int. J. Polym. Mater.* **2006**, *55*, 441–455.

[66] Y. Murali Mohan, M. Padmanabha Raju, K. Mohana Raju, Synthesis, Spectral and DSC Analysis of Glycidyl Azide Polymers Containing Different Initiating Diol Units, *J. Appl. Polym. Sci.* **2004**, *93*, 2157–2163.

[67] D. Guanaes, E. Bittencourt, M. N. Eberlin, A. A. Sabino, Influence of polymerization conditions on the molecular weight and polydispersity of polyepichlorohydrin, *Eur. Polym. J.* **2007**, *43*, 2141–2148.

[68] J. S. Kim, D. Ki Kim, J. Ohk Kweon, J. M. Lee, S. T. Noh, S. Y. Kim, The Influence of Initiator Diol-BF_3 Complex Solubility and Other Factors on the Induction Period in BF_3 Catalyzed Cationic Ring Opening Polymerization of Epichlorohydrin, *Macromol. Res.* **2014**, *22*, 436–444.

[69] J. Su Kim, J. Ohk Kweon, S. Tae Noh, Online Monitoring of Reaction Temperature During Cationic Ring Opening Polymerization of Epichlorohydrin in Presence of BF_3 and 1,4-Butanediol, *J. Appl. Polym. Sci.* **2014**, *131*, 39912.

[70] Y. M. Mohan, M. P. Raju, K. M. Raju, Synthesis and Characterization of GAP-PEG Copolymers, *Int. J. Polym. Mater.* **2005**, *54*, 651–666.

[71] K. Subramanian, Hydroxyl-terminated poly (azidomethyl ethylene oxide-*b*-butadiene-*b*-azidomethyl ethylene oxide) – synthesis, characterization and its potential as a propellant binder, *Eur. Polym. J.* **1999**, *35*, 1403–1411.

[72] V. Vasudevan, G. Sundararajan, Synthesis of GAP-PB-GAP Triblock Copolymer and Application as Modifier in AP/HTPB Composite Propellant, *Propellants Explos. Pyrotech.* **1999**, *24*, 295–300.

[73] M. S. Eroğlu, B. Hazer, O. Güven, B. M. Baysal, Preparation and Thermal Characterization of Block Copolymers by Macroazonitriles Having Glycidyl Azide and Epichlorohydrin Moieties, *J. Appl. Polym. Sci.* **1996**, *60*, 2141–2147.

[74] M. S. Eroğlu, B. Hazer, O. Güven, Synthesis and characterization of hydroxyl terminated poly(butadiene)-*g*-poly(glycidyl azide) copolymer as a new energetic propellant binder, *Polym. Bull.* **1996**, *36*, 695–701.

[75] Y. M. Mohan, K. M. Raju, Synthesis and characterization of HTPB-GAP cross-linked co-polymers, *Des. Monomers Polym.* **2005**, *8*, 159–175.

[76] H. Arslan, M. S. Eroğlu, B. Hazer, Ceric ion initiation of methyl methacrylate from poly(glycidyl azide)-diol, *Eur. Polym. J.* **2001**, *37*, 581–585.

[77] K. Al-Kaabi, A. J. Van Reenen, Synthesis of Poly(methyl methacrylate-*g*-glycidyl azide) Graft Copolymers Using *N,N*-Dithiocarbamate-Mediated Iniferters, *J. Appl. Polym. Sci.* **2009**, *114*, 398–403.

[78] Y. Zhang, J. Zhao, P. Yang, S. He, H. Huang, Synthesis and Characterization of Energetic GAP-*b*-PAEMA Block Copolymer, *Polym. Eng. Sci.* **2012**, *52*, 768–773.

[79] S. Pisharath, H. G. Ang, Synthesis and thermal decomposition of GAP – Poly(BAMO) copolymer, *Polym. Degrad. Stab.* **2007**, *92*, 1365–1377.

[80] A. Kanti Sikder, S. Reddy, Review on Energetic Thermoplastic Elastomers (ETPEs) for Military Science, *Propellants Explos. Pyrotech.* **2013**, *38*, 14–28.

[81] A. M. Kawamoto, J. A. S. Holanda, U. Barbieri, G. Polacco, T. Keicher, H. Krause, M. Kaiser, Synthesis and Characterization of Glycidyl Azide-r-(3,3-bis(azidomethyl)oxetane) Copolymers, *Propellants Explos. Pyrotech.* **2008**, *33*, 365–372.

[82] U. Barbieri, G. Polacco, R. Massimi, Synthesis of Energetic Polyethers from Halogenated Precursors, *Macromol. Symp.* **2006**, *234*, 51–58.

[83] A. M. Kawamoto, M. F. Diniz, V. L. Lourenço, M. F. K. Takahashi, T. Keicher, H. Krause, K. Menke, P. B. Kempa, Synthesis and Characterization of GAP/BAMO copolymers applied at high energetic composite propellants, *J. Aerosp. Technol. Manage.* **2010**, *2*, 307–322.

[84] T. Keicher, S. Steinert, M. Doerich, H. Krause, M. Raab, U. Schaller, W. Schweikert in Proceedings of the 44th Annual Conference of ICT, Karlsruhe, Germany, Fraunhofer ICT, **2013**.

[85] T. Keicher, W. Janitschek, U. Schaller, H. Krause, M. Kaiser in Proceedings of the 45th International Annual Conference of ICT, Karlsruhe, Germany, Fraunhofer ICT, **2014**.

[86] J.-F. Pei, F.-Q. Zhao, H.-L. Lu, X.-D. Song, R. Zhou, Z.-F. Yuan, J. Zhang, J.-B. Chen, Compatibility study of BAMO–GAP copolymer with some energetic materials, *J. Therm. Anal. Calorim.* **2016**, *124*, 1301–1307.

[87] Y. M. Mohan, K. M. Raju, Synthesis and Characterization of GAP-THF Copolymers, *Int. J. Polym. Mater.* **2006**, *55*, 203–217.

[88] B. J. Lee, I. J. Bae, J. S. Kim, S. H. Kim, *US Patent*, 2014/0135453 A1, **2014**.

[89] Q. Dong, Y. Li, F. Wu, H. Li, X. Liu, C. Huang, Synthesis, Characterization and Thermal Properties of Poly(glycidyl azide-*r*-3-azidotetrahydrofuran) as Azido Binder for Solid Rocket Propellants, *Propellants Explos. Pyrotech.* **2017**, *42*, 1143–1148.

[90] E. H. Immergut, H. F. Mark, Principles of Plasticization in *Plasticization and Plasticizer Processes*, (Ed.: N. A. Platzer), Advances in Chemistry 48, American Chemical Society, Washington D.C., **1965**, pp. 1–26.

[91] A. Davenas, Solid Rocket Motor Design in *Tactical Missile Propulsion*, (Eds.: G. E. Jensen, D. W. Netzer), Progress in Astronautics and Aeronautics 170, American Institute of Aeronautics and Astronautics, Washington, D.C., **1996**, pp. 57–113.

[92] R. G. Stacer, D. M. Husband, Molecular Structure of the Ideal Solid Propellant Binder, *Propellants Explos. Pyrotech.* **1991**, *16*, 167–176.

[93] N. Wingborg, C. Eldsäter, 2,2-Dinitro-1,3-Bis-Nitrooxy-Propane (NPN): A New Energetic Plasticizer, **2002**, *27*, 314–319.

[94] A. Wypych, *Plasticizer Databook*, 2nd ed., ChemTec Publishing, Toronto, **2013**.

[95] P. C. Tfelt-Hansen, J. Tfelt-Hansen, Nitroglycerin headache and nitroglycerin-induced primary headaches from 1846 and onwards: a historical overview and an update, *Headache* **2009**, *49*, 445–456.

[96] D. Drees, D. Löffel, A. Messmer, K. Schmid, Synthesis and Characterization of Azido Plasticizer, *Propellants Explos. Pyrotech.* **1999**, *24*, 159–162.

[97] G. Wypych, *Handbook of Plasticizers*, 2nd ed., ChemTec Publishing, Toronto, **2012**.

[98] J. Libardi, S. P. Ravagnani, A. M. F. Morais, A. R. Cardoso, Study of plasticizer diffusion in a solid rocket motor's bondline, *J. Aerosp. Technol. Manage.* **2009**, *1*, 223–229.

[99] J. Libardi, S. P. Ravagnani, A. M. F. Morais, A. R. Cardoso, Diffusion of plasticizer in a solid propellant based on hydroxyl-terminated polybutadiene, *Polimeros* **2010**, *20*, 241–245.

[100] D. Venkatesan, M. Srinivasan, K. A. Reddy, V. V. Pendse, The Migration of Plasticizer in Solid Propellant Grains, *Polym. Int.* **1993**, *32*, 395–399.

[101] L. Gottlieb, S. Bar, Migration of Plasticizer between Bonded Propellant Interfaces, *Propellants Explos. Pyrotech.* **2003**, *28*, 12–17.

[102] Z.-p. Huang, H.-y. Nie, Y.-y. Zhang, L.-m. Tan, H.-l. Yin, X.-g. Ma, Migration kinetics and mechanisms of plasticizers, stabilizers at interfaces of NEPE propellant/HTPB liner/EDPM insulation, *J. Hazard. Mater.* **2012**, *229-230*, 251–257.

[103] M. Pröbster, R. H. Schmucker, Ballistic anomalies in solid rocket motors due to migration effects, *Acta Astronaut.* **1986**, *13*, 599–605.

[104] D. Kumari, R. Balakshe, S. Banerjee, H. Singh, Energetic plasticizers for gun & rocket propellants, *Rev. J. Chem.* **2012**, *2*, 240–262.

[105] K. Menke, P. Gerber, E. Geißler, G. Bunte, H. Kentgens, R. Schöffl, Characteristic Properties of an End Burning Grain with Smoke Reduced Ferrocene Containing Composite Propellant, *Propellants Explos. Pyrotech.* **1999**, *24*, 126–133.

[106] N. W. Gregornik, Barrier Films for MK 12 Mod 2 Cartridge Plug, Report AD-A043253, Minnesota, **1974**.

[107] J. K. Sears, J. R. Darby, *The Technology of Plasticizers*, Wiley & Sons, Hoboken, New Jersey, **1982**.

[108] A. Marcilla, S. Garcia, J. C. Garcia-Quesada, Study of the migration of PVC plasticizers, *J. Anal. Appl. Pyrolysis* **2004**, *71*, 457–463.

[109] C. E. Rehberg, C. H. Fisher, Preparation and Properties of the *n*-Alkyl Acrylates, *J. Am. Chem. Soc.* **1944**, *66*, 1203–1207.

[110] S. Rogers, L. Mandelkern, Glass Formation in Polymers 1: The Glass Transitions of the Poly-(*n*-Alkyl Methacrylates), *J. Phys. Chem.* **1957**, *61*, 985–991.

[111] L. A. White, S. Jönson, C. E. Hoyle, L. J. Mathias, Synthesis of 3-alkylated-1-vinyl-2-pyrrolidones and preliminary kinetic studies of their photopolymerizations, *Polymer* **1999**, *40*, 6597–6605.

[112] J. R. Sasthav, F. W. Harris, Internal plasticization of polyimides with alkyl 3,5-diaminobenzoate compounds, *Polymer* **1995**, *36*, 4911–4917.

[113] M. Ma, Y. Shen, Y. Kwon, C. Chung, J. S. Kim, Reactive Energetic Plasticizers for Energetic Polyurethane Binders Prepared via Simultaneous Huisgen Azide-Alkyne Cycloaddition and Polyurethane Reaction, *Propellants Explos. Pyrotech.* **2016**, *41*, 746–756.

[114] M. Ma, Y. Kwon, Reactive cycloalkane plasticizers covalently linked to energetic polyurethane binders *via* facile control of an *in situ* Cu-free azide–alkyne 1,3-dipolar cycloaddition reaction, *Polym. Chem.* **2018**, *9*, 5452–5461.

[115] Deutsches Institut für Normung (DIN), DIN 66137-2: Determination of solid state density - Part 2: Gaspycnometry, **2004**.

[116] Deutsches Institut für Normung (DIN), DIN 53420-2: Determination of hydroxyl value - Part 2: Method with catalyst, **2007**.

[117] NATO Standardization Office, NATO STANAG 4515: Explosives. Thermal Analysis using Differential Thermal Analysis (DTA), Differential Scanning Calorimetry (DSC), Heat Flow Calorimetry (HFC) and Thermogravimetric Analysis (TGA), **2015**.

[118] Deutsches Institut für Normung (DIN), DIN 51900-2: Testing of solid and liquid fuels - Determination of the gross calorific value by the bomb calorimeter and calculation of the net calorific value - Part 2: Method using isoperibol or static, jacket calorimeter, **2003**.

[119] NATO Standardization Office, NATO STANAG 4489: Explosives. Impact Sensitivity Tests, **1999**.

[120] United Nations (UN), UN Recommendations on the Transport of Dangerous Goods; Manual of Testis and Criteria, **2009**.

[121] NATO Standardization Office, NATO STANAG 4487: Explosives. Friction Sensitivity Tests, **2002**.

[122] T. M. Klapötke, M. Stein, J. Stierstorfer, Salts of 1*H*-Tetrazole – Synthesis, Characterization and Properties, *Z. Anorg. Allg. Chem.* **2008**, *634*, 1711–1723.

[123] A. F. Holleman, E. Wiberg, N. Wiberg, *Lehrbuch der Anorganischen Chemie*, 101st ed., Walter de Gruyter, Berlin, **1995**.

[124] M. Szwarc, 'Living' Polymers, *Nature* **1956**, *178*, 1168–1169.

[125] M. Szwarc, M. Levy, R. Milkovich, Polymerization Initiated by Electron Transfer to Monomer. A New Method of Formation of Block Polymers, *J. Am. Chem. Soc.* **1956**, *78*, 2656–2657.

[126] *Controlled and Living Polymerizations*, (Eds.: A. H. E. Müller, K. Matyjaszewski), Wiley-VCH, Weinheim, **2009**.

[127] S. Penczek, M. Cypryk, A. Duda, P. Kubisa, S. Słomkowski, Living ring-opening polymerizations of heterocyclic monomers, *Prog. Polym. Sci.* **2007**, *32*, 247–282.

[128] E. J. Goethals, F. Du Prez, Carbocationic polymerizations, *Prog. Polym. Sci.* **2007**, *32*, 220–246.

[129] D. Baskaran, A. Müller, Anionic vinyl polymerization – 50 years after Michael Szwarc, *Prog. Polym. Sci.* **2007**, *32*, 173–219.

[130] T. Yokozawa, A. Yokoyama, Chain-growth polycondensation: The living polymerization process in polycondensation, *Prog. Polym. Sci.* **2007**, *32*, 147–172.

[131] G. J. Domski, J. M. Rose, G. W. Coates, A. D. Bolig, M. Brookhart, Living alkene polymerization: New methods for the precision synthesis of polyolefins, *Prog. Polym. Sci.* **2007**, *32*, 30–92.

[132] W. A. Braunecker, K. Matyjaszewski, Controlled/living radical polymerization: Features, developments, and perspectives, *Prog. Polym. Sci.* **2007**, *32*, 93–146.

[133] S. Carlotti, A. Labbé, V. Rejsek, S. Doutaz, M. Gervais, A. Deffieux, Living/Controlled Anionic Polymerization and Copolymerization of Epichlorohydrin with Tetraoctylammonium Bromide – Triisobutylaluminum Initiating Systems, *Macromolecules* **2008**, *41*, 7058–7062.

[134] T. Endo, General Mechanisms in Ring-Opening Polymerization in *Handbook of Ring-Opening Polymerization*, (Eds.: J.-M. Raquez, O. Coulembier, P. Dubois), Wiley-VCH, Weinheim, **2009**, pp. 53–63.

[135] E. J. Goethals, Cyclic Oligomers in the Cationic Polymerization of Heterocycles, *Pure Appl. Chem.* **1976**, *48*, 335–341.

[136] *Cationic Ring-Opening Polymerization: 2. Synthetic Applications*, (Eds.: S. Penczek, P. Kubisa, K. Matyjaszewski), Springer, Berlin, **1985**.

[137] S. Penczek, Cationic Ring-Opening Polymerization (CROP) Major Mechanistic Phenomena, *J. Polym. Sci. Part A: Polym. Chem.* **2000**, *38*, 1919–1933.

[138] H. Bouchékif, M. I. Philbin, E. Colclough, A. J. Amass, Non-steady-state living polymerization: a new route to control cationic ring-opening polymerization (CROP) of oxetane via an activation chain end (ACE) mechanism at ambient temperature, *Chem. Commun.* **2005**, 3870–3872.

[139] S. Penczek, P. Kubisa, K. Matyjaszewski, Cationic Ring-Opening Polymerization of Heterocyclic Monomers in *Cationic Ring-Opening Polymerization Part 2: Synthetic Applications*, Advances in Polymer Science 68/69, Springer, Berlin, **1985**.

[140] A. Carpmael, *GB Patent*, 477843, **1938**.

[141] J. M. Baggett, M. E. Pruitt, *US Patent*, 2871219, **1959**.

[142] S. Ishida, Polyethers 1. Stereospecific Polymerization of Epihalohydrins, *Bull. Chem. Soc. Jpn.* **1960**, *33*, 727–730.

[143] E. J. Vandenberg, Organometallic catalysts for polymerizing monosubstituted epoxides, *J. Polym. Sci. Part A: Polym. Chem.* **1960**, *47*, 486–489.

[144] E. J. Vandenberg, *US Patent*, 3158580, **1964**.

[145] E. J. Vandenberg, *US Patent*, 3065188, **1962**.

[146] E. J. Vandenberg, *US Patent*, 3158581, **1964**.

[147] E. J. Vandenberg, A New Class of Polyethers – Poly(1,4-Dichloro-2,3-Epoxybutane)s – Synthesis, Mechanism and Property Aspects, *Pure Appl. Chem.* **1976**, *48*, 295–306.

[148] S. Brochu, G. Ampleman, Synthesis and Characterization of Glycidyl Azide Polymers Using Isotactic and Chiral Poly(epichlorohydrin)s, *Macromolecules* **1996**, *29*, 5539–5545.

[149] J. M. Hammond, J. F. Hooper, W. G. P. Robertson, Cationic Copolymerization of Tetrahydrofuran with Epoxides. 1. Polymerization Mechanism in the Presence of a Glycol, *J. Polym. Sci. Part A-1: Polym. Chem.* **1971**, *9*, 265–279.

[150] M. D. Baijal, L. P. Blanchard, Kinetic Aspects of the Copolymerization of Tetrahydrofuran with Propylene Oxide. Part 2, *J. Polym. Sci. Part C: Polym. Symp.* **1968**, *23*, 157–167.

[151] K. Ito, N. Usami, Y. Yamashita, Cationic Oligomerization of Epichlorohydrin, *Polym. J.* **1979**, *11*, 171–173.

[152] Y. Okamoto, *US Patent*, 4391970, **1983**.

[153] Y. Okamoto, Cationic Ring-Opening Polymerization of Epichlorohydrin in the Presence of Ethylene Glycol in *Ring-Opening Polymerization: Kinetics, Mechanisms and Synthesis*, (Ed.: J. E. McGrath), ACS Symposium Series 286, American Chemical Society, Washington, D.C., **1985**, pp. 361–372.

[154] B. Johannessen, *US Patent*, 5741997, **1998**.

[155] T. Biedron, P. Kubisa, S. Penczek, Polyepichlorohydrin Diols Free of Cyclics: Synthesis and Characterization, *J. Polym. Sci. Part A: Polym. Chem.* **1991**, *29*, 619–628.

[156] A. U. Francis, S. Venkatachalam, M. Kanakavel, P. V. Ravindran, K. N. Ninan, Structural characterization of hydroxyl terminated polyepichlorohydrin obtained using boron trifluoride etherate and stannic chloride as initiators, *Eur. Polym. J.* **2003**, *39*, 831–841.

[157] T. Biedron, R. Szymanski, P. Kubisa, S. Penczek, Kinetics of polymerization by activated monomer mechanism, *Makromol. Chem. Macromol. Symp.* **1990**, *32*, 155–168.

[158] M. A. Mohd Noor, V. Sendijarevic, H. Abu Hassan, I. Sendijarevic, T. N. M. Ismail, H. Seng Soi, N. A. Hanzah, R. Ghazali, Polyether polyols as GPC calibration standards for determination of molecular weight distribution of polyether polyols, *J. Appl. Polym. Sci.* **2015**, *132*, 42698.

[159] N. Kubota, T. Sonobe, Combustion Mechanism of Azide Polymer, *Propellants Explos. Pyrotech.* **1988**, *13*, 172–177.

[160] Y. Haas, Y. B. Eliahu, S. Welner, Infrared Laser-Induced Decomposition of GAP, *Combust. Flame* **1994**, *96*, 212–220.

[161] M. S. Eroğlu, O. Güven, Thermal Decomposition of Poly(glycidyl azide) as Studied by High-Temperature FTIR and Thermogravimetry, *J. Appl. Polym. Sci.* **1996**, *61*, 201–206.

[162] E. Diaz, P. Brousseau, G. Ampleman, R. E. Prud'homme, Heats of Combustion and Formation of New Energetic Thermoplastic Elastomers Based on GAP, PolyNIMMO and PolyGLYN, *Propellants Explos. Pyrotech.* **2003**, *28*, 101–106.

[163] NIST Chemistry WebBook, National Institute of Standards and Technology, https://webbook.nist.gov/chemistry/ (visited on 05/04/2019).

[164] Deutsches Institut für Normung (DIN), DIN EN 13631-4: Explosives for civil uses – High explosives – Part 4: Determination of sensitiveness to impact of explosives, **2002**.

[165] Deutsches Institut für Normung (DIN), DIN EN 13631-3: Explosives for civil uses – High explosives – Part 3: Determination of sensitiveness to friction of explosives, **2004**.

[166] A. Dadieu, R. Damm, E. W. Schmidt, *Raketentreibstoffe*, Springer, Wien, **1968**.

[167] K. Klager, Raketentreibstoffe, *Chem. Unserer Zeit* **1976**, *10*, 97–105.

[168] K. Sellers, *Perchlorate: Environmental Problems and Solutions*, CRC Press, Boca Raton, **2007**.

[169] A. Larsson, N. Wingborg, Green Propellants Based on Ammonium Dinitramide (ADN) in *Advances in Spacecraft Technologies*, (Ed.: J. Hall), InTech, **2011**, pp. 139–156.

[170] S. Venkatachalam, G. Santhosh, K. Ninan Ninan, An Overview on the Synthetic Routes and Properties of Ammonium Dinitramide (ADN) and other Dinitramide Salts, *Propellants Explos. Pyrotech.* **2004**, *29*, 178–187.

[171] Oleg A. Luk'yanov, Vladimir A. Tartakovsky, Synthesis and Characterization of Dinitramidic Acid and Its Salts in *Solid Propellant Chemistry, Combustion, and Motor Interior Ballistics*, (Eds.: T. B. Brill, V. Yang), Progress in Astronautics and Aeronautics 185, AIAA, Virginia, **2000**, pp. 207–220.

[172] T. Brinck, Introduction to Green Energetic Materials in *Green Energetic Materials*, (Ed.: T. Brinck), John Wiley & Sons, Chichester, West Sussex, United Kingdom, **2014**.

[173] ADN Product Information Data Sheet, Eurenco Bofors, http://www.eurenco.com/content/explosives/defence-security/oxidizers-energetic-polymers/adn/ (visited on 03/02/2019).

[174] J. de Flon, S. Andreasson, M. Liljedahl, C. Oscarson, M. Wanhatalo, N. Wingborg in Proceedings of the 47th AIAA/ASME/SAE/ASEE Joint Propulsion Conference & Exhibit, San Diego, California, American Institute of Aeronautics and Astronautics, **2011**.

[175] N. Wingborg, S. Andreasson, J. de Flon, M. Johnsson, M. Liljedahl, C. Oscarsson, Å. Pettersson, M. Wanhatalo in Proceedings of the 46th AIAA/ASME/SAE/-ASEE Joint Propulsion Conference & Exhibit, Nashville, TN, American Institute of Aeronautics and Astronautics, **2010**.

[176] D. Trache, T. M. Klapötke, L. Maiz, M. Abd-Elghany, L. T. DeLuca, Recent advances in new oxidizers for solid rocket propulsion, *Green Chem.* **2017**, *19*, 4711–4736.

[177] A. Davenas, *Solid Rocket Propulsion Technology*, Pergamon Press, Oxford, **1993**.

[178] P. Mackey, Introduction to elastomers in *The Polyurethanes Book*, (Eds.: D. Randall, S. Lee), Wiley & Sons, New York, **2002**.

[179] S. Keskin, S. Özkar, Kinetics of Polyurethane Formation Between Glycidyl Azide Polymer and a Triisocyanate, *J. Appl. Polym. Sci.* **2001**, *81*, 918–923.

[180] R. P. Houghton, A. W. Mulvaney, Mechanism of tin(IV)-catalysed urethane formation, *J. Organomet. Chem.* **1996**, *518*, 21–27.

[181] T. H. Hagen, T. L. Jensen, E. Unneberg, Y. H. Stenstrøm, T. E. Kristensen, Curing of Glycidyl Azide Polymer (GAP) Diol Using Isocyanate, Isocyanate-Free, Synchronous Dual, and Sequential Dual Curing Systems, *Propellants Explos. Pyrotech.* **2014**, *40*, 275–284.

[182] B. S. Min, Y. C. Park, J. C. Yoo, A Study on the Triazole Crosslinked Polymeric Binder Based on Glycidyl Azide Polymer and Dipolarophile Curing Agents, *Propellants Explos. Pyrotech.* **2012**, *37*, 59–68.

[183] K. Menke, T. Heintz, W. Schweikert, T. Keicher, H. Krause, Formulation and Properties of ADN/GAP propellants, *Propellants Explos. Pyrotech.* **2009**, *34*, 218–230.

[184] T. Keicher, W. Kuglstatter, S. Eisele, T. Wetzel, H. Krause, Isocyanate-Free Curing of Glycidyl Azide Polymer (GAP) with Bis-Propargyl-Succinate (II), *Propellants Explos. Pyrotech.* **2009**, *34*, 210–217.

[185] R. Huisgen, 1,3-Dipolare Cycloadditionen Rückschau und Ausblick, *Angew. Chem.* **1963**, *75*, 604–637.

[186] C. S. Kim, C. H. Youn, P. N. Noble, A. Gao, Developement of Neutral Polymeric Bonding Agents for Propellants with Polar Composites Filled with Organic Nitramine Crystals, *Propellants Explos. Pyrotech.* **1992**, *17*, 38–42.

[187] E. Landsem, T. L. Jensen, F. K. Hansen, E. Unneberg, T. E. Kristensen, Neutral Polymeric Bonding Agents (NPBA) and Their Use in Smokeless Composite Rocket Propellants Based on HMX-GAP-BuNENA, *Propellants Explos. Pyrotech.* **2012**, *37*, 581–591.

[188] G. A. Fluke, Composite Solid Propellant Processing Techniques in *Propellants Manufacture, Hazards, and Testing*, (Eds.: C. Boyars, K. Klager), Advances in Chemistry 88, American Chemical Society, Washington, D. C., **1969**.

[189] T. Smith, Solid Propellants...Elastomeric-Binder and Mechanical-Property Requirements for Solid Propellants, *Ind. Eng. Chem.* **1960**, *52*, 776–780.

[190] F. Volk, H. Bathelt, ICT Thermodynamic Code, version 2014.1.0, Fraunhofer ICT, Pfinztal, Germany, **2014**.

[191] F. Volk, H. Bathelt, ICT Database of Thermochemical Values, version 2008.8.0, Fraunhofer ICT, Pfinztal, Germany, **2008**.

[192] J. Köhler, R. Meyer, *Explosivstoffe*, 10th ed., Wiley-VCH, Weinheim, **2009**.

[193] Oxsoft GPO: Product information data sheet, Oxea.

[194] Palatinol TOTM: Product information data sheet, BASF, http://www.plasticizers.basf.com/portal/streamer?fid=277354 (visited on 05/01/2019).

[195] Plastomoll DOA: Product information datasheet, BASF, http://www.plasticizers.basf.com/portal/load/fid228835/Plastomoll_DOA.pdf (visited on 01/04/2019).

[196] Palatinol N: Product information data sheet, BASF, http://www.plasticizers.basf.com/portal/load/fid247440/Pal_N_e_09_13.pdf (visited on 02/02/2019).

[197] BASF, https://www.weichmacher.basf.com/portal/load/fid247491/TI_Hexamoll_DINCH_20170705.pdf (visited on 03/02/2019).

[198] Triacetin: Product information data sheet, Lanxess.

[199] K. Selim, S. Özkar, L. Yilmaz, Thermal Characterization of Glycidyl Azide Polymer (GAP) and GAP-based Binders for Composite P ropellants, *J. Appl. Polym. Sci.* **2000**, *77*, 538–546.

[200] S. K. Manu, T. L. Varghese, S. Mathew, K. N. Ninan, Compatibility of Glycidyl Azide Polymer with Hydroxyl Terminated Polybutadiene and Plasticizers, *J. Propul. Power* **2009**, *25*, 533–536.

[201] T. G. Fox, Influence of Diluent and of Copolymer Composition on the Glass Temperature of a Polymer System, *Bull. Am. Phys. Soc.* **1956**, *1*, 123.

[202] E. Jenckel, R. Heusch, Die Erniedrigung der Einfriertemperatur organischer Gläser durch Lösungsmittel, *Kolloid-Z.* **1953**, *130*, 89–105.

[203] M. Gordon, J. S. Taylor, Ideal Copolymers and the Second-Order Transitions of Synthetic Rubbers. I. Non-Crystalline Copolymers, *J. Appl. Chem.* **1952**, *2*, 493–500.

[204] M. H. Baghersad, A. Habibi, A. Heydari, Synthesis, characterization, thermal and computational studies of novel tetra–azido compounds as energetic plasticizers, *J. Mol. Struct.* **2017**, *1130*, 447–454.

[205] M.-S. Chi, Compatibility of Cross-Linked Polymers with Plasticizers by Glass Transition Temperature Measurement and Swelling Tests, *J. Polym. Sci. Polym. Chem. Ed.* **1981**, *19*, 1767–1779.

[206] I. M. Kalogeras, W. Brostow, Glass Transition Temperatures In Binary Polymer Blends, *J. Polym. Sci. Part B: Polym. Phys.* **2009**, *47*, 80–95.

[207] T. Heintz, H. Pontius, J. Aniol, C. Birke, K. Leisinger, W. Reinhard, Ammonium Dinitramide (ADN)-Prilling, Coating, and Characterization, *Propellants Explos. Pyrotech.* **2009**, *34*, 231–238.

[208] T. Heintz, M. Herrmann, K. Leisinger, W. Reinhard in Proceedings of the 47th International Annual Conference of ICT, Karlsruhe, Germany, Fraunhofer ICT, **2016**.

[209] T. Heintz, K. Leisinger, W. Reinhard, M. Heil, M. Herrmann in Proceedings of the 49th International Annual Conference of ICT, Karlsruhe, Germany, Fraunhofer ICT, **2018**.

[210] Desmodur N100: Product information data sheet, Covestro.

[211] Baymedix AP501: Product information datasheet, Convestro.

[212] Information about the centrifugal mixer principle, www.thinkyusa.com (visited on 01/05/2019).

[213] V. Gettwert, V. Weiser, C. Tagliabue, S. Hafner, S. Fischer, Environment-Friendly Composite Propellants Based on Ammonium Dinitramide, *Int. J. Energ. Mater. Chem. Propul.* **2019**, *18*, 31–49.

[214] GRAIL – Green advanced high energy propellants for launchers, European Union, http://grail-h2020.eu/ (visited on 05/06/2019).